UNIVERSITA' DEGLI STUDI DI MILANO

Facoltà di Scienze Matematiche, Fisiche e Naturali

Dipartimento di Chimica Inorganica, Metallorganica ed Analitica "Lamberto Malatesta"

PhD in Chemical Sciences

XXIII Cycle

Use of poliphosphanes in the assembly of discrete or polymeric coordination compounds

(Chim 03)

Matteo Daghetta

Supervisor: Prof. LUIGI GARLASCHELLI

Coordinator: Prof. SILVIA ARDIZZONE

A.A. 2009/2010

"L'Illuminismo è l'uscita dell'uomo dallo stato di minorità che egli deve imputare a se stesso.
Minorità è l'incapacità di valersi del proprio intelletto senza la guida di un altro.
Imputabile a se stessa è questa minorità, se la causa di essa non dipende da difetto di intelligenza, ma dalla mancanza di decisione e del coraggio di far uso del proprio intelletto senza essere guidati da un altro.
Sapere aude! Abbi il coraggio di servirti della tua propria intelligenza!
È questo il motto dell'Illuminismo"

Immanuel Kant - Risposta alla domanda: che cos'è l'illuminismo?, in *Scritti politici e di filosofia della storia e del diritto*

Index

Abstract

Although phosphanes show useful features for the coordination chemistry, their use as pure structural building blocks, to join metal centres in larger aggregates, has not been yet well explored.

In this work, synthesis and characterization of discrete and polymeric coordination compounds are presented.

As metal centres both monometallic and cluster compounds have been used, whereas as ligands we have used poliphosphanes both commercially available and synthesised in our laboratories.

For simplicity we can classify them in: rigid diphosphanes, flexible diphosphanes and rigid poliphosphanes.

Rigid diphosphanes

Bis(diphenylphosphano)acetylene (dppa) and trans-1,2-bis(diphenylphosphano)ethane (t-dppethe)

These diphosphanes (Fig. 1 and 2) have been used to obtain the first rhodium and iridium carbonyls based 1D coordination polymers.

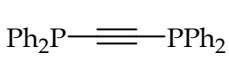

Fig. 1 dppa

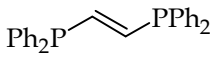

Fig. 2 t-dppethe

Reaction of $[Ir_4Br(CO)_{11}]^-$ with dppa and t-dppethe gave two analogous products where two cluster units are linked by one ligand molecules (Fig.3 a-b).

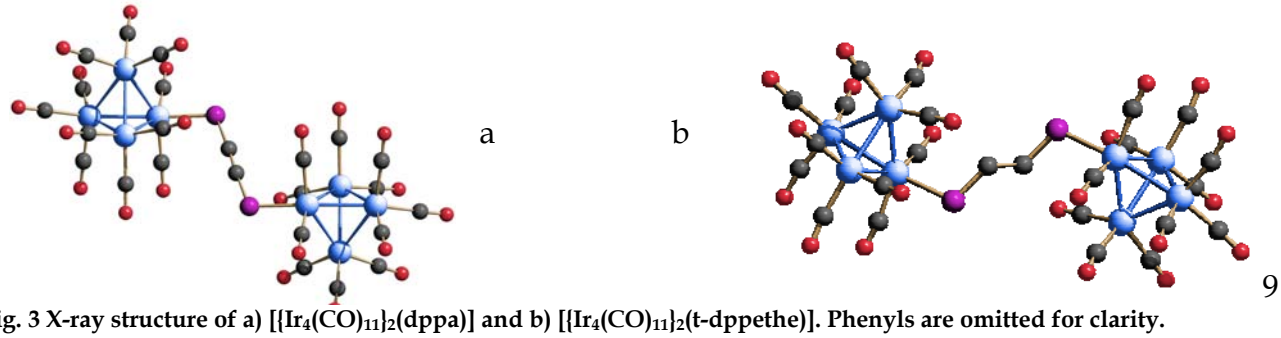

Fig. 3 X-ray structure of a) $[\{Ir_4(CO)_{11}\}_2(dppa)]$ and b) $[\{Ir_4(CO)_{11}\}_2(t\text{-}dppethe)]$. Phenyls are omitted for clarity.

X-ray structures show that in both cases iridium clusters coordinate only terminal COs, as in the parent cluster $[Ir_4(CO)_{12}]$. This fact is confirmed by Nujol-IR spectrum. On the contrary, ATR-IR spectrum, a technique in which the sample is monitored under pressure, shows either bridging and terminal CO stretching bands.

It is possible to suggest that pressure induce a change in the coordination mode of three COs, from terminal to bridging.

1,4-bis(diphenylphosphanomethyl)benzene (dppmb),

4,4' bis(diphenylphosphano)biphenyle (dppbp) and

4,4'-bis(diphenylphosphanomethyl)biphenyle (dppmbp)

The aromatic spacers give rigidity to these diphosphanes, a desirable feature in the assembly of robust coordination polymer (Fig 4, 5 and 6).

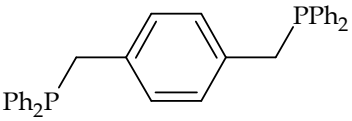

Fig. 4 dppmp

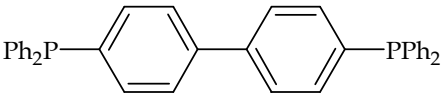

Fig. 5 dppbp

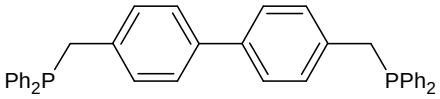

Fig. 6 dppmbp

Monometallic compounds

Reaction of $[MCl_2(CO)_2]^-$ (M= Rh, Ir) with dppbp and dppmb leads to the formation of polymeric species of formula $[MCl(CO)(L)]_n$. We were not able to grow crystals suitable for X-ray analysis. In one case, crystals of the cyclic dimer $[MCl(CO)(L)]_2$ (M=Rh, L=dppmb), supposed to be the polymer precursor in a ring opening polymerization mechanism, were obtained (Fig. 7).

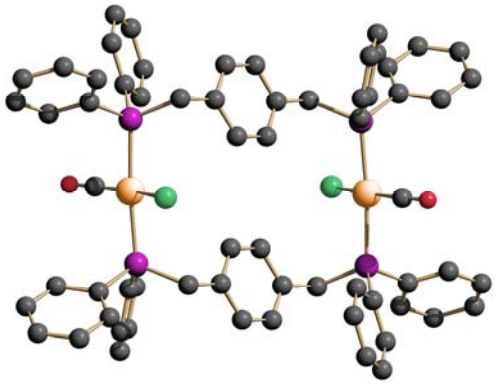

Fig. 7 X-ray structure of $[RhCl(CO)(dppmb)]_2$

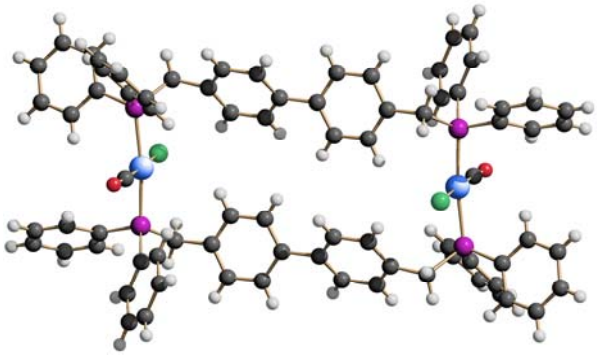

Fig. 8 X-ray structure of $[IrCl(CO)(dppmbp)]_2$

Reaction of $[MCl_2(CO)_2]^-$ with dppmbp leads only to the formation of the cyclic dimer both with rhodium and iridium salts (Fig. 8). Due to the insolubility of the cyclic dimer, its evolution towards polymeric products is prevented.

Cluster compounds

All previous ligands react with $[Ir_4Br(CO)_{11}]^-$ to give $[\{Ir_4(CO)_{11}\}_2(L)]$. The formulation is proposed on the basis of elemental analysis, IR and ^{31}P-NMR spectra.

VT-^{31}P-NMR experiments on the species with L=dppmb show a fluxionality phenomenon. attributed to the presence of three isomers, differing in the P coordination positions with respect to the cluster triangular base (Fig. 9). No fluxionality was not observed in the case of dppbp and dppmbp as ligands.

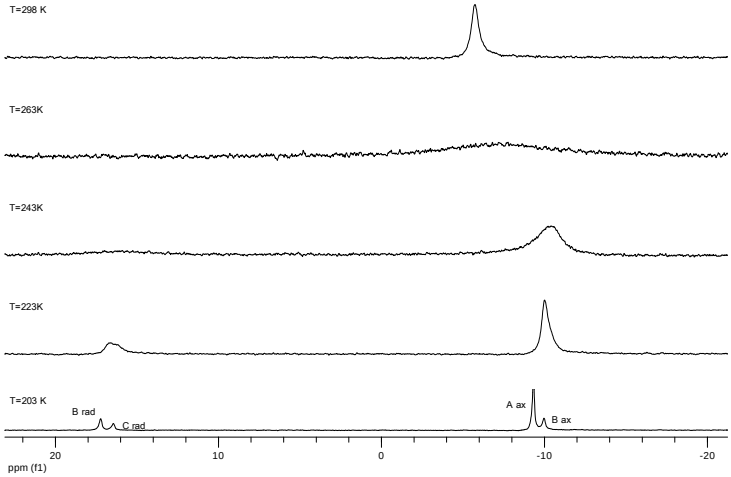

Fig. 9 VT-^{31}P-NMR of $[\{Ir_4(CO)_{11}\}_2(dppmb)]$ in CD_2Cl_2

$[Ir_4(CO)_{12}]$ reacts with dppmb in solvothermal conditions leading to the formation of crystalline $[\{Ir_4(CO)_9\}_4(dppmb)_6 \cdot (SOLV)_5]$ (Fig. 10).

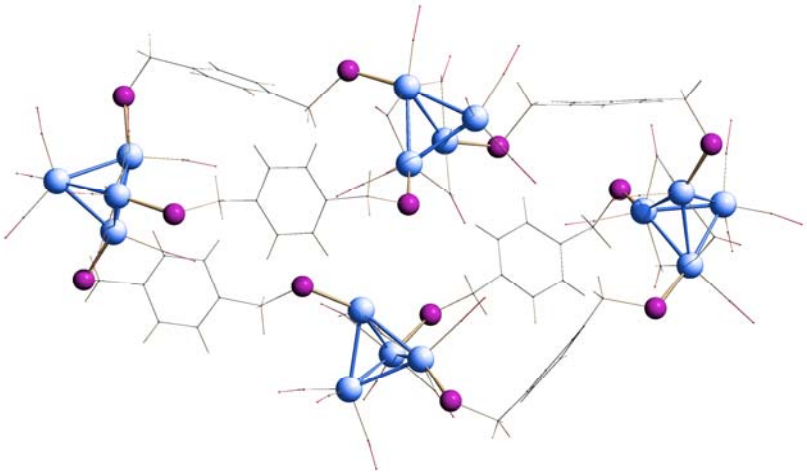

Fig. 10 X-Ray structure of $[\{Ir_4(CO)_9\}_4(dppmb)_6 \cdot (SOLV)_5]$

The whole molecule consists of two $[Ir_4(CO)_9(dppmb)]_2$ cyclic dimers joined by two dppmb ligands. Thus, every Ir_4 tetrahedron has a triply substituted basal face defined by three edge-bridged CO molecules. Each dppmb molecule owning to a cyclic dimer is radial-axial coordinated, whereas the ligands joining the cycles are both radial-radial coordinated. Thus every Ir_4 cage presents two radially and one axially coordinated P atoms.

Flexible diphosphanes

1,4-bis(diphenylphosphano)butane (dppbut)

This flexible and rather short ligand (Fig. 11) was tested with $[Ir_4(CO)_{12}]$ in solvothermal condition.

Fig. 11 dppbut

Orange crystals of $[\{Ir_4(CO)_9(\mu\text{-dppbut})\}_2(dppbut)]$ were obtained (Fig. 12). Two Ir_4 clusters are joined by a radial-radial coordinated dppbut ligand. Each Ir_4 cluster is also chelated by another axial-axial coordinated diphosphane lying under the tetrahedron basal plane.

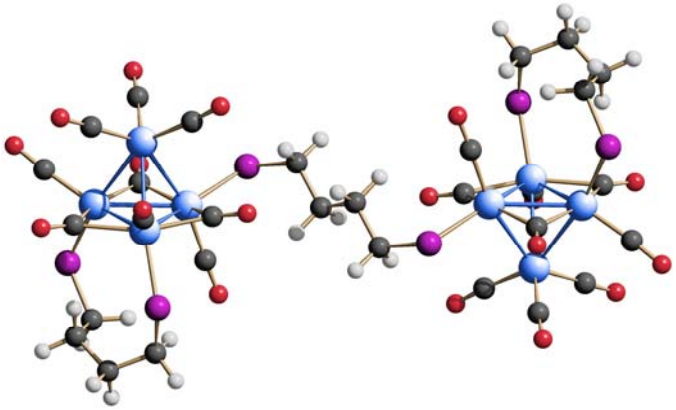

Fig. 12 X-ray structure of $[\{Ir_4(CO)_9(\mu\text{-dppbut})\}_2(dppbut)]$. Phenyls are omitted for clarity

1,6-bis(diphenylphosphano)hexane (Dpphex)

We used dpphex with $[RhCl_2(CO)_2]^-$ to obtain the porous 1D coordination polymer $[RhCl(CO)(dpphex) \cdot 0{,}5THF \cdot 0{,}5CH_2Cl_2]_n$. Starting from this result, we explored dpphex with $[Ir_4Br(CO)_{11}]^-$ and $[Ir_4(CO)_{12}]$. Reaction with the neutral cluster needs for thermal activation and leads to a species insoluble in all common solvents. This insolubility

prevented re-crystallization. ATR-IR shows carbonyl stretching bands typical for triply substituted Ir_4 moieties.

Reactions with $[Ir_4Br(CO_{11}]^-$ in different conditions offered a series of compounds where two tetrahedral carbonyl clusters are bridged by one, two or three dpphex molecules (Fig. 13, 14 and 15).

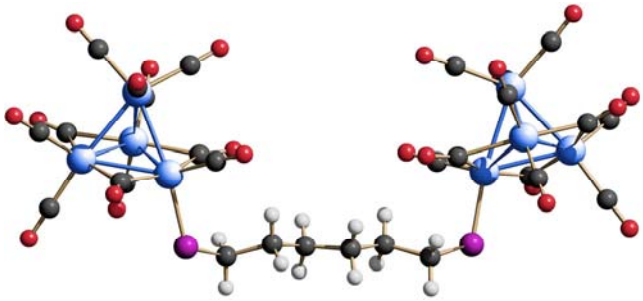

Fig. 13 X-ray structure of $[\{Ir_4(CO)_{11}\}_2(dpphex)]$

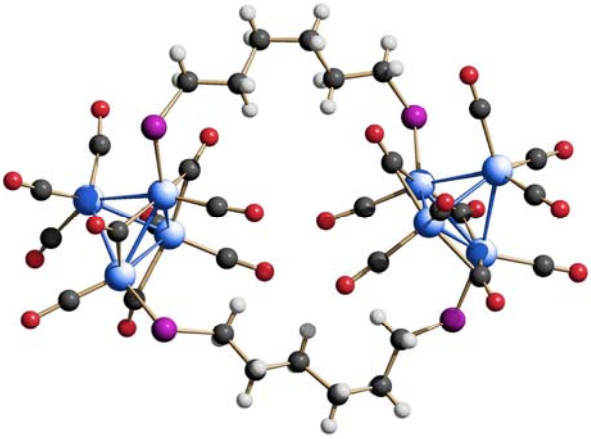

Fig. 14 X-ray structure of $[Ir_4(CO)_{10}(dpphex]_2$

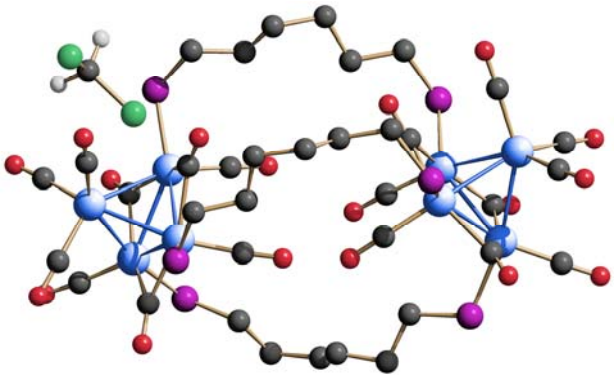

Fig. 15 X-ray structure of $[\{Ir_4(CO)_{11}\}_2(dpphex)_3 \bullet CH_2Cl_2]$

1,8-bis(diphenylphosphano)octane (dppo) and 1,12-bis(diphenylphosphano)dodecane (dppdod)

In order to evaluate the ligand length influence on the polymer formation, we tested the reactivity of dppo (Fig. 16) and dppdod (Fig. 17) towards Rh(I) and Ir(I) halocarbonyl.

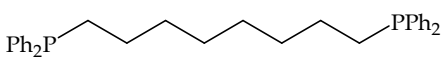

Fig. 17 dppo

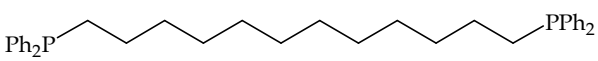

Fig. 16 dppdod

In fact, for a general $PPh_2(CH_2)_nPPh_2$ ligand, polymer has been onbtained only for n=6.

We found that with dppo a 1D coordination polymer is formed (Fig. 18), while with dppdod reaction does not proceed further than the cyclic dimer (Fig. 19). As we think that

this kind of polymer is formed through a ring-opening mechanism, it is possible to state that in the case of dppdod the polymer can not be obtained because the cyclic dimer has a high kinetic stability. An attempt to isolate an oxidized form of the desired product, based on $[RhClI_2(CO)(L)]$ centres, resulted in the crystallization of a octahedral Rh(III) species with the ligand chelating trans positions of the metal centre (Fig. 20). This is quite unusual as, from the entropic point of view, a "long" ligand is expected to hardly chelate.

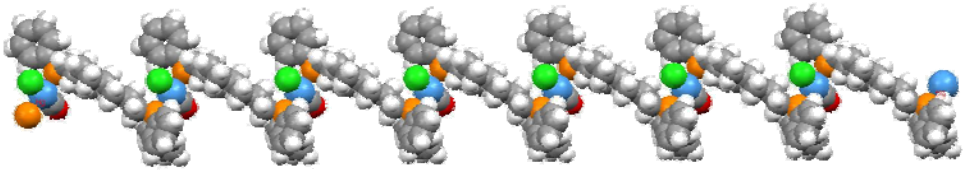

Fig. 18 Fragment of the infinite chain of $[RhCl(CO)(dppo)]_n$ 1D polymer

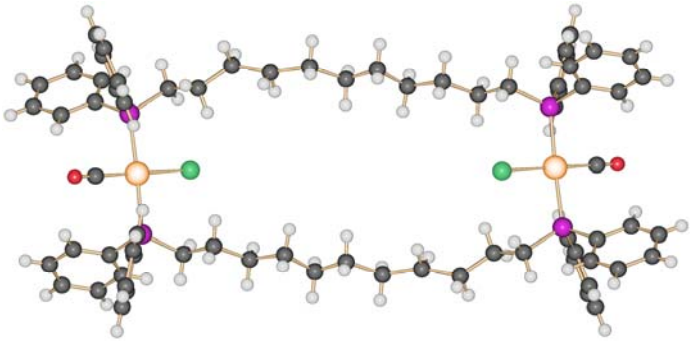

Fig. 19 X-ray structure of $[RhCl(CO)(dppdod)]_2$

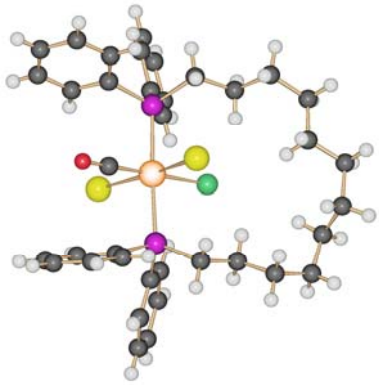

Fig. 20 X-ray structure of $[RhClI_2(CO)(\mu\text{-dppdod})]$

Rigid poliphosphanes

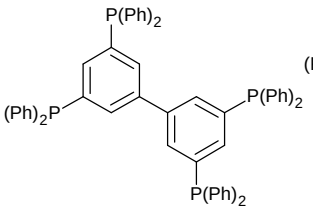

1

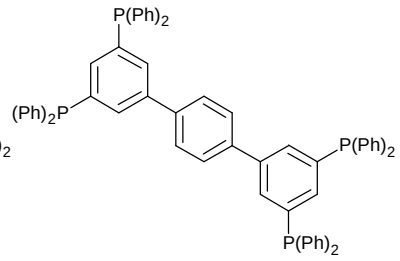

2

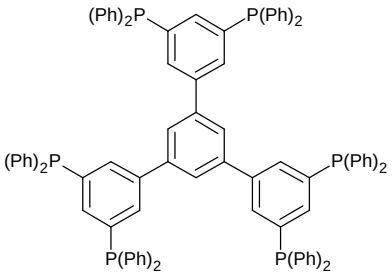

3

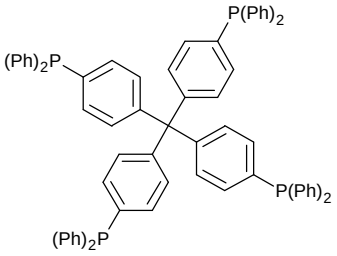

4

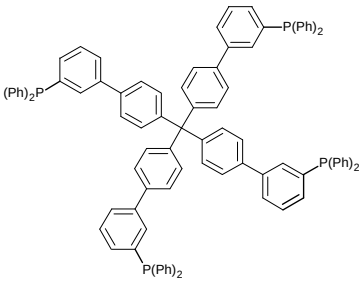

5

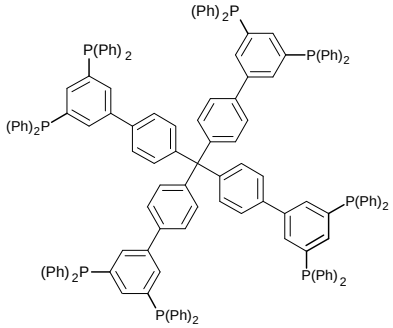

6

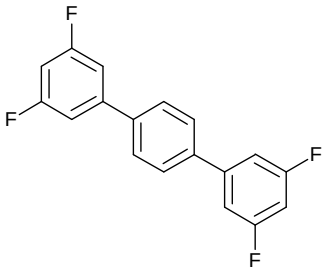

7

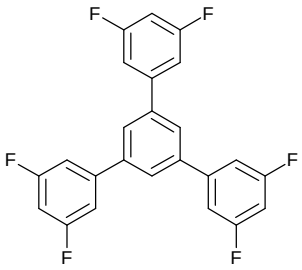

8

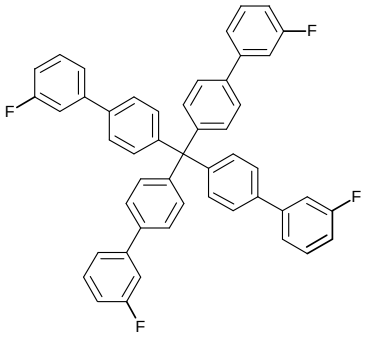

9

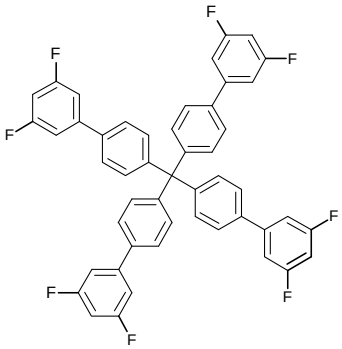

10

Except for **4**, ligands **1-6** have been synthesised from the corresponding fluoro precursors by reaction with $KPPh_2$. Four of these fluoro compounds (**7÷10**) are unprecedented as well, being obtained via Suzuky coupling reaction of the suitable boronic acids with bromo-3,5-difluorobenzene or with bromo-3-fluorobenzene in the case of **9**.
All these new phosphane ligands exhibit fluorescence.

Monometallic compounds

$[MCl_2(CO)_2]^-$ (M= Rh, Ir)

Ligands 1-6 have been used in reaction with $[MCl_2(CO)_2]^-$ (M= Rh, Ir) in a suitable molar ratio: M:L = 2:1 for 1, 2, 4 (L^4) and 5, 3:1 for 3 (L^6) and 4:1 for 6 (L^8). As the halocarbonyls are known to react with phosphanes by coordinating two of them and substituting one CO and one Cl^-, those ratios should saturate the coordination sites with the minimum number of ligands. Air stable, insoluble products have been obtained in all cases and the elemental analyses are in accordance with an hypothetical formula $[\{MCl(CO)\}_{n/2}(L^n)]_m$.
Unfortunately we were unable to grow crystals of these compounds.
Anyway we can suppose their structure on the basis of the ligands and complex geometrical constraints. For example in the case of 3 (Fig. 21), the molecule should contain cyclic dimers as repeating motif.

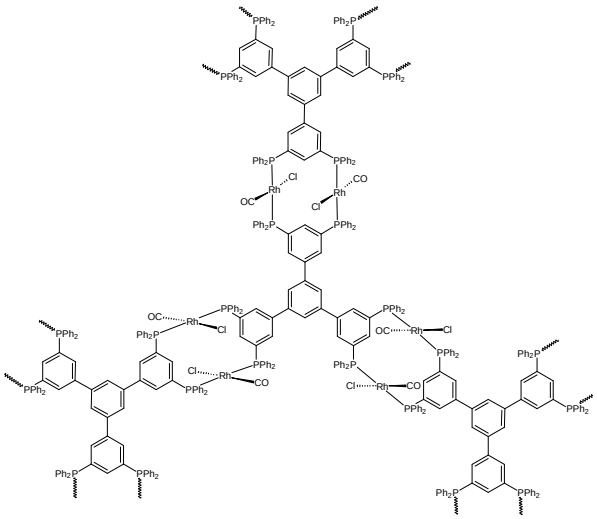

Fig. 21 Proposed structure for $[\{RhCl(CO)\}_3(3)]_n$

AuCl(THT)

Reaction between ligands **1-6** and stoichiometric amount of AuCl(THT) (THT= tetrahydrothiophene) in n:1 Au:L^n molar ratio gave the corresponding gold(I)phosphanes where all the available P atoms bond a AuCl fragment.

The products are air and light stable and, as expected, their fluorescence change with respect to the free ligands.

$NiBr_2$

Ligands **1-6** have been used in reaction with $NiBr_2$ with the same molar ratios used in the case of $[MCl_2(CO)_2]^-$. Also in this case very insoluble products have been obtained and the elemental analyses agree with a formula $[\{NiBr_2\}_{n/2}(L^n)]_m$. In the case of **1** we obtained crystals suitable for X-ray diffraction, Fig. 22.

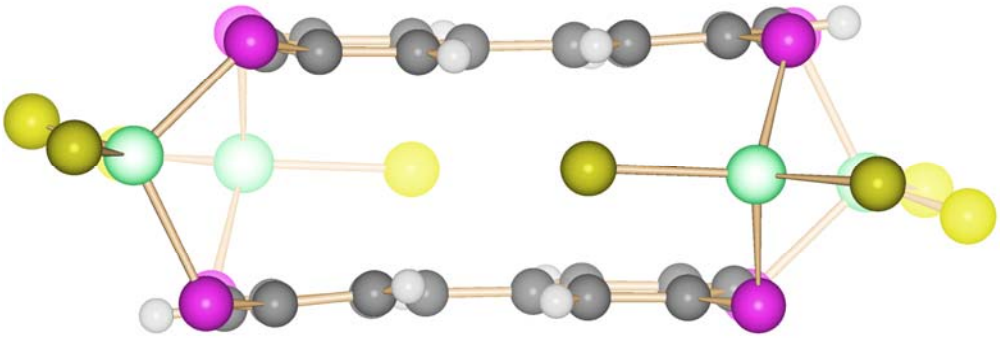

Fig. 22 X-ray structure of $[\{NiBr_2\}_4(1)_2]$. Phenyls are omitted for clarity.

Magnetic measurements revealed that each Ni centre behaves as an isolated spin with a magnetic moment of 3,21 μ_B.

Carbonyl clusters

$[Ir_4Br(CO)_{11}]^-$

We exploited the high easiness and selectivity of bromine substitution in $[Ir_4Br(CO)_{11}]^-$ by phosphane ligands to obtain various compounds where a $[Ir_4(CO)_{11}]$ fragment is bonded to each available phosphorous atom. Elemental analyses, IR and ^{31}P-NMR spectra are in agreement with the expected formula $[\{Ir_4(CO)_{11}\}_n(L^n)]$.

In the case of **1** and **2** we were able to obtain crystals suitable for X-ray analysis and the structures confirm our hypothesis, Fig. 23 and 24.

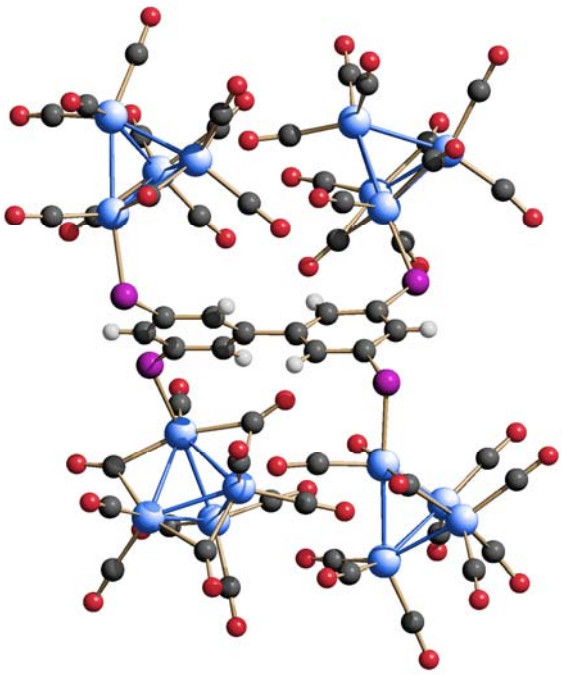

Fig. 23 X-ray structure of [{$Ir_4(CO)_{11}$}$_4$(1)]

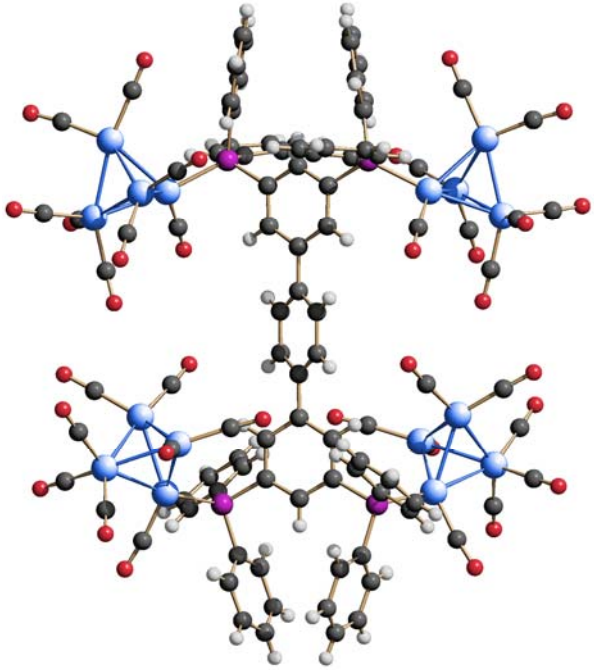

Fig. 24 X-ray structure of [{$Ir_4(CO)_{11}$}$_4$(2)]

$[Pt_{19}(CO)_{22}]^{4-}$ and $[Ir_6(CO)_{15}]^{2-}$

These carbonyl clusters are known to easily react with $[Au(PPh_3)]^+$.

So we used gold(I)phosphanes obtained from **1**, **2** and **3** in order to get aggragates similar to those ones synthesised with $[Ir_4Br(CO)_{11}]^-$.

Although we were unable to get crystals of the products, elemental analyses, IR and ^{31}P-NMR spectra agree with the proposed formula $[\{Ir_6(CO)_{15}\}_n(L^n)]^{n-}$ or $[\{Pt_{19}(CO)_{22}\}_n(L^n)]^{3n-}$.

We are currently investigating redox behaviour of these compounds through cyclovoltammetry.

Chapter 1 – Introduction

Generalities on phosphanes as ligands

Phosphanes are very versatile ligands as their steric and electronic properties can be systematically varied by changing R substituents. P atom has a lone pair that can form a coordination bond with a metal. Thanks to the softer character with respect to N and O donor ligans, phosphanes prefer to react with soft ions. They are also π acid, as more as R electron-withdrawing increases. For example $P(CH_3)_3$ is weakly π acid, the acidity increases for aryl and alkoxy groups and PF_3 is as great π acid as CO. Electron density coming from the metal is localized in P—R σ* orbitals (Fig. 25).[1]

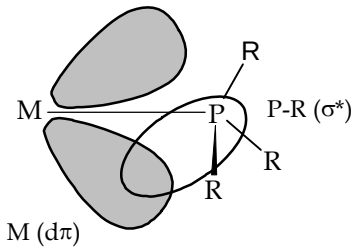

Fig. 25 Molecular orbitals diagram for M-PR_3 system. The more electronegative are the atoms bonded to P, the more low in energy become s* orbital and so more available for metal back donation.

An increase of R group electronegativity means that the orbital that it uses to bond to P becomes lower in energy and more stable. This implies that the σ* orbital of the P−R bond becomes more stable too. At the same time, the phosphorus contribution to σ* increases, and so the size of the σ* lobe that points toward the metal increases. Both of these factors make the empty σ* more accessible for back donation. The final order of increasing π-acid character is

$$PMe_3 \approx P(NR_2)_3 < PAr_3 < P(OMe)_3 < P(OAr)_3 < PCl_3 < CO \approx PF_3$$

Occupation of the P−R σ* by back bonding from the metal also implies that the P−R bonds should lengthen slightly on binding. In practice, this is masked by a simultaneous shortening of the P−R bond due to donation of the P lone pair to the metal, and the consequent decrease in P(lone pair)–R(bonding pair) repulsions. To eliminate this

complication, Orpen[1a] has compared the crystal structures of pairs of complexes, such as $[(\eta^3\text{-}C_8H_{13})Fe\{P(OMe)_3\}_3]^{n+}$,where n = 0 or 1. The M−P σ bonds are similar in both cases, but the cationic iron in the oxidized complex is less π basic and so back-donates less to the phosphite; this leads to a longer Fe−P distance (difference: +0.015 ± 0.003 Å), and a shorter P−O distance (−0.021 ± 0.003 Å). Once again, as in the case of CO, the M−L π bond is made at the expense of a bond in the ligand, but this time it is a σ , not a π, bond.

The electronic effect of various PR_3 ligands can be adjusted by changing the R group as quantified by Tolman,[2] who compared the ν_{CO} frequencies of a series of complexes of the type $LNi(CO)_3$, containing different PR_3 ligands. A stronger donor phosphanes increase the electron density on Ni, which passes some of this density along to the COs by back donation. This, in turn, lowers ν_{CO} as shown in Fig. 26.

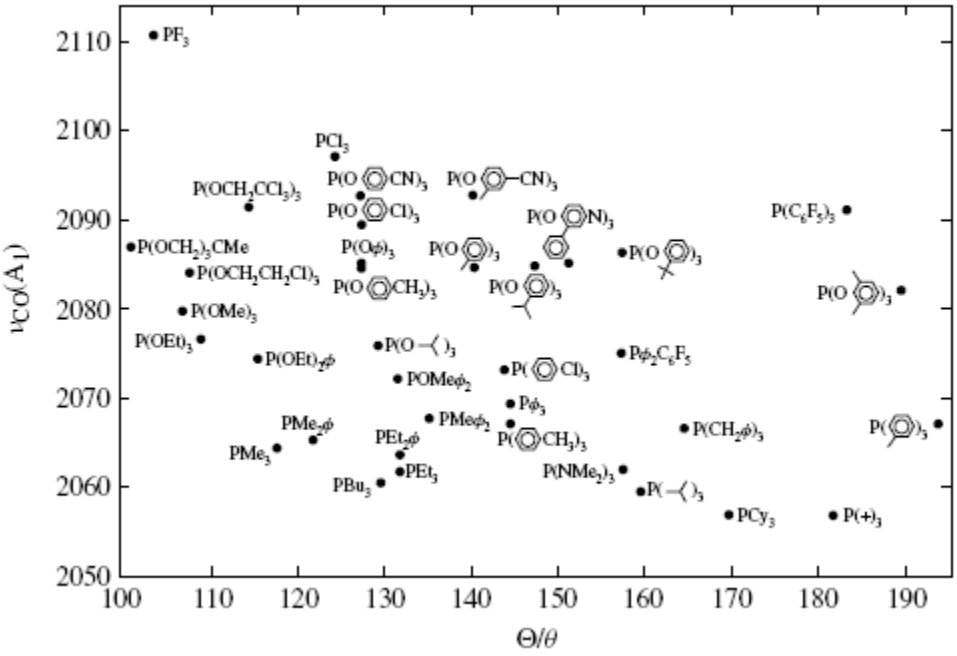

Fig. 26 Electronic and steric effects of phosphanes as plotted by Tolman in ref. 2

Particularly for chelating ligands, the ν(CO) frequencies of $L_2Mo(CO)_4$ can also be used for this purpose because ν_{Mo} correlates with ν_{Ni}.[3]

The second important feature of PR_3 as a ligand is the variable steric size, which can be adjusted by changing R. Carbonyl ligand is so small that as many can bind as are needed to achieve 18e. In contrast, the same is rarely true for phosphanes, where only a certain number of phosphanes can fit around the metal, due to the larger steric hindrance. This

fact can be used as an advantage, because it makes possible to access low-coordinate metals or to coordinate small but weakly binding ligands, which would be excluded by a direct competition with a smaller ligand such as PMe_3 or CO.

Usually the maximum number of phosphanes that can bind to a single metal is two for PCy_3 or $P(i\text{-}Pr)_3$, three or four for PPh_3, four for PMe_2Ph, and five or six for PMe_3.

Examples of stable complexes showing these rules are $Pt(PCy_3)_2$ and $[Rh(PPh_3)_3]^+$: both of them do not reach 18 electrons but they are stabilized by bulky phosphanes. Moreover $W(PMe_3)_6$, a rare case of a hexakis–phosphane complex.

Tolman has also introduced the concept of *cone angle* to quantify the steric effects of phosphanes. This is obtained by taking a space-filling model of the $M(PR_3)$ group, folding back the R substituents as far as they will go, and measuring the angle of the cone that will just contain all of the ligand, when the apex of the cone is at the metal, Fig. 27. Although the procedure may look rather approximate, the angles obtained have been very successful in rationalizing the behavior of a wide variety of complexes. The results of these studies also appear on Fig. 26 with the electronic parameters.

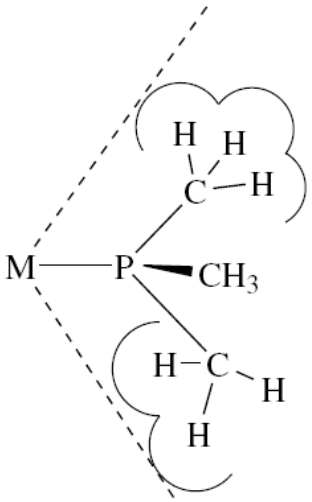

Fig. 27 A view of Tolman angle in the case of PMe_3

Activity and selectivity of homogeneous catalysts, reversibility of binding of a ligand, facility of decomposition and therefore stability of a complex can all be set by varying steric and electronic features of coordinated ligands. So that, desired properties can be optimized. A key feature of the PR_3 series of ligands is that is possible to relatively easily

change electronic effects without changing steric effects [e.g., by moving from PBu_3 to $P(O^iPr)_3$] or change steric effects without changing electronic effects [e.g., by moving from PMe_3 to $P(o\text{-tolyl})_3$]. One outcome of increasing the ligand electron donor strength, for example, might be to perturb an oxidative addition/reductive elimination equilibrium in favor of the oxidative addition product. Likewise, increasing the steric bulk is expected to favor low-coordination-number species. Chemistry of a phosphine-containing complex should be expected to vary with the position of the phosphane in the Tolman map.

Reaction between phosphanes and metal carbonyls

Fred Basolo has deeply investigated the reactions of metal carbonyls with phosphanes,[4] a class of reactions that forms the basis for understanding organometallic substitution reactions in general.

In these studies phosphane is usually refluxed with the carbonyl in an organic solvent, such as ethanol or toluene. It is possible to distinguish two extreme mechanisms for substitution, one dissociative, labeled D, and the other associative, labeled A. Intermediate cases are often labeled I and in particular Ia if closer to A and Id if closer to D. [5]

Dissociative mechanism

The dissociative extreme involves a slow initial loss of a CO to generate a vacant site at the metal, which is trapped by the incoming ligand L. In general, a dissociative step precedes an associative step. Because the rate-determining step is dissociation of CO, the reaction is usually independent of the concentration of L, and the rate is the same for any of a series of different L ligands. This leads to a simple rate equation:

$$r = k_1[\text{complex}]$$

$$L_n\text{-M-CO} \underset{+CO,\ k_{-1}}{\overset{-CO,\ k_1}{\rightleftharpoons}} L_n\text{-M-}\square \xrightarrow{+L',\ k_2} L_n\text{-M-L}'$$

Sometimes back reaction k_{-1} becomes important. This happens when the intermediate, $L_nM-\square$, partitions between the forward and back reactions.[6] Increasing the concentration of L should now have an effect on the rate because k_2 now competes with k_{-1}. The rate equation becomes now:

$$\frac{k_1 k_2[\mathrm{L}][\mathrm{complex}]}{k_{-1}[\mathrm{CO}]+k_2[\mathrm{L}]}$$

Note that it reduces to the previous equation if the concentration of CO, and therefore the rate of the back reaction, is negligible.

The overall rate is usually controlled by the rate at which the leaving ligand dissociates. Ligands that bind less well to the metal dissociate faster than does CO. For example, $Cr(CO)_5L$ shows faster rates of substitution of L in the order:

$$\mathrm{L} = \mathrm{CO} < \mathrm{Ph_3As} < \mathrm{Py}.$$

As expected, this mechanism tends to be follow by 18e carbonyls. In fact, the alternative, initial associative attack of a phosphane would generate a 20e, unfavoured species. Although it is not forbidden to have a 20e transition state (as an example $NiCp_2$ is a stable 20e species), a 16e intermediate provides a lower-energy path in many cases. This is a reminiscent of the S_N1 mechanism of substitution in alkyl halides where halide dissociates. The activation enthalpy required for the reaction is normally close to the M−CO bond strength because this bond is largely broken in going to the transition state.

Depending on the behavior of the d^6 ML_5 intermediate formed after initial dissociation of L, a dissociative substitution of a d^6 ML_6 complex may go with or without retention of the starting stereochemistry. Unlike the d^8 ML_5 situation, where a trigonal bipyramid (TBP) is preferred, a d^6 ML_5 species is unstable in a TBP geometry and tends to undergo a distortion. Fig. 28 shows this is behaviour.[6]

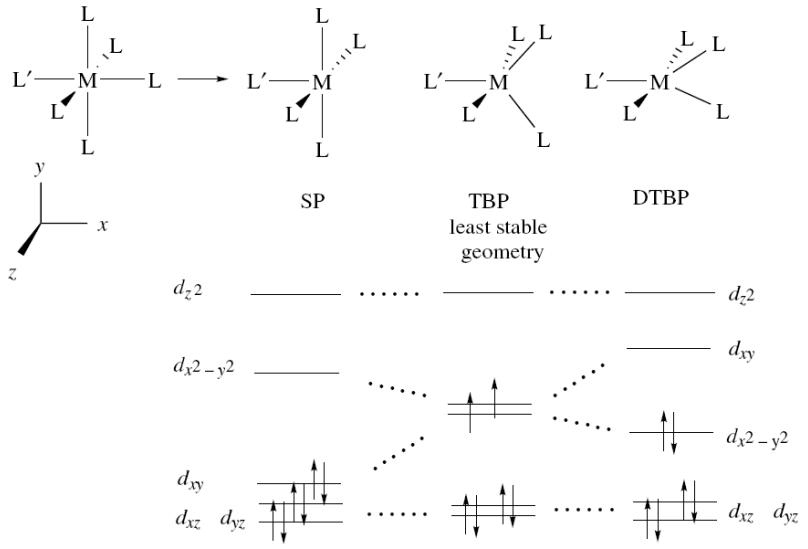

Fig. 28 For a d^6 ML_5 intermediate, a TBP geometry is the least stable, so it turns to squared pyramid if L' has a high trans-effect, or to distorted TBP if L' is a π donor ligand.

The pure TBP geometry requires that two electrons occupy the two highest filled orbitals. Hund's rule predicts a triplet paramagnetic ground state for such a situation. The distortion may take place either to the square pyramidal (SP) geometry or to the distorted TBP (DTBP) geometry. In both cases, the system is stabilized because the two electrons can pair up and occupy the lower-lying orbital. An SP geometry is favored when L' is a high-trans-effect ligand such as H and a DTBP geometry when L' is a π donor such as Cl.

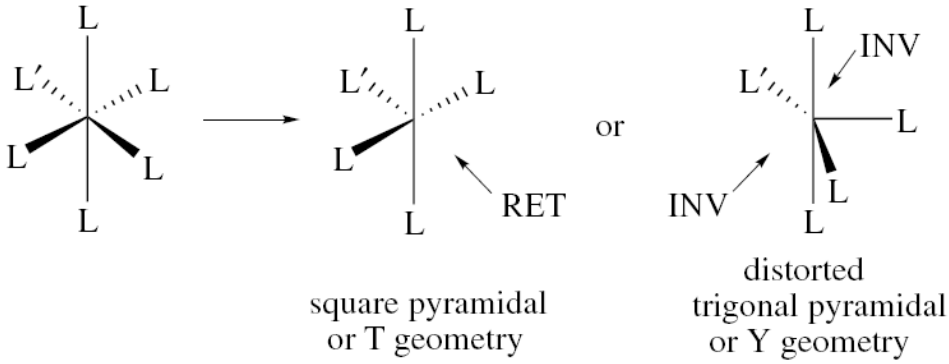

Fig. 29 Possible geometries for a d^6 ML_5 intermediate

If the SP geometry is adopted for the intermediate in Fig. 29, the incoming ligand can simply replace the leaving group and we may have retention of stereochemistry. On the contrary, if the DTBP geometry is favoured, inversion of the stereochemistry is more probable.

It is found that dissociative mechanism tends to be most favoured in TBP d^8, followed by d^{10} tetrahedral and then d^6 octahedral. For example, d^8 $CO_2(CO)_8$ has a half-life for CO dissociation of a few tens of minutes at 0° C, but for d^6 $Mn_2(CO)_{10}$ at room temperature the half-life is about 10 years. This order is consistent with the relative stabilities of the stereochemistries of the starting material and of the intermediates in each case, as predicted by crystal field arguments. Substitution rates tend to follow the order 3rd row < 2nd row > 1st row.[18] For example, at 50° C, the rate constants for CO dissociation in $M(CO)_5$ are Fe 6×10^{-11},Ru 3×10^{-3},and Os $5 \times 10^{-8} s^{-1}$. The rate for Fe is exceptionally slow, perhaps because $Fe(CO)_4$, but not the Ru or Os analog, has a high-spin ground state having low stability, leading to a higher activation energy for CO loss.

Whereas 18e organometallic complexes are usually diamagnetic, non-18e intermediates may have more than one possible spin state, such as singlet (↓↑)and triplet (↑↑) for $M(CO)_4$ (M = Fe, Ru, Os). Different spin states are isomers with different structures and different potential-energy surfaces; the reaction pathways favored by the various possible spin states can in principle differ greatly.

Phosphanes do not replace all the carbonyls in a complex, even in a case where the particular phosphane is sterically small enough to do so. The reaction of $Mo(CO)_6$ with a monodentate alkylphosphane never proceeds further than the *fac*-$Mo(CO)_3L_3$ stage. This is in part because the phosphanes are much more electron donating than the carbonyls they replace. The remaining COs therefore benefit from increased back donation and are more tightly held in consequence. The fac stereochemistry (Fig. 30), in which the PR_3 ligands occupy a face of the octahedron, is preferred electronically to the mer arrangement, in which the ligands occupy a meridian. This is because the COs have a higher trans effect than do the phosphanes, and so substitution continues until there are no COs trans to a CO. The mer arrangement is less sterically encumbered, however, and is seen for bulky L groups.

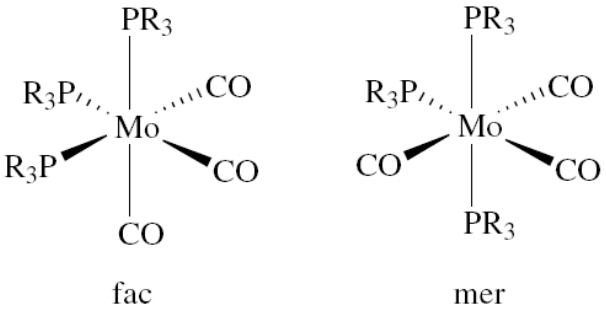

Fig. 30 Fac and mer isomers of $Mo(PR_3)_3(CO)_3$

Dissociation of a ligand is accelerated for bulky ligands. The degree of dissociation can be predicted from the appropriate cone angles, and the bulky phosphate $P(O\text{-}o\text{-}tolyl)_3$ gives one of the very best catalysts. Triphenylphosphane is very useful in a wide variety of catalysts for the same reason.

Dissociation can sometimes be encouraged in various ways. For example, a chloride ligand can often be substituted in the presence of Ag^+ because AgCl is precipitated. Tl^+ is used in cases where Ag^+ oxidizes the complex and is therefore unsatisfactory. Protonation can also be used to remove ligands such as alkyl or hydride groups. Weakly bound solvents are often synthetically useful ligands because they can be readily displaced. As a π donor, THF is a poor ligand for W(0), and $W(CO)_5(THF)$ readily reacts with a wide range of ligands L to give $W(CO)_5L$.

Substitution of halide for alkyl or hydride is often carried out with RMgX or $LiAlH_4$. Cyclopentadienyls may be prepared from CpNa or CpTl, in which case the insoluble TlCl precipitates and helps drive the reaction.

Certain types of ligand are more likely to dissociate than others. The chelate effect means that polydentate ligands will dissociate less easily, for example. Carbon-donor ligands of the L_n type, such as η^6-C_6H_6 (L_3 type) or CO (L), will tend to dissociate more easily than L_nX ligands such as η^5-Cp (L_2X) or Me (X). This is because L_n ligands tend to be stable in the free state, but L_nX ligands would have to dissociate as radicals or ions, which is usually less favourable. Among non-carbon-donor ligands, the anions or cations can be very stable in solution (e.g., H^+ or Cl^-) and may well dissociate in a polar solvent. The electronic

configuration of the metal is also important: substitution-inert d^6 octahedral complexes are much less likely to dissociate a ligand than are substitution-labile d^8 TBP metals.

Associative mechanism

The slow step in associative substitution[7] is the attack of the incoming ligand L^- on the complex to form an intermediate that rapidly expels one of the original ligands L. In general, an associative step precedes a dissociative step.

$$L_nM \xrightarrow{+L',\, k_1} L_nM{-}L' \xrightarrow{-L,\ \text{fast}} L_{n-1}M{-}L'$$

The rate of the overall process is now controlled by the rate at which the incoming ligand can attack the metal in the slow step, and so L^- appears in the rate equation:

$$r = k_1[L'][\text{complex}]$$

This mechanism is often adopted by 16e complexes because the intermediate is now 18e, and so can usually provide a lower energy route than the 14e intermediate that would be formed in a dissociative substitution. The reaction is analogous to the nucleophilic attack of OH^- on a C=O in ester hydrolysis, for example.

The classic examples of the associative mechanism are given by 16e, d^8 square planar species, such as complexes of Pt(II), Pd(II), and Rh(I). The 18e intermediate is a trigonal bipyramid with the incoming ligand in the equatorial plane. By microscopic reversibility, if the entering ligand occupies an equatorial site, the departing ligand must leave from an equatorial site. Loss of an equatorial ligand gives a stable square, planar species, but loss of an axial ligand would leave a much less favorable tetrahedral fragment. This has important consequences for the stereochemistry of the product and provides a simple rationale for the trans effect. In Fig. 31 the incoming ligand is labeled L^i, the departing ligand L^d. We need to postulate that L^t, the ligand of highest trans effect, has the highest tendency to occupy the equatorial sites in the intermediate. This will ensure that the ligand

L^d, trans to L^t, will also be in an equatorial site. Now, either L^t or L^d may be lost to give the final product; since L^t, as a good π-bonding ligand, is likely to be firmly bound, L^d, as the most labile ligand in the equatorial plane, is forced to leave. This is equivalent to saying that L^d is labilized by the trans effect of L^t. Good π-acid ligands are high in the trans effect series because they find the more π-basic equatorial sites in the TBP intermediate more congenial—the metal is a better π donor to these sites. Hydrogen also has a high trans effect, in part because of the lack of lone pairs, such as would be found for Cl^- , for example, minimize the ligand—metal (dπ) repulsions.

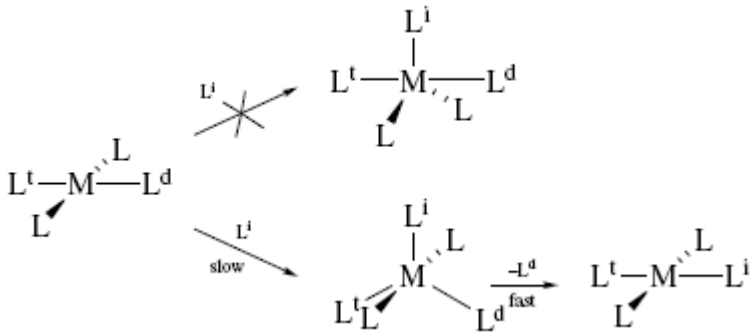

Fig. 31 Associative mechanism for a d^8 square planar complex

It is not uncommon for the solvent, present as it is in such high molarity, to act as L^i and expel L^d to give a solvated 4-coordinate intermediate. This intermediate can then undergo a second associative substitution with the ultimate ligand to give the final product. Substitutions of one halide for another on Pd and Pt(II) can follow this route:[8]

$$L_2MCl_2 \xrightarrow{+solv.\ slow} [L_2M(solv)Cl]^+ \xrightarrow{+Br^-,\ fast} L_2MBrCl$$

It is easy to imagine that, because it is cationic, the solvated intermediate would be much more susceptible to Br^- attack than the starting complex. Because the solvent concentration cannot normally be varied without introducing rate changes due to solvent effects, the [solv] term does not usually appear in the experimental rate equation, which therefore has the form

$$\text{Rate} = k_s[\text{complex}] + k_a[\text{complex}][L']$$

where the first term refers to the solvent-assisted associative route, and the second to the direct associative reaction, which will become relatively more important as less strongly ligating solvents are used. If k_a is zero, this type of reaction can wrongly appear to be dissociative.

Eighteen-electron complexes can also undergo associative substitution. Such complexes usually contain a ligand capable of rearranging and accepting an extra pair of electrons, so that the metal can avoid a 20e configuration. Nitrosyls, with their bent to linear rearrangements, can do this. For example, $Mn(CO)_4(NO)$ shows a second-order rate law and a negative entropy of activation, $S^{\ddagger}$, consistent with this mechanism:

$$(CO)_4Mn(lin\text{-}NO) \xrightarrow{L,\ slow} (CO)_4LMn(bent\text{-}NO) \xrightarrow{-CO,\ fast} (CO)_3LMn(lin\text{-}NO)$$

$$\text{Rate} = k_a[\text{complex}][L]$$

Phosphanes as building block in self-assembly chemistry

Since 60th of the Twentieth Century phosphanes have played a key role in the development of coordination chemistry and homogeneous catalysis.[9] These ligands form a large variety of complexes with late transition metals and they are able to stabilize uncommon species that can be isolated or intermediates during catalyzed reactions. Fig. 32 reports some phosphanes and their complexes examples of historical and topical importance.

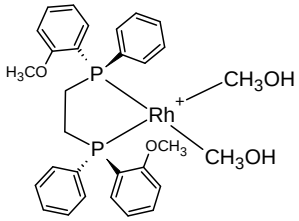

Catalyst for L-DOPA synthesys (Asymmetric catalysis

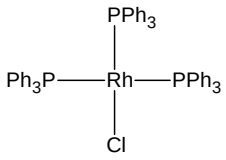

Wilkinson catalyst

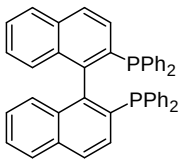

BINAP

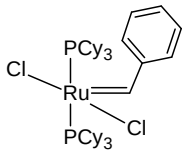

Grubbs catalyst

Fig. 32 Some examples of famous phosphanes and complexes

Although phosphanes show useful features for the coordination chemistry, their potentiality as pure structural building blocks, to join metal centres in larger aggregates, have not been yet well explored.

Fig. 33 indicates that, unlikely rigid building blocks widely used as 4,4'-bipyridine,[10] a rigid structurally similar diphosphane will hardly behave as well as. Even in a non-chelating phosphane, phosphorous atom pyramidal geometry and the free rotation of P-C bond, allow a wide range of lone pairs available orientations. Moreover, from Fig. 33 emerge phosphane's larger hindrance and irregularity.

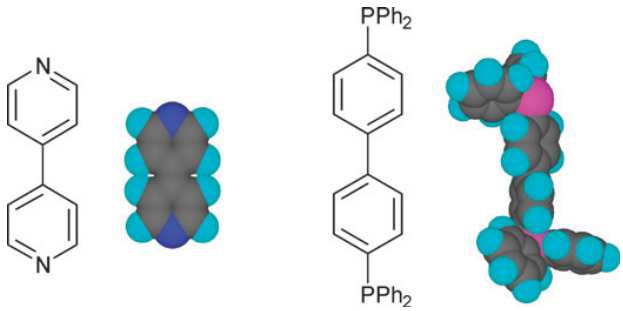

Fig. 33 Comparison between similar N and P ligand: phosphane is more hindred and irregular

Steric effects, which consequences are not easily predictable, are so important in determining the self-assembly. Anyhow, although these complications, phosphanes assemble with metal ions giving coordination compounds structurally "precise" with high selectivity. The low predictability can even become an advantage, in revealing self-assembly unusual aspects which would not be obvious by using an approach only based on molecular design. Another distinctive advantage of phsopshoroud ligands is the relative easiness in monitoring the reaction with ^{31}P NMR spectroscopy. Finally, by using arylic substituent on phosphorous, phosphanes become more stable towards oxidation and they can be use and store in air.

Generalities on CO as ligand

In 1884 Ludwig Mond observed that his nickel valves were being eaten away by CO. So he tried to heat Ni powder in a CO stream and a volatile compound formed. It was $Ni(CO)_4$: the first metal carbonyl was born. Mond used this reaction to refine nickel because the carbonyl can be decomposed to give pure nickel by further heating. Lord Kelvin was so impressed by this result that he stated "Mond has given wings to nickel."

Unlike a simple alkyl, CO is an unsaturated ligand, by virtue of the C−O multiple bond. Such ligands are soft because they are capable of accepting metal d_π electrons by back bonding; that is, these ligands are π acceptors. This contrasts to hard ligands, which are σ donors, and often π donors too (e.g., H_2O, alkoxides). CO can act as a spectator or an actor ligand.

It has to look first at the frontier orbitals of M and L because these usually dominate the M−L bonding. The electronic structure of free CO is shown in Fig. 34. At the beginning, both the C and the O are *sp* hybridized. The singly occupied *sp* and p_z orbitals on each atom form a σ and a ıı bond, respectively.

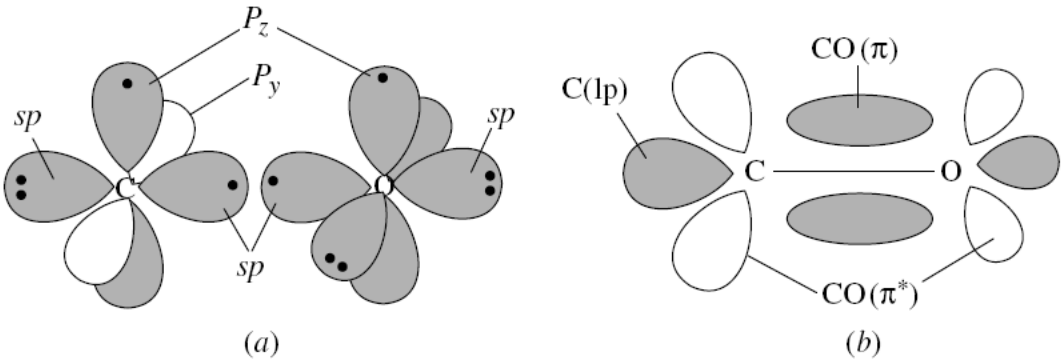

Fig. 34 Electronic structure of CO. Shading are occupied orbitals

This leaves the carbon π orbital empty, and the oxygen py orbital doubly occupied, and so the second π bond is formed only after we have formed a dative bond by transfer of the lone pair of O(π) electrons into the empty C(π) orbital. This transfer leads to a C^-−O^+ polarization of the molecule, which is almost exactly canceled out by a partial C^+−O^- polarization of all three bonding orbitals because of the higher electronegativity of oxygen.

The free CO molecule therefore has a net dipole moment very close to zero. In Fig. 35 the reason for the polarization of the πz orbital is shown in MO terms.

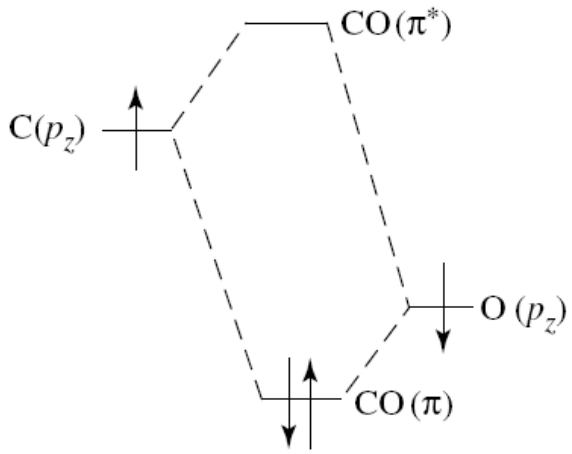

Fig. 35 π bond of CO

An orbital is always polarized so as to favor the AO that is closest in energy and so the C−O π MO has more O than C character. The valence bond picture of CO and one form of the MCO system are shown in Fig. 36.

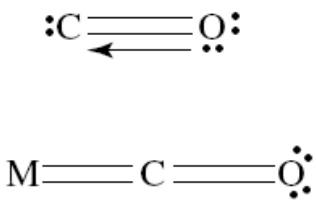

Fig. 36 Valence bond of CO and MCO fragment

It is not surprising that the metal binds to C, not O, because the ligand HOMO is the C, not the O lone pair; this is because O is more electronegative and so its orbitals have lower energy. In addition, the CO(π^*) LUMO is polarized toward C, and so M−CO π overlap will also be optimal at C not O. Fig. 37 shows how the CO HOMO, the carbon lone pair, donates electrons to the metal LUMO, the empty M(dσ) orbital, and metal HOMO, the filled M(dπ) orbital, back donates to the CO LUMO.

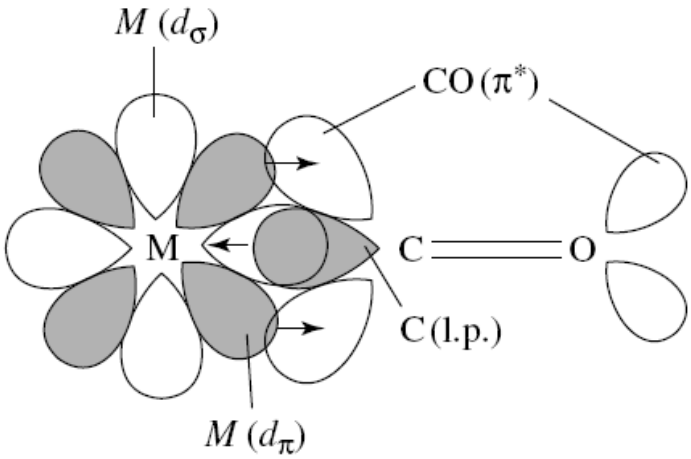

Fig. 37 Molecular orbitals of MCO fragment

While the former removes electron density from C, the latter increases electron density at both C and O because CO(π*) has both C and O character. The result is that C becomes more positive on coordination, and O becomes more negative. This translates into a polarization of the CO on binding.

This metal-induced polarization chemically activates the CO ligand. It makes the carbon more sensitive to nucleophilic and the oxygen more sensitive to electrophilic attack. The polarization will be modulated by the effect of the other ligands on the metal and by the net charge on the complex. In $L_nM(CO)$, the CO carbon becomes particularly ∂^+ in character if the L groups are good π acids or if the complex is cationic [e.g., $Mo(CO)_6$ or $[Mn(CO)_6]^+$], because the CO-to-metal σ -donor electron transfer will be enhanced at the expense of the metal to CO back donation. If the L groups are good donors or the complex is anionic [e.g., $Cp_2W(CO)$ or $[W(CO)_5]^{2-}$], back donation will be encouraged, the CO carbon will lose its pronounced ∂^+ charge, but the CO oxygen will become significantly ∂^-. The range can be represented in valence bond terms as Fig. 38a, the extreme in which CO acts as a pure σ donor, through Fig. 38b and c, the extreme in which both the π_x^* and π_y^* are both fully engaged in back bonding.

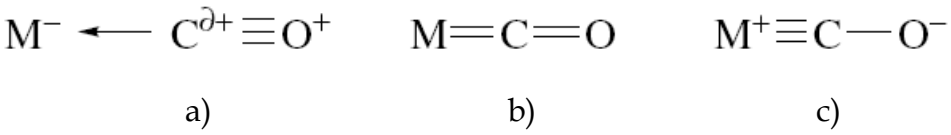

Fig. 38 Extreme representations of M-CO bond

Neither extreme is reached in practice, but each can be considered to contribute differently to the real structure according to the circumstances. In general, polarization effects are of great importance in determining the reactivity of unsaturated ligands. Note that, on the covalent model, the electron count of CO in Fig. 38a-c is 2e. The same e count applies to all true resonance forms.

We can tell where any particular CO lies on the continuum between Fig. 38a and Fig. 38c, by looking at the IR spectrum. Because Fig.38c has a lower C=O bond order than Fig. 38a, the greater the contribution of Fig. 38c to the real structure, the lower the observed C stretching frequency, ν_{CO}; the normal range is 2200-1600 cm^{-1}. The MO picture leads to a similar conclusion. As the metal to CO π* back bonding becomes more important, we populate an orbital that is antibonding with respect to the C=O bond, and so we lengthen and weaken the CO bond. In a metal carbonyl, the M−C π bond is made at the expense of the C=O π bond. The high intensity of the CO stretching bands, also partly a result of polarization on binding, means that IR spectroscopy is extremely useful. From the band position, we can tell how good the metal is as a π base. From the number and pattern of the bands, we can tell the number and stereochemistry of the COs present.

Carbonyls bound to very poor π-donor metals, where Fig. 38a is the predominant contributor to the bonding, have very high ν_{CO} bands as a result of weak back donation. When these appear to high energy of the 2143 cm^{-1} band of free CO, the complexes are sometimes called *nonclassical carbonyls*. Even d^0 species can bind CO, for example, the nonclassical, formally d^0 Zr(IV) carbonyl complexes, $[Cp^*_2Zr(\kappa^2\text{-}S_2)(CO)]$, prepared from reaction of d^2 $[Cp^*_2Zr(CO)_2]$ with S_8 at 80° C, has a ν_{CO} stretching frequency of 2057 cm^{-1}. One of the most extreme weak π-donor examples is $[Ir(CO)_6]^{3+}$ with ν_{CO} bands at 2254,

2276, and 2295 cm^{-1}. The X-ray structure of the related complex $[IrCl(CO)_5]^{2+}$ shows the long M−C [2.02(2) Å] and short C−O [1.08(2) Å] distances expected from structure Fig. 38a**.** The highest oxidation state carbonyl known is *trans*$[OsO_2(CO)_4]^{2+}$ with ν_{CO} = 2253 cm^{-1}.[11] Carbonyls with exceptionally low ν_{CO} frequencies are found for negative oxidation states (e.g., $[Ti(CO)_6]^{2-}$ ν_{CO} = 1747 cm^{-1}) or where a single CO is accompanied by non-π-acceptor ligands (e.g., $[ReCl(CO)(PMe_3)_4]$ ν_{CO} = 1820 cm^{-1}); these show short M−C and long C−O bonds.

Although Fig. 38a-c represent three ideal structures in the bonding range possible for CO, no one structure can be said to perfectly represent the situation for any particular case. There is therefore considerable looseness in the way carbonyls are represented in organometallic structures. Often, M−CO or M−C=O are used. Whatever picture is chosen for graphical representation, the bonding picture discussed above still applies.

Metal carbonyl clusters

According to Cotton, a metal atom cluster is a "finite group of metal atoms which are held together mainly, or at least to a significant extent, by bonds directly between the metal atoms, even though some nonmetal atoms may also be intimately associated with the cluster."[12]

Ir_4 carbonyl clusters

Almost all tetranuclear carbonyl clusters show a tetrahedral geometry, except for few cases in which they adopt a butterfly structure.

As for rhodium analogous, $[Ir_4(CO)_{12}]$ is one of the most easily available species to conduct studies on low valence metallic clusters.

There are reported a number of $[Ir_4(CO)_{12}]$ syntheses that do not need high CO pressure.[13] One of this procedure leading to the desired compound does not use gaseous CO but Ir(III) or Ir(IV) chloride and concentrated formic acid:[14] by heating these reactants in an

autoclave at 120°C for about 12 hours, it is possible to isolate $[Ir_4(CO)_{12}]$ with a quantitative yield. In this reaction formic acid acts both as reductant and CO source, as it is possible to see in this stoichiometry:

$$4IrCl_3 + 18HCOOH \xrightarrow[12h]{100\ °C} Ir_4(CO)_{12} + 12H_2O + 6CO_2 + 12H^+ + 12Cl^-$$

It is possible to distinguish $[Ir_4(CO)_{12}]$ structure from the cobalt and rhodium analogous - $[Co_4(CO)_{12}]$, $[Rh_4(CO)_{12}]$ – ones, in the contrast with them, it shows CO ligands all terminally coordinated and equally distributed among the four metal atoms. Polyhedron having carbonyls carbon (or oxigen) atoms as vertex is a cuboctahedron for $[Ir_4(CO)_{12}]$, and a icosahedron in the case of $[Co_4(CO)_{12}]$ and $[Rh_4(CO)_{12}]$.

Reactions with nucleophiles

$[Ir_4(CO)_{12}]$ with nucleophiles as hydroxides and alcoxides have been deeply studied.
Final products are sensible to presence or absence of water and to excess of CO too. $[Ir_4(CO)_{12}]$ reacts under CO atmosphere with alcoxides in anhydrous alcohol giving carboxilate anion $[Ir_4(CO)_{11}COOR]^-$ in good yield.[15]
Ester group in these complexes undergo to alcolhisys reaction with primary alcohol.[40] If $[Ir_4(CO)_{11}COOR]^-$ is exposed to alkaline conditions in presence of water, anionic hydride[16] $[Ir_4H(CO)_{11})]^-$ is formed. This species could be deprotonated with a base in anhydrous conditions giving $[Ir_4(CO)_{11}]^{2-}$ dianion or it could lose one CO ligand forming $[Ir_4H_2(CO)_{10}]^{2-}$ dihydride dianion, when water is present. [41] Neutral dihydride $Ir_4H_2(CO)_{11}$ is formed when $[Ir_4H(CO)_{11})]^-$ is treated with acetic acid under.[41] The following scheme (Fig. 39) summarizes the described reactions:

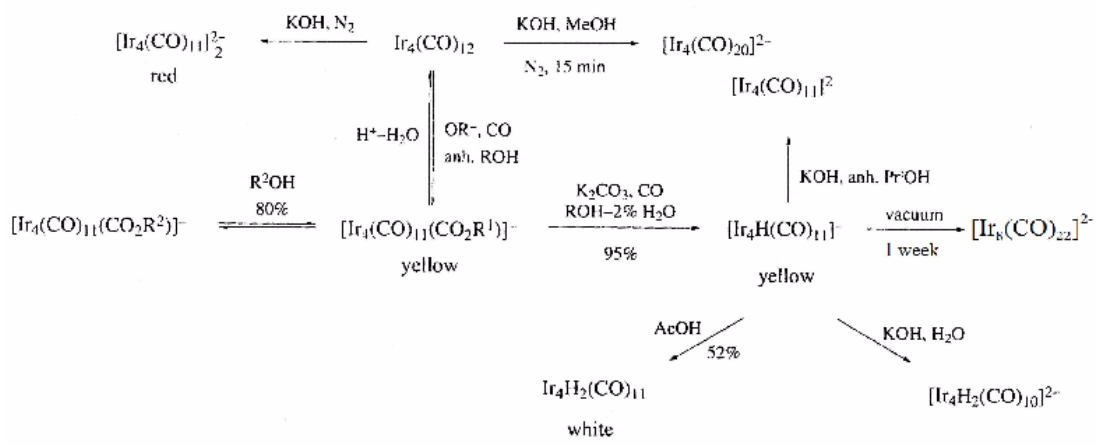

Fig. 39 Reactions of $[Ir_4(CO)_{12}]$ with nucleophiles

In alkaline solution $[Ir_4(CO)_{12}]$ is active for water-gas shift reaction:[17]

$$H_2O + CO \rightleftharpoons H_2 + CO_2$$

Catalytic reaction shows a first order dependance on $[Ir_4(CO)_{12}]$, concentration, but it does not depend on CO pressure in the system. Spectroscopic IR and NMR studies reveal the presence of $[Ir_4H(CO)_{11}]^-$ and $[Ir_4H_2(CO)_{10}]^{2-}$hydrides; it has been then stated that they are both independently active in the reaction.

A proposed mechanism for the catalytic reaction involving two hydride species is shown in Fig. 40:

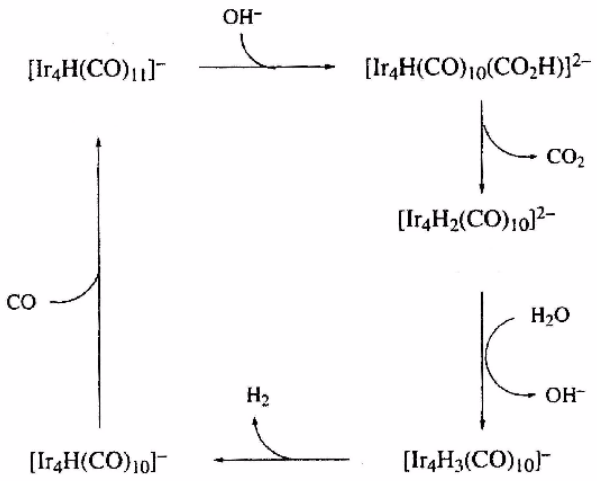

Fig. 40 Hydrido carbonyl clusters catalyzed hydroformilation reactions

It has been postulated that the rate determining step is then transformation of $[Ir_4H(CO)_{11}]^-$ in $[Ir_4H_2(CO)_{10}]^{2-}$ with the contemporary formation of CO_2. The formation of $[Ir_8(CO)_{20}]^{2-}$ from $[Ir_4H(CO)_{11}]^-$ in alkaline conditions has been demonstrated to be a deactivation pathway of the catalyst.

$Ir_4(CO)_{12}$ derivatives

Preparation

It has been developted several methods to prepare substituted neutral derivatives of formula $[Ir_4(CO)_{12-n}L_n]$ (n=1-4).[18] For many ligands as phosphanes, arsines, and isonitryls, high temperature reaction of $Ir_4(CO)_{12}$ with an excess of ligand leads to a mixture of tri- and tetrasubstituted products.[19]

$$Ir_4(CO)_{12} + L\ (\text{excess}) \xrightarrow{70\text{–}110\ ^\circ C} Ir_4(CO)_9L_3 + Ir_4(CO)_8L_4$$

$L = PPh_2Me, PPr_3, P(OPh)_3, AsPhMe_2$

The facile substitution of bromide in $[Ir_4Br(CO)_{11}]^-$ complex is used for the preparation of many monosubstituted complexes and with diphosphanes bridging two cluster units.[20]
Finally, treatment of $[Ir_4(CO)_{12}]$ with N_3^- ion gives monoisocyanide derivative.[21]
As happens with cobalt and rhodium, by using anionic ligands as halogenides, cyanides or tiocyanides, only one CO in the coordination sphere of $[Ir_4(CO)_{12}]$ can be substituted, even by heating with a large excess of ligand.[22]

Structures

The solid state structure of anionic or neutral monosubstituted derivatives can be classified into two categories:

- For good π-acceptor and not too bulky ligands, it has been observed a general structure in which every ligands are terminally coordinated to the metal atoms, like as dodecacarbonyl precursor.
- The second structure motif to be observed is analogous to that one found in Co_4 e Rh_4 clusters: three CO ligands are bridging coordinated on the same number of edges belonging to a tetrahedron face. So, this face is going to be distinguished from the others as the "basal face"; each iridium atoms on the base coordinate two more CO molecules, except for that one carrying the ligand that coordinates only one CO. It is possible to distinguish between the equatorial position (if it is comprehended in the base plane) and the axial position (if it is perpendicular to the base plane). The fourth iridium terminally coordinates the remaining three CO molecules (so-called apical) and the molecule has a C_{3v} idealized simmetry.

Clusters with good σ- and π-donor (Br^-, $[CH_2CO_2Me]^-$) or sterically hindred ligand (PPh_3) show this second structure in the solid state. (Fig. 41, $[Ir_4Br(CO)_{11}]^-$ structure) with the only non CO ligand axially coordinate, perpendicularly to the basal plane Ir_3.

C_{3v} is observed whenever more than one CO is substituted by another ligand.

In $Ir_4(CO)_{10}(PPh_3)_2$, one PPh_3 ligand is axially coordinated under the basal face while the second one occupies a radial position nearly lying in the plane determined by bridging CO ligands.

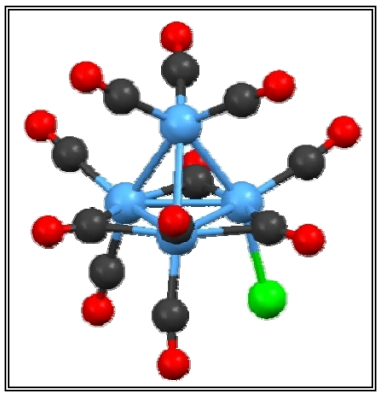

Fig. 41 X-ray structure of $[Ir_4Br(CO)_{11}]^-$

By using the suitable stechiometry and conducting the reaction at low temperature, it is possible to obtain the various mono- and disubstituted products. (Fig. 42)

In most of $[Ir_4(CO)_{10}(diphosphane)]$ compound, the bidentate ligand chelates an Ir-Ir edge on the basal plane. In few cases a second isomer, that is supposed to have the bidenate ligand chelating on the same metal atom, has been observed by NMR.[44]

Bo Keun Park and co-workers have reported the structure of $[Ir_4(CO)_{10}(o\text{-dppbz})]$ (*o*-dppbz= 1,2-bis(diphenylphosphano)benzene) which shows both the phosphorous atoms coordinated by one iridium atom.[23]

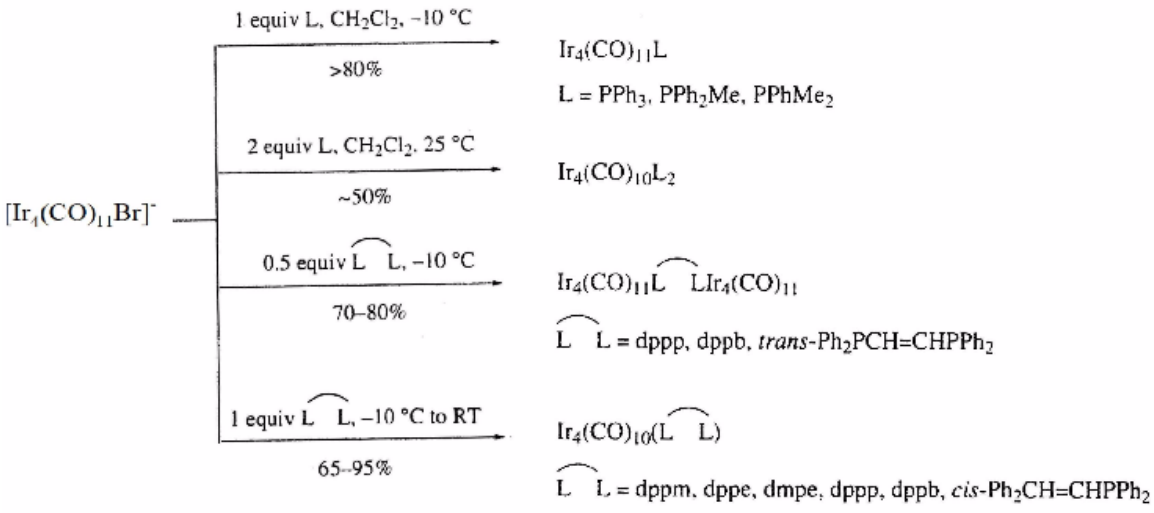

Fig. 42 Strategies to synthesise Ir_4 phosphane derivatives

CO fluxionality

A number of investigations on COs fluxional behavior in $[Ir_4(CO)_{12}]$ monosubstituted derivatives have been conducted. Thanks to the development of two dimensional NMR techniques like DANTE[24] and EXSY and through traditional VT-NMR studies, two basic mechanisms has been individuated to justify position exchange among carbonyl ligands.

The first one is an adaptation of the Cotton[25] "merry–go-round" mechanism. It provides for all the radial COs exchange with those bridging ones through an opening – reclosing concerted movement. The formation of a new C_{3v} structure, with a different CO combination, leads to the position exchange of the other coordinated ligands.

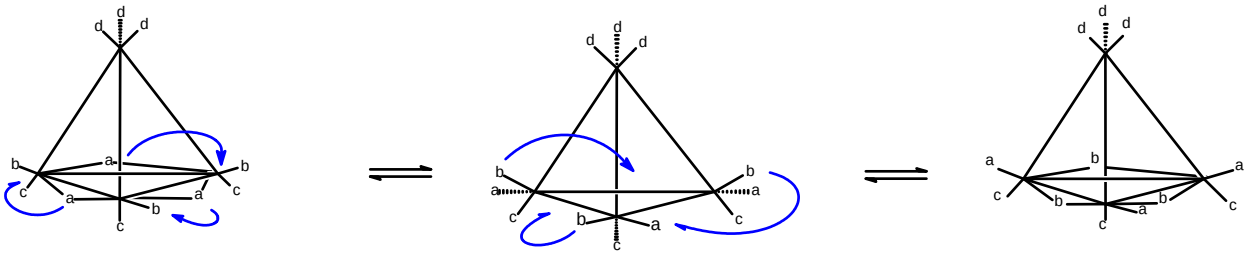

The second mechanism is called "change of basal face" [26] and leads to exchange the face on which three COs are closed with a concerted opening and closing of carbonyls: this process provide for the exchange $CO_{ap} \longleftrightarrow CO_{p}$, $CO_{p} \longleftrightarrow CO_{ap}$ position, actually passing through an intermediate species in which one CO is triply coordinated on a tetrahedron

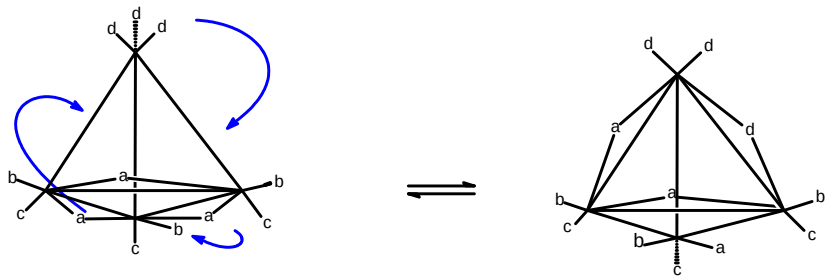

face. It interesting to underline that, through the movement of only three carbonyls, all the others invert their position: $CO_{ap} \longleftrightarrow CO_{ax}$, $CO_{p} \longleftrightarrow CO_{ap}$. On the contrary, two bridging CO groups maintain their position at the of the exchange process too. Consequently, the ligand position changes, from axial to radial and vice-versa.

The specific adopted mechanism varies according to the steric and electronic effects of the involved ligands.

Kinetic studies

In 1974 Karel and Norton[27] have published a comparison among the CO substitution rate by PPh_3, for a series of tetrahedral complexes of formula $[Ir_4(CO)_{12-n}(PPh_3)_n]$ (n = 0-3).

The substantial increment in the substitution rate with the increase of PPh_3 ligands in the starting cluster has been formerly interpreted as an evidence of the exclusive electronic effects. Further investigations on the substitution kinetics of carbonyls in $Ir_4(CO)_{12}$, on its cobalt analogous and on other clusters, have leaded to a detailed comprehension of the factors influencing the rate of these reactions.[28]

As is observed for cobalt, COs substitution rate in $[Ir_4(CO)_{12}]$ derivatives follow a general two terms rate law:

$$Rate = \{k_1+k_2[L]\}[Ir_4(CO)_{12}]$$

- The first term k_1 is related to the dissociative COs substitution and it does not depend upon the ligand concentration. For all the $[Ir_4(CO)_{12-n}L_n]$ (n=1-4) complexes, but not for $[Ir_4(CO)_{12}]$, this term dominates the total substitution rate.
- The second term k_2 describes the associative COs substitution exhibited by these compounds and it is the dominant factor only for the parent cluster.[29]

Although CO substitution rate for the dissociative pathway in $[Ir_4(CO)_{11}L]$ [30] and $[Ir_4(CO)_{10}L_2]$ [31] does not depend upon the ligand concentration, it is anyway related with the σ-donor strength of the ligand or the ligands in the starter complex.[32] This correlation has been interpreted in terms of stabilization of a common transition state involved in this reaction.[53]

Independent studies on $[Ir_4(CO)_9L_3]$ [33] and $[Ir_4(CO)_8L_4]$ [34] have been also revealed that the steric hindrance of a ligand (as measured by the Tolman cone angle)[35,36] influences the dissociative substitution CO rate. So the original notion of cooperation among the metallic centres, increasing the substitution rate of ligands in $[Ir_4(CO)_{12}]$, appears to be mainly composed of predictable steric and electronic properties of the present ligands.

Reaction with alkens

Many alken ligands could formally substitute CO in $[Ir_4(CO)_{12}]$ by using bromide derivative as starting material.

$[Ir_4Br(CO)_{11}]^-$ anion reacts, at low temperature and in presence of $AgBF_4$, with an excess of alken to give the monosubstituted species.[37]

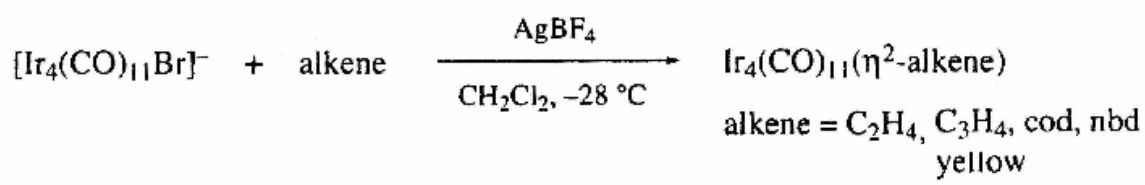

These mild condition alllows to isolate the complex $[Ir_4(CO)_{11}(\eta\text{-}C_2H_4)]$, that is stable only with an ethylene excess or at low temperature. Moreover, by using this method, complexes with diene ligands like 1,4-cyclooctadiene (COD) and norbornadiene (NBD), coordinating only one double bond, can be isolated.

By heating at more than 30°C, COD and NBD coordinating clusters give disubstituted complexes and an equivalent of $[Ir_4(CO)_{12}]$.

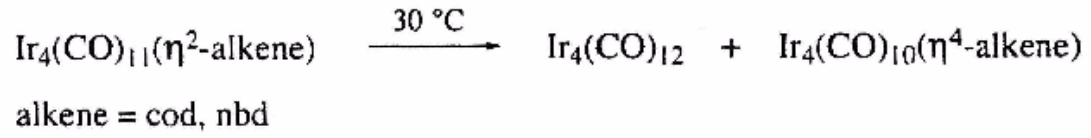

Exposure of alkenic monodentate derivatives to CO turns into the instant formation of the parent cluster.

Spectroscopic properties are in agreement with a C_{3v} structure with three bridging COs. η^4-diene ligands (COD,NBD) chelates on only one metal atom.[38] The COs fluxional behaviour found in COD coordinating clusters is considered to be a "merry-go-round" process.[39]

When $Ir_4(CO)_{11}L$ (L = PMe_2Ph, PMe_2Ph, PPh_3, $AsPh_3$) monophosphane or monoarsane derivatives are treated with an excess of diene (COD, NBD, COT= 1,3,5 cyclooctatriene), in the presence of (Me_3NO), substitution of two or four COs occurs, to give $[Ir_4(CO)_9L(\eta^4\text{-diene})]$ and $[Ir_4(CO)_7L(\eta^4\text{-diene})_2]$ complexes .[40]

Assembly of metal carbonyl clusters

Synthesis of high nuclearity clusters and molecules containing clusters with high molecular weight and well defined structure and composition is a challenge that is continuing to attract much interest. This is stimulated both by purely academic and practic reason. The peculiar structures of transition metal cluster and their potential behaviour as electronic capacitors suggest their use as versatile building block to synthesise molecular networks, macromolecules and nanomaterials. These materials could find application in nano electronic, non linear optics, sensoristic and so on.[41,42,43,44] The molecule and desired materials architecture is in principle predictable and their properties could be point up by varying the substituents of the clusters. In this context, a key role is played by bridging polifunctionalized ligands, that can connect cluster fragments acting as spacers at the same time, determining the electronic connection (or not connection) within the network.

Bridge-linked cluster have received considerable attention for the last 15 years. Most of the structures contain various functionalized organic molecules[45,46,47,48,49] or phosphanes as linking group among metallic subunites.[50,51,52,53,54,55,56] It should be stressed that the number of complexes where three or more carbonyl clusters are linked by phosphanes are still very limited.[60,64,65,66,57] The relatively slow advances in this field are likely caused by the absence of suitable and easily accessible ligands, that could be used in the design of supramolecular aggregates.

As we will see shortly, with this work we have contributed to make the previous sentence less true. Anyway, functionalized 4,4'-bipyridile and related ligands can be used for the synthesis of different supramolecular organometallic complexes. Use of rigid aromatic N-donor ligands favours in most cases their complexation to positive oxidation state metal centres.[58,59,60] Non labile N-heteroaryl groups containing carbonyl clusters normally show additional metal-ligand interaction as, for example, ortometallic bond C-M[61,62,63,64] and dative bond M-N[65,66,67] or M-P.[68,69, 70,71]

So, functionalization of 4,4'-bipyridile (with the introduction of additional coordinating groups that could strongly bind to metal core) could considerably amplify coordination chemistry of these ligands.

Condensation of metal carbonyl clusters have been obtained in several ways. Some of these methods are the following:

1. Oxidation of anionic MCCs with formation of new direct homometallic M-M bonds (for example oxidation of $[Pt_6(CO)_{12}]^{2-}$ to $[Pt_{12}(CO)_{24}]^{2-}$, $[Pt_{18}(CO)_{36}]^{2-}$ ...).[72]
2. Condensation of anionic MCCs with $[M']^{z+}$ (z=1-3) cations, through the complete elimination of counter ion and, in some cases, carbon monoxide. This process results in the formation of heteronuclear M-M'-M bonds (for example $\{Ag[Rh_6C(CO)_{15}]_2\}^{3-}$,[73] $\{Hg[Os_{10}C(CO)_{24}]_2\}^{2-}$,[74] $[M_2Ru_{12}C_2(CO)_{30}]^{2-}$ (M = Pd, Ag),[75,76] $[Pd_3Os_{18}C_2(CO)_{42}]^{2-}$,[77] and $[Ni_{12}(\mu_6\text{-}In)(\eta_2\text{-}\mu_6\text{-}In_2Br_4OH)(CO)_{22}]^{4-}$).[78]
3. Condensation of anionic MCCs with Groups 11-13 salts like $M'X_n$, and partial or no elimination of X counter ions and formation of M-M'X_{n-1}-M or M-M'$_nX_m$-M metal heteronuclear interactions (for example $[H_2Ru_{12}Cu_6Cl_2(CO)_{34}]^{2-}$,[79] $[H_4Ru_{20}Cu_6Cl_2(CO)_{48}]^{4-}$,[80] and $[Ag_3Ru_{10}C_2(CO)_{28}Cl])^{2-}$).[81]
4. Condensation of anionic MCCs with Group 11-13 $M'X_n$ salts, with limited or no elimination of X counter ions and formation of hereeonuclear M-M' interactions and M'-X→M' bridges (for example $\{Cd_2Cl_3[Ni_6(CO)_{12}]_2\}^{3-}$).[82]

Condensation of anionic, neutral or cationic MCCs with neutral or anionic bridging ligands as diamines, diphosphanes, ditiolates, and formation of M-L-L-M bonds (for example $\{H_2N\text{–}(CH_2)_4\text{–}NH_2)\text{-}[Rh_5(CO)_{14}]_2\}^{2-}$,[83] $\{[Rh_6(CO)_{14}]_2(dpbp)\}$ and $\{[Ru_6C(CO)_{15}(dpbp)_3]Ir_4(CO)_8\}$ (dpbp = 2,2'-bis(diphenylphosphano)-4,4'- bipyridine), Fig. 43).[84]

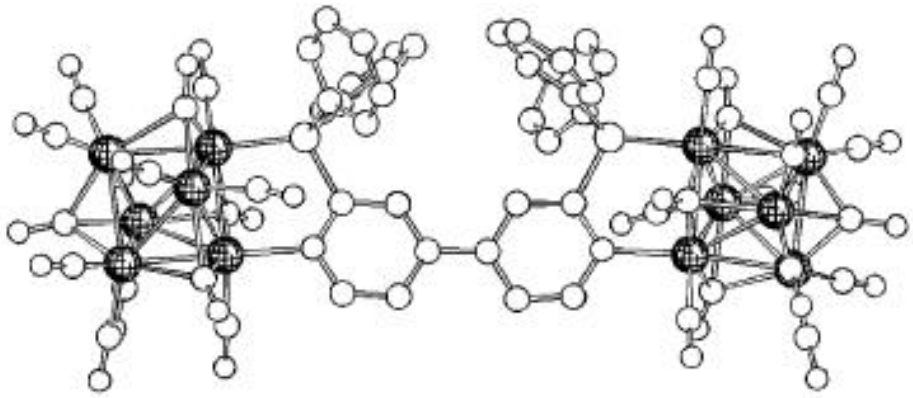

Fig. 43 Structure of $\{[Ru_6C(CO)_{15}(dpbp)_3]Ir_4(CO)_8\}$ (dpbp = 2,2'-bis(diphenylphosphano)-4,4'-bipyridine)

Procedures 1-3 lead to the formation of new bigger MCCs, meaning architectures supported only (or nearly only) by M-M or M'-M metallic bonds.

Procedures 4-5 lead to species where metal carbonyl clusters are not jointed by direct M-M or M'-M bonds but bridging ligands that could be conducting or isolating.

Predicted properties of some of these aggragates, obtained by assembling redox active MCCs, are a better electrons sink behaviour and the mixing valence. As an example, bis fullerene shows a weak electronic communication within the space and exhibits 2 electrons reductions with a ΔEs of about 0.45V, practically equal to those ones of C_{60}.[85,86,87] On the contrary, MCC bridges in $[Rh_6(CO)_5(dppm)_2(CNCH_2Ph)(C_{60})_2]$ enormously improve communication between C_{60} groups. This species exhibits 1 electron reduction and shows a ΔEs between two consecutive redox couples decreased at 0.19-0.29V.[88] So that species, depending on the conducting behavior of the bridge, could allow studies on intramolecular electronic transfer processes between two MCC units and more.

In principle, all the procedures 1-5 can also make possible the self-assembly of a variety of 1D molecular wires. Both Physics and Chemists are fascinating by 1D and pseudo 1D materials. As this subject covers both organic and inorganic – organometallic chemistry, an impressive mole of literature is yet available.

These are some historical example:

- 1D stacked square planar d^8 coordination compounds have short M-M contacts along the axes perpendicular to the planes due to a doping (for example $K_2[Pt(CN)_4]X_{0.3} \cdot 3H_2O$)[89]
- Organic molecules based compounds with almost parallel array (for example [TTF][M(dmit)$_2$] (M= Ni, Pd; dmit = 4,5-dimercapto-1,3-dityole-2-tione)[90], α-[EDTTTF][Ni(dmit)$_2$] (EDT-TTF = ethilendityotetratia fulvalene[91])
- Compounds with mixing valence planes of donor – acceptor organic molecules as [TTF][TCNQ] (TTF = tetratiafulvalene, TCNQ= 7,7',8,8'-tetracianoquinodimetano)[92]) or $[TMTSF]_2[ClO_4]$ (TMTSF = tetrametiltetraselenafulvalene)[93]
- Conducting organic polymers like as polyacetylene, pirrols and tiophens[94,95].

The discovery of their conducting and superconducting behavior, combined with Phisic theories anticipating 1D high T_C superconductors,[96,97] have fed the interest for this research field.

An example of metallic molecular wire coming from coordination chemistry is $\{[Rh(CH_3CN)_4][BF_4]_{1.5}\}_\infty$, obtained through electrocrystallization of $[Rh_2(CH_3CN)_{10}][BF_4]_4$ on Pt electrode[98,99]. Anyway, despite the presence of an infinite sequence of alternated Rh-Rh contacts (2.84 and 2.93 Å) and mixing valence Rh centres, those molecular wires show a semiconducting behavior.[109]

Molecular 1D e 2D aggregates from the self-assembly of metal carbonyl clusters

Metallic molecular wires involving positive oxidation state metal centres and CO are known for a long time. For example many halo-carbonyls like $Ir(CO)X_3$ (X=Cl, Br),[102] $Rh(CO)_2(acac)$[100] or $Pt(CO)_2Cl_2$[101] crystallizes as infinite stacks with a M-M 10-20% longer with respect to the massive metal. Some of them show metallic conductivity under doping.[100] A more recent example regarding M-M ligands supported by ligands is $\{[Rh_2(CF_3COO)_4][Rh_2(CF_3COO)_2(CO)_4]_2\}_\infty$.[102,103]

Metallic molecular wires basing on zero or negative valence metal centres and COs are more rare. The first structurally characterized example has been $[CuCo(CO)_4]_\infty$.[104] This compound derives from the self-assembly of $[Co(CO)_4]^-$ with Cu^+ cations, that ca lead both to a tetrameric cycle, $[Cu_4\{Co(CO)_4\}_4]$, and to an infinite sia 1D compound, $[CuCo(CO)_4]_\infty$ showing a zig-zag chain of metal atoms, as a result of crystallization process.

The structure of a linear polymer of formula $[Ru(CO)_4]_\infty$, obtained starting from $Ru_3(CO)_{12}$,[105] has been determined by X-ray powder diffraction.

Anyhow, in 1D aggregates, the most pertinent example is the superwire $\{[AgRu_6C(CO)_{16}]^-\}_\infty$.[87] It has been obtained with quantitative yield from the reaction between $[Ru_6C(CO)_{16}]^{2-}$ cluster and Ag^+ ions. So it can be considered an example of the condensation procedure 2. The formation of infinite ruthenium cluster – silver atoms chian in crystalline phase is supposed to be favoured by the suitable size of $[N(PPh_3)_2]^+$ or $[PPh_4]^+$ cations with respect to the cluster.

Both the salts are soluble in acetone, probably because polymer breaks into oligomers. The product can be re-obtained by precipitation.[87] This de-assembly and re-assembly is an important characteristic for possible future applications.

An incipient self-assembly of MCC units is shown by the salt $[NMe_4]_2[Ni_6(CO)_{12}]$.[106,107] $[Ni_6(CO)_{12}]^{2-}$ cluster ions are stacked in ordered columns, so there is an infinite sequence of staggered and eclipsed $Ni_3(CO)_6$ groups, alternatively separated by bonding contacts of about 2.5Å and non-bonding contacts of about 4.5Å. A further evidence that not completely shielded clusters like $[M_{3n}(CO)_{6n}]^{2-}$ (M = Ni, Pt) and $[Pt_{26}(CO)_{32}]^{2-}$ can aggregate into oligomers containing up to twenty or thirty units come from mass spectroscopy.[108]

In the research of such materials, Longoni and co-workers has as first suggested the use of redox active and not coordinating dications. Possible examples of these dications are 4,4'-bipyridils (viologens),[109] that show a formal redox potential comparable with MCC and tunable by changing 1,1' substituents. So $[Pt_{3n}(CO)_{6n}]^{2-}$ metathesis with 4,4'-diethyl-bipyridile (EtV^{2+}) leads to the formation of mixed salt $[EtV^{2+}][EtV^{\bullet+}]_2[Pt_{15}(CO)_{30}]_2$, containing both initial EtV^{2+} and monocationic radical $EtV^{\bullet+}$.[110] Two images of the crystal packing of $[EtV^{2+}][Et–V^{\bullet+}]_2[Pt_{15}(CO)_{30}]_2$, are shown in Fig. 44.

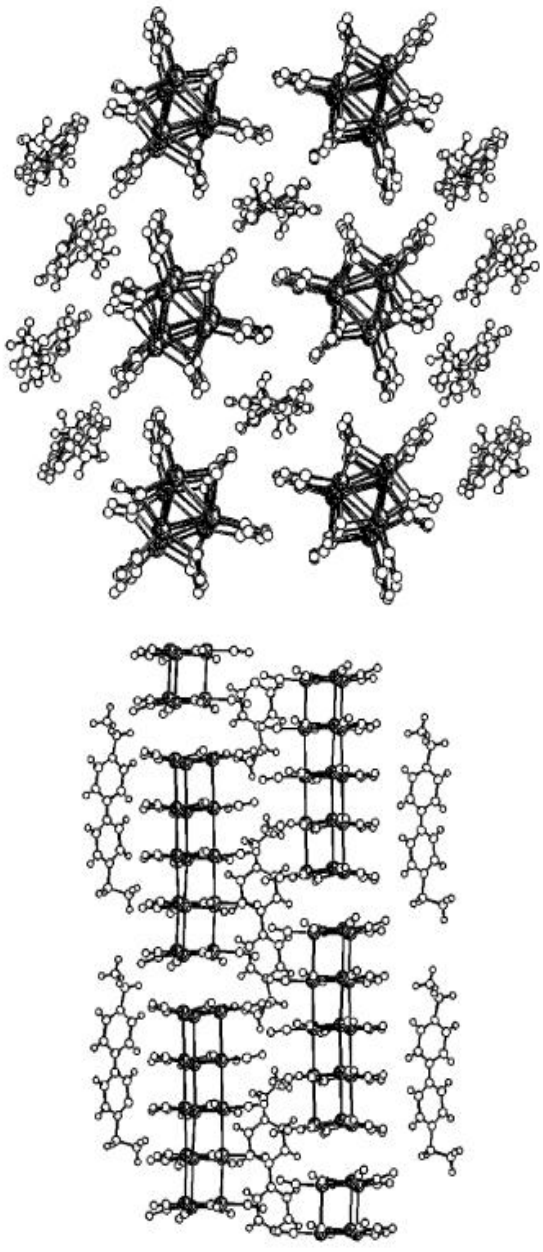

Fig. 44 Two images of crystal packing in $[EtV^{2+}][EtV^{\bullet+}]_2[Pt_{15}(CO)_{30}]_2$

The two different diethylviologen dications are clearly distinguishable for their frequence in the structure and because EtV^{2+} is bent, while $EtV^{\bullet+}$ is nearly planar. The most interesting feature of this structure is that dianionic groups $[Pt_{15}(CO)_{30}]^{2-}$, although maintaining their molecular identity, are assembled into infinite

columns. Inside each molecular ion, distance between $Pt_3(CO)_6$ planes is slightly lower than 3.1Å, whereas intermolecular distance (circa 3.9Å) is shorter than in $[NMe_4]_2[Ni_6(CO)_{12}]$ (4.5 ° Å) and near to the double of usually van der Waals radius usual for platinum(0).

Gold(I) phosphane complexes

Puddephatt and co-workers have deeply studied the self-assembly of gold based rings and polymers, often by using diphosphanes as ligands.[111,112] From a structural point of view, the high tendency to linear coordination and to the formation of weak aurophilic contacts are important in gold(I) complexes.

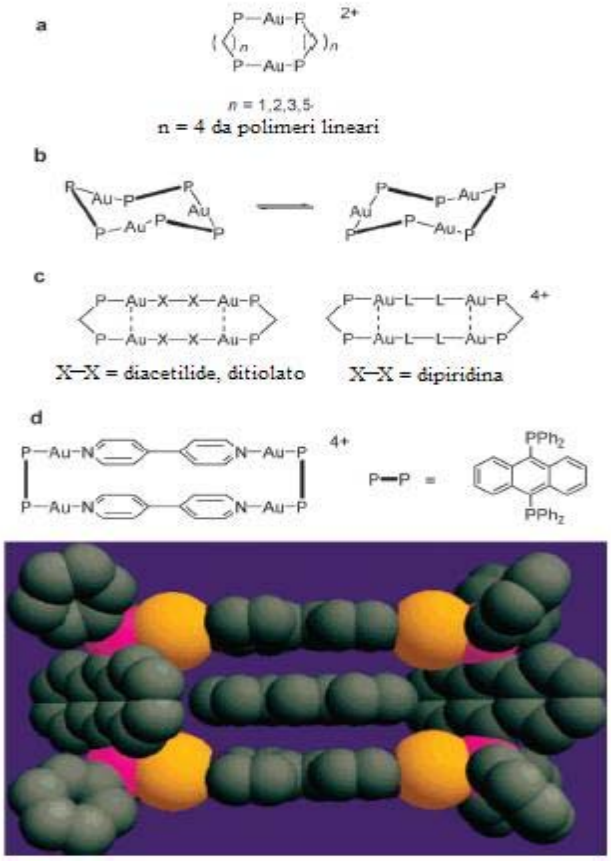

Fig. 45 Gold diphosphanes based rings: (a) homoleptic 2:2 rings based on a flexible diphosphane, (b) rings with mixed diacetylide, dityolide or dipyridile ligands, (c) Au_4 rectangles based on 9,10-bis(diphenylphosphano)antracene, (d)Au_4 based on 9,10-bis(diphenylphosphano) antracene and 4,4'-bipyridile acting as host for organic compounds; crystal structure of d with antracene as host.

For cationic complexes, oxoanionic based anionic bridges do not look to be an important factor, unlike observed with silver(I).

With diphosphanes of formula $Ph_2P(CH_2)_nPPh_2$, with n = 1, 2, 3 o 5, Au(I) forms rings M : L = 2 : 2 similar to those ones obtained with Ag(I) but without the coordination of trifluoroacetate anions[113] (Fig. 45a). For n = 4, open ring structures have been obtained. This is justifiable with the transannular aurophilic contacts, which are allowed in a shorter structure (n = 1 e 2) and for those higher and odd values for which a syn conformation, favouring the ring formation, is natural. More rigid diphosphanes too, like as xantphos and nixantphos, form 2 : 2 rings that maintain their structure in solution and show interesting conformational and dynamic features.[114,115,116] A larger homoleptic ring M : L = 3 : 3, including a ClO_4^- anion in the has been obtained with 9,10-bis(diphenylphosphano)antracene, (Fig 45b). The higher nuclearity is likely due to the divergent orientation of the P doublets. Fluxionality in

solution is attributed to a ring inversion process, reminiscent of the cyclohexane chair-chair inversion.[117]

The combined use of diphosphanes with other bridging ligands like diacetylides, dityolides or dipyridiles leads to a variety of larger rings. (Fig. 45c, d).[10] For short diphosphanes L and linear coligands L', $Au_4L_2L'_2$ tetranuclear rings are usually formed. This can be seen as an extended version of a dinuclear homoleptic ring. Short diphosphanes, in particular dppm, promote aurophilic contacts stabilizing the ring. An increase in the diphosphane length and in the non linearity of coligand favour open polymeric chains.

Yip and co-workers have developted the functionality of these type of rings with mixed ligands by using 9-10bis(diphenylphosphano)antracene combined with 4,4'-bipyridile. A luminescent $Au_4L_2L'_2$ rectangle, that acts as receptor for aromatic guests, has been obtained.[118]

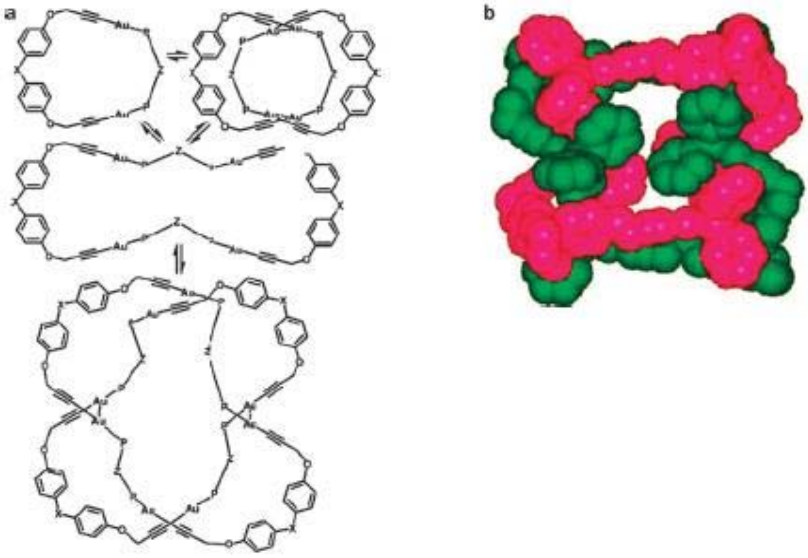

Fig. 46 a) Equilibrium between rings and catenane b) structure of a double fold interpenetrated catenane $\{Au_4\}_2$

Dynamic equilibrium structures have been observed by using, longer diacetylides and diphosphanes as connectors. (Fig. 46).[119-120] These structures do not include only di- and tetragold rings, but $\{Au_2\}_2$ and $\{Au_4\}_2$ catenanes too. A systematic switch from discrete rings to catenanes has been found when the diphosphanes spacers move from two to five CH_2 groups. Aurophilic contacts favour the formation of catenanes, but, as observed, their occurrence are not critical for catenanes formation.

Metal Organic Materials (MOMs)

Metal–organic materials, MOMs, (Fig. 47) are comprised of metal moieties and organic ligands and are exemplified by a diverse group of discrete (e.g. metal–organic polyhedra, spheres or nanoballs, metal–organic polygons) or polymeric structures (e.g. porous coordination polymers, PCPs, metal–organic frameworks, MOFs, or hybrid inorganic–organic materials).

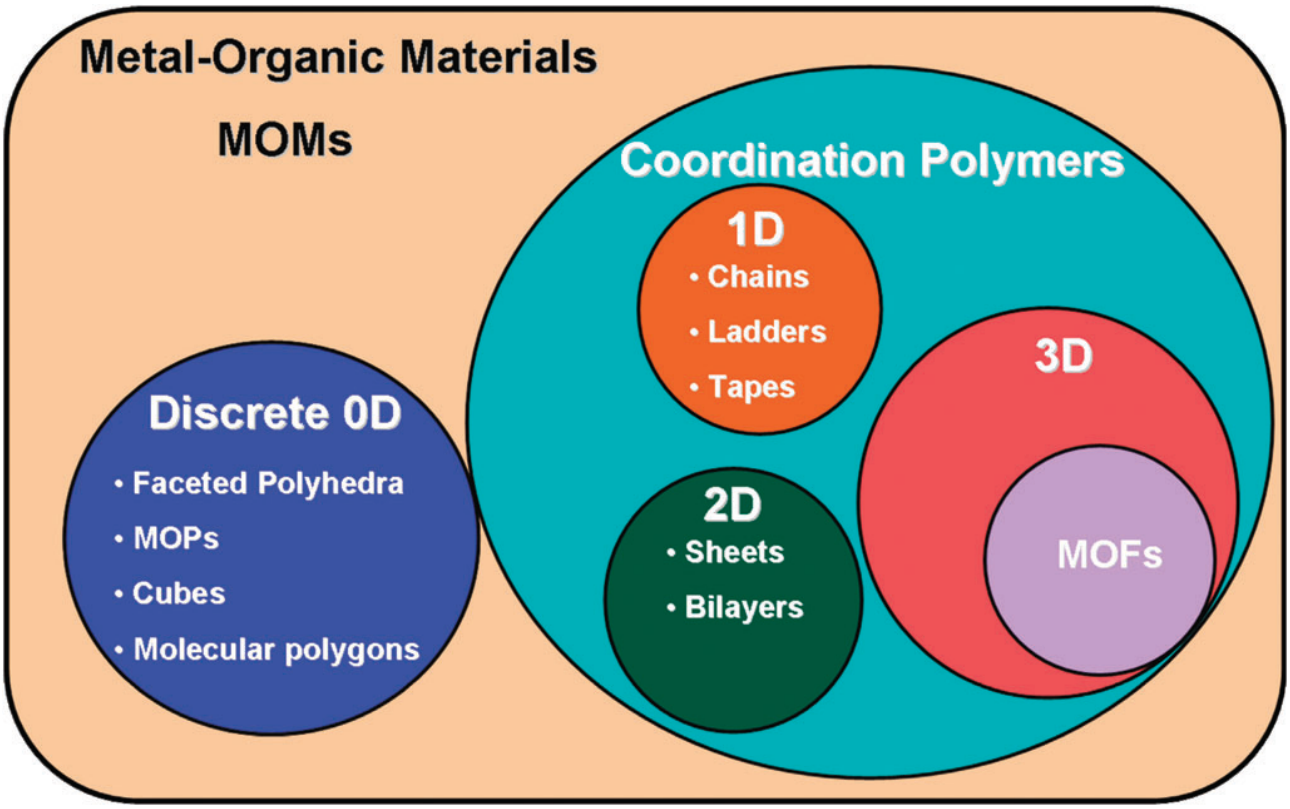

Fig. 47 Metal–organic materials encompass discrete as well as extended structures with periodicity in one, two, or three dimensions. The latter have also been referred to as coordination polymers, metal–organic frameworks, and hybrid inorganic–organic materials.

Although MOMs have existed for several decades[121] it has been necessary to wait until the early 1990's to see a broad increase of attention about them as it became evident that MOMs are typically simple to prepare, aesthetically pleasing and, because of their inherent modularity, prototypal for a diverse range of structures that are amenable to

crystal engineering design strategies.[122] The foundation for today's activity in MOMs resides with the seminal work of A. F. Wells[123] who introduced the simple and practically useful ''node and spacer'' interpretation of inorganic crystal structures. Inorganic crystal structures can thereby be described as networks defined by metal ions (nodes) linked together via bonds (spacer or edge). An important aspect of this approach is that the resultant network topology is reliant on the geometry and coordination environment of the nodes as the spacer is simply a linear connection between adjacent nodes. For example, if a given metal ion preferably adopts a tetrahedral geometry and two equivalents of a linear bifunctional ligand are coordinated to this metal, then a cubic or hexagonal diamondoid network is the likely outcome (Fig. 48). In a similar vein, octahedral metals can sustain square grid or octahedral nets depending upon the metal : ligand stoichiometry (Fig. 48). Such an approach is inherently modular, meaning that any existing network structure is in principle prototypal, i.e. it might serve as a blueprint for the study of the crystallochemistry of many compounds with the same topology but with a different chemical composition.

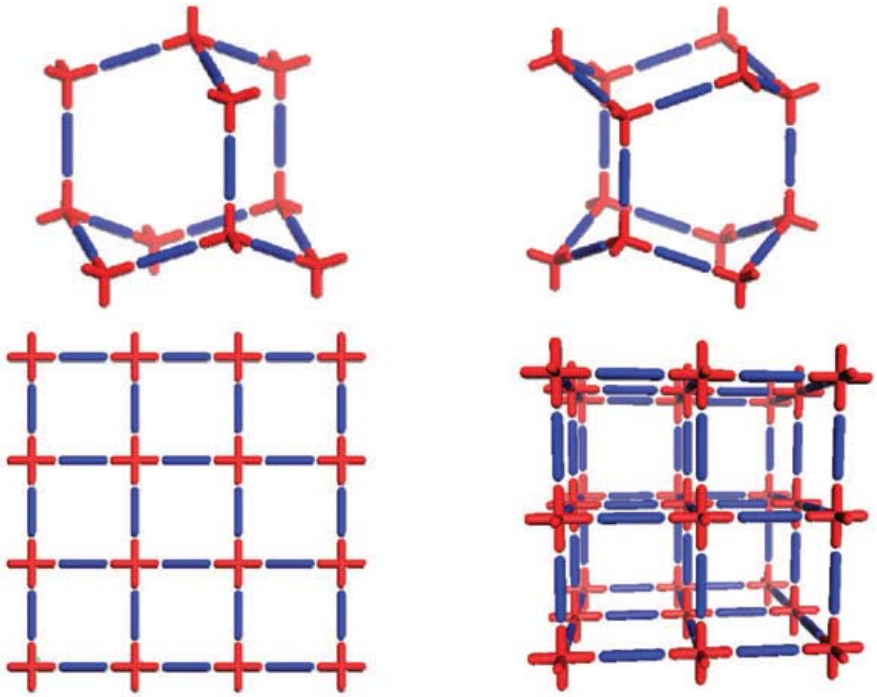

Fig. 48 Schematic illustration of the node (red) and linear spacer (blue) approach for design of networks based upon tetrahedral (above left cubic diamondoid, above right hexagonal diamondoid) or octahedral metal nodes (below left square grid, below right octahedral network).

Design

In the early 1990's, R. Robson[124] and others[125] applied the ''node and spacer'' approach to generate coordination polymers, most typically via coordination of linear ditopic organic molecules such as 4,4'-bipyridyl to transition metal cations. The resulting compounds can exist as 1-periodic, 2-periodic or 3-periodic nets that are at the very least rational based upon the geometry of the node and the node : spacer stoichiometry.

0-Periodic structures based upon 4,4'-bipyridyl and square planar metal moieties were developed concurrently.[126] These ''molecular squares'' and polygons served as precursors to the metal–organic polyhedra that are discussed below. 3-Periodic nets such as the diamondoid net were studied[127] through judicious selection of a tetrahedral metal ion and two equivalents of a spacer ligand, thereby affording a considerable degree of predictability and control over the scale and topology of the resulting compounds. Extension of this crystal engineering[128] paradigm across a wide range of metals and organic ligands created a degree of chemical diversity greater than that typically encountered in purely inorganic or purely organic materials and in turn afforded a plethora of prototypal MOMs. Indeed, given that crystal engineering design principles are equally applicable to crystals that are sustained by hydrogen bonds, there are also examples of diamondoid networks sustained by multiple[129] (i.e. nodes and spacers) or single components[130] (i.e. tectons) that are complementary in terms of their hydrogen bonding.

Properties

As the nascent field of MOMs advanced, the level of complexity increased and researchers began to address the functionality of this emerging class of materials. There were early indications that 3-periodic MOMs could survive guest exchange[131] and, in the late 1990's, the research groups of O. M. Yaghi and S. Kitagawa reported the first examples of MOMs that exhibit permanent porosity.[132] These new materials could aptly be considered as second generation MOMs for which Yaghi and Kitagawa coined the terms metal–organic frameworks (MOFs)[133] and porous coordination polymers (PCPs), respectively.[134] Subsequent MOMs possess the lowest densities and highest surface areas per gram known to mankind.[135] Furthermore, many of these MOMs exhibit air/water stability and thermal stability that is much improved over that of first generation MOMs. However, perhaps even more important than any one particular MOM has been the realization that such compounds are certainly rational if not predictable in terms of their structure and porosity. For example, Yaghi and O'Keeffe developed the versatile and fruitful design strategy of reticular chemistry,[136] a strategy that exploits secondary building units (SBUs)[137] as molecular polygons or polyhedra for the construction of MOFs. A SBU (Fig. 49) is a metal cluster or molecular complex which is rigid in nature, and, when the points of extension are considered, prediction of network topologies that might exist when these molecular building blocks are linked via polytopic organic linkers is relatively facile.

As discussed above, first generation MOMs consist of a single metal ion node that is linked by polytopic organic ligands. In this context the use of SBUs to generate porous MOMs can be viewed as an important evolution in terms of design and utility because the greater relative size of SBUs afford much greater surface area and increased pore and cavity sizes. Additionally, the use of multiple metal ions in a cluster bridged by multiple coordinating ligands tends to enhance the robustness of the MOM. SBUs are also important from a design perspective as they provide a means of controlling the coordination environment of otherwise promiscuous transition metals which might be capable of adopting any of several coordination modes.

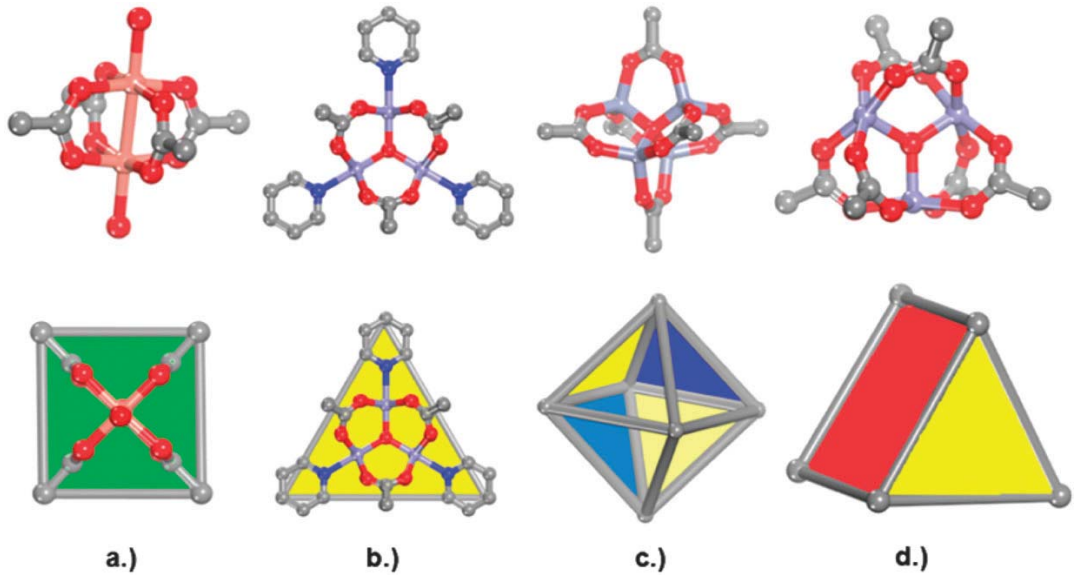

Fig. 49 Examples of prototypal secondary building units (SBUs) commonly used in the construction of periodic MOMs. (a.) Cupric acetate is a dimetal tetracarboxylate square paddlewheel cluster [$M_2(O_2CR)_4L_2$] (M = transition metal, L = axial ligand) which mimics a molecular square. Basic chromium(III) acetate, a m_3-oxo trimetallic hexacarboxylate cluster [$M_3O(O_2CR)_6L_3$] can be used as either a molecular triangle (b.) or a triangular prism (d.). (c.) Basic zinc acetate is a m_4-oxo tetrametallic hexacarboxylate cluster, [$M_4O(O_2CR)_6$], that is prototypal for a molecular octahedron.

Thus, the inclusion of SBUs into the chemists' toolbox facilitated rapid development of MOMs with enhanced properties and structures that can be readily understood and exploited for design purposes.

It should therefore be unsurprising that interest in MOMs exploded as their synthetic accessibility was soon combined with a range of functional properties: unprecedented levels of permanent porosity,[138] catalysis,[139] molecular magnetism,[140] chemical separations and sensing,[141] luminescence,[142] and NLO properties[143] among others.[144] Furthermore, that MOMs are inherently modular and can be generated through self-assembly means that they are amenable to fine-tuning of both structure (e.g. scale, functional groups) and bulk physical properties through either pre-synthetic or post-synthetic modification.[145]

Indeed, today there is a general realization that there already exist a plethora of MOMs that are amenable to control over their structure– property relationships in a manner that was hither to unprecedented in materials chemistry. This degree of control means that the incorporation of more than one useful property into a single material becomes feasible, i.e. multi-functional MOMs.

Chapter 2- Results and discussion

Although phosphanes show useful features for the coordination chemistry, their use as pure structural building blocks, to join metal centres in larger aggregates, has not been yet well explored.

In this work, synthesis and characterization of discrete and polymeric coordination compounds are presented.

As metal centres both monometallic and cluster compounds have been used, whereas as ligands we have used poliphosphanes both commercially available and synthesised in our laboratories.

For simplicity we can classify them in: rigid diphosphanes, flexible diphosphanes and rigid poliphosphanes.

RIGID DIPHOSPHANES

As rigid diphosphanes we mean ligands where the PPh_2 groups are separated by an aromatic or insatured organic spacers that does not allow the chelation on a same metal centre.

Reactions of bis(diphenylphosphano)acetylene (dppa) and trans-1,2-bis(diphenylphosphano)ethane (t-dppethe) with $[Ir_4Br(CO)_{11}]^-$

As rigid diphosphanes bis(diphenylphosphano)acetylene (dppa) and *trans*-1,2-bis(diphenylphosphano)ethane (t-dppethe) have been tested.

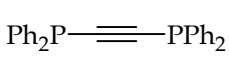

Fig. 50 dppa

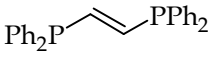

Fig. 51 t-dppethe

By conducting the reaction in dichloromethane at room temperature with a 2:1 cluster/phosphane molar ratio, and monitoring it by IR spectroscopy, an upshift of the carbonyl stretching bands, after adding ligand to the cluster solution, is noted. This is what we would expect moving from anionic to neutral species (Fig. 52). Shape and position of the bands, according to literature data, show the formation of a monosubstituted species. It becomes so clear that bromine is substituted by a phosphorous atom.

After about two hours a neutral compounds precipitates from the solution. It was the fully characterized as $[\{Ir_4(CO)_{11}\}_2(P\text{-}P)]$, the predictable product basying on the set stoichiometry.

$$2[Ir_4Br(CO)_{11}]^- + P\text{-}P \longrightarrow [\{Ir_4(CO)_{11}\}_2(P\text{-}P)] + 2Br^-$$

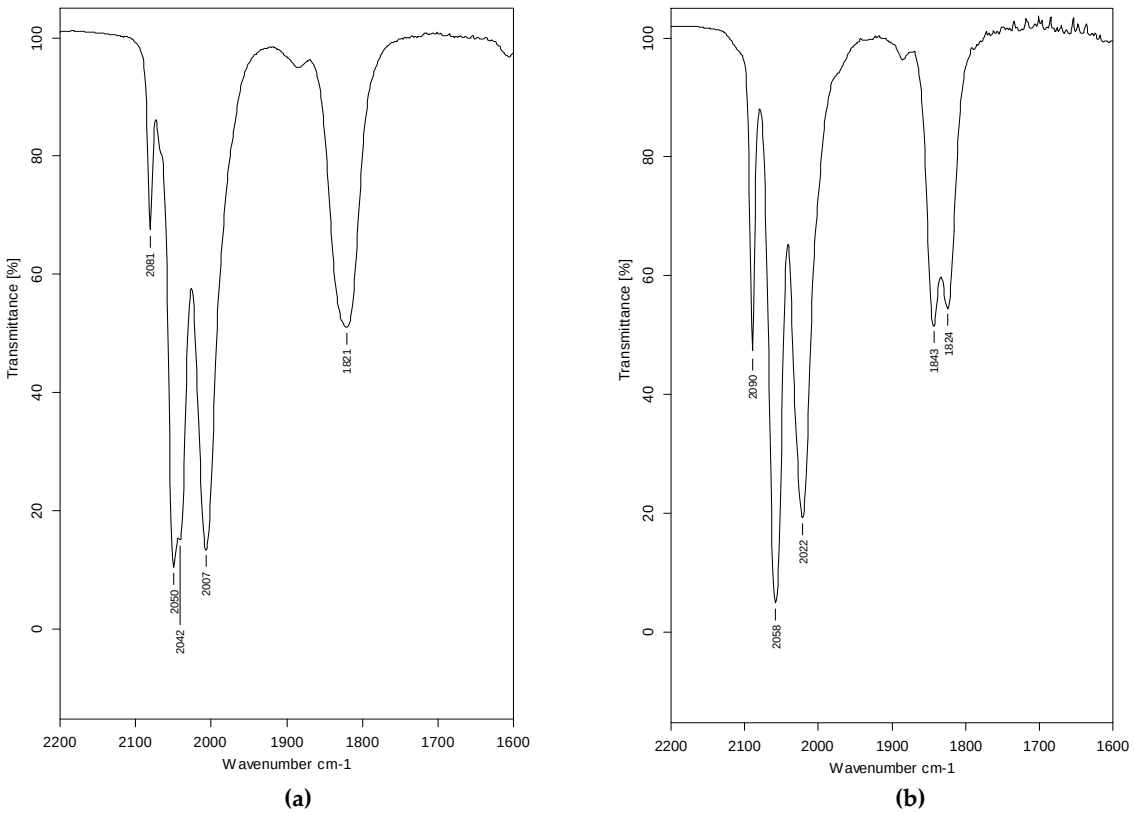

Fig. 52 CH_2Cl_2 IR spectra of a) $[Ir_4Br(CO)_{11}]^-$ b) $[Ir_4(CO)_{11}(P\text{-}P)]$ species

By conducting the reaction in dichloromethane with a 1:1 cluster/phosphane molar ratio, it has not been possible to characterize a 1D coordination polymer or the derivative where the tetrahedral cluster coordinates a pendant diphosphane. As in the previous case,

formation of $[Ir_4(CO)_{11}(P\text{-}P)]$ (ν_{CO}= 2087, 2055, 2018 cm^{-1} terminal COs and 1843, 1819 cm^{-1} bridging COs) is observed. This species has not been yet structurally characterized.

In the case of dppa, after about 2 hours, some $[\{Ir_4(CO)_{11}\}_2(dppa)]$ precipitates, while the IR spectra is roughly unvaried. Then a low downshift of the CO stretching bands is observed, (ν_{CO}= 2075, 2049, 2014 cm^{-1} terminal COs and 1825, 1802 cm^{-1} bridging COs), suggesting a further substitution. These values are in agreement with the formation of a $[Ir_4(CO)_{12}]$ disubstituted species (Fig. 53, after 3 days stirring).

It is possible to assume a three steps mechanism affording to the observed result:

$$3\,[Ir_4(CO)_{11}Br]^- + 3\,dppa \longrightarrow 3\,[Ir_4(CO)_{11}(dppa)] + 3Br^-$$

$$2\,[Ir_4(CO)_{11}(dppa)] \longrightarrow [\{Ir_4(CO)_{11}\}_2(dppa)] + dppa$$

$$dppa + [Ir_4(CO)_{11}(dppa)] \longrightarrow [Ir_4(CO)_{10}(dppa)_2] + CO$$

$$3\,[Ir_4(CO)_{11}Br]^- + 3\,dppa \longrightarrow [\{Ir_4(CO)_{11}\}_2(dppa)] + [Ir_4(CO)_{10}(dppa)_2] + CO + 3Br^-$$

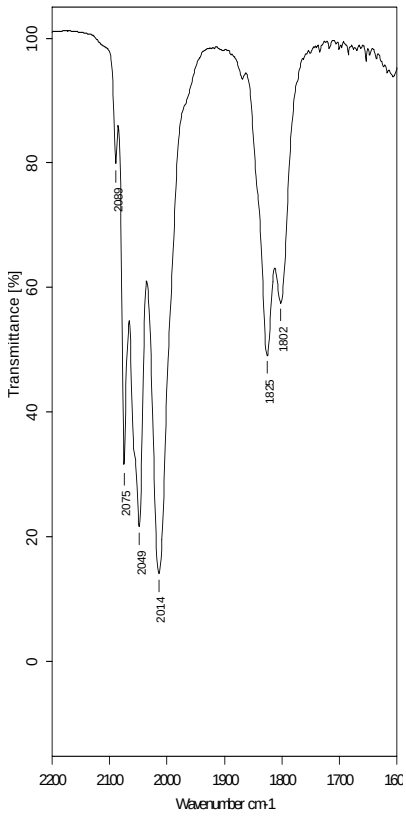

Fig. 53 CH_2Cl_2 IR spectra of $[Ir_4(CO)_{10}(dppa)_2]$

On the contrary, with t-dppethe ligand precipitation of [{$Ir_4(CO)_{11}$}$_2$(*t*-dppethe)] was not observed but anyway in the IR spectrum slowly appears a weak band at 1796 cm^{-1}, which can be attributed to the presence of a small amount of bisubstituted species.

Finally, by conducting the reaction in dichloromethane with a 1:2 cluster/phosphane molar ratio, formation of the monosubstituted derivative [$Ir_4(CO)_{11}$(P-P)] (ν_{CO}= 2087, 2055, 2018 cm^{-1} terminal COs and 1843, 1819 cm^{-1} bridging COs) is first observed. Then COs stretching bands slowly downshift, indicating a second substitution (ν_{CO}= 2065, 2038, 2002 cm^{-1} terminal CO and 1817, 1792 cm^{-1} bridging COs), Fig. 54.

$$[Ir_4(CO)_{11}Br]^- + 2\ P\text{-}P \longrightarrow [Ir_4(CO)_{10}(P\text{-}P)_2] + Br^- + CO$$

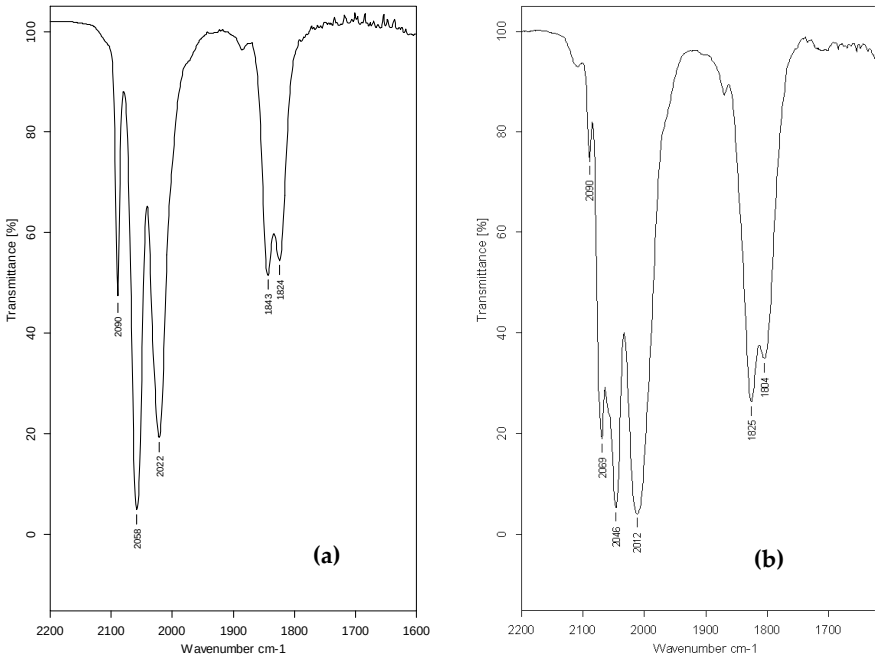

Fig. 54 CH_2Cl_2 IR spectra of a) [$Ir_4(CO)_{11}$(PP)] b) [$Ir_4(CO)_{10}$(PP)$_2$]

Synthesis and characterization of $[\{Ir_4(CO)_{11}\}_2(dppa)]$

During the reaction of $[PPh_4][Ir_4Br(CO)_{11}]$ and dppa in acetonitrile 2:1 molar ratio an almost immediate precipitation of yellow – microcrystalline of $[\{Ir_4(CO)_{11}\}_2(dppa)]$ occurs, that is then insoluble in all the common organic solvents.

$$2[PPh_4][Ir_4Br(CO)_{11}] + dppa \longrightarrow [\{Ir_4(CO)_{11}\}_2(dppa)] + 2[PPh_4]Br$$

Crystals, suitable for X-ray diffraction, have been obtained for slow diffusion of a n-heptane solution of the ligand into a dichloromethane solution of the cluster.

Solid state structure

The molecule consists of two $Ir_4(CO)_{11}$ tetrahedral cages linked by a dppa molecule. The conformation of the two clusters at the P-C≡C-P axis is *trans,* as the molecule lies on a crystallographic inversion centre.
Each cluster moiety terminally coordinates eleven CO molecules, Fig. 55.
In the following table some significant bond lengths are reported.

Bond	Å
Ir-Ir (average)	2,696
C-O (average)	1,136
Ir-P	2,299
C≡C	1,171

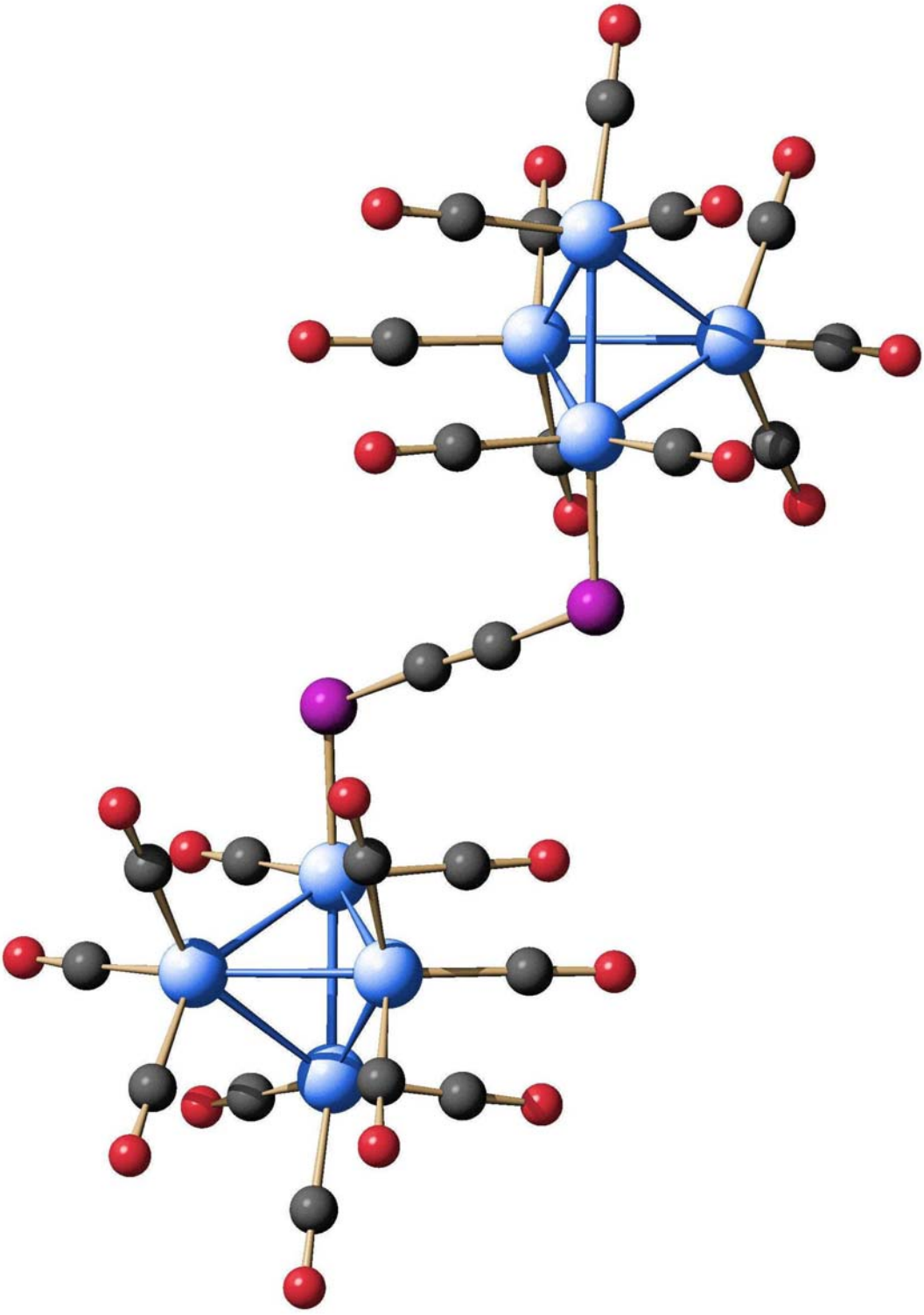

Fig. 55 X-ray structure of [{$Ir_4(CO)_{11}$}$_2$(dppa)]. Phenyls are omitted for clarity

ATR-IR spectra of the new derivative has been registered on a total attenuated reflectance spectrophotometer (Thermonicolet- Avatar 360 FT-IR- with Smart Endurance accesory). The experiment consists in deposing a small amount of sample on a ZnSe crystal, and applying a pression through a mechanic press. This IR spectra, more and more times registered on different crystals for which the elemental cell was checked, have given always the same result (Fig. 56a). In this spectra two bands in the typical region of edge-bridging COs are present. Anyway, XRD analysis determined only the presence of terminal coordinated COs. Actually Nujol IR spectra shows only terminal COs stretching bands 8Fig. 56b).

This phenomenom allows us to suppose that the pressure applied to register the first spectrum causes a structural re-arrangment and some carbonyl ligands would change their coordination mode, from terminal to edge-bridging.

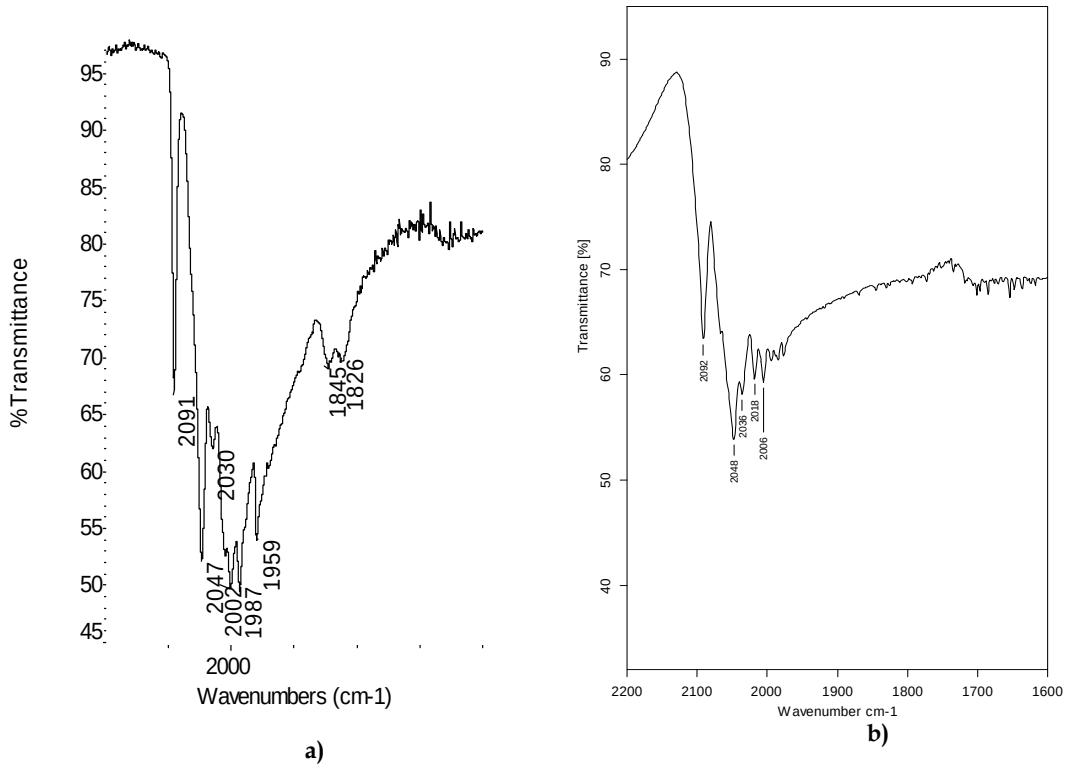

Fig. 56 a) ATR-IR spectrum and b) Nujol-IR of [{$Ir_4(CO)_{11}$}$_2$(dppa)]

Synthesis and characterization of [{$Ir_4(CO)_{11}$}$_2$(*t*-dppethe)]

By reacting [PPh_4][$Ir_4Br(CO)_{11}$] and *t*-dppethe in acetonitrile in 2:1 molar ratio a yellow microcristalline powder of [{$Ir_4(CO)_{11}$}$_2$(*t*-dppethe)] precipitates very quickly (yield 70%). This solid is then insoluble in all common organic solvents.

2[PPh_4][$Ir_4Br(CO)_{11}$] + *t*-dppethe ⟶ [{$Ir_4(CO)_{11}$}$_2$(*t*-dppethe)] + 2[PPh_4]Br

Crystals suitable for X.ray analysis have been obtained by reaction in dichloromethane and cooling the resulting solution at 4°C for some days.
This species has a low solubility in CH_2Cl_2. Anyway, with 38000 scansions, it has been possible to obtain a satisfaying ^{31}P-NMR spectrum, Fig. 57, showing a singlet at -18,8 ppm.

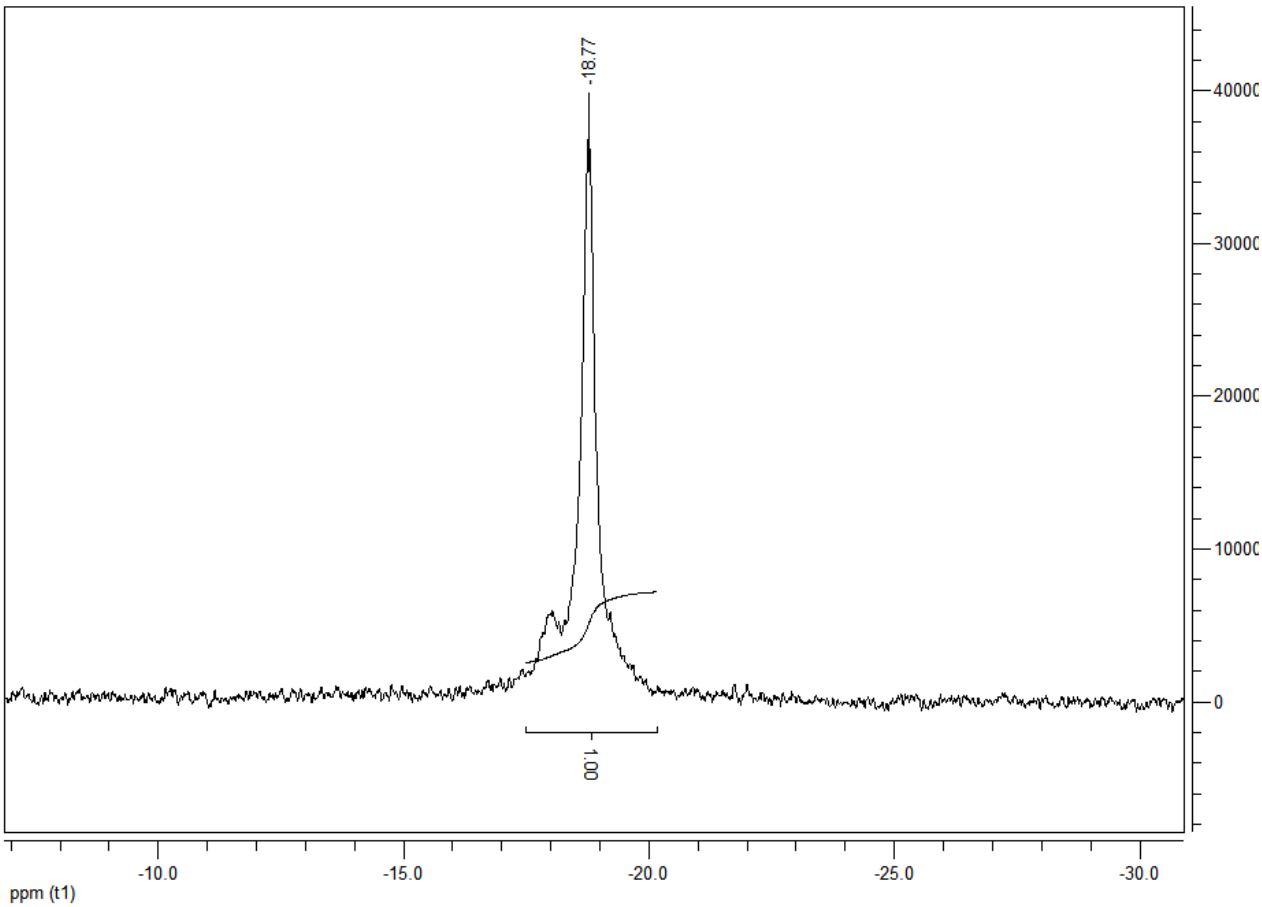

Fig. 57 CD_2Cl_2 ^{31}P-NMR of [{$Ir_4(CO)_{11}$}$_2$(*t*-dppethe)]

Solid state structure

The structure is analogous to that of [{$Ir_4(CO)_{11}$}$_2$(dppa)]: the molecule is constituted by two $Ir_4(CO)_{11}$ tetrahedral cages linked by a diphosphanoethylenic bridge. The conformation of the cages at the axe of the two phosphorous atoms is trans because the molecule lies on a inversion crystallographic centre. Each cluster unit coordinates eleven terminal COs: two for the iridium atom bonding the phosphorous and three for the others (Fig. 58).
In the following table some significant bond lenghts are reported:

Bond	[{$Ir_4(CO)_{11}$}$_2$(dppa)] Å	[{$Ir_4(CO)_{11}$}$_2$(*t*-dppethe)] Å
Ir-Ir (average)	2,696	2,691
C-O (average)	1,136	1,097
Ir-P	2,299	2,336
C≡C	1,171	-
C=C	-	1,319

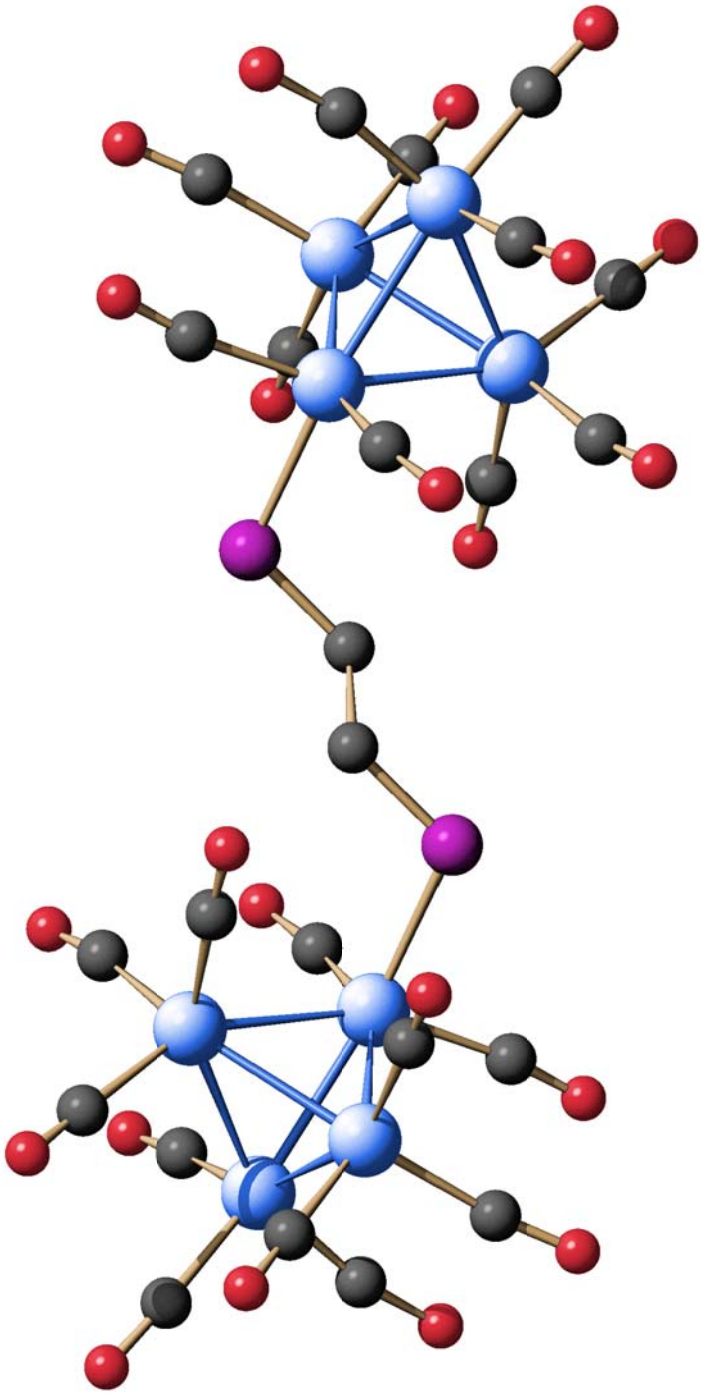

Fig. 58 Solid state structure of [{$Ir_4(CO)11$}$_2$(t-dppethe)]. Phenyls omitted for clarity)

By collecting the IR spectra it has been observed the same phenomenon described for [{$Ir_4(CO)_{11}$}$_2$(dppa)]: in nujol-IR there are not bands for edge-bridging COs (Fig. 59a), which are present in the ATR-IR registered under pressure (Fig. 59b)

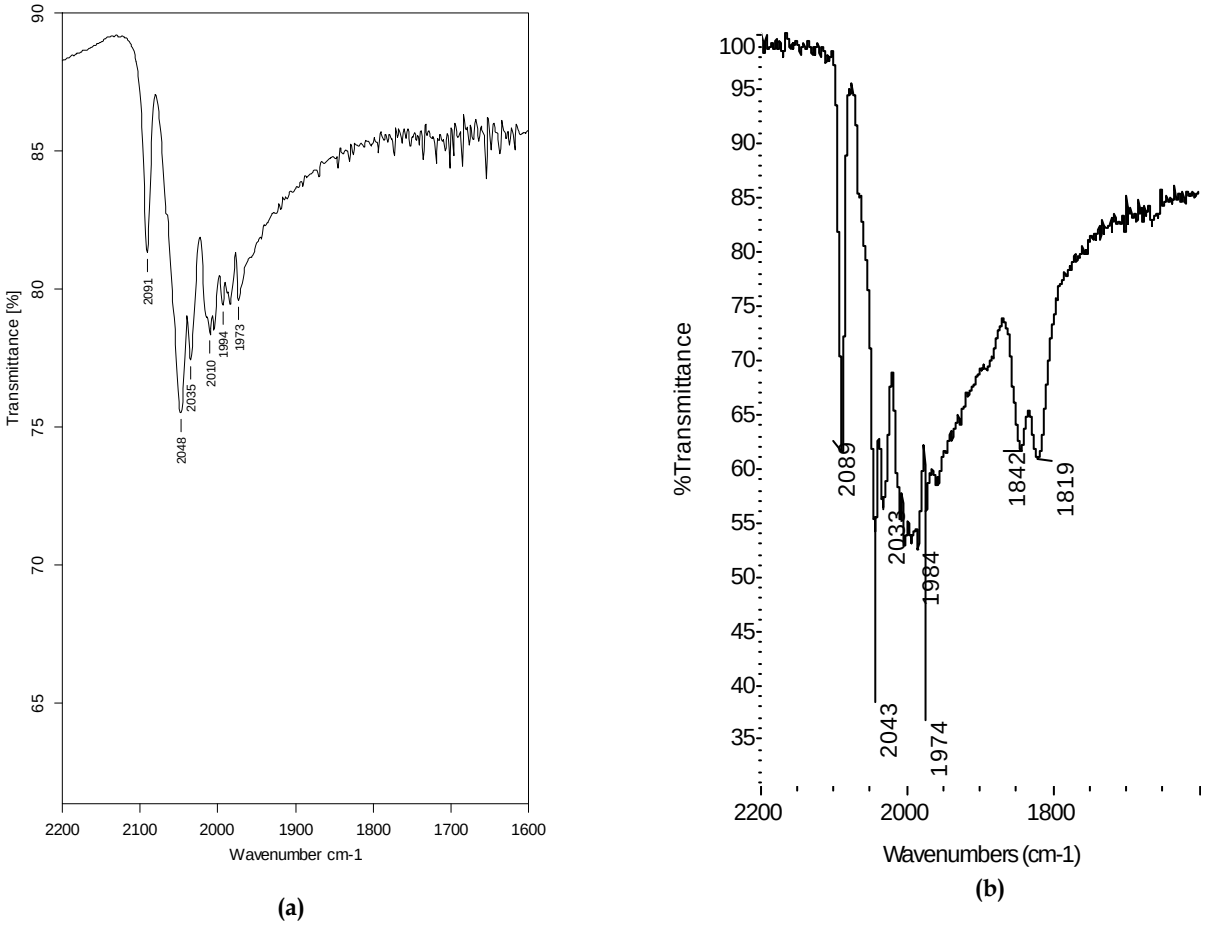

(a) **(b)**

Fig. 59 a) Nujol-IR and b) ATR-IR of [{$Ir_4(CO)_{11}$}$_2$(*t*-dppethe)]

1,4-bis(diphenylphosphanomethyl)benzene (dppmb)

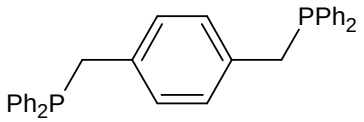

Fig. 60 dppmb

Reaction[146] of *p*-bis(chloromethyl)benzene with potassium diphenylphosphide in dry THF (inert atmosphere), at 263 K for half an hour and then at room temperature, leads in few hours to the desired product (Fig. 60) which is isolated adding water to the reaction mixture, filtering and washing with water and methanol.

$$ClCH_2(C_6H_4)CH_2Cl + 2KPPh_2 \xrightarrow[263\ K,\ T_{amb},\ ca\ 5h]{THF,\ N_2} Ph_2PCH_2(C_6H_4)CH_2PPh_2 + 2KCl$$

Reaction of 1,4-bis(diphenylphosphanomethyl)benzene with $[MCl_2(CO)_2]^-$ (M = Rh, Ir)

1,4-bis(difenilfosfinometil)benzene quickly reacts with $[RhCl_2(CO)_2]^-$ and after about 20 minutes a microcrystalline yellow powder separates, presenting in the ATR-IR spectrum a carbonyl stretching band at 1964(s) cm^{-1}. By monitoring the raction *via* IR it is observed that the reactant CO stretching bands quickly disappeared and a band at 1974(s) cm^{-1} appear. Instead, by monitoring the reaction *via* ^{31}P-NMR we observe that, just after the addition of the ligand to the metal solution (molar ratio M:L = 1:1) there are two peaks, a doublet at 29,9 ppm ($^3J_{Rh\text{-}P}$ 126,4 Hz) and a doublet at 34,5 ppm ($^3J_{Rh\text{-}P}$ 129,8 Hz) in 10:1 ratio; after 10 minutes the minor doublet disappears and the other decreases. After 20 minutes also the remaining peaks disappeared and a yellow precipitate is present in the NMR tube.

By layering a solution of the ligand in dichloromethane with a solution of the complex in ethanol two crystalline species have been obtained.

The first one was the cyclic dimer $[RhCl(CO)(dppmb)]_2$ (Fig. 61).

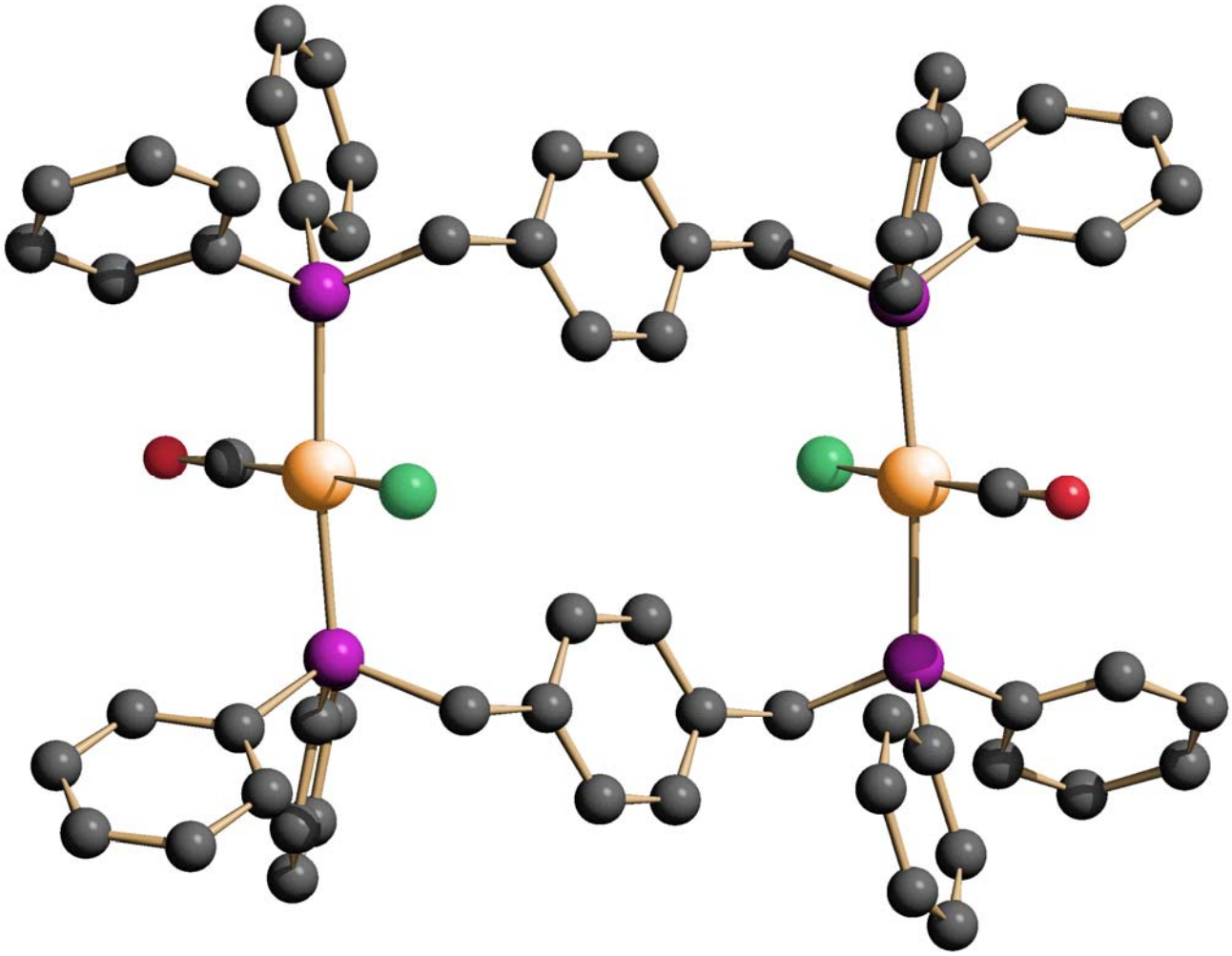

Fig. 61 X-ray structure of $[RhCl(CO)(dppmb)]_2$

The second one loosed very quickly its crystallinity as soon as removed from the solvent. So it has not been possible a diffrattometric analysis. An analogous behaviour was yet described for the polymer $[RhCl(CO)(dpphex)]_\infty$. So we could hypotize that also in this case we have obtained a polymeric species, $[RhCl(CO)(dppmb)]_\infty$.

The crystallized cyclic dimer $[RhCl(CO)(dppmb)]_2$ is the observed species with the CO stretching band at 1974 cm^{-1} and the ^{31}P-NMR doublet at 29,9 ppm, whereas the doublet at 34,5 could be attributed to a small amount of a larger size ring. Subsequently the cyclic dimer evolves to the corresponding 1D polymer $[RhCl(CO)(dppmb)]_\infty$ with a ring opening mechanism.

Reaction of dppmb with iridium halocarbonyl leads to a mixture whose spectrum shows three carbonyl bands at 1984(w), 1959(m), 1937(s) cm^{-1}. From this solution precipitates a yellow powder with a CO stretching band at 1953 cm^{-1} (ATR-IR). Also in this case the product results insoluble in all common solvents.

Reaction of 1,4-bis(diphenylphosphanomethyl)benzene with $[Ir_4Br(CO)_{11}]^-$ and $[Ir_4(CO)_{12}]$

$$2[PPh_4][Ir_4Br(CO)_{11}] + dppmb \xrightarrow[R.T., 24h]{CH_2Cl_2} [\{Ir_4(CO)_{11}\}_2(dppmb)] + 2PPh_4Br$$

Room temperature reaction between $[Ir_4Br(CO)_{11}]^-$ and dppmb, conducted in dichloromethane with 2:1 molar ratio, results in the substitution of bromine by the phosphorous, as usual for this class of reactions and as shown by the shift of the carbonyl stretching bands to higher wave numbers (Fig. 62-63).

The IR spectrum changes after about 15 minutes and the bands of the anionic cluster are not present anymore.

Actually, a TLC (thin layer chromatography) analysis shows the presence of the starting cluster and a second more polar species, identifiable as $[Ir_4(CO)_{11}(dppmb)]$ (*vide infra*) and the reaction needs about 24 hours to complete.

The stretching bands at 2087, 2055 and 2018 cm^{-1} are due to terminally coordinated COs, while the bands at 1843, 1818 cm^{-1} are due to edge-bridging COs.

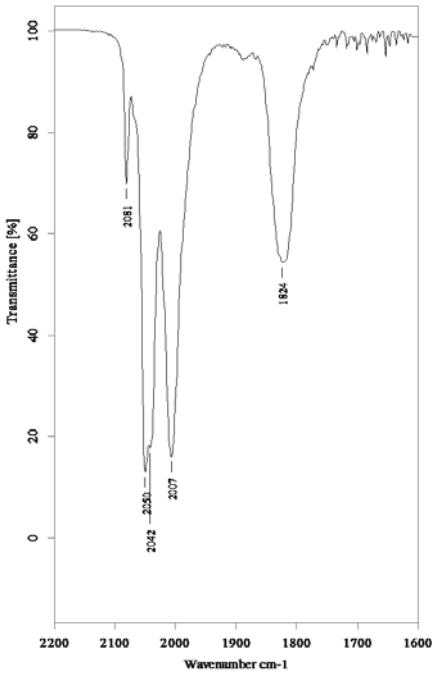

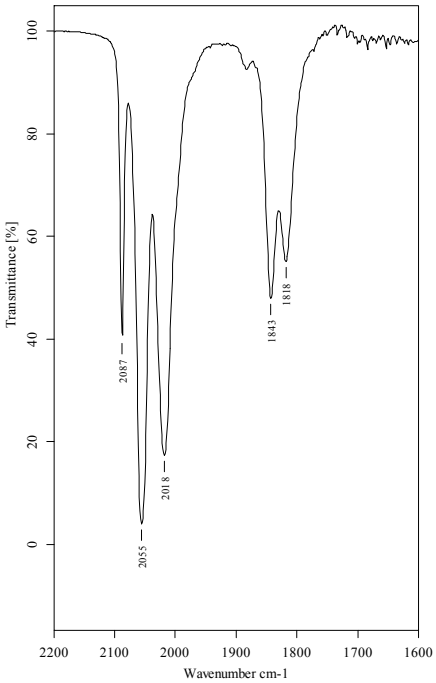

Fig. 62 IR spectra in CH_2Cl_2 of $[Ir_4Br(CO)_{11}]^-$ **Fig. 63 IR spectra in CH_2Cl_2 of $[\{Ir_4(CO)_{11}\}_2(dppmb)]$**

The product, separated from PPh_4Br by extraction with toluene, results to be, according to spectroscopic, analytic (CHN) and experimental evidences, $[\{Ir_4(CO)_{11}\}_2(dppmb)]$.
The reaction was repeated starting from $[Ir_4I(CO)_{11}]^-$, giving similar results. Unfortunately, it has not been possible to obtain crystals suitable for X-ray analysis.

Spectroscopic characterization of $[\{Ir_4(CO)_{11}\}_2(dppmb)]$

CD_2Cl_2 RT ^{31}P-NMR shows one broad peak at -5,7 ppm. The signal broadness suggests the species is fluxional. Actually, by cooling the solution at 243 K, a coalescence phenomenon is observed and then, at 203 K, four sharp peaks, at 16,45/ 17,23/ -9,97/ -9,32 ppm, 1:2:2:12 molar ratio, are obtained (Fig. 64).
These ratios and the reported chemical shifts for analogous compounds allow to state these peaks are due to three different isomers, with formula $[\{Ir_4(CO)_{11}\}_2(dppmb)]$, different in the coordination mode of P atoms:

- Isomer A with both the phosphorous atoms in axial position (A_{ax}-9,32 ppm) (12)
- Isomer B with one axial (B_{ax}-9,97 ppm) (2) and one radial (B_{rad}17,23 ppm) (2) P atom
- Isomer C with both the P atoms radially coordinated (C_{rad}, 16,45 ppm) (1)

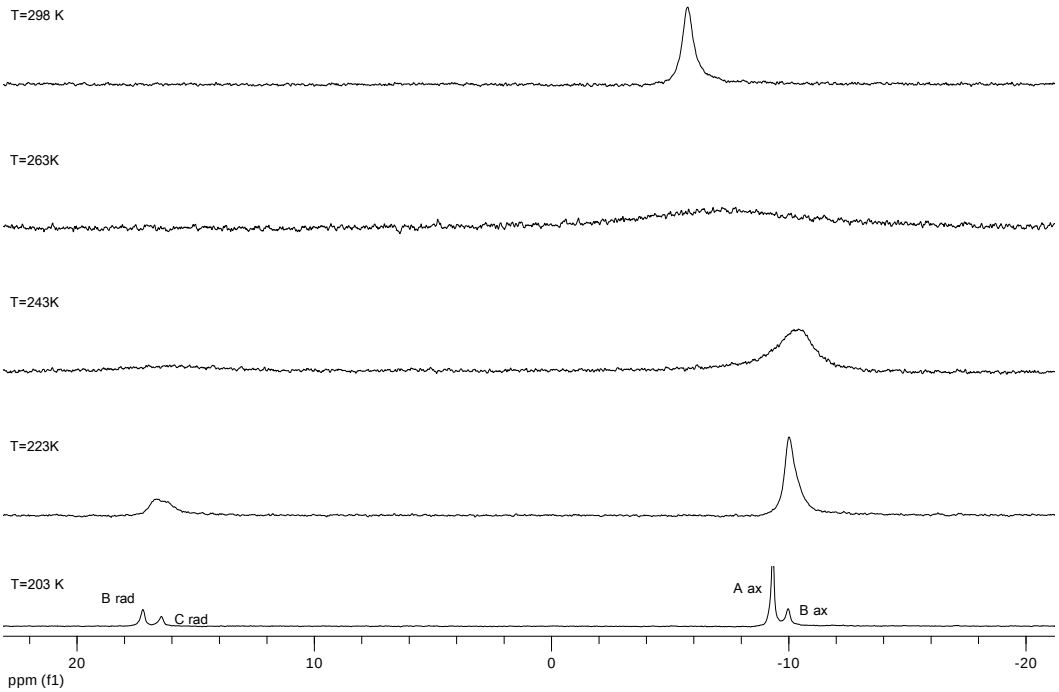

Fig. 64 CD_2Cl_2 VT-^{31}P-NMR of [{$Ir_4(CO)_{11}$}$_2$(dppmb)]

So, the ratio among A, B and C isomers is approximately 12:4:1. The experimental data agrees with the principle according to axial position is preferentially occupied respect to radial one.

It is interesting to compare the behaviour in solution of this species (and [$Ir_4(CO)_{11}$(dppmb)], *vide infra*) with that of [{$Ir_4(CO)_{11}$}$_2$(dppbp)] (and [$Ir_4(CO)_{11}$(dppbp)]), *vide infra* (dppbp = 4,4'-bis(diphenylphosphano)biphenyl)).

Substitution products of 1,4-bis(difenilfosfinometil)benzene (dppmb) are fluxional, whereas 4,4'-bis(diphenylphosphano)biphenyl are not. This difference is likely due to the different steric hindrance at the phosphorus atom. Dppmb ligand is less hindered and so, although axial position is preferred, isomers with one or two P atoms in radial position are present. Instead, dppbp is more hindered, phosphorus atom is not able to coordinate in radial position and so there is not fluxionality.

NMR spectrum with EXSY (2D-EXchange SpectroscopY) technique it has been registered. The experiment is conducted applying the pulses scheme summarized in Fig. 65. It is similar to NOESY tecnique: while the last one regards Overhauser effect, EXSY technique shows magnetization

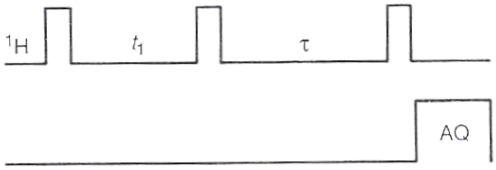

Fig. 65 EXSY pulses scheme

Exchange among the nuclei. It is one of the most versatile approach in the study of both bond nature and reaction equilibria when in solution different species are present.

Experiment at 213 K (Fig 66) has shown that among the three species a magnetization exchange is present: there are cross-peaks between signals at 16,3 ppm (C_{rad}) and 17,1 ppm (B_{rad}) and between signals at -10,12 (B_{ax}) and -9,50 (isomer A). This result can be explained with a carbonyls scrambling fluxional process, widely reported in the literature.[147]

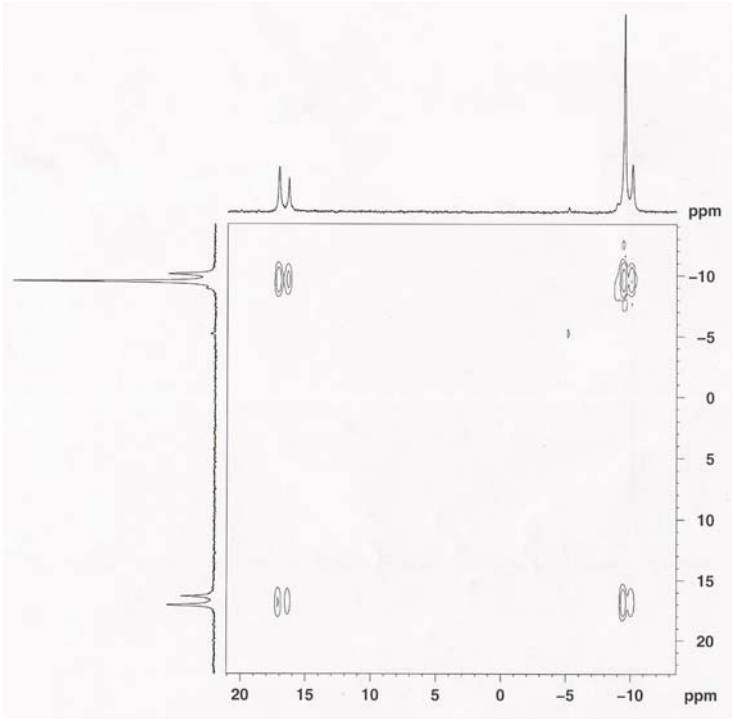

Fig. 66 EXSY ^{31}P-NMR of [{$Ir_4(CO)_{11}$}$_2$(dppmb)]

Synthesis and characterization of [{$Ir_4(CO)_9$}$_4$(dppmb)$_6$]

1,4-bis(diphenylphosphanomethyl)benzene easily gives a policyclic compound, namely [{$Ir_4(CO)_9$}$_4$(*dppmb*)$_6$] (**1**) (Fig. 67).

Initially, we synthesized this compound via a solvothermal approach, keeping [$Ir_4(CO)_{12}$] and *dppmb* (molar ratio 1:3) in a Teflon lined steel autoclave with an ethanol/toluene 3:2 mixture and heating in an oven at 130°C for 14 hours. Then the vessel was allowed to slowly cool down to room temperature and orange crystals, suitable for X-ray analysis, were recovered.

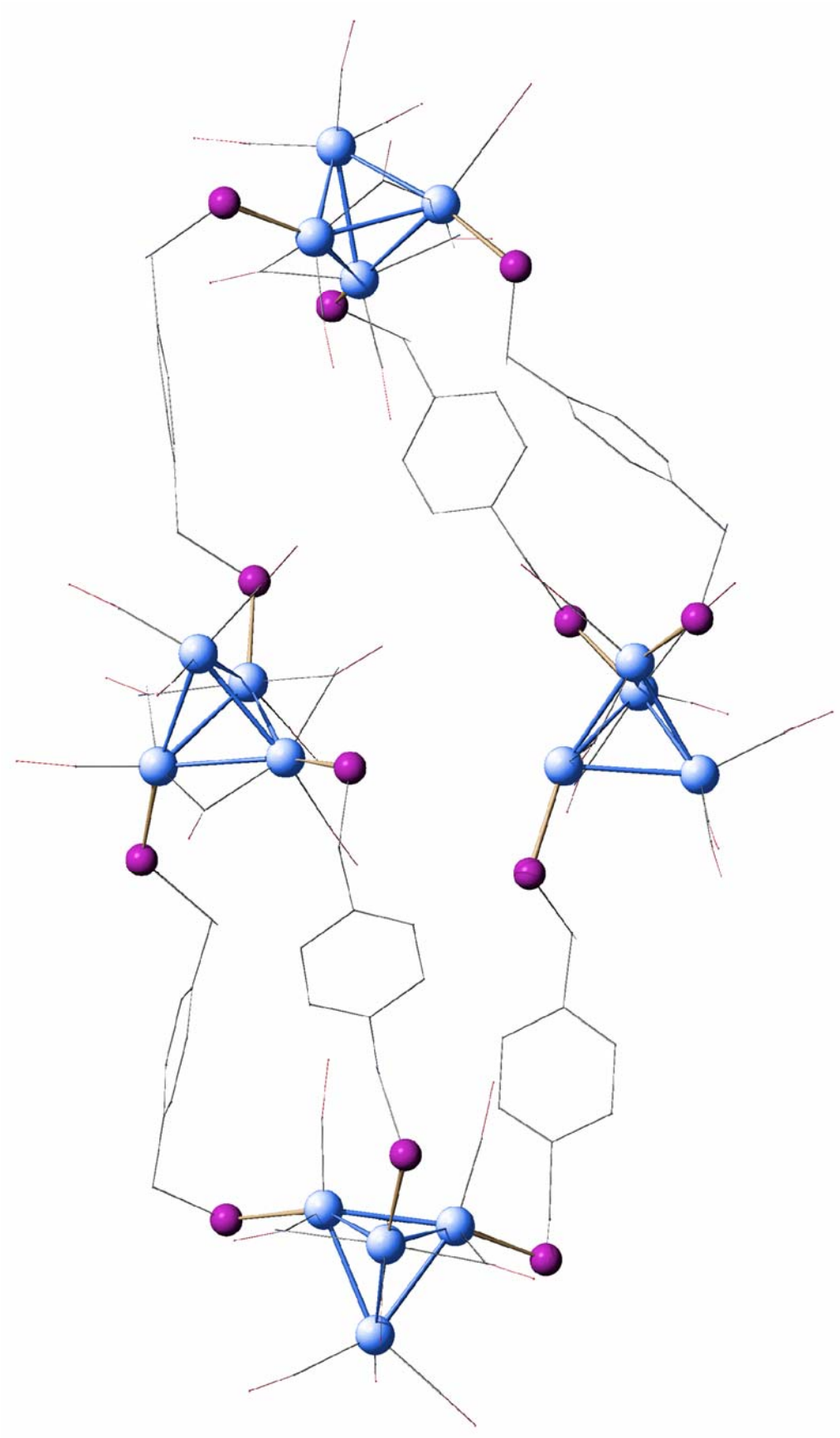

Fig. 67 X-ray structure of [{$Ir_4(CO)_9$}$_4$(*dppmb*)$_6$]. Phenyls are omitted for clarity.

Subsequently, also $[PPh_4][Ir_4Br(CO)_{11}]$ was successfully used as starting material to obtain **1** in good yield. Reactions can be summarized as follow:

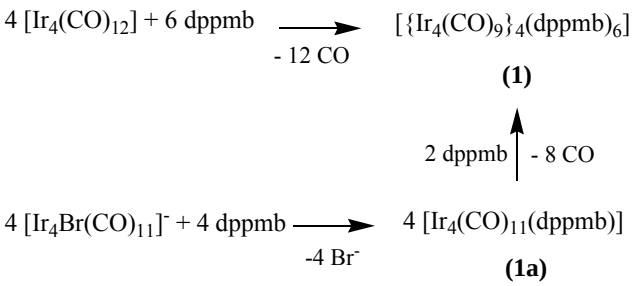

Furthermore, the bromide species was successfully used also for the synthesis at atmospheric pressure: in fact, it reacts at room temperature in dichloromethane with one equivalent of *dppmb* to give a mono-substituted species (**1a**) that, extracted with toluene and refluxed with a second equivalent of *dppmb*, gives **(1)** as a microcrystalline powder.

Compound **1** is insoluble in all common organic solvents. The absence of other solid products has been verified by comparison between simulated and measured X-ray powder diffraction and by the good agreement between calculated and found elemental analysis.

Despite **1** is only oligomeric, the result appears extremely interesting for some reasons. First of all, **1** proves the hypothesis that the metal clusters are very flexible *connectors* (as in fact each cluster moiety in **1** bears three diphosphano ligands, attached in a multistep procedure). Secondly, the structure of **1** is very peculiar (see Fig. 68): four tetra-iridium clusters are connected by six *dppmb* to form a poly-cyclic assembly.

In each cluster unit, the phosphano ligands are coordinated in the basal plane (where three bridging carbonyls reinforce the three iridium trigonal face). However, two ligands are equatorially bound, whereas one is axially bound, see Fig. 69.

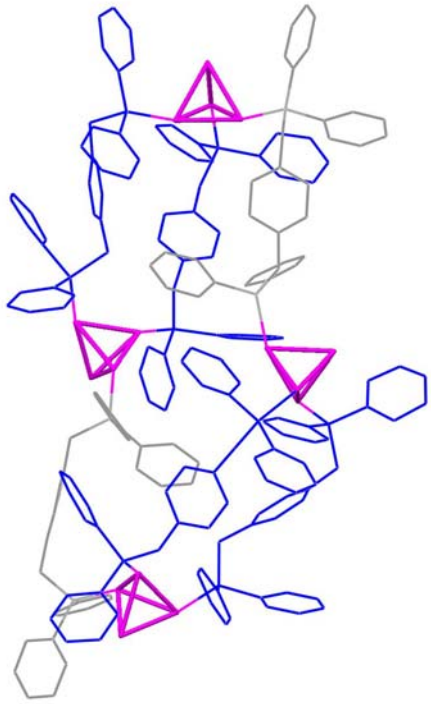

Fig. 68 The structure of 1. The four Ir_4 units are highlighted in purple. The CO ligands are omitted for clarity. The diphosphano ligands are in blue (those forming a short circuit between two Ir_4 units) or in gray (simple connection between two Ir_4 units).

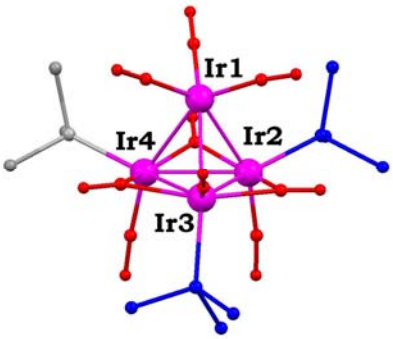

Fig. 69 One Ir_4 unit, showing the different stereochemistries of each Ir atom (diphosphano ligands, in blu or gray as in Figure 64, are truncated at the first C atoms). CO ligands are in red.

Interestingly, if we consider each cluster unit as a *node*, the overall shape is rhombic, but with a peculiarity: each *node* is involved in a short cycle (20 covalent bonds) with one of its two neighbours (see blue ligands in Fig. 68), whereas it is interconnected with just one ligand (in gray) to the other neighbour *node*. The structure is schematically drawn in Fig. 70.

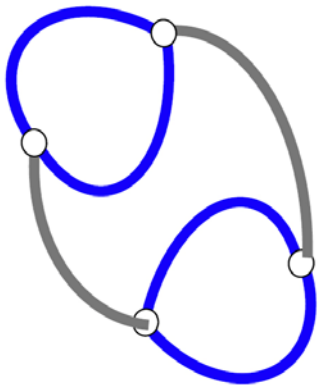

Fig. 70 Schematic structure of 1 highlighting the policyclic connection.

Otherwise, if each metal centre is considered as a *node*, then according to Wells[148] we recognize three different metal atoms: 1) Ir1 is not part of any inter-cluster cycle, hence its topology is the same as in the monomer (3^3); 2) Ir2 and Ir3 are part of octa-fold and tetra-fold cycles (hence they are $8^1 4^1 3^3$); 3) Ir4 is part of two octa-fold rings (hence it is $8^2 3^3$). Notably, if the small four metal cycles (in blue in Fig. 68-70) were not formed, the resulting "dangling" diphosphano ligands would be prompt for a polymeric coordination (several configurations being possible, of course). The resulting network could have large cavities because the octa-metal cycle might also relax, whereas in **1** the octa-cycles are quite tensioned.

4,4'-bis(diphenylphosphano)biphenyl (dppbp)

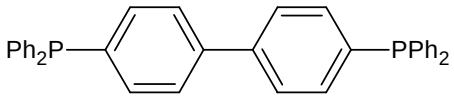

Fig. 71 dppbp

4,4'-dibromobiphenyl reacts[149] with two equivalents of *n*-buthyl lithium at 240 K in dry THF (inert atmosphere) to give the dilithium derivative. Addition of stoichiometric amount of chlorodiphenylphosphane affords 4,4'-bis(diphenylphosphano)biphenyl (Fig. 71).

Reaction of 4,4'-bis(diphenylphosphano)biphenyle with $[MCl_2(CO)_2]^{2-}$ (M = Rh, Ir)

Also dppbp reacts with the rhodium and iridium halocarbonyls, although the dppbp is less reactive than diphosphanes having an alkyl group directly bonded to phosphorus atom. This is likely explainable by considering that in dppbp the P lone pair is less available for donation, because of its partial delocalization on the aromatic π system. Anyhow, when dppbp is added to $[MCl_2(CO)_2]^-$, the IR spectrum changes showing carbonyl bands at 1979(s) cm^{-1} for Rh and 1930(s), 1967(m) cm^{-1} for Ir (the former probably due to a cyclic dimer analogous to others reported, the latter to a mixture) and then a microcrystalline powder separates from the solution, displaying typical IR bands in the CO region at 1966(s) cm^{-1} for Rh and 1981(vw), 1960(w), 1922(vs), 1899(vw) cm^{-1} for Ir. These products are, as usual, sparingly soluble in all organic solvents. I have tried many times to get X-ray suitable crystals of these materials. In the best cases the crystals diffract but the molecules are very disordered and the model does not converge satisfying. Despite of the poor quality of the data, it is possible to state the polymeric nature of these species.

Reactivity of $[Ir_4X(CO)_{11}]^-$ with 4,4'-bis(diphenylphosphano)biphenyl (X=Br, I)

Synthesis and characterization of $[\{Ir_4(CO)_{11}\}_2(dppbp)]$

$$2[PPh_4][Ir_4Br(CO)_{11}] + dppbp \xrightarrow[\text{R.T., 30 min}]{CH_2Cl_2} [\{Ir_4(CO)_{11}\}_2(dppbp)] + 2PPh_4Br$$

Reaction between $[Ir_4Br(CO)_{11}]^-$ and 4,4'-bis(diphenylphosphano)biphenyl (dppbp), at RT and 2:1 molar ratio results, in about 30 minutes, in the substitution of bromine by the P atom, as demonstrated by IR spectra: carbonyl stretching bands shift to higher wavenumbers, meaning the formation of a neutral compound from an anionic one (Fig. 72, 73).

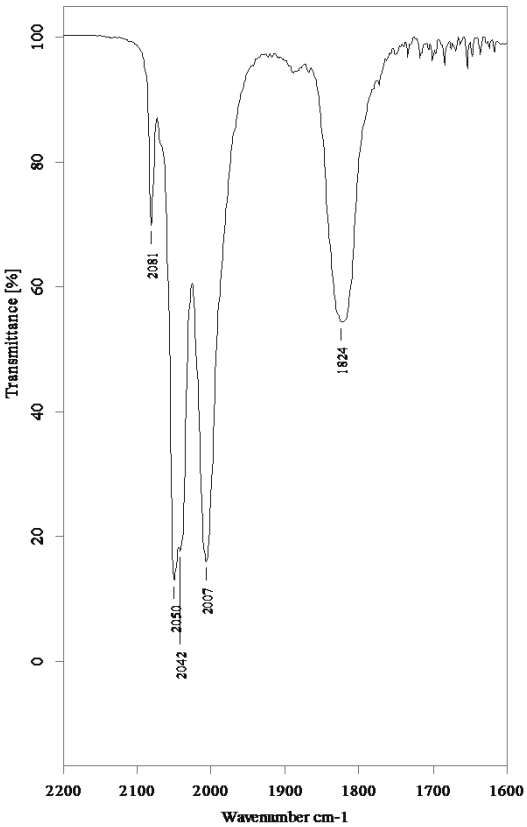

Fig. 72 CH_2Cl_2 IR spectrum of $[Ir_4Br(CO)_{11}]^-$

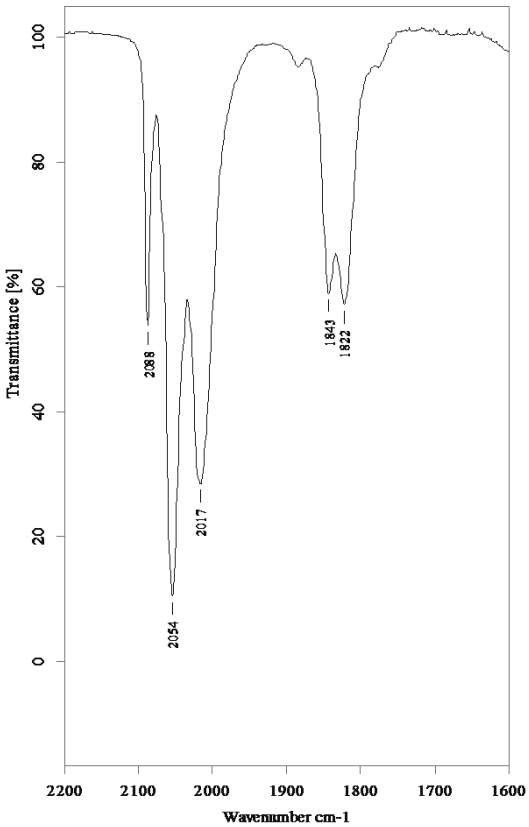

Fig. 73 CH_2Cl_2 IR spectrum of $[\{Ir_4(CO)_{11}\}_2(dppbp)]$

Furthermore, bands position, according to the literature, indicate the presence of a monosubstituted product. The reaction is slower than in the case of alkyl diphosphane like as 1,6 bis(diphenylphosphano)hexane (dpphex) (*vide infra*). This fact is attributed to the lower basic nature of dppbp respect of dpphex, becuase the former has three aromatic substituent of place of two like the latter, making the P lone pair less available for the donation to the metal.

Elemental analysis, IR and ^{31}P-NMR spectra are in agreement with the formula $[\{Ir_4(CO)_{11}\}_2(dppbp)]$. Unfortunately, attempts to grow crystals for this species did not give any results. The reaction has been then repeating in the same conditions starting from $[Ir_4I(CO)_{11}]^-$. The reaction is slower than starting from bromide cluster but it lets to isolate the same product.

Spectroscopic characterization

As we said, IR spectrum is typical of a neutral monosubstituted product of $[Ir_4(CO)_{12}]$. It shows carbonyl stretching bands at 2088, 2054, 2017 cm^{-1}, for terminal COs and at 1845, 1822 cm^{-1} for edge-bridging COs.

CD_2Cl_2 RT ^{31}P-NMR spectrum (Fig. 74) shows a singlet at -11,59 ppm, with an up-field shift respect to the free ligand (-5,8 ppm). Spectrum registered at 183 K shows only a slight down-field shift (-11,37 ppm), explainable as a simple effect of temperature.

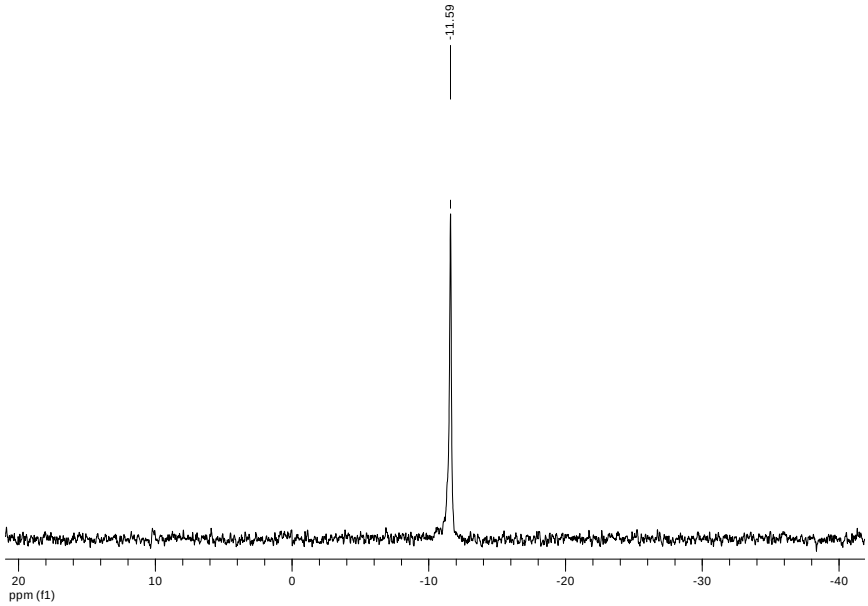

Fig. 74 CD_2Cl_2 ^{31}P-NMR of $[\{Ir_4(CO)_{11}\}_2(dppbp)]$

As previously underlined, it is interesting to note that, unlike analogous species like as $[\{Ir_4(CO)_{11}\}_2(dpphex)]$[150] (*vide infra*), this product does not show carbonyls fluxionality. non sono presenti fenomeni di flussionalità dei carbonili. The chemical shift, according to literature data, can be assigned to axially coordinated phosphourus atoms.

In Fig. 75 the proposed structure for $[\{Ir_4(CO)_{11}\}_2(dppbp)]$ is reported: analogously to the XRD structure of $[\{Ir_4(CO)_{11}\}_2(dpphex)]$ *(vide infra)*, each Ir_4 cage coordinate three COs on the edges of a face (namely basal face) and seven terminal COs. The cluster are linked by the phosphane ligand and both the P atoms are axially bonded.

The cages could lie both on the same side respect of P-P axe (as shown in the figure) or on opposite sides.

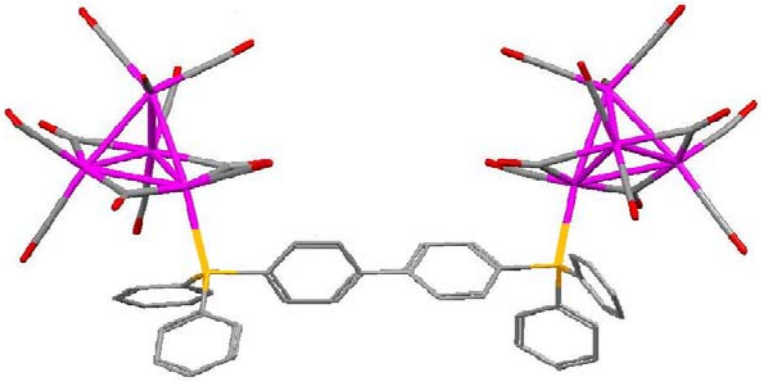

Fig. 75 Supposed structure of $[\{Ir_4(CO)_{11}\}_2(dppbp)]$

Synthesis and characterization of $[Ir_4(CO)_{11}(dppbp)]$

Addition of dppbp ligand to an acetonitrile solution of $[Ir_4I(CO)_{11}]^-$ (molar ratio 1:1) leads, in 24 hours, to the precipitation of a yellow powder. This material, well soluble in dichloromethane, shows the IR spectrum in Fig. 76b.

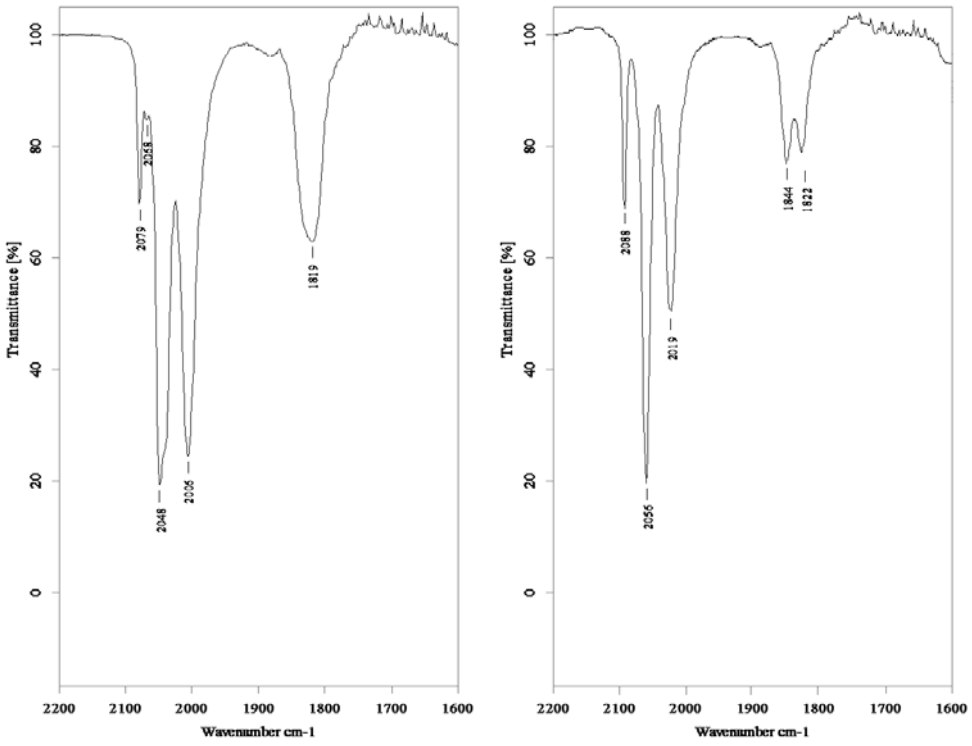

a) **b)**

Fig. 76 CH_2Cl_2 IR spectrum of a) $[Ir_4I(CO)_{11}]^-$ and b) $[Ir_4(CO)_{11}(dppbp)]$

The bands at 2088, 2055, 2019 cm^{-1} are due to terminal COs, while those ones at 1844, 1822 cm^{-1} are due to edge-bridging COs.

$$[PPh_4][Ir_4I(CO)_{11}] + dppbp \xrightarrow[R.T., 24h]{CH_3CN} [Ir_4(CO)_{11}(dppbp)] + PPh_4I$$

Also in this case an up-shift in the frequencies is observed.

Elemental analysis and ^{31}P-NMR spectrum agree with the proposed formula $[Ir_4(CO)_{11}(dppbp)]$.

The reaction has been repeated in dichloromethane at room temperature but in this way it is not possible to obtain the desired product selectively. Basing on ^{31}P-NMR spectrum, TLC and elemental analysis is clear that a mixture of $\{[Ir_4(CO)_{11}]_2(dppbp)\}$ and $[Ir_4(CO)_{11}(dppbp)]$ is formed. Clearly, when the latter species begins to be present in solution, becomes competitive with the free ligand in the reaction with the anionic cluster and so a mixture is obtained.

On the contrary, when $[Ir_4(CO)_{11}(dppbp)]$ is formed in the acetonitrile reaction, it precipitates from the solution and does not lead to further reactions.

The reaction was repeated starting from $[Ir_4Br(CO)_{11}]^-$ with both the solvents but the selectivity, in the case of acetonitrile too, was lost.

It has been found that the iodide substitution by dppb as well as by other phosphane ligands is slower than bromide reaction.

This experimental data is explainable with the higher nucleoficity of I^- respect to Br^- in polar aprotic solvents.

Spectroscopic characterization of $[Ir_4(CO)_{11}(dppbp)]$

CD_2Cl_2 RT ^{31}P-NMR of $[Ir_4(CO)_{11}(dppbp)]$ shows two sharp peaks, one at -5,5 ppm, attribuibile ad un fosforo non coordinato (free ligand -5,8 ppm) and the other at -11,6 ppm, due to an axially coordinated P atom. At low temperature (183 K) the spectrum does not change and so there is not fluxionality for the carbonyls in the range T_{amb}-183 K.

We can so assume a structure like the one shown in Fig. 77.

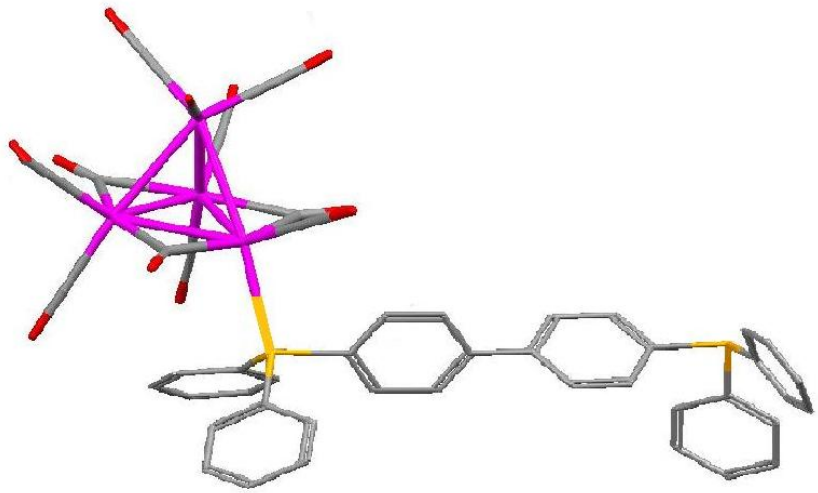

Fig. 77 Supposed structure of $[Ir_4(CO)_{11}(dppbp)]$

The cluster should show a C_{3v} geometry with an axial position ocupied by the phosphane ligand which acts like a monodentate ligand.

Room temperature ^{31}P-NMR shows two peaks at -5,5(s) and -11,8(s) ppm). These peaks do not have an integer ratio of 1:1, as we would expert for $[Ir_4(CO)_{11}(dppbp)]$, but 2 (-11,8 ppm, coordinated phosphorus) to 1 (-5,5 ppm, uncoordinated phosphorus). We registered the spectrum in dichloromethane with a D_1 of 1 second. This time is usually sufficient for these kind of compounds.

Then we registered further spectra with longer D_1 (15, 60, 120 seconds) at room or low temperature. In this way the ratio turns to be almost 1:1, as we expert (Table 1). In Fig. 78 the spectrum at 183 K with D_1= 15 sec is reported: there are two peaks at -9,07(s) and -11,37(s) ppm, with the ratio 0,88 :1,0. Toluene spectra resulted similar.

So the coordinated phosphorus has a very long relaxing time, much more than those usually found for these compounds. This phenomenon is connected with the coordination.

D_1 (sec); temperature (K)	Uncoordinated phosphorus (relative intensity)	Coordinated phosphorus (relative intensity)
1; 300	0,44	1,0
15; 295	0,61	1,0
60, 300	0,81	1,0
15, 183	0,88	1,0
120, 300	0,91	1,0

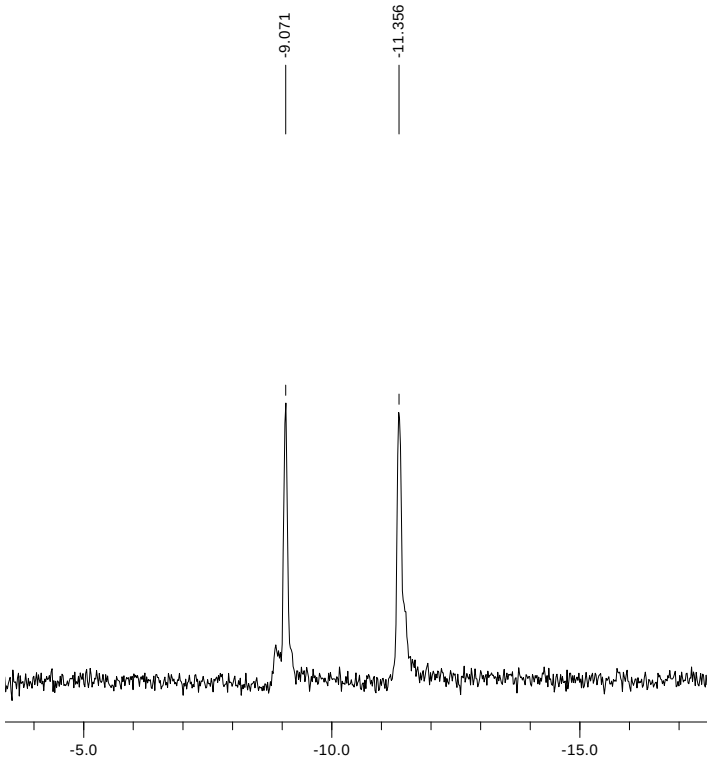

Fig. 78 CD_2Cl_2 ^{31}P-NMR of $[Ir_4(CO)_{11}(dppbp)]$. T= 183 K, D_1= 15 sec.

4,4'-bis(diphenylphosphanomethyl)biphenyl (dppmbp)

This ligand[151] (Fig. 79a) can be structurally viewed as "a merge" of dppmb and dppbp. So we considered interesting to study its behaviour in the reactivity with the usual halocarbonyls.

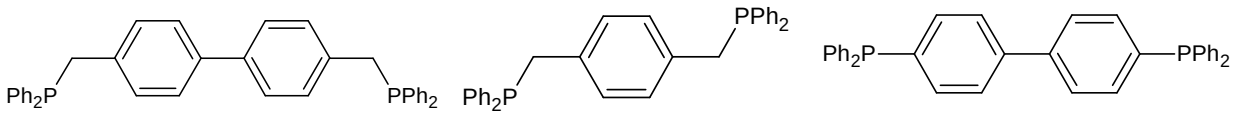

a **b** **c**

Fig. 79 a) dppmbp b) dppmb c) dppbp

Reactivity of $[MCl_2(CO)_2]^-$ (M = Rh, Ir) with 4,4'-bis(diphenylphosphanomethyl)biphenyl

Respect of other phosphane ligands, dppmbp is air-sensitive and shows a very low solubility, in the order of 1 mg/mL (dichloromethane).

This fact became a hard limit in the study of its reactivity and so we quickly left this ligand.

Reactions of $[MCl_2(CO)_2]^-$ with dppmbp in dichloromethane at room temperature (molar ratio M:L = 1:1) result in the precipitation of a yellow powder, insoluble in all organic solvents, showing in the ATR-IR a CO stretching band at 1969 cm^{-1} for Rh and 1956 cm^{-1} for Ir.

The same products are obtained by refluxing the reagents in ethanol for some hours.

Crystals suitable for X-ray analysis were obtained in solvothermal condition, by heating the reagents in dichloromethane at 90°C.

Fig. 80 shows the structure of the compound obtained from Ir(I) salt, the cyclic dimer $[IrCl(CO)(dppmbp)]_2$; the structure obtained from Rh(I) is very similar.

Their high insolubilities are likely to prevent the evolution, through a ring opening polymerization, to the corresponding 1D polymers.

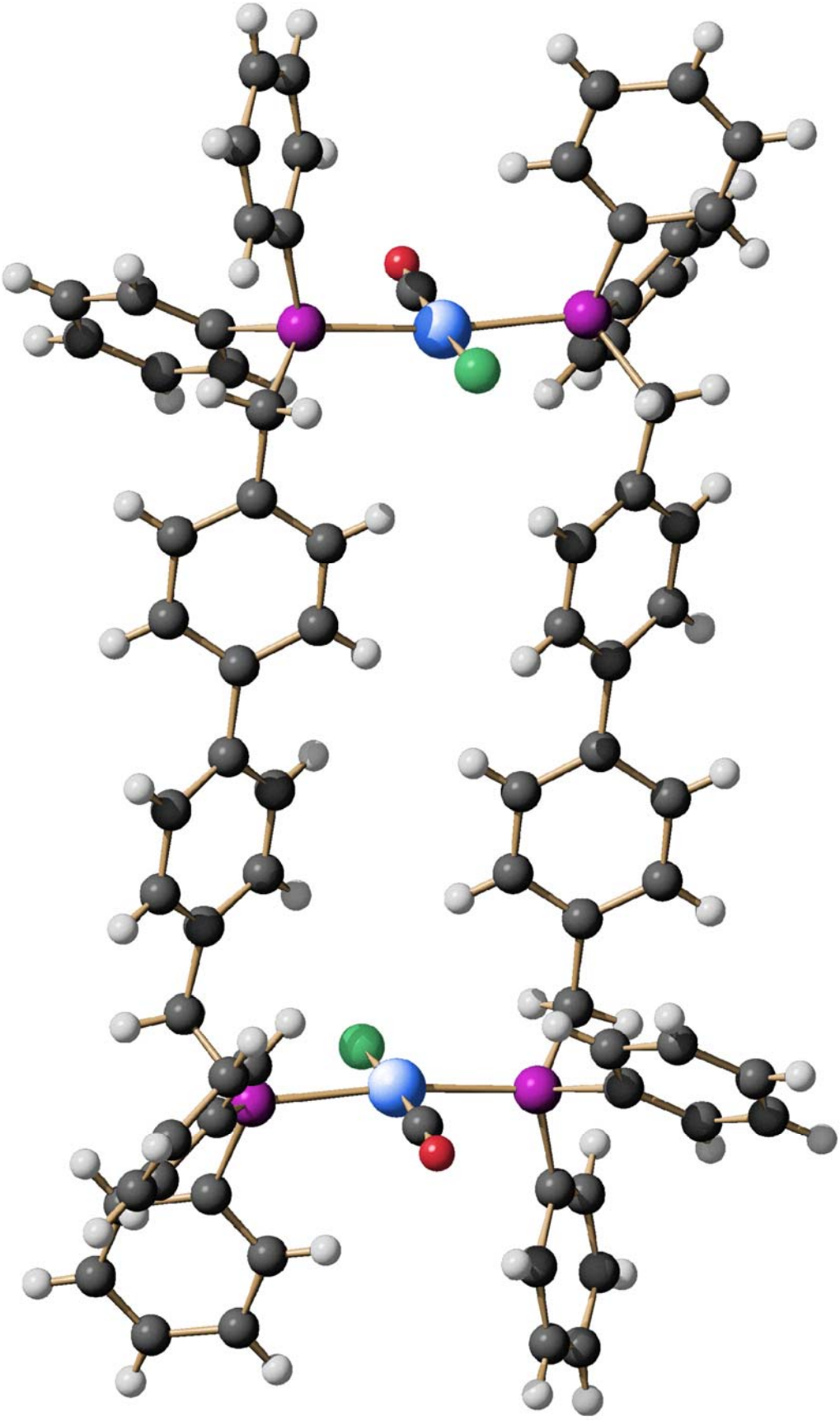

Fig. 80 X-ray structure of $[IrCl(CO)(dppmbp)]_2$

FLEXIBLE DIPHOSPHANES

Flexible diphosphanes typically have a saturated alkyl chain as spacer and so the general formula is $Ph_2P(CH_2)_nPPh_2$. We focused our attention on the ligands with n = 4, 6, 8, 10, 12. The most interesting results have been obtained with n = 6, both for $[RhCl_2(CO)_2]^-$ and $[Ir_4Br(CO)_{11}]^-$ or $[Ir_4(CO)_{12}]$.

Reactivity of $[Ir_4(CO)_{12}]$ with 1,4-bis(diphenylphosphano)butane (dppbut)

This commercially available diphosphane (Fig. 81) is flexible and rather short to be able both to chelate on the edge of a cluster and to link two of them.

Fig. 81 dppbut

In literature is reported the formation of a cyclic dimer starting from $[Rh_2Cl_2(CO)_2]$.[152]
We used dppbut with $[Ir_4(CO)_{12}]$ in solvothermal condition and orange crystals of $[\{Ir_4(CO)_9(\mu\text{-dppbut})\}_2(dppbut)]$ were obtained (Fig. 82).
Two Ir_4 clusters are joined by a radial-radial coordinated dppbut ligand. Each Ir_4 cluster is also chelated by another axial-axial coordinated diphosphane lying under the tetrahedron basal plane.

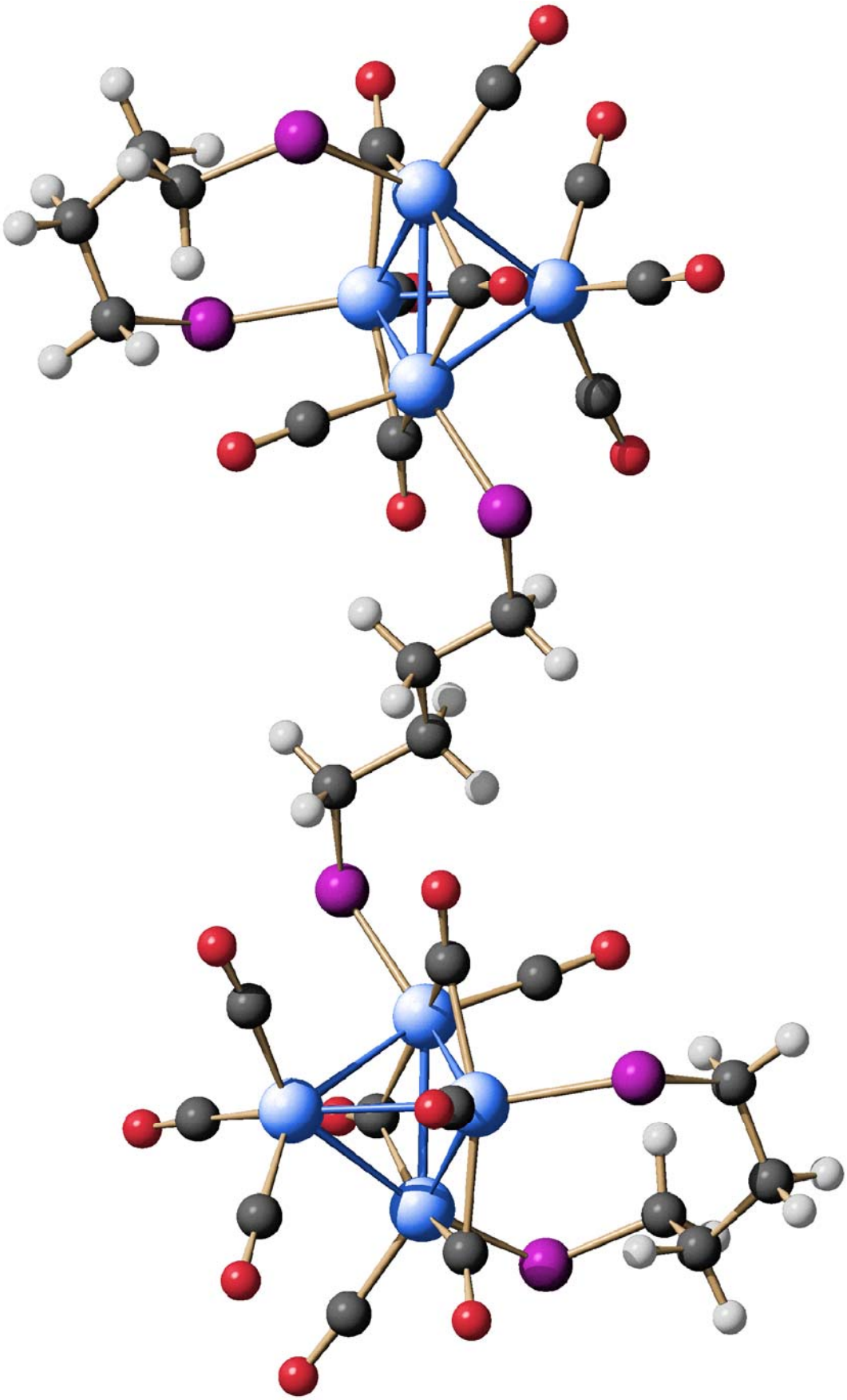

Fig. 82 X-ray structure of [{$Ir_4(CO)_9$(μ-dppbut)}$_2$(dppbut)]. Phenyls are omitted for clarity

Reactivity of $[Ir_4Br(CO)_{11}]^-$ with 1,6-bis(diphenylphosphano)hexane (dpphex)

1,6-bis(diphenylphosphano)hexane (dpphex) has an alkyl chain long enough to prevent the formation of chelated species.

It has been recently used to obtain a 1D coordination polymer, [RhCl(CO)(dpphex)·SOLV]. So we continued the study of its reactivity by considering $[Ir_4Br(CO)_{11}]^-$ and $[Ir_4(CO)_{12}]$.

As for other phosphane ligands, the substitution reaction of Br^- group in the anionic cluster (RT and dichloromethane as solvent) is fast and selective, leading to neutral species that are soluble in THF, toluene and chlorinated solvents but insoluble in acetonitrile or methanol. IR spectra (Fig. 83) clearly show an up-shift of the carbonyl stretching bands to higher wavenumbers. Bands at 2087, 2055, 2018 cm^{-1} are due to terminal COs, while bands at 1843, 1819 cm^{-1} are due to edge-bridging COs. This is a typical spectrum for a monosubstituted species of $[Ir_4(CO)_{12}]$.

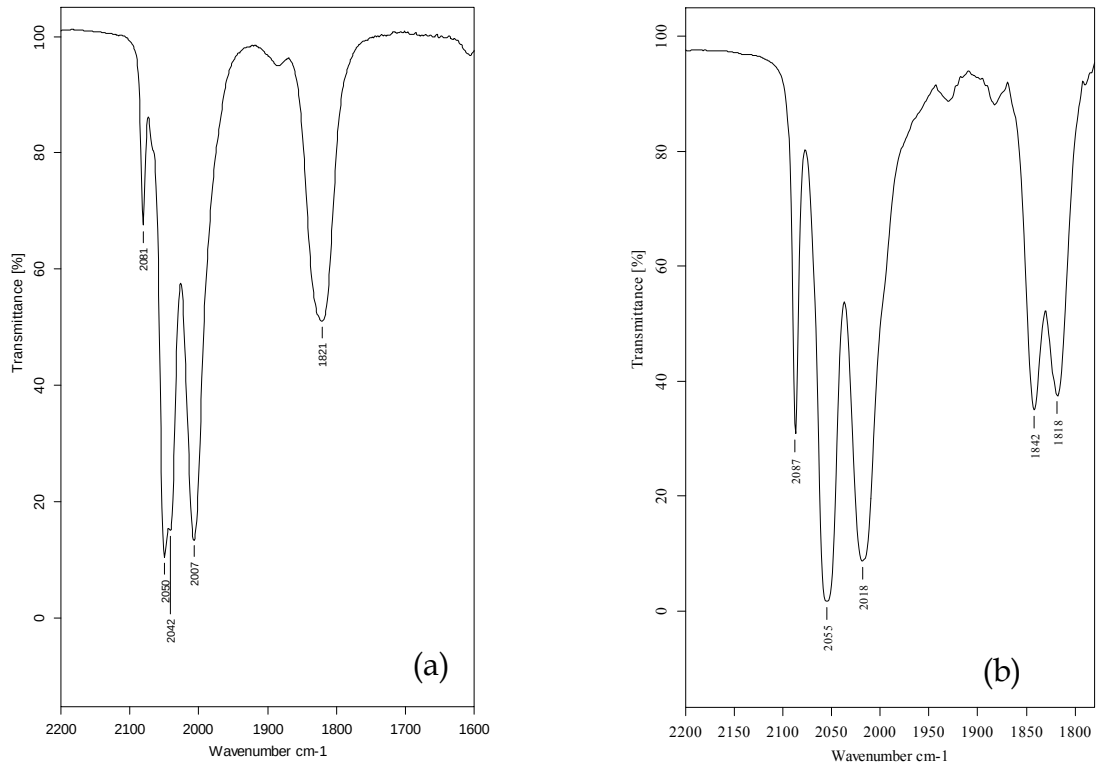

Fig. 83 CH_2Cl_2 IR spectra of (a) $[Ir_4Br(CO)_{11}]$- and (b) $[\{Ir_4(CO)_{11}\}_2(dpphex)]$

Synthesis and characterization of [{$Ir_4(CO)_{11}$}$_2$(dpphex)]

This compound is obtained in the reaction of the anionic cluster and the ligand, by using a M : L = 2 : 1 molar ratio and dichloromethane as solvent at room temperature.

$$2[Ir_4Br(CO)_{11}]^- + \text{dpphex} \longrightarrow [\{Ir_4(CO)_{11}\}_2\text{dpphex}] + 2Br^-$$

[{$Ir_4(CO)_{11}$}$_2$(dpphex)] can be isolated removing the solvent and washing the crude with acetonitrile (58% yield) or extracting the neutral product with toluene(53% yield).
Elemental analysis agrees with the proposed formula.

Solid state structure of [{$Ir_4(CO)_{11}$}$_2$(dpphex)]

Single crystals, suitable for X-ray analysis, have been obtained by layering a solution in dichloromethane with n-heptane. The molecule (Fig. 84) is constituted by two $Ir_4(CO)_{11}$ tetrahedral units connected by a bridging dpphex ligand. Each cage has a C_{3v} symmetry with the same COs stereochemistry of the parent cluster $[Ir_4Br(CO)_{11}]^-$: three COs are bridged coordinated on the edges of a tetrahedron face, becoming the basal face, while the others are terminally bonded. In addition the basal Ir atoms coordinate two terminal COs (or one when the phosphane group is present). One is normally directed to the base plane (axial coordination), while the other is nearly contained in the plane (radial or equatorial coordination). The apical Ir atom coordinates three carbonyl groups.

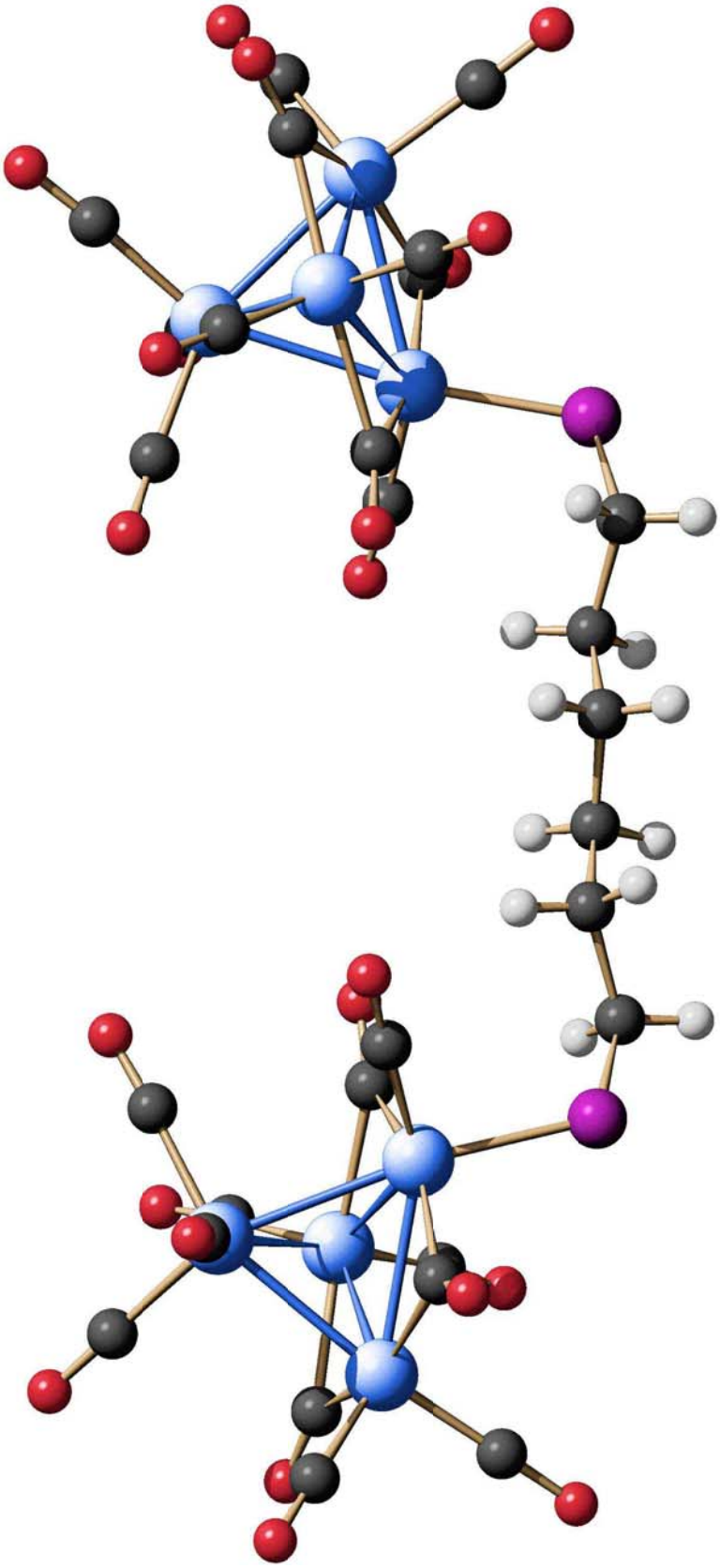

Fig. 84 X-ray structure of [{$Ir_4(CO)_{11}$}$_2$(dpphex)]. Phenyls are omitted for clarity.

In the following table significant bond lenghts are reported.

Bond	**[{$Ir_4(CO)_{11}$}$_2$(dpphex)] (Å)**
Ir-Ir (average)	2,727
C-O (average)	1,132
Ir-P	2,331

Actually in the unit cell two molecules are present, differing for the reciprocal position of the clusters respect to the P-P axe, cisoid or transoid (Fig. 85).

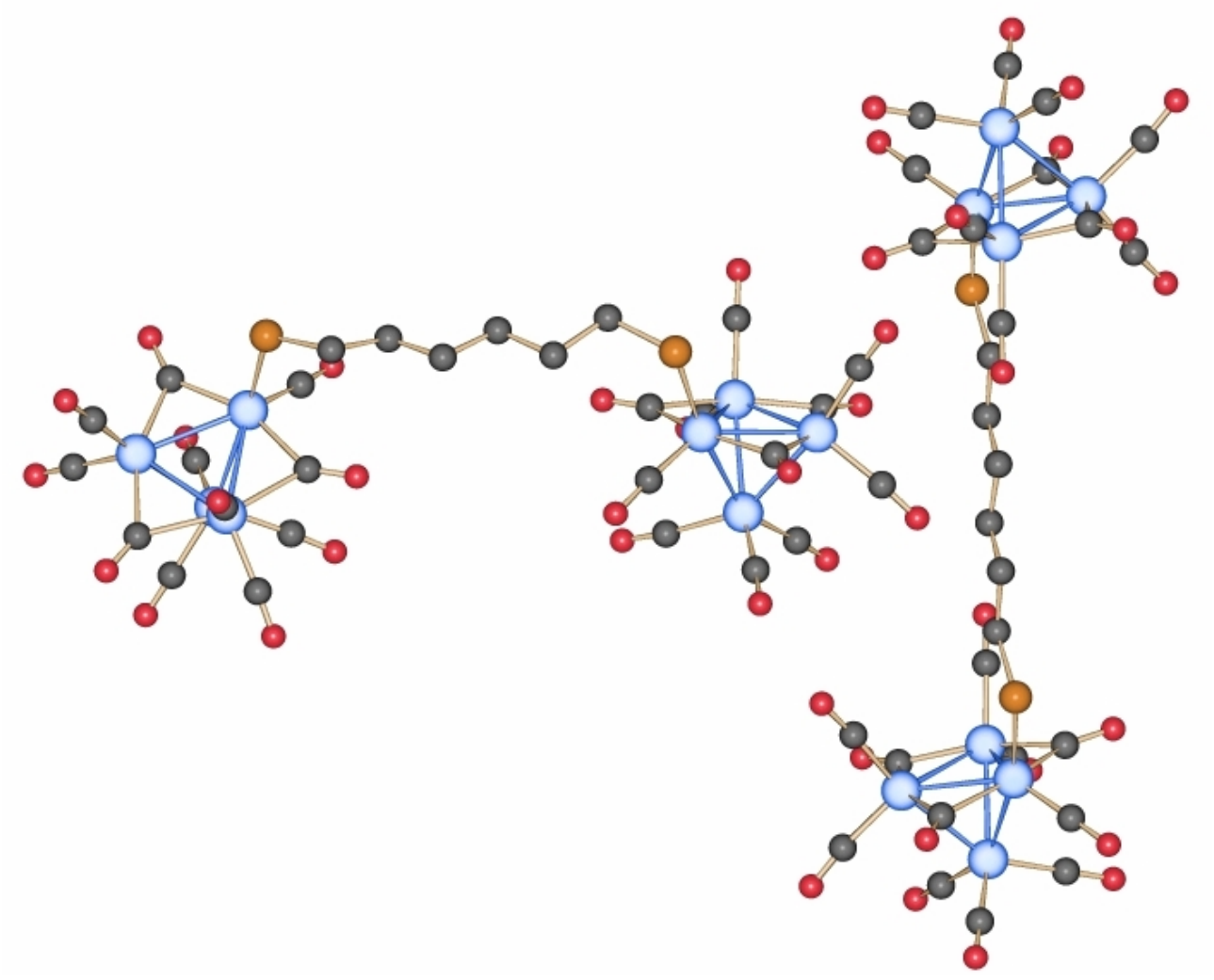

Fig. 85: Molecules of [{$Ir_4(CO)_{11}$}$_2$(dpphex)] in the crystallographic cell

Spectroscopic characterization

CH_2Cl_2 IR spectrum, reported in Fig. 86, is in agreement with the solid state X-ray structure, showing bands at 2087, 2055, 2018 (terminal COs) and 1842, 1818 (edge-bridging COs).

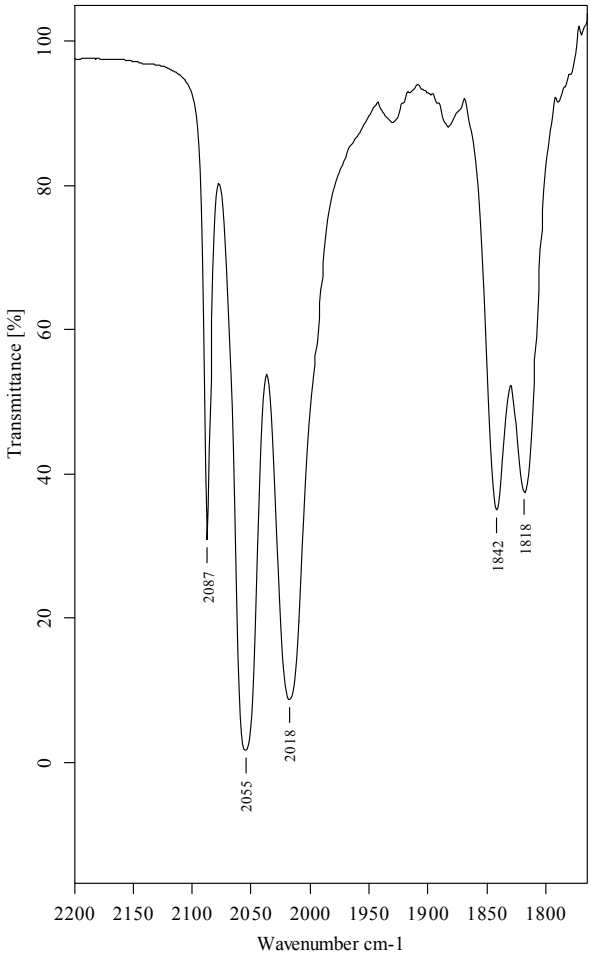

Fig. 86: CH_2Cl_2 IR spectrum of [{$Ir_4(CO)_{11}$}$_2$(dpphex)]

Room temperature CD_2Cl_2 ^{31}P-NMR spectrum shows one broad singlet at -14 ppm (free ligand has a singlet at -15,7 ppm). At 273 K the coalescence phenomenon is observed and finally at 213 K there are three peaks, relative intensity 1:1:8 at 6 ppm, -17,2 ppm and -17,4 ppm rispectively: the chemical shift and the integration ratio agree with the presence of two stereoisomers. The main species **A** shows the same structure observed in the solid

state, with both the P atoms axially coordinated; isomer **B** has one phosphorus atom in axial position (B_{ax}) and the second one in radial position (B_{rad}) (Fig. 87).

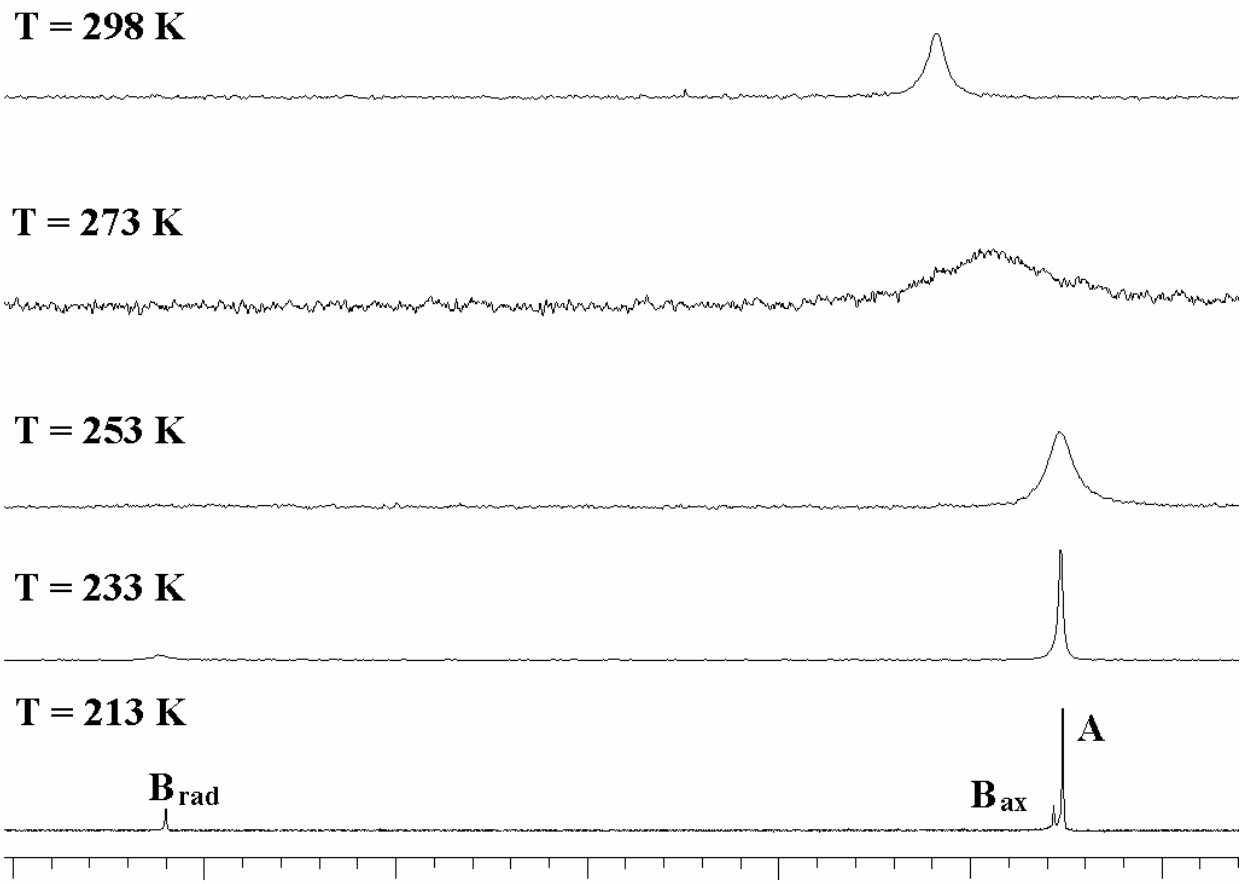

Fig. 87: CD_2Cl_2 **VT** ^{31}P-NMR spectra of $[\{Ir_4(CO)_{11}\}_2(dpphex)]$

It has been then registered an EXSY (2D-EXchange SpectroscopY spectrum).

The experiment, conducted at 203K (Fig. 88) shows the magnetization transfer between the two species. The cross peak between the peak at 6 ppm (B_{rad}) and the peak at -17,4 (isomer A) is evident, while the signals at -17,2 and -17,4 are too close to appreciate the cross-peak. This result is explainable with a scrambling fluxional process of the COs, widely documented in the literature.[153]

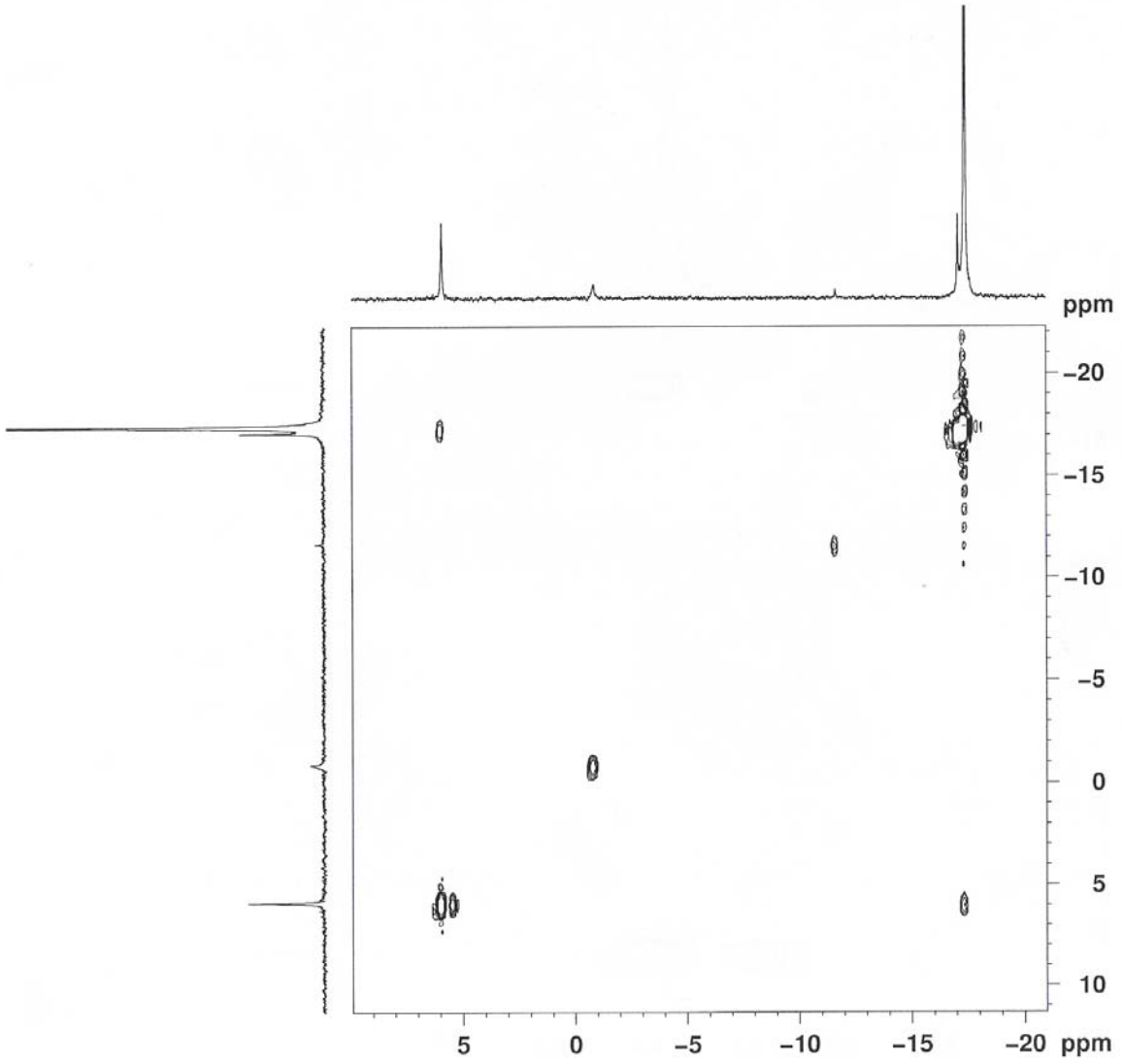

Fig. 88 CD_2Cl_2 EXSY ^{31}P-NMR spectrum of [{$Ir_4(CO)_{11}$}$_2$(dpphex)]

In our case the mechanism of this process should involves exchanging the basal plane of bridging CO ligands between two faces of the Ir_4 tetrahedron (Fig. 89). A concerted movement of three CO ligands inverts the position of all the other ligands, except for two bridging COs that maintain their original position at the end of the process. Consequently to the movement of COs, P atoms exchange position too, moving from radial to axial position and *vice-versa*.

^{13}C-NMR, registered on a ^{13}CO enriched sample (Fig. 90), shows in the carbonylic region seven peaks at 206.27, 195.70, 172.96, 171.12, 158.59, 157.14 and 156.35 ppm due to the main isomer A. They can be assigned by considering the typical chemical shifts trend for CO

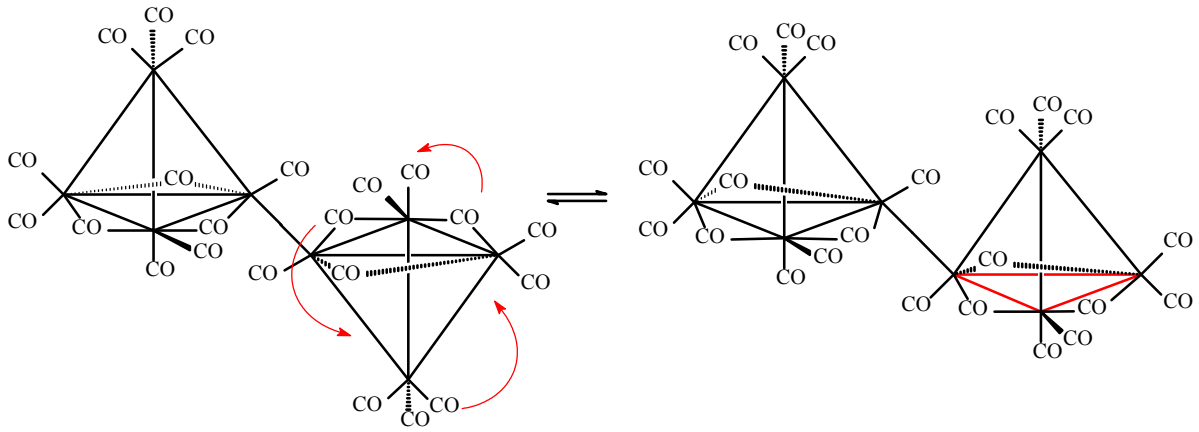

Fig. 89: Scrambling CO mechanism in [{$Ir_4(CO)_{11}$}$_2$(dpphex)]

ligands in substituted $Ir_4(CO)_{11}L$ compounds that is bridging>radial>axial≈apical.[154]
So, signals at 206,27 and 195,70 can be assigned to the μ-COs, 172,96 and 171,12 to radial COs, 158,59 and 157,14 to axial and apical COs and finally 156,35 to axial COs coordinated on the same Ir of P atoms.

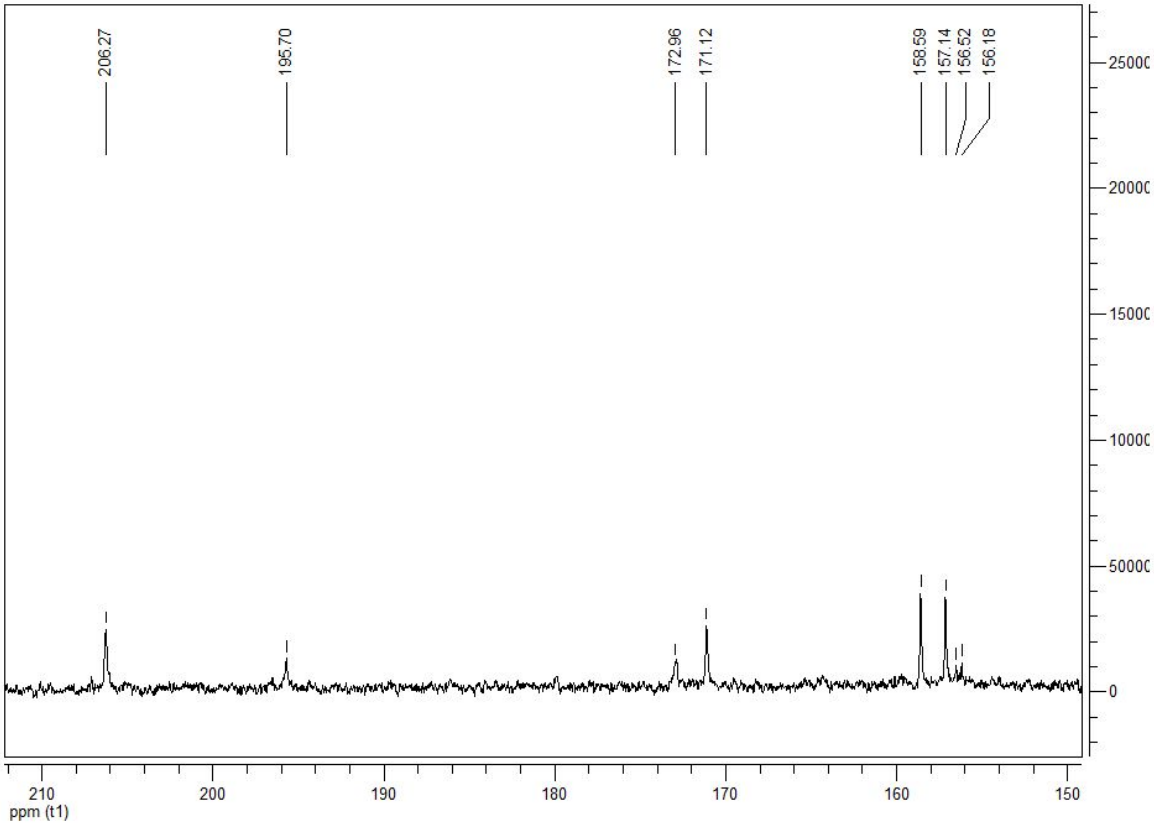

Fig. 90 ^{13}C-NMR of [{$Ir_4(CO)_{11}$}$_2$(dpphex)] registered at RT in $CDCl_3$

Synthesis and characterization of $[Ir_4(CO)_{11}(dpphex)]$

As in the previous case, the reaction of anionic cluster and dpphex in 1:1 molar ratio (RT and dichloromethane as solvent) leads to the fast substitutuion of Br- by the phosphane with formation of $[Ir_4(CO)_{11}(dpphex)]$, where dpphex acts like a monodentate ligand

$$PPh_4][Ir_4Br(CO)_{11}] + dpphex \longrightarrow [Ir_4(CO)_{11}(dpphex)] + [PPh_4]Br$$

Removing the solvent and washing the crude with acetonitrile the product is isolated with 54% yield, which can be enhance up to 62% conducting the reaction in acetonitrile. In this case the product precipitates from the solution.

Unfortunately all the attempts to get crystals suitable for X-ray analysis failed. Anyhow, basing on elemental analysis and spectroscopic data, it is possible to propose the structure in Fig. 91.

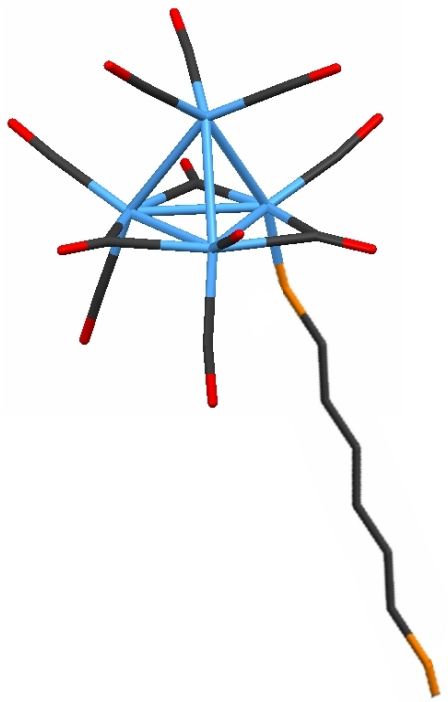

Fig. 91 Proposed structure of $[Ir_4(CO)_{11}(dpphex)]$

Spectroscopic characterization

Dichloromethane IR spectrum (Fig. 92) is very similar to those ones of [{$Ir_4(CO)_{11}$}$_2$(dpphex)] and others previously shown species.

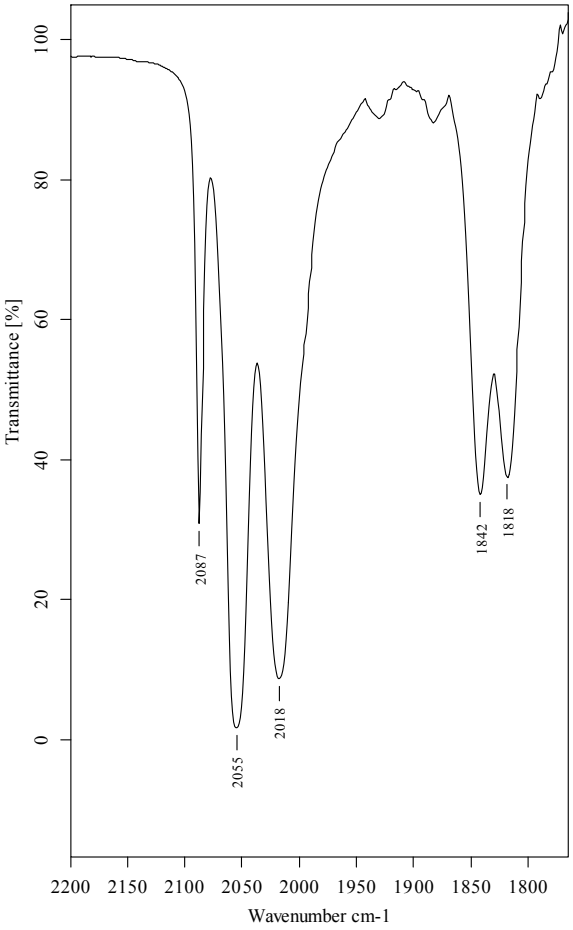

Fig. 92: CH_2Cl_2 IR spectrum of [$Ir_4(CO)_{11}$(dpphex)]

This fact is not strange, if we consider that the factors influencing the frequency and the shape of the carbonyl stretching bands (number and type of non carbonyl ligands and global charge of the molecule) are nearly the same for all these species.

^{31}P-NMR shows a broad peak at -14 ppm (due to the coordinated P atom) and one at -15,9 ppm (for the uncoordinated P atom) with 1:1 relative intensity. The peaks are attributed considering the free ligand chemical shift (-15,7 ppm), and the signal of {$Ir_4(CO)_{11}$}$_2$(dpphex)] at -14 ppm.

Synthesis and spectroscopic characterization of $[Ir_4(CO)_{10}(dpphex)]_2$

Conducting the reaction in CH_2Cl_2 a fast substitution of Br^- by a P atom is observed and the species $[Ir_4(CO)_{11}(dpphex)]$ (**2a**) shows carbonylic stretching band at 2087(s), 2055(vs), 2018(vs) cm-1 for terminal COs and 1842(s), 1818(s) cm^{-1} for edge-bridged COs. ^{31}P-NMR spectrum shows two peaks with 1:1 ratio at -14 ppm and -15,9 ppm. As the free ligand has a peak at -15,7 ppm, it is reasonable to attribute the first peak to the coordinated P atom and the second to the uncoordinated one. This solution evolves and while the bands of the P monosubstituted species decrease, lower frequencies bands due to a P disubstituted species appear. After *ca* 4 days a yellow powder of $[Ir_4(CO)_{10}(dpphex)]_2$, recognized by ATR-IR, elemental analysis and X-ray powder diffraction, precipitates in low yield. The solution shows carbonyl stretching bands at 2087(vw), 2066(s), 2041(vs), 2006(vs) cm^{-1} and 1821(m), 1796(m) cm^{-1} (Fig. 92). ^{31}P-NMR shows lot of peaks and thin layer chromatography confirms the presence of more than one species. They are likely to be variously substituted species like $[Ir_4(CO)_{10}(\mu\text{-}dpphex)]$ (**2b**), $[\{Ir_4(CO)_{10}(\mu\text{-}dpphex)\}\{Ir_4(CO)_{11}(dpphex)\}]$ (**2d**) and $[\{Ir_4(CO)_{10}(dpphex)\}\{Ir_4(CO)_{11}(dpphex)\}]$ (**2c**). This lack of selectivity can explain the low yield obtained. Fig. 93 summarizes the possible reaction paths.

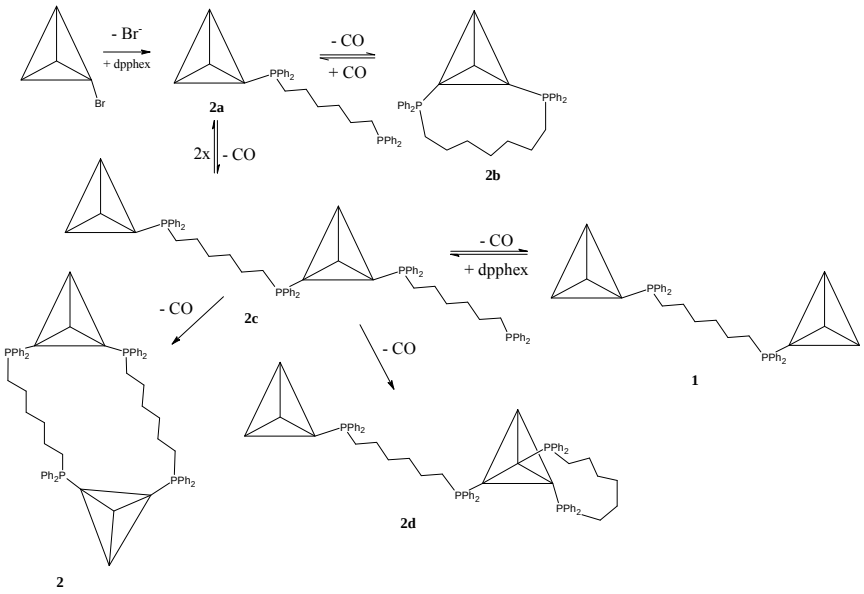

Fig. 93 Possible reaction paths and equilibra

Synthesis of **2** from **1** and an equivalent of dpphex works with a higher yield than starting directly from $[Ir_4Br(CO)_{11}]^-$ likely because formation of **2b** is hindered.

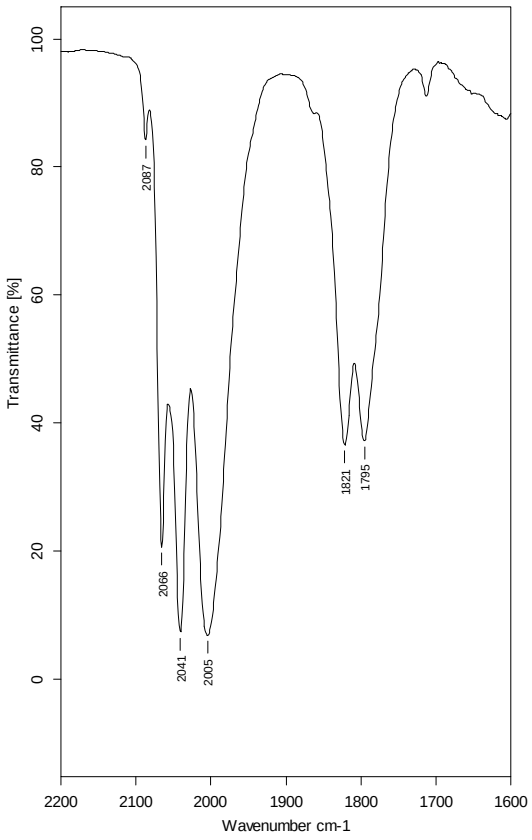

Fig. 94 From this solution $[Ir_4(CO)_{10}(dpphex)]_2$ precipitates

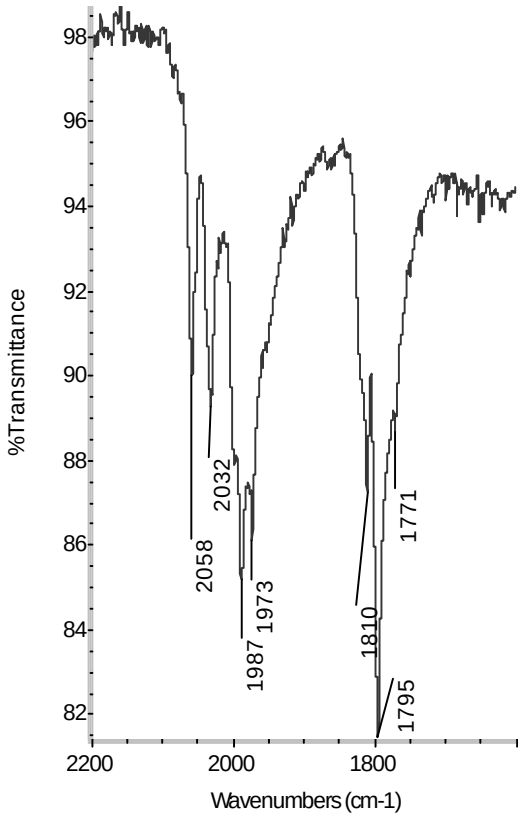

Fig. 95 ATR-IR of $[Ir_4(CO)_{10}(dpphex)]_2$

Solid state structure

Crystals suitable for X-ray diffraction have been obtained by layering a dichloromethane solution of cluster with a n-heptane solution of dpphex (Fig. 96).

$[Ir_4(CO)_{10}(dpphex)]_2$ has a ring structure including the Ir_4 cages and the dpphex ligands. Each cage has a pseudo-C_{3v} stereochemistry with a basal plane defined by the three edge-bridged COs. Two coordination sites are occupied by the phosphane groups, one in axial and the other in radial position.

This configuration is likely induced by the steric demand of the ligands.

So, only one Ir-Ir edge lying in the basal plane belongs to the twenty terms ring. Each cluster coordinate ten CO groups too: three edge bridged and seven terminal.

Unlike $[Ir_4(CO)_{10}(dpppent)]_2$ (dpppent = 1,5-bis(diphenylphosphano)pentane), an analogous species previously synthesised, this ring has a low symmetry.

This is because phosphourus atoms of a same ligand occupy the same coordination positions on the cages. This means that one dpphex is axial-axial bonded, while the other is radial-radial bonded, locating the tetrahedrons unsimmetrically respect to the centre of the ring.

Moreover the radial-radial dpphex is more contracted than the other. For steric reasons, the cages are exo-cyclic arranged, with two axial COs pointing to the centre of the ring.

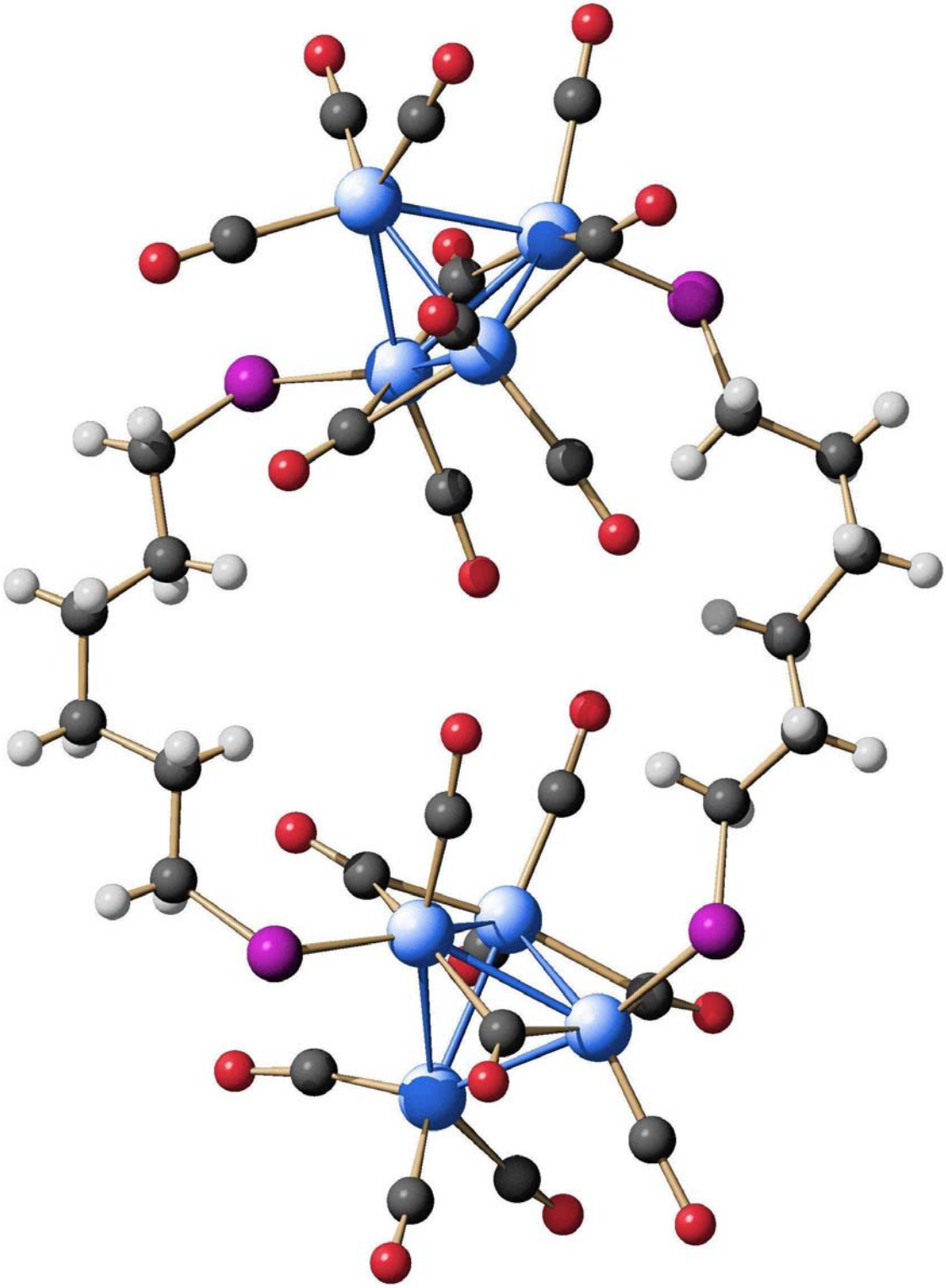

Fig. 96 Solid state structure of $[Ir_4(CO)_{10}(dpphex)]_2$. Phenyls are omette for clarity.

The conformations at each C-C bond are not all trans and this decrease the molecular volume. In fact there is not accessible volume for guest molecules inside the rings but only in the intermolecular regions.

In the following table some significant bond lengths are reported.

Bond	$[Ir_4(CO)_{10}(dpphex)]_2$ Å
Ir-Ir (average)	2,760
C-O (average)	1,176
Ir-P	2,340

Synthesis and characterization of $[\{Ir_4(CO)_9\}_2(dpphex)_3]$

Solvothermal reaction of $Ir_4(CO)_{12}$ with dpphex (CH_2Cl_2/ n-heptane 1:2, T = 403 K, t = 16 h) gave yellow crystals of $[\{Ir_4(CO)_9\}_2(dpphex)_3 \bullet (CH_2Cl_2)]$, 51% yield (Fig. 95).

Two $Ir_4(CO)_9$ cages are linked by three dpphex molecules, two radial-radial coordinated, with a P-P distance of 7,718 and 7,975 Å, and one axial-axial, with a P-P distance of 8,631 Å.

So, each Ir_4 tetrahedron has two radially and one axially coordinated P atoms. Nine COs, three edge-bridged and six terminal, complete the coordination sphere at each cluster; a dichloromethane molecule is also chlatrated. ATR-IR spectrum shows carbonyl stretching bands at 2036(m), 1998(m), 1972(s), 1952(s) cm^{-1} (terminal COs) and 1774(s), 1760(vs) cm^{-1} (edge-bridged COs) (Fig. 97).

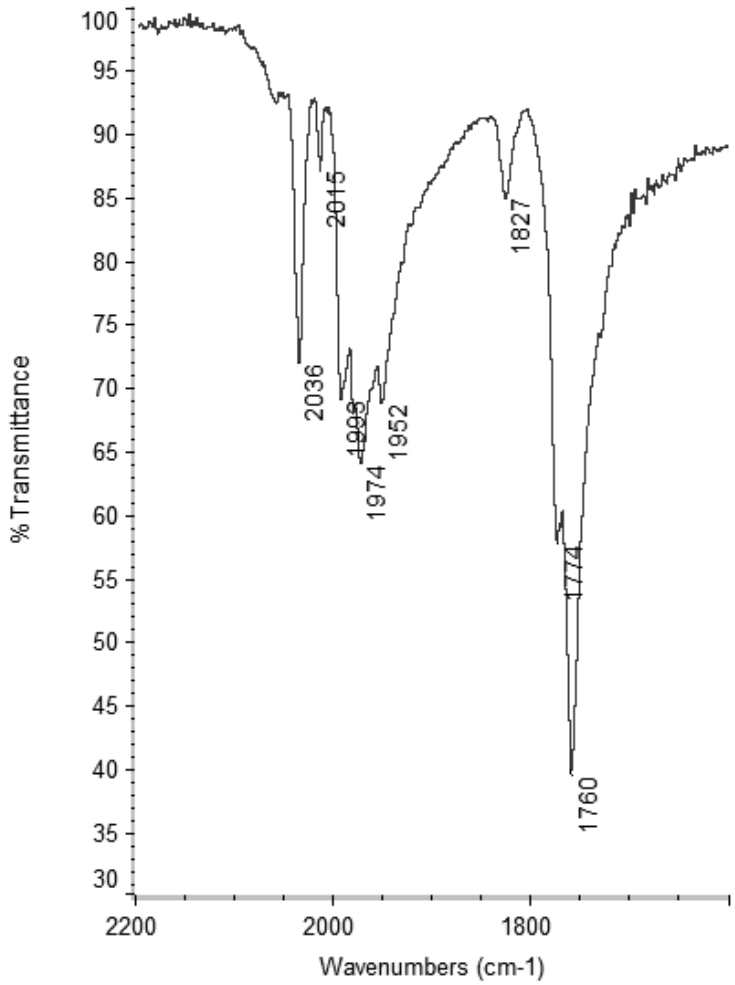

Fig. 97 ATR-IR spectrum of $[\{Ir_4(CO)_9\}_2(dpphex)_3]$

This new compound is closely related with the two others previously reported,[155] $\{[Ir_4(CO)_{11}]_2(dpphex)\}$ and $[Ir_4(CO)_{10}(dpphex)]_2$.

They can be considered as a series in which two Ir_4 cluster are linked by one, two, or three dpphex ligands. As the double linked cyclic dimer compound, also $[\{Ir_4(CO)_9\}_2(dpphex)_3 \bullet (CH_2Cl_2)]$ is sparingly soluble in all common solvents, preventing NMR or other in-solution studies.

In the following table some significant bond lengths are reported.

Bond	$[\{Ir_4(CO)_9\}_2(dpphex)_3]$ Å
Ir-Ir (average)	2,728
C-O (average)	1,153
Ir-P (average)	2,304

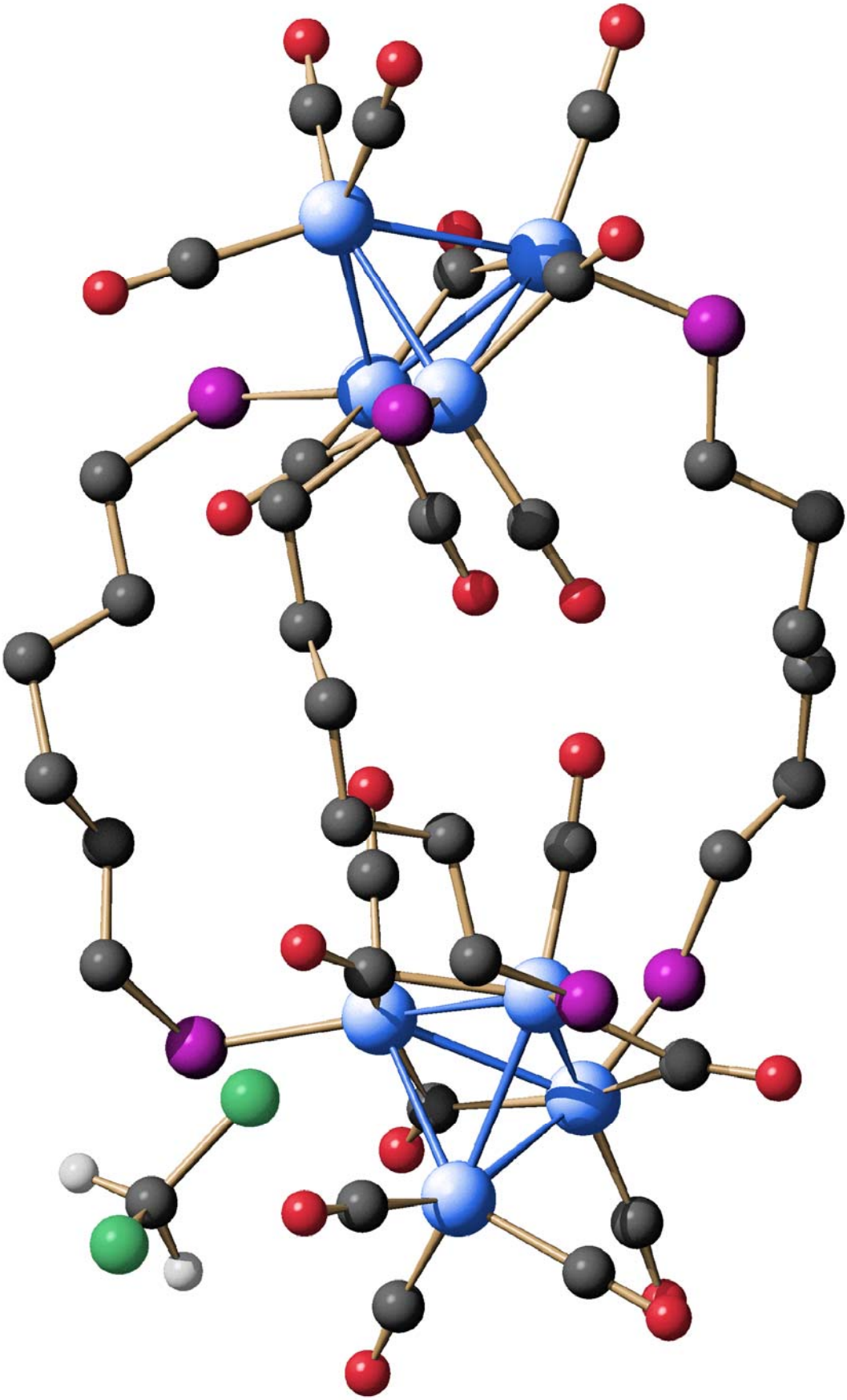

Fig. 98 X-ray structure of [{$Ir_4(CO)_9$}$_2$(dpphex)$_3$•(CH_2Cl_2)]. Phenyl groups are omitted for clarity.

Reactivity of $[RhCl_2(CO)_2]^-$ with flexible diphosphanes

Diphosphanes containing a flexible alkyl chain, with general formula $PPh_2(CH_2)_nPPh_2$ (n = 1-4), easily reacts with $[RhCl_2(CO)_2]^-$ or $[Rh_2Cl_2(CO)_4]$ leading to a neutral species, according to a substitution reaction favoured by the elimination of a chloride ion and a CO molecule on each rhodium atom:

$$m[PPh_4][RhCl_2(CO)_2] + mPPh_2(CH_2)_nPPh_2 \rightarrow [RhCl(CO)(PPh_2(CH_2)_nPPh_2)]_m + mPPh_4Cl + mCO$$

m = 1 o 2

Depending on the alkyl chain length, different species have been described:[156] the formation of cyclic molecules is usually observed, where two diphosphane ligands bridge two metal atom, whose coordination spheres are completed by a chloride ion and a CO molecule (Fig. 99/1a).

The only exception is 1,2-bis(diphenylphosphano)ethane (n = 2) that prefers the chelation on the same rhodium atom (Fig. 99/1b).

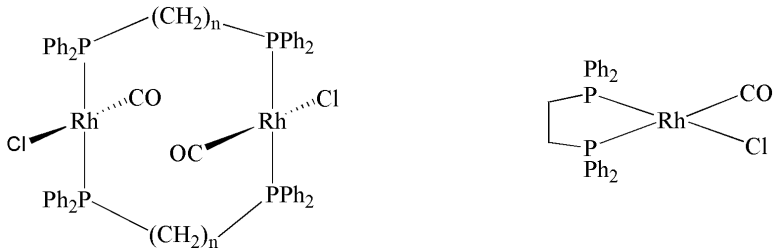

1a 1b

Fig. 99 Cyclic species obtained starting from $[RhCl_2(CO)_2]^-$ and $PPh_2(CH_2)_nPPh_2$

These data suggested to study deeper this coordination chemistry field, by exploring the reactivity of phosphanes having five and six C atoms alkyl chains. With 1,5-bis(diphenylphosphano)pentane a cyclic dimer was isolated;[157] with 1,6-bis(diphenylphosphano)hexane, the cyclic dimer and a 1D coordination polymer were characterized.

To enrich our knowledge, we have here explored the reactivity of long chain phosphanes, with n = 8, 10 and 12, to verify if the dpphex were the only to give the polymer.
Actually with 1,8-bis(diphenylphosphano)octane a polymer has been obtained, while with the other phosphanes we found only discrete species.

Reactivity of $[RhCl_2(CO)_2]^-$ with 1,8-bis(diphenylphosphano)octane (dppo)

The reaction between $[RhCl_2(CO)_2]^-$ and 1,8-bis(diphenylphosphano)octane (RT and dichloromethane as solvent) is fast, as observed monitoring by IR spectroscopy. The bands at 2069 and 1991 cm^{-1} (A) disappeared for a band at 1968 cm^{-1} (B) (Fig. 100). In the ^{31}P-NMR a broad doublet at 25 ppm is observed (Fig. 101).

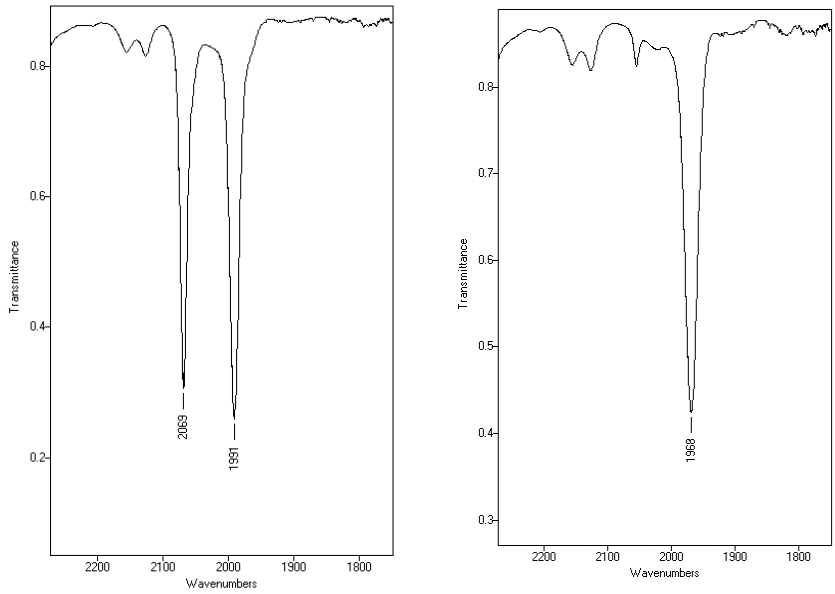

a) **b)**

Fig. 100 CH_2Cl_2 IR spectrum of a) $[RhCl_2(CO)_2]$ and b) $[RhCl(CO)(dppo)]_2$

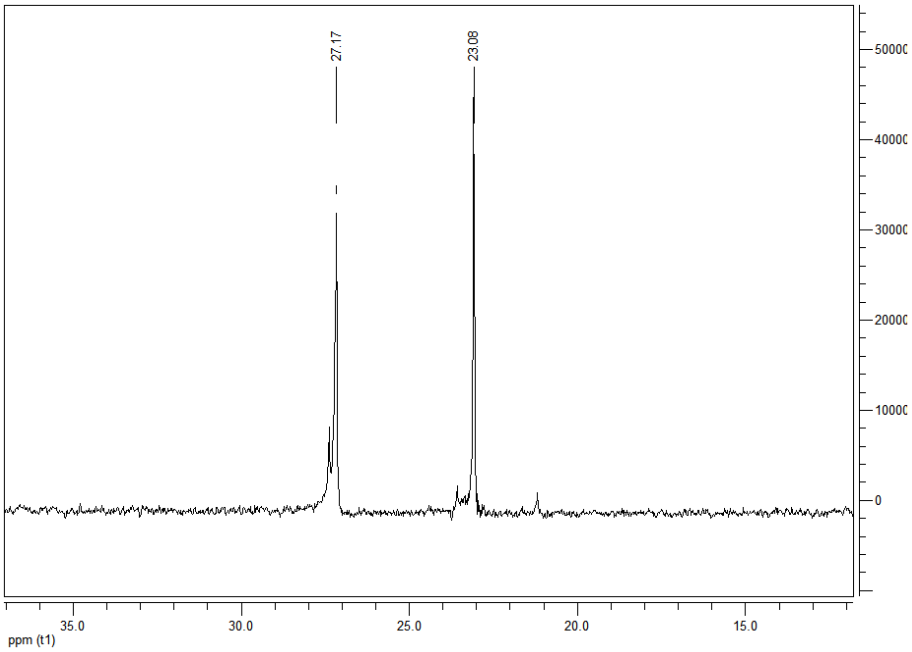

Fig. 101 Acetone ^{31}P-NMR of [RhCl(CO)(dppo)]$_2$

Spectroscopic data suggest the idea that a cyclic species is formed, like the ones described for the other diphosphanes (Fig. 102).

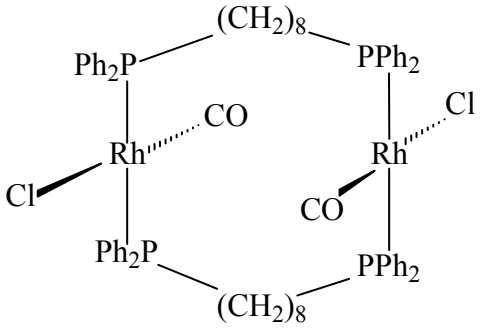

Fig. 102 Hyphotized cyclic dimer for dppo

Unlike observed for other phosphanes, from this solution does not precipitate any solid, nor after several hours. This solution was layered with 2-propanol, obtaining crystals suitable for X-ray analysis. These yellow crystals were insoluble in all common organic solvents, being characterized by a carbonyl stretching band at 1978 cm^{-1} (ATR-IR, Fig. 103).

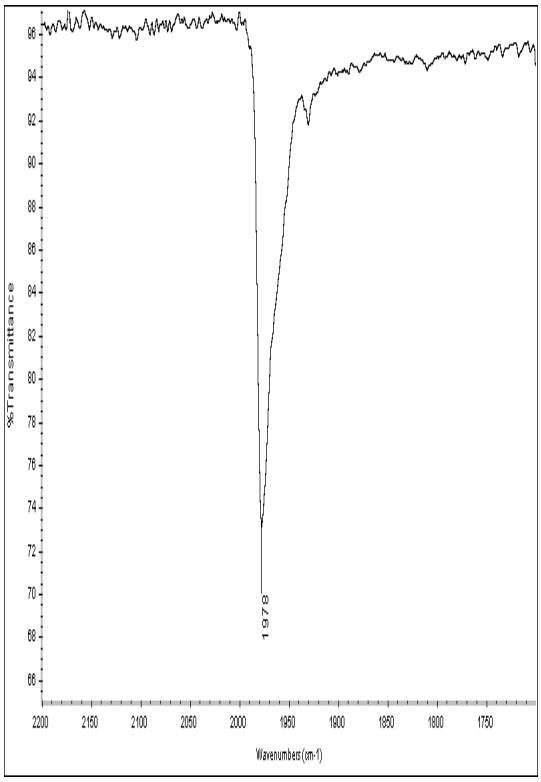

Fig. 103 ATR- IR spectrum of [RhCl(CO)(dppo)]$_\infty$

Surprisingly, the crystallized species was not the same observed in solution, but a 1D coordination polymer of formula [RhCl(CO)(dppo)]$_\infty$. We can so image that the ring is the precursor of the polymer that is believed to form with a ring-opening-polymerization mechanism (Fig. 104), yet described by James for an Ag(I) – dppa system.[158]

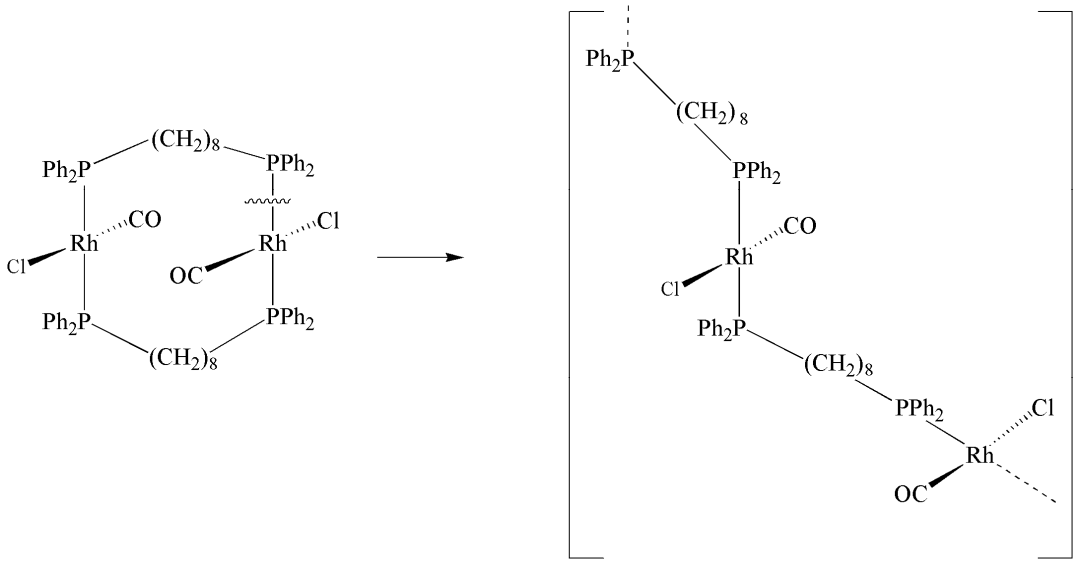

Fig. 104 Ring opening polymerization mechanism

If the reaction is conducted at higher concentration (about 0,1 M), the product directly precipitates from the dichloromethane solution as microcrystalline powder, that can be checked by XRPD.

Even if we do not know the average molecular weight, supposing that speaks about average molecular weight for a coordination polymer makes sense, it is possible to calculate the reaction yield.

If the repeating unit is known, the yield is the ratio between the rhodium amount in the reactant and the amount in the product.

$$n[PPh_4][RhCl_2(CO)_2] + n\ dppo \rightarrow [RhCl(CO)(dppo)]_n + n\ CO + n\ [PPh_4]Cl$$

$$Yield\% = [(m_\infty \cdot n_\infty)/ (m_r \cdot n_r)]*100$$

Where: n_r is the weight metal ratio in the reactant

m_r is the weight of the reactant

n_∞ is the weight metal ratio in the repeating unit.

m_∞ is the weight of the polymer

Crystals, suitable for X-ray analysis, were also obtained by layering a dichloromethane solution of Rh(I) salt with a THF solution of the ligand.

Finally this product was prepared in solvothermal condition, by heating the reagent in M : L 1:2 molar ratio at 90°C (ethanol as solvent).

Solid state structure

The solid state structure was obtained by single crystal X ray diffraction (Fig. 105).

This material is composed by polymeric chain where the rhodium atoms are linked by diphosphanes. The metallic centre is in square planar geometry and it bonds two P atoms, owning to different ligand molecules, in trans position, a chlorine atom and a CO molecule.

The alkyl chain are not completely extended, because one C-C bond is in gauche conformation, as it is possible to see in Fig. 106.

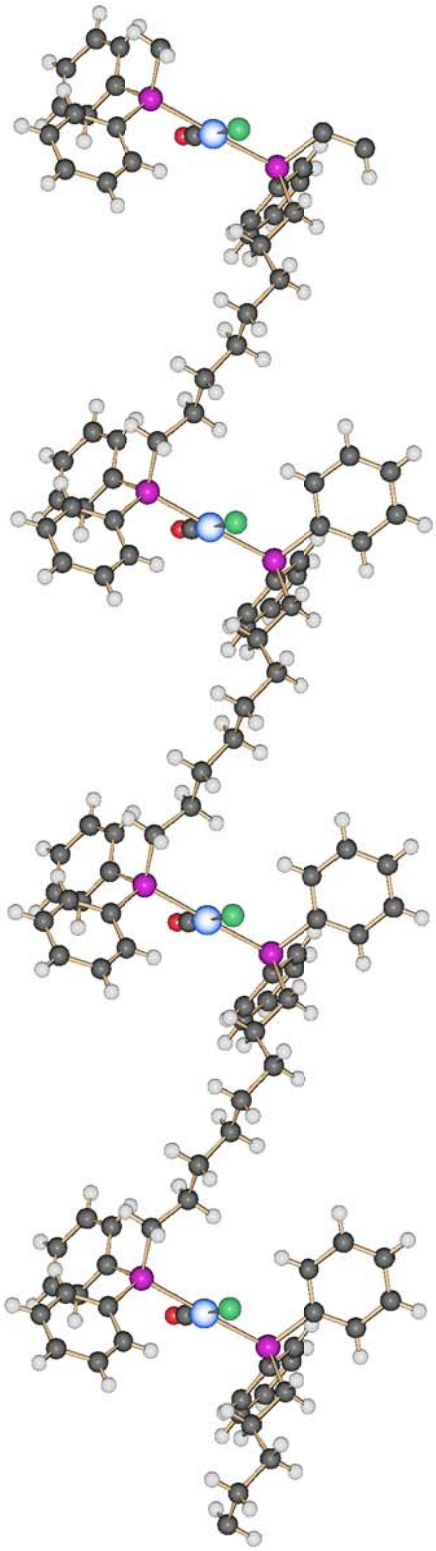

Fig. 105 View along b of a chain fragment of [RhCl(CO)(dppo)]$_\infty$

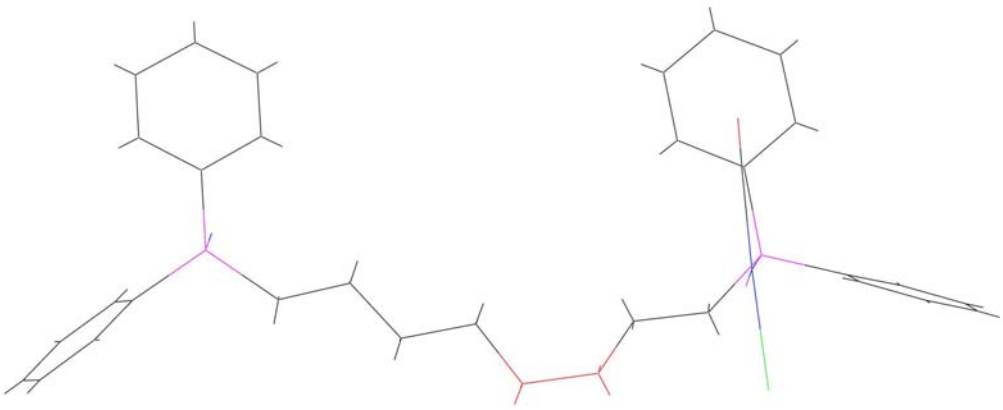

Fig. 106 Repeating unit of $[RhCl(CO)(dppo)]_\infty$. The C-C bond in gauche conformation is in red.

The polymer crystallizes without chlatrated molecules, unlike $[RhCl(CO)dpphex]_\infty$; the chains arrange in parallel with the ac plane closely and the crystal packing does not leave any space to host guest molecules (Fig. 107).

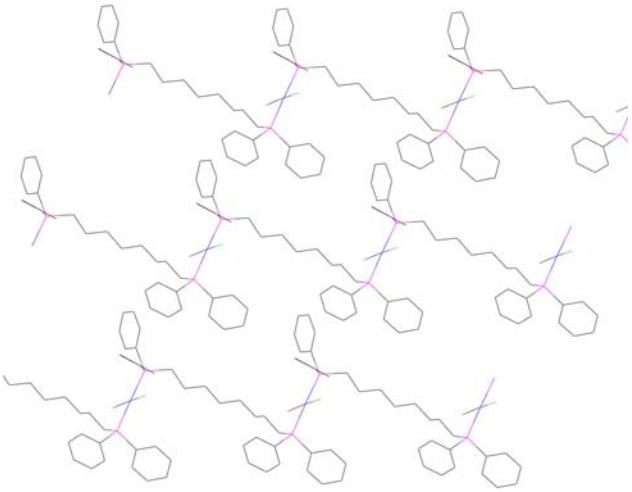

Fig. 107 Chain packing in the ac plane

Reactivity of $[RhCl_2(CO)_2]^-$ and 1,10-bis(diphenylphosphano)decane (dppdec)

The reaction between $[RhCl_2(CO)_2]^-$ and 1,10-bis(diphenylphosphano)decane (RT and dichloromethane as solvent) is fast as observed monitoring the reaction by IR spectroscopy. The reactant bands at 2069 e 1991 cm^{-1} (Fig. 108a) disappeare for a band at 1968 cm^{-1}(Fig. 108b).

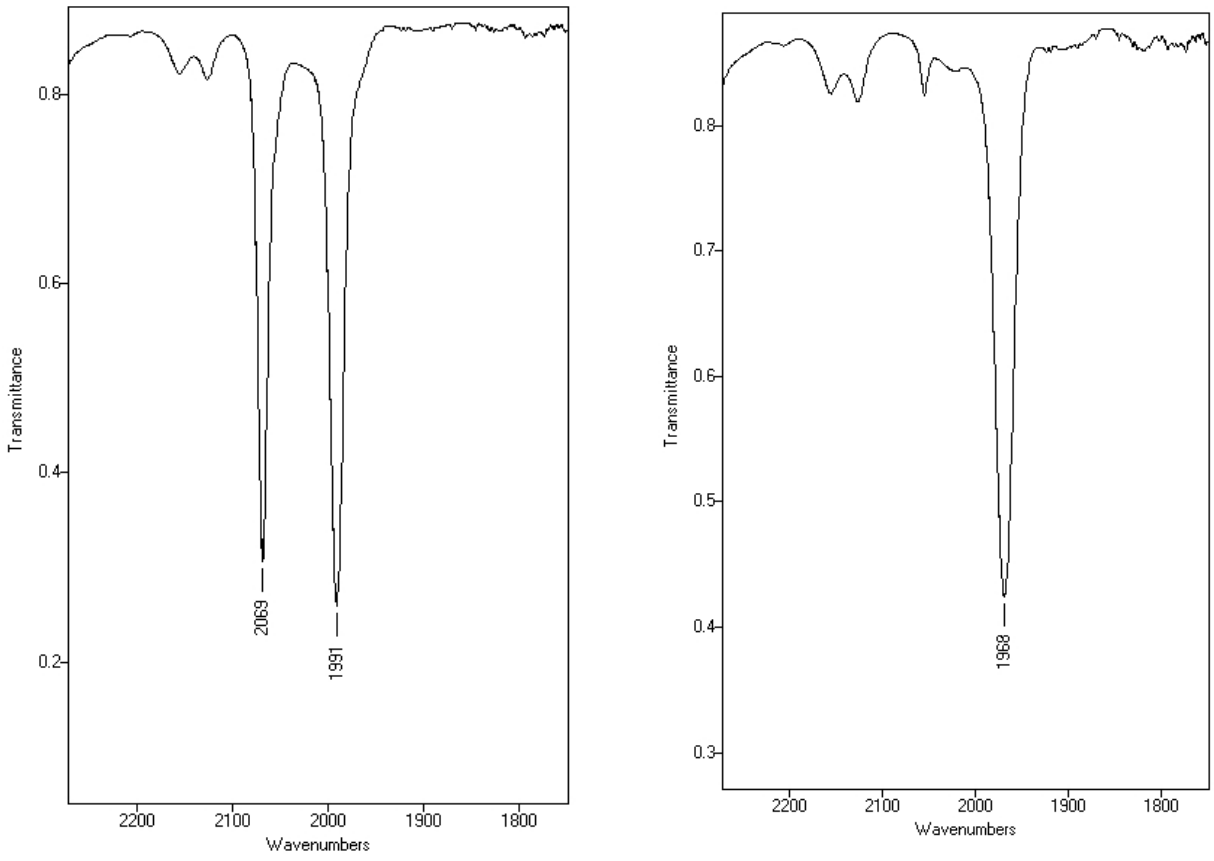

a **b**

Fig. 108 CH_2Cl_2 IR of a) $[RhCl_2(CO)_2]^-$ and b) $[RhCl(CO)(dppdec)]_2$

^{31}P-NMR spectrum shows one doublet at 28,5 ppm ($^3J_{Rh\text{-}P}$ = 103,4 Hz) (Fig. 109).

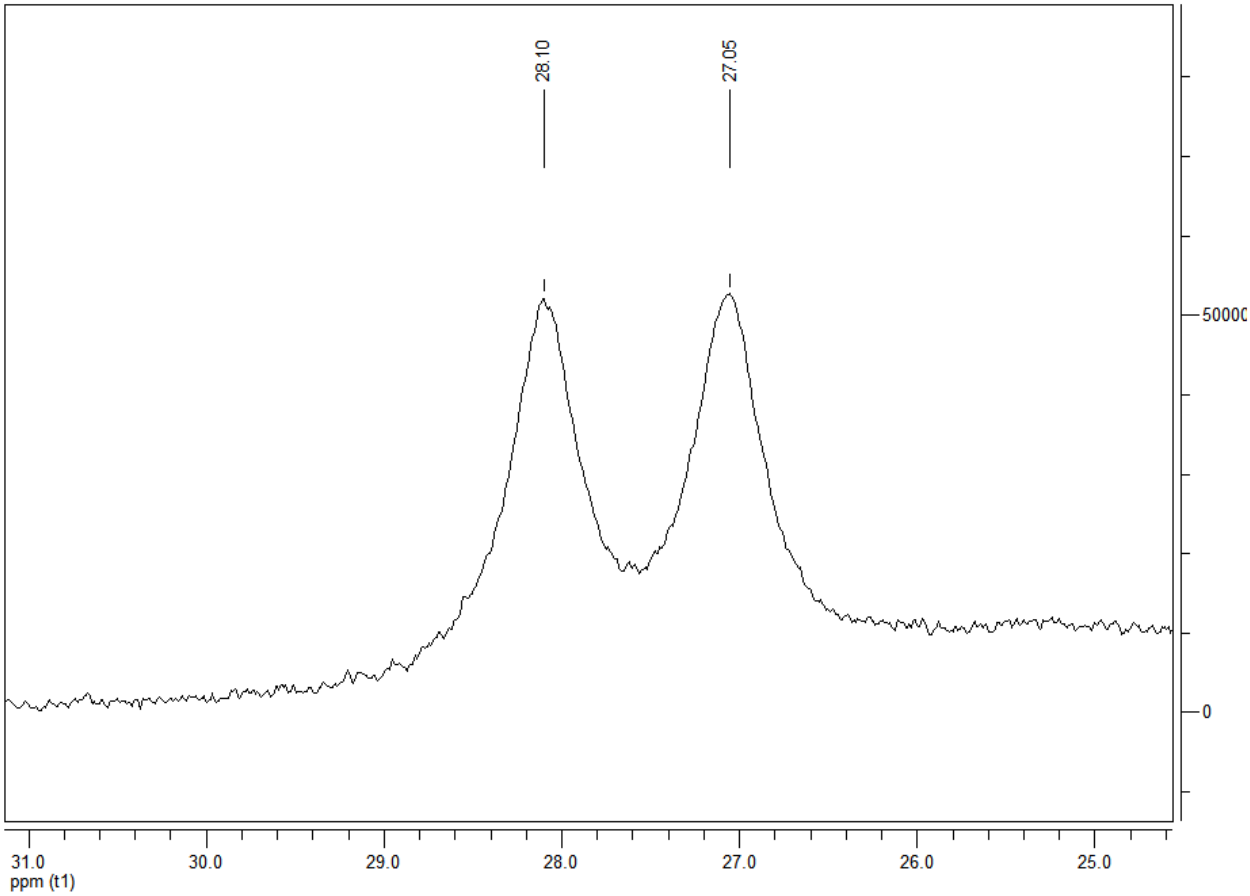

Fig. 109 $CDCl_3$ ^{31}P-NMR spectrum of $[RhCl(CO)(dppdec)]_2$

As for dppo, spectroscopic data agree with the formation of a cyclic dimer, $[RhCl(CO)_2(dppdec)]_2$ (Fig. 110), but in this case it does not evolve to a polymeric species in any condition.

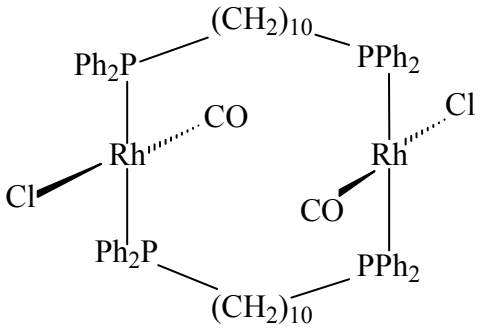

Fig. 110 Cyclic dimer observed with dppdec

Reactivity of $[RhCl_2(CO)_2]$- and 1,12-bis(difenilfosfino)dodecano (dppdod)

As for dppo and dppdec, the reaction of $[RhCl_2(CO)_2]^-$ and 1,12-bis(diphenylphosphano)dodecane (RT and dichloromethane as solvent) results in the appearance of a carbonyl stretching band at 1968 cm^{-1} in place of those at 2069 and 1991 cm^{-1}. This solution was layered with 2-propanol, obtaining yellow crystals that resulted to be $[RhCl(CO)(dppdod)]_2$. These crystals was than dissolved in dichloromethane, showing in the IR spectrum a CO stretching band at 1968 cm^{-1} (Fig. 111) and in the ^{31}P-NMR spectrum a doublet at 26,1 ppm ($^3J_{Rh\text{-}P}$ = 125,0 Hz, Fig. 112).

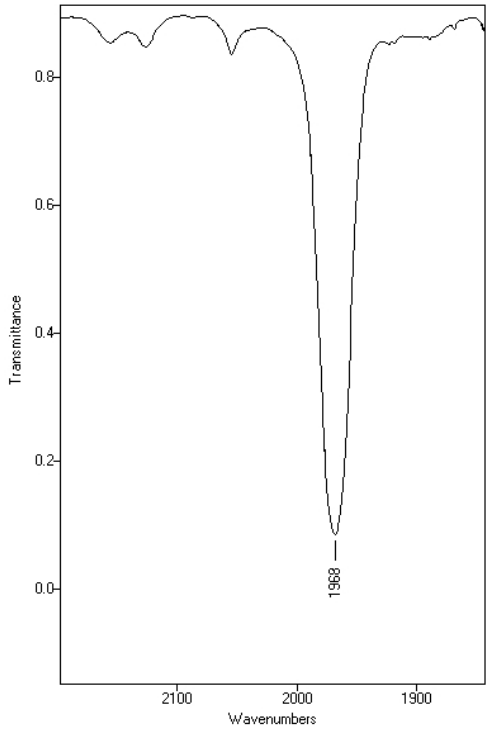

Fig. 111 CH_2Cl_2 IR of crystals of $[RhCl(CO)(dppdod)]_2$

Even repeating the reaction at high concentration, or heating the reactants in refluxing ethanol, formation of polymeric species was not observed, but again the cyclic dimer was obtained.

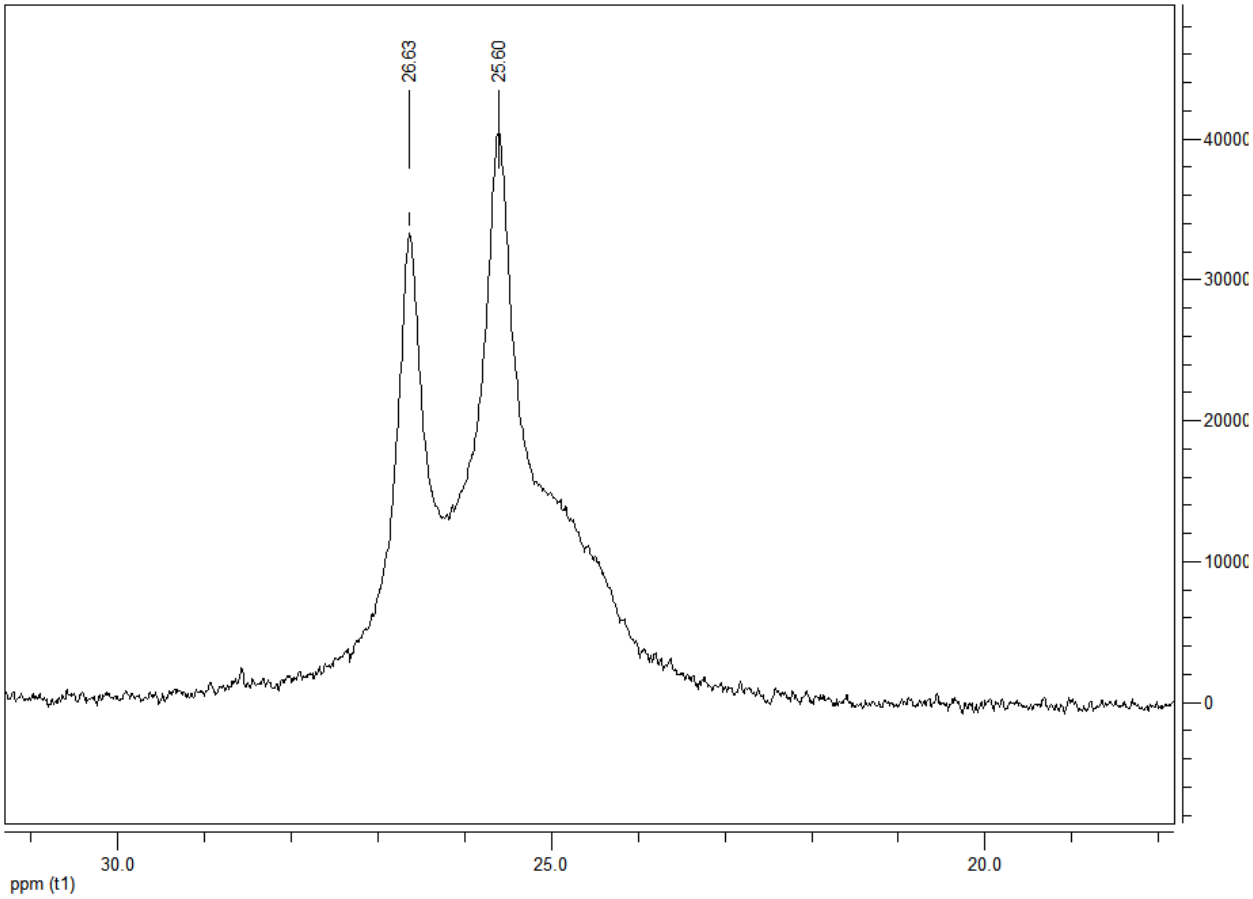

Fig. 112 CD_2Cl_2 ^{31}P-NMR of $[RhCl(CO)(dppdod)]_2$

Solid state structure

The structure was obtained by single crystal X ray diffraction. The molecule is a 30 – membered ring where two dppdod ligands bridge two squared planar Rh(I) centres, beig coordinated in trans positions (Fig. 110). A chlorine atom and a CO molecules complete the coordination sphere at each metal atom. So, this is an example of Vaska-type compound.

In Fig. 113 only eleven CH_2 groups instead of 12 are shown because the alkyl are higly disordered and the best disorder rationalization fits with the arbitrarily removing of a carbon atom.

The compound crystallizes without any solvent molecule.

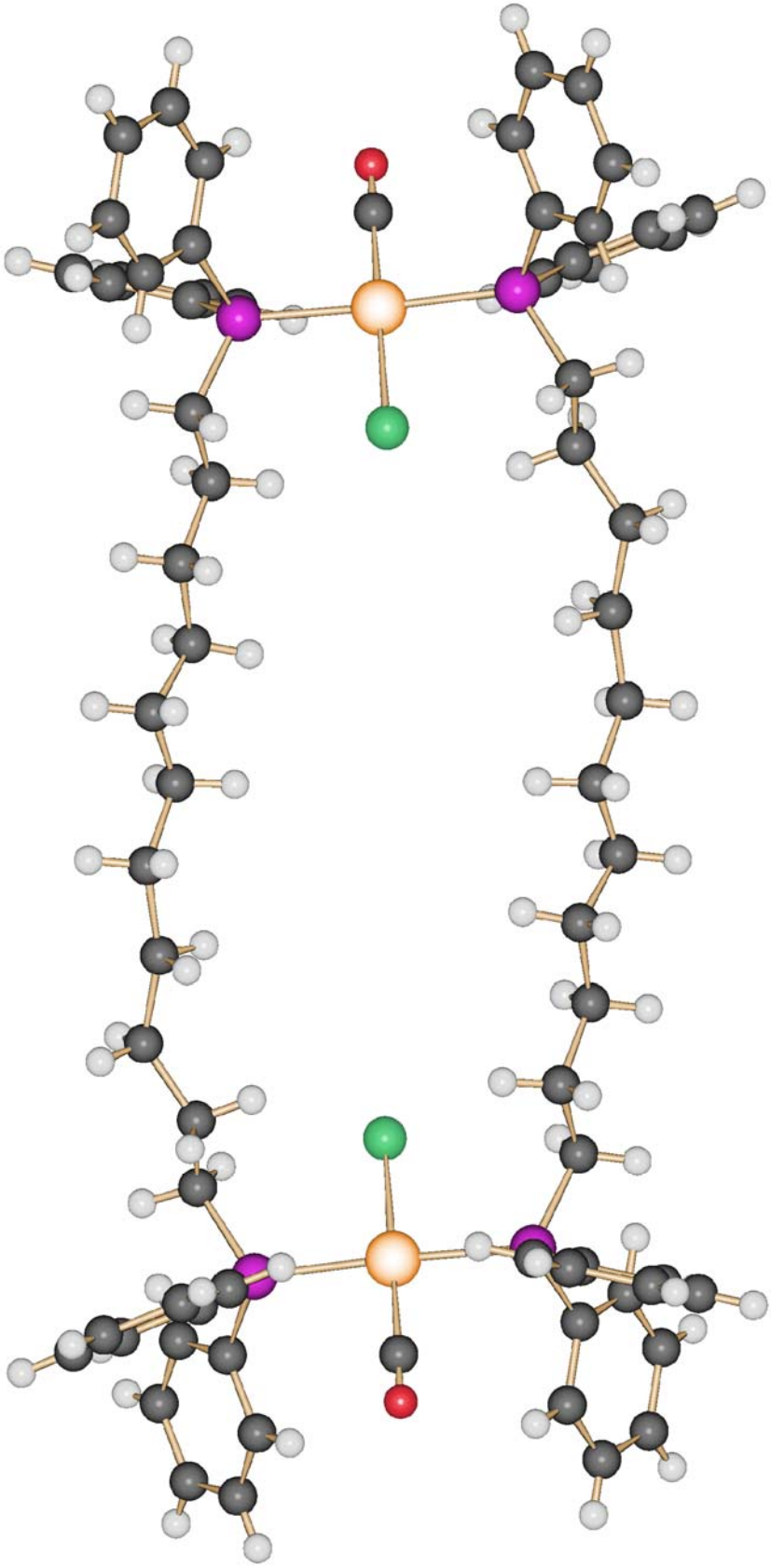

Fig. 113 Solid state structure of $[RhCl(CO)(dppdod)]_2$

This result lets us to indirectly confirm the identity of the products obtained in the case of dppo and dppdec.

We can so conclude that these diphosphanes have a very similar reactivity, although only in the case of dppo the cyclic dimer evolves to give the corresponding coordination polymer.

Synthesis of [$RhClI_2(CO)(dppdod)$]

We know that Vaska-type 1D coordination polymer react with RI or I_2 to give the oxidative addiotion, forming Rh(III) centres.

So, while we were not able to obtain a polymer based on Rh(I) and dppdod, we thought to synthesised an oxidized form of it, by reacting Rh(I), I_2 and dppdod.

Surprisingly we did not get the desired product but a ring molecule where a dppdod chelates a Rh(III) centre with the P atoms in trans positions.

The compound shows, in the ATR-IR spectrum, a carbonyl stretching band at 2079 cm^{-1} (Fig. 114), in agreement with the reported data for CO coordinated to a Rh(III) centre.

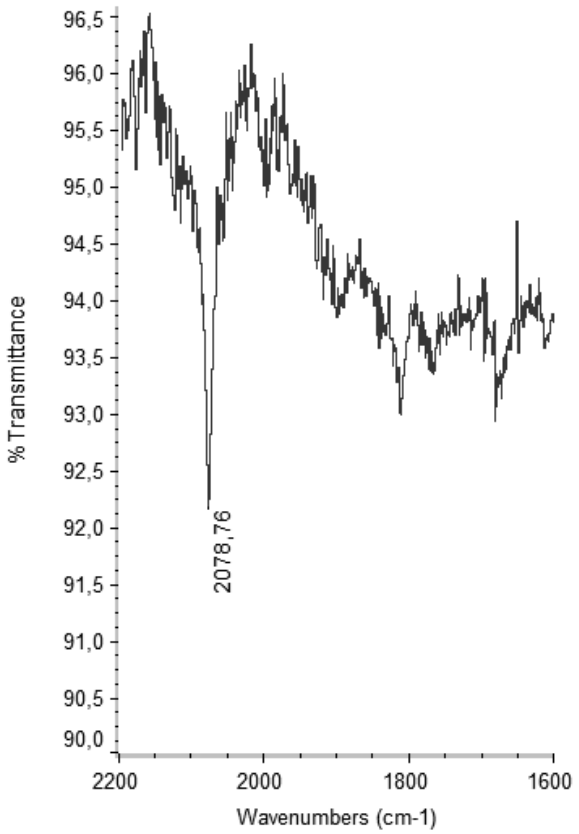

Fig. 114 ATR-IR spectrum of [$RhClI_2(CO)(dppdod)$]

In the ^{31}P-NMR there are three signals: a triplet at 10,22 ppm, a multiplet at 3,04-0,39 ppm and a doublet at -8,02 ppm, with a relative ratio of about 1 : 2,5 : 1 (Fig. 115).

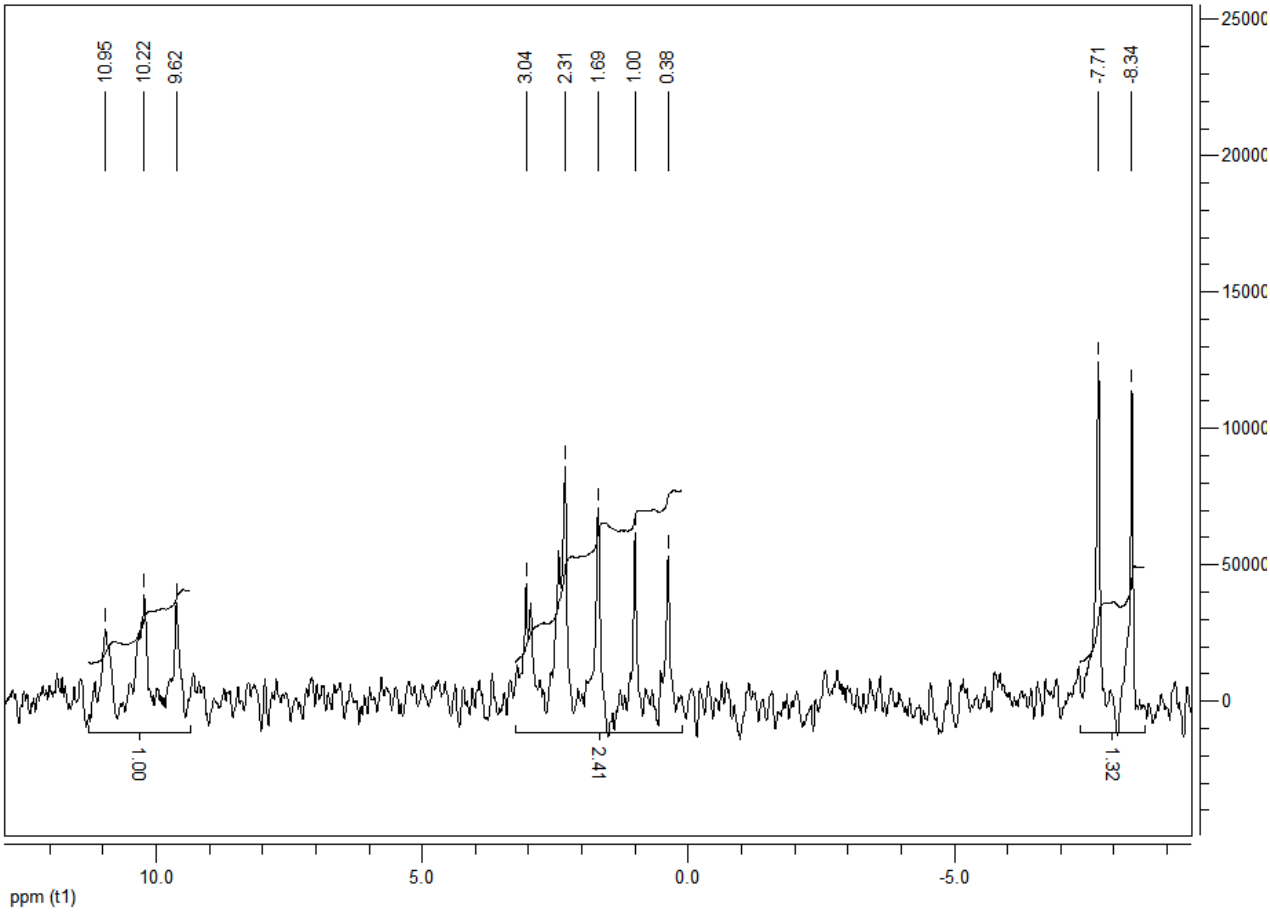

Fig. 115 $CDCl_3$ ^{31}P-NMR registered for [$RhClI_2$(CO)(dppdod)]

Solid state structure

The solid state structure was obtained by single crystal X-ray diffraction. The 18e$^-$ Rh(III) centre in octahedral geometry is part of a 15 members ring (Fig. 116). The dppdod molecule chelates two trans position of the metal and two other trans position are occupied by the iodine atoms.

The geometry is completed by a CO molecule and a chlorine atom.

This result quite unusual as, from an entropic point of view, a "long" ligand is expected to hardly chelate.

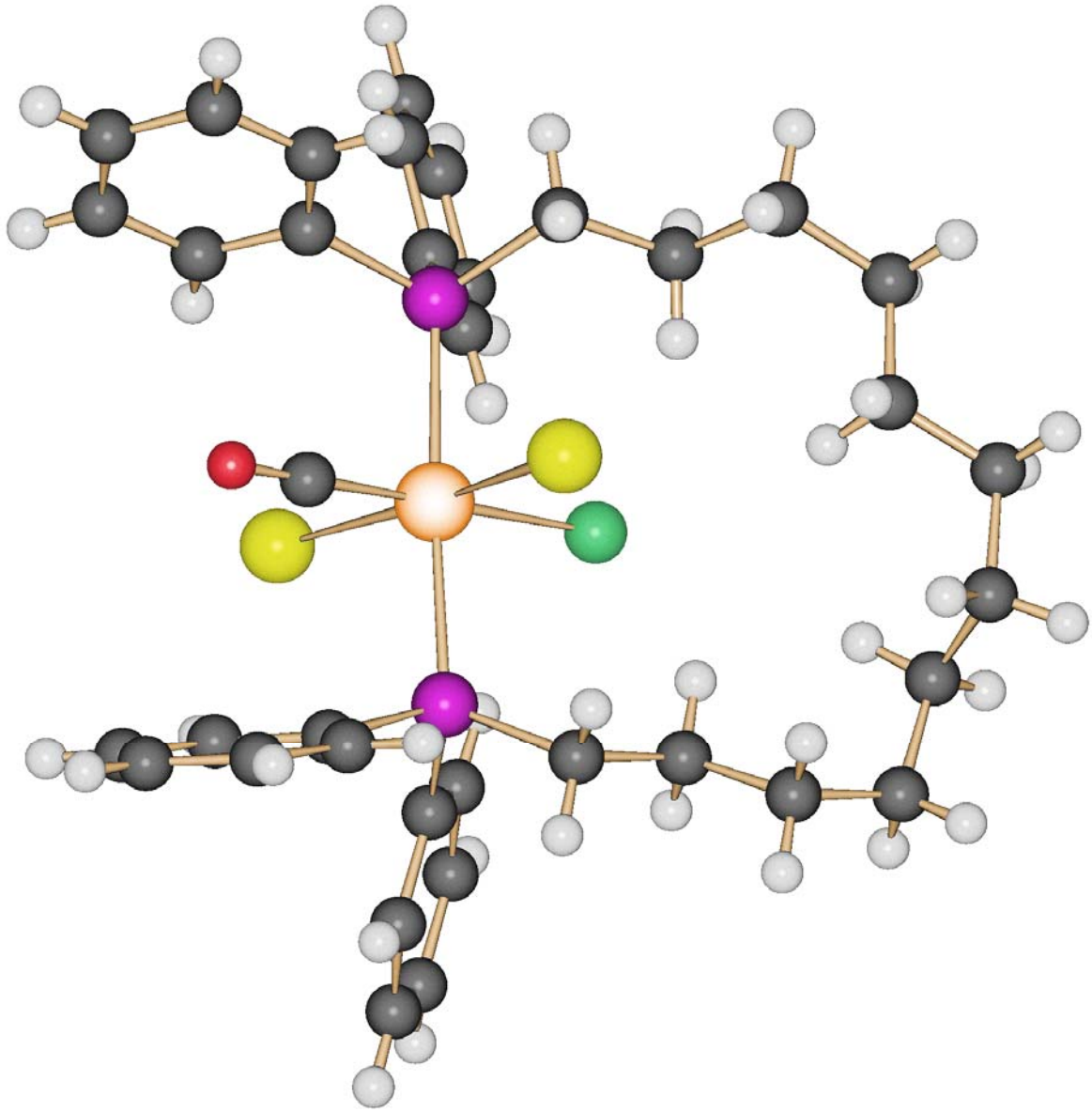

Fig. 116 X-ray structure of [$RhClI_2(CO)$(dppdod)]

RIGID POLIPHOSPHANES

Six rigid poliphosphanes ligands, having an aromatic skeleton as spacer and fuor, six or eight PPh_2 groups have been synthesised.

3,3′-5,5′-tetrakis(diphenylphosphano)biphenyle (180tetraphos)

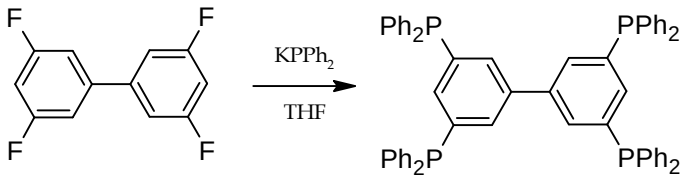

Reaction between 3,3′-5,5′-tetrafluorobiphenyle[159] with $KPPh_2$ in refluxing THF leads to the corresponding phosphane in high yield

One singlet at -3,86 ppm ($CDCl_3$) is present in the 31P-NMR spectrum (Fig. 117)

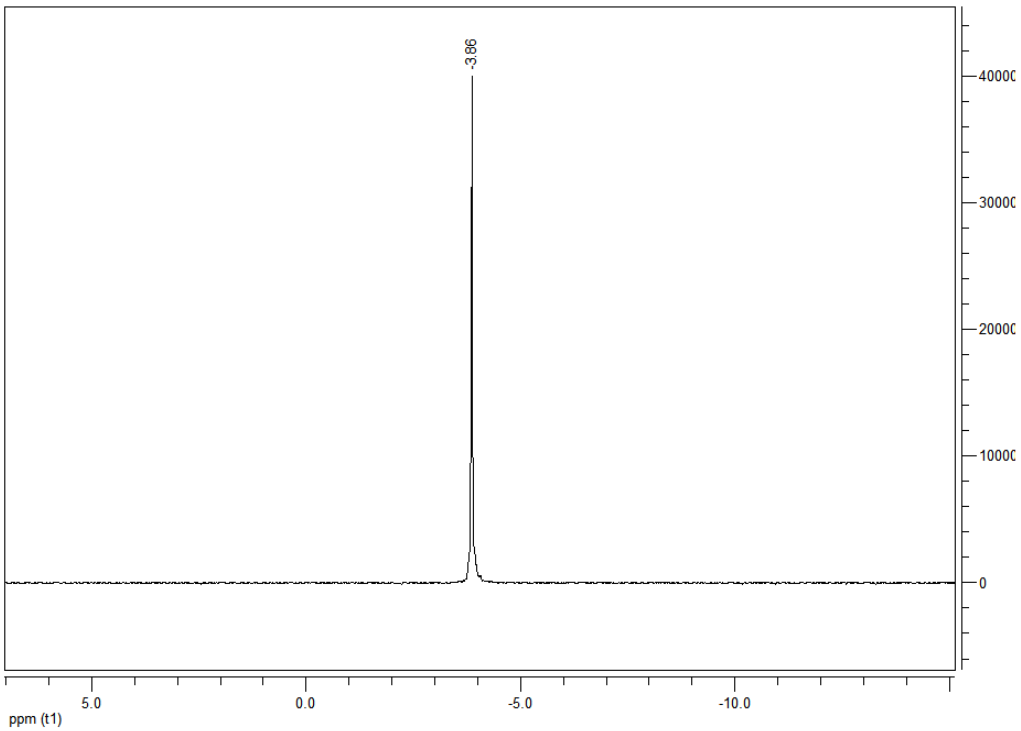

Fig. 117 $CDCl_3$ ^{31}P-NMR of 180tetraphos

^{1}H NMR is consistent with the structure, showing a multiplet for the hydrogen owning to phosphorus phenyls, a triplet of triplet for the hydrogen in 3, 3′ positions and a doublet of doublet for the hydrogen in 1,1′ – 5, 5′ positions (Fig. 118)

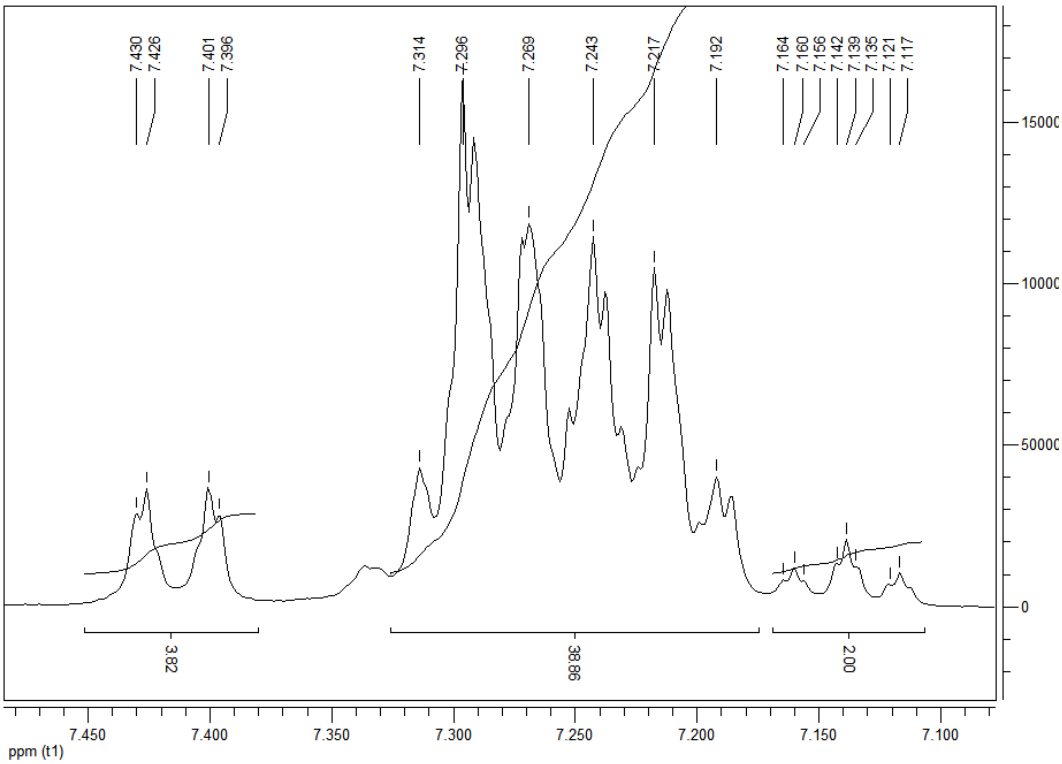

Fig. 118 $CDCl_3$ ^{1}H-NMR of 180tetraphos

This phosphane, like all the others we will show, is fluorescent. This behaviour can be due to an energy transfer from the n P lone pairs to the antibonding π* orbitals of the aromatic systems.

In Fig. 119 the excitation and emission spectra of 180tetraphos, registered in degassed dichloromethane, are shown.

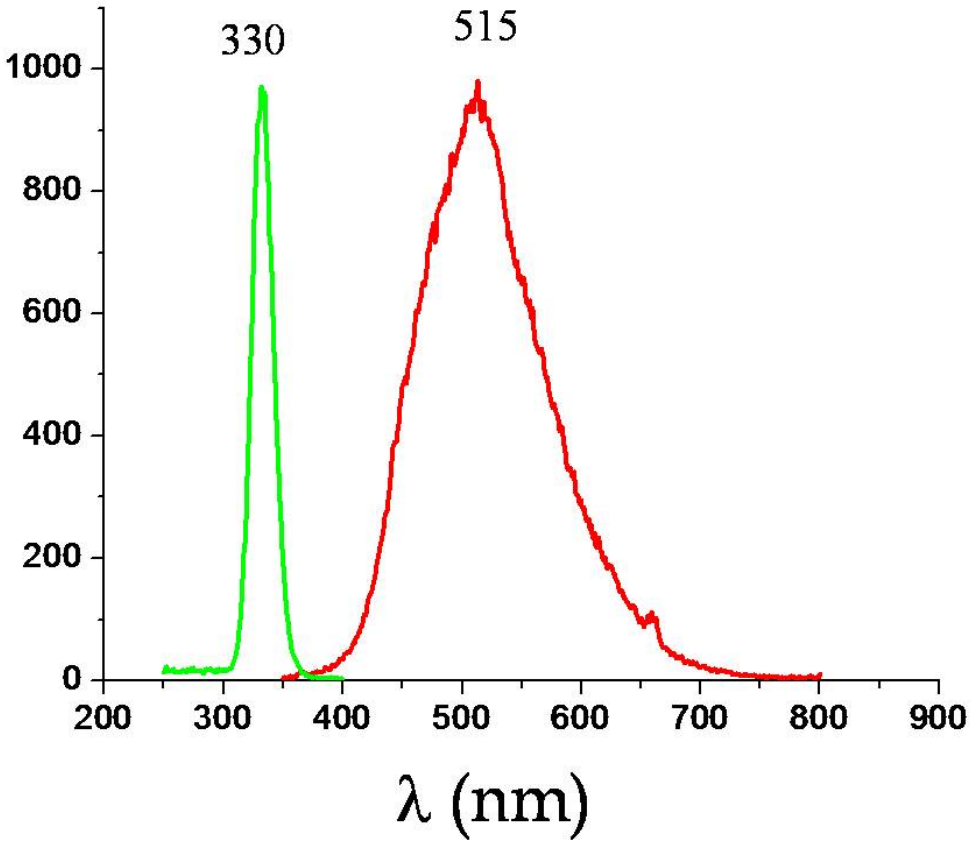

Fig. 119 Excitation (green) and emission (red) spectra of 180tetraphos

3,3′′-5-5′′-tetrakis(diphenylphosphano)-1,1′:4′,1′′-terphenyl

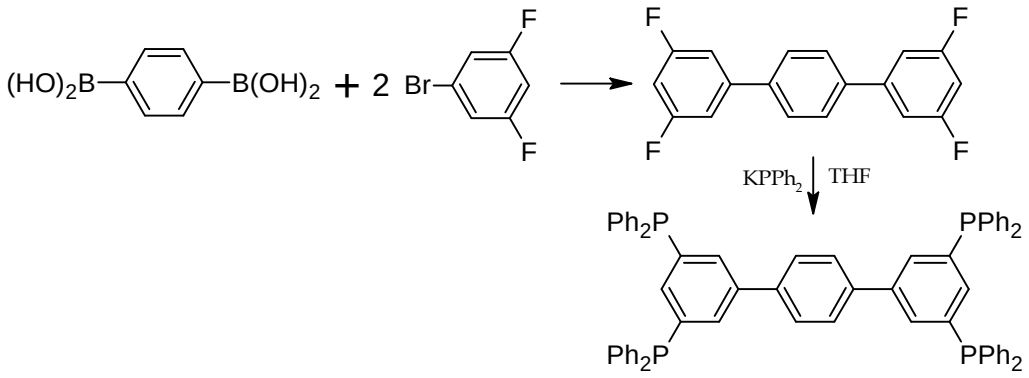

In this case the tetrafluro precursor was not available and so it has been synthesised with a Suzuky coupling reaction between 1,4-benzodiboronic acid and 2-bromo-3,5-difluorobenzene.

The reaction with $KPPh_2$ gave 180tertetraphos in high yield.

In the following figures NMR spectra of the tetrafluoro and the tetraphosphane derivatives are shown.

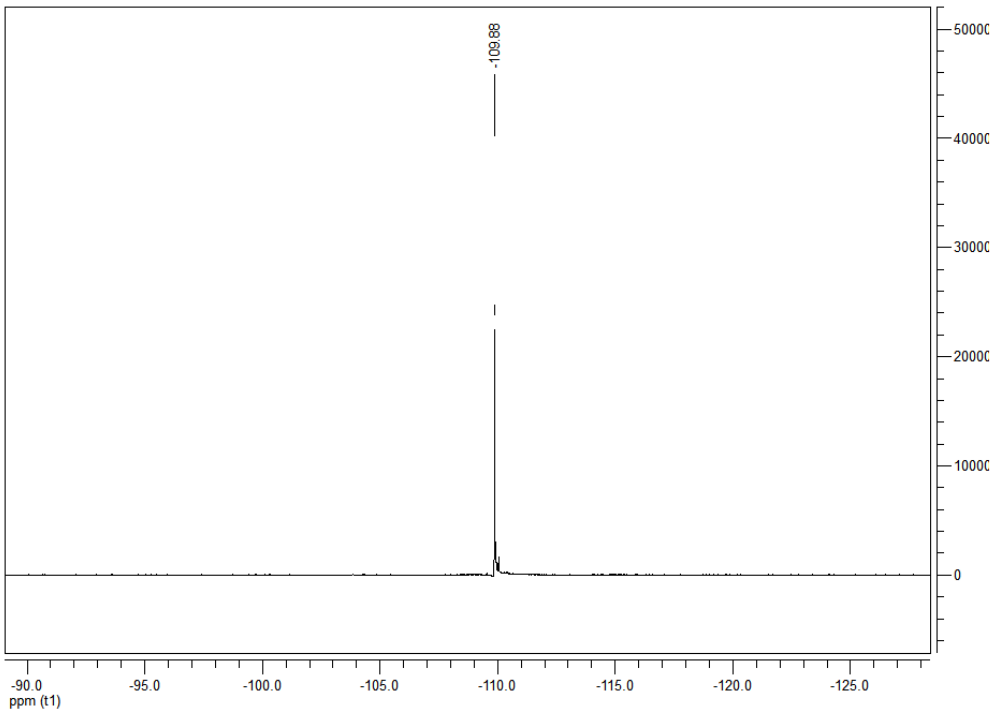

Fig. 120 $CDCl_3$ ^{19}F-NMR of 3,3′′-5-5′′-tetrafluoro-1,1′:4′.1′′-terphenyl

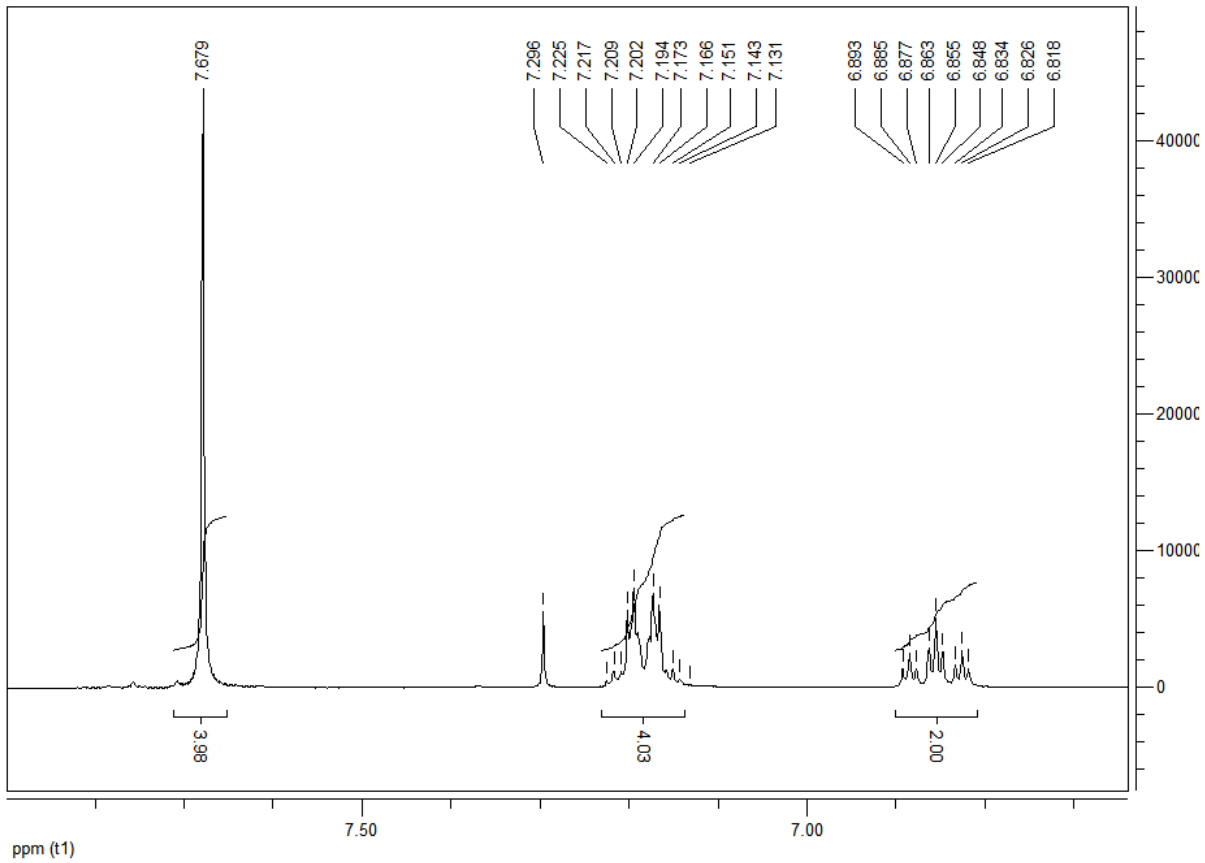

Fig. 121 $CDCl_3$ ^{1}H-NMR of 3,3′′-5-5′′-tetrafluoro-1,1′:4′.1′′-terphenyl

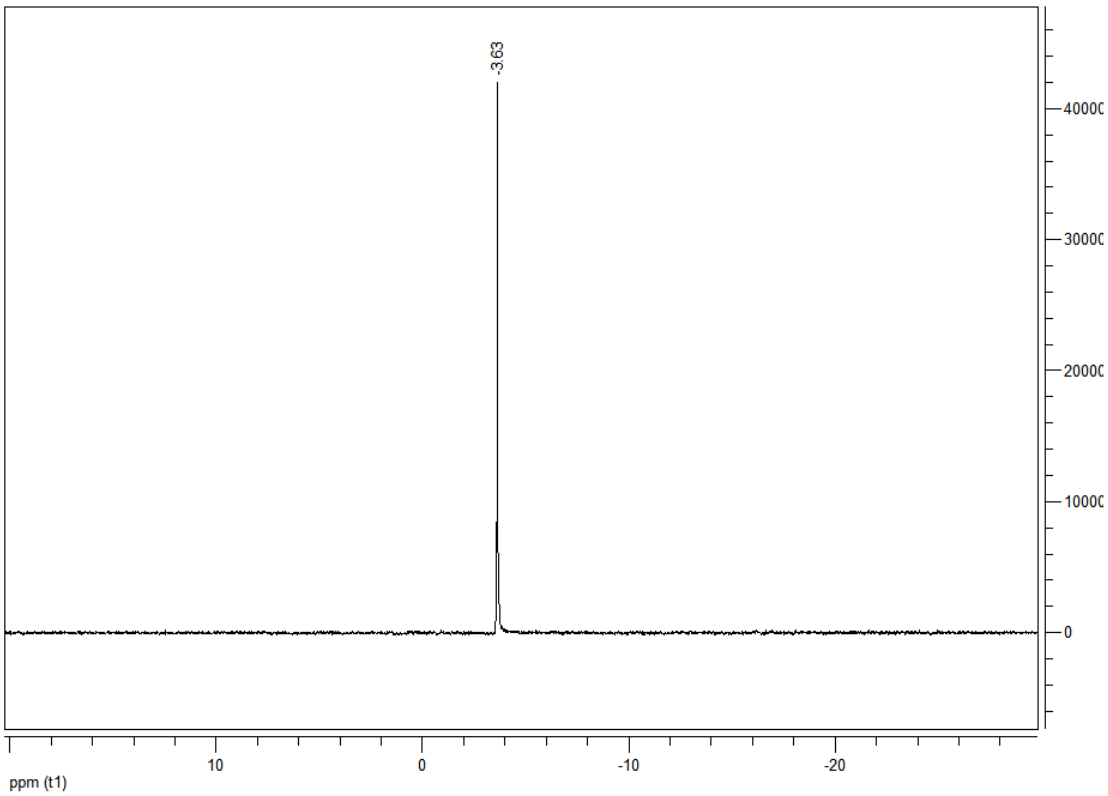

Fig. 122 $CDCl_3$ ^{31}P-NMR of 3,3′′-5-5′′-tetrakis(diphenylphosphano)-1,1′:4′,1′′-terphenyl

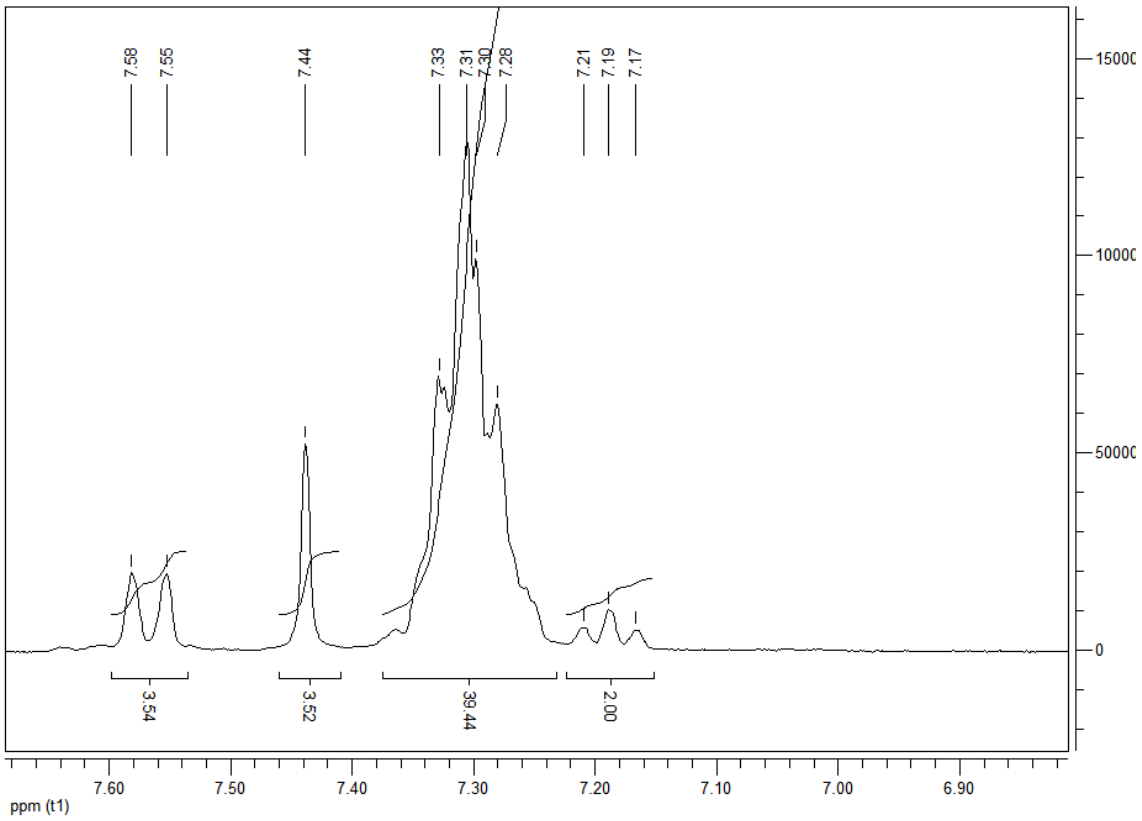

Fig. 123 $CDCl_3$ ^{1}H-NMR of 3,3''-5-5''-tetrakis(diphenylphosphano)-1,1':4',1''-terphenyl

Finally, in Fig. 124 are reported the excitation and emission spectra of 180tertetetraphos, registered in degassed dichloromethane.

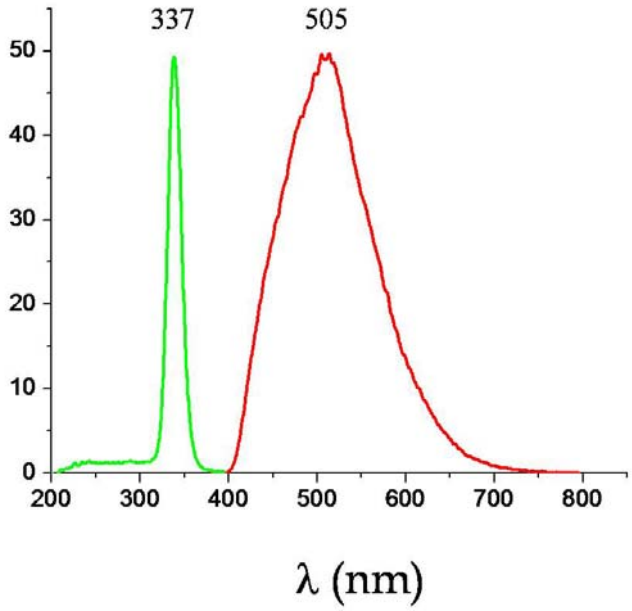

Fig. 124 Excitation (green) and emission (red) spectra of 180tertetraphos

1,3,5-tris[3′-5′-bis(diphenylphosphano)phenyl]benzene

This is the first ligand of this series we have synthesised. So it was rather laborious but it showed the right way to the other ligands too.

The first approach to get **B** has been the lithiation of **A** followed by electrophilic substitution with PPh_2Cl. Compound **A** has been obtained as described in the literature.[160]

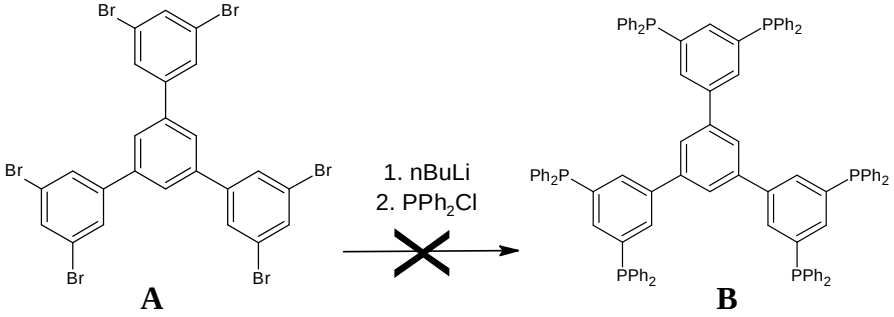

The multiple bromine – lithium exchange step did not work, likely because, after substitution of one bromine by a lithium on each benzene ring, the resulting species is very electron rich and could not bear further substitutions.

So I decided to synthesize the exafluoro precursor **C**, as it is known that polifluorinated benzene rings very efficiently give nucleophilic substitution with $KPPh_2$.[161]

Firstly, I tried the same approach used to obtain the parental bromo molecule **A**, consisting in cyclization – dehydration of three molecules of 3,5-difluorobenzacetamyde.

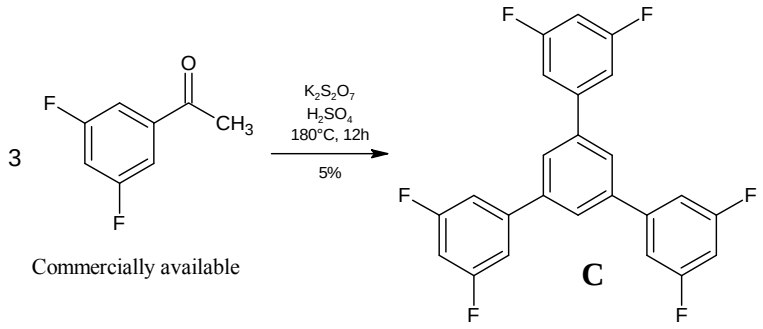

The reaction worked but with a very low yield and several attempts, varying the reaction conditions, could not improve the yield.

So I turned my attention to Suzuky coupling in order to obtain the desired product

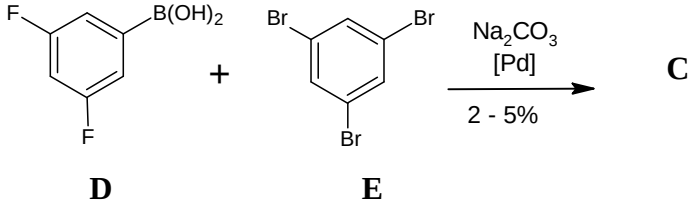

But this Suzuky reaction is very lazy and I have not been able to obtain acceptable yields even by changing the solvent, the catalyst, the temperature and the reacting time. This experimental observation might be explained with the particular electron deficiency of the boronic acid, due to the presence of two fluorine substituents on the ring, that affects its reactivity. Actually the same reaction conducted by using phenyl boronic acid works with a quantitative yield.[162]

Then, by changing approach, so using bromo-3,5-difluorobenzene **F** and 1,3,5-tris(boronic acid)benzene **G**, I have synthesised **C** with satisfactory yield:

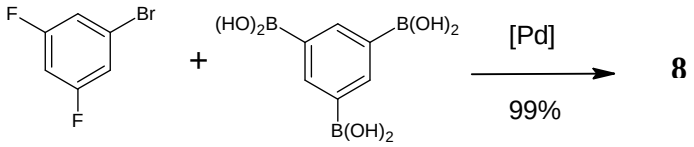

F **G**

Triboronic acid **G** has been obtained as described in the literature[163] whereas **F** is commercially available.

Finally, **C** has been converted into the desired phosphane **B** by reaction with $KPPh_2$ in high yield (93%).

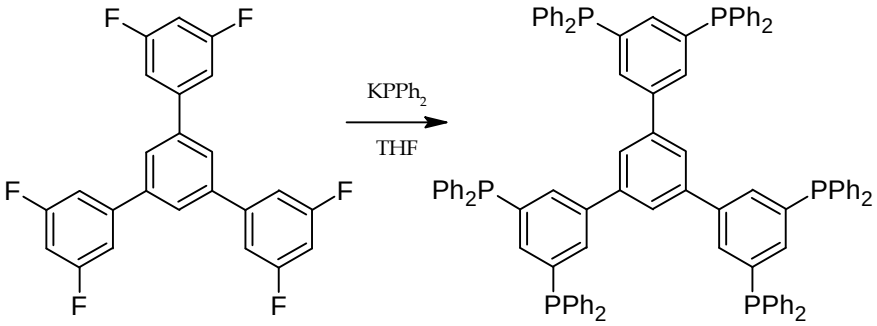

In the following figures NMR spectra of **C** and **B** are reported.

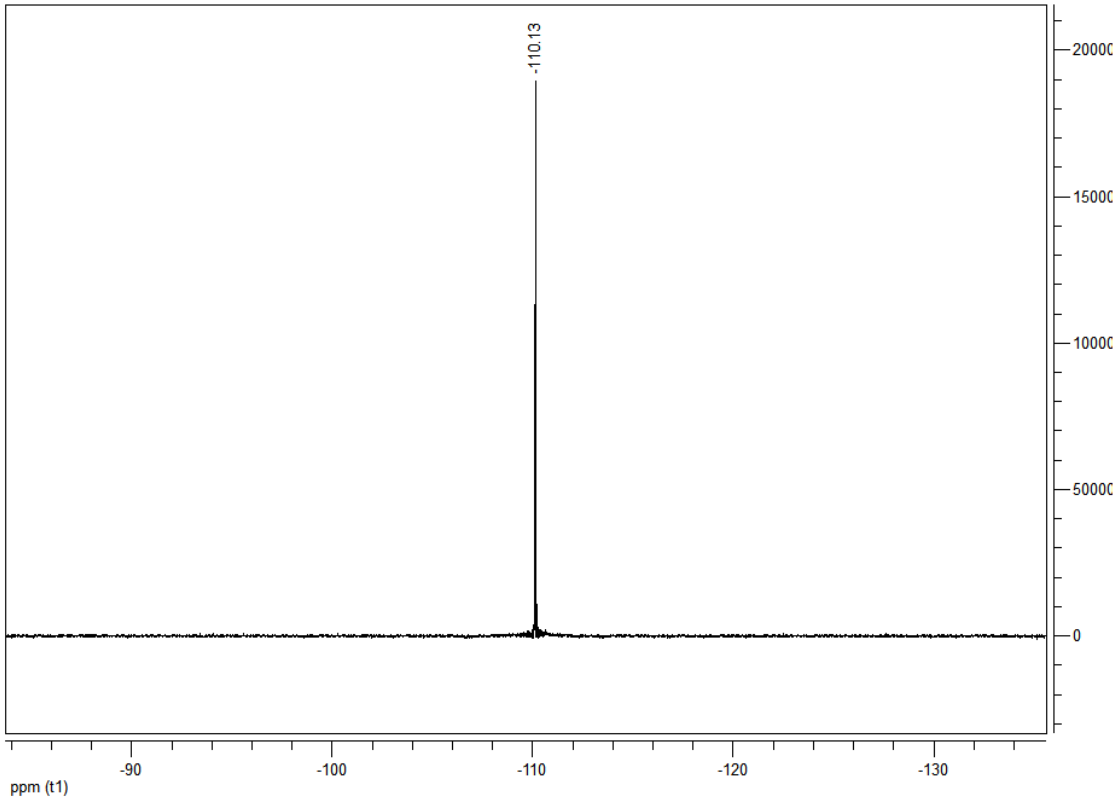

Fig. 125 DMSO ^{19}F of 1,3,5-tris(3′-5′-difluorophenyl)benzene

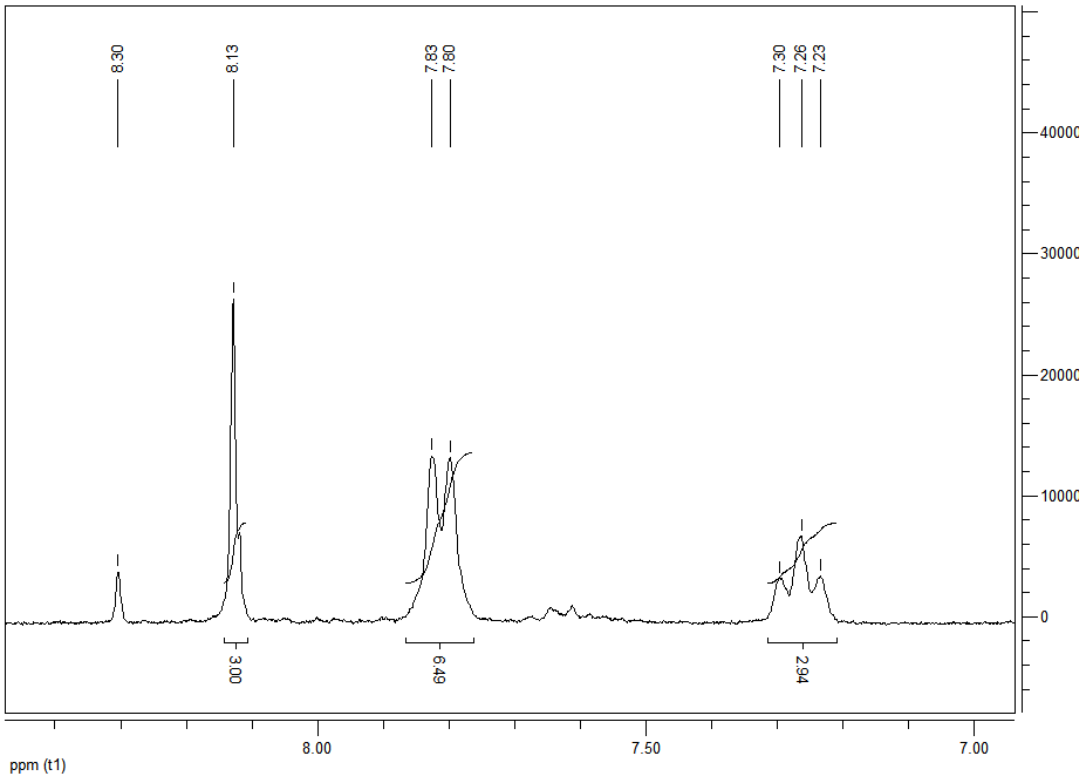

Fig. 126 DMSO ^{1}H-NMR of 1,3,5-tris(3′-5′-difluorophenyl)benzene

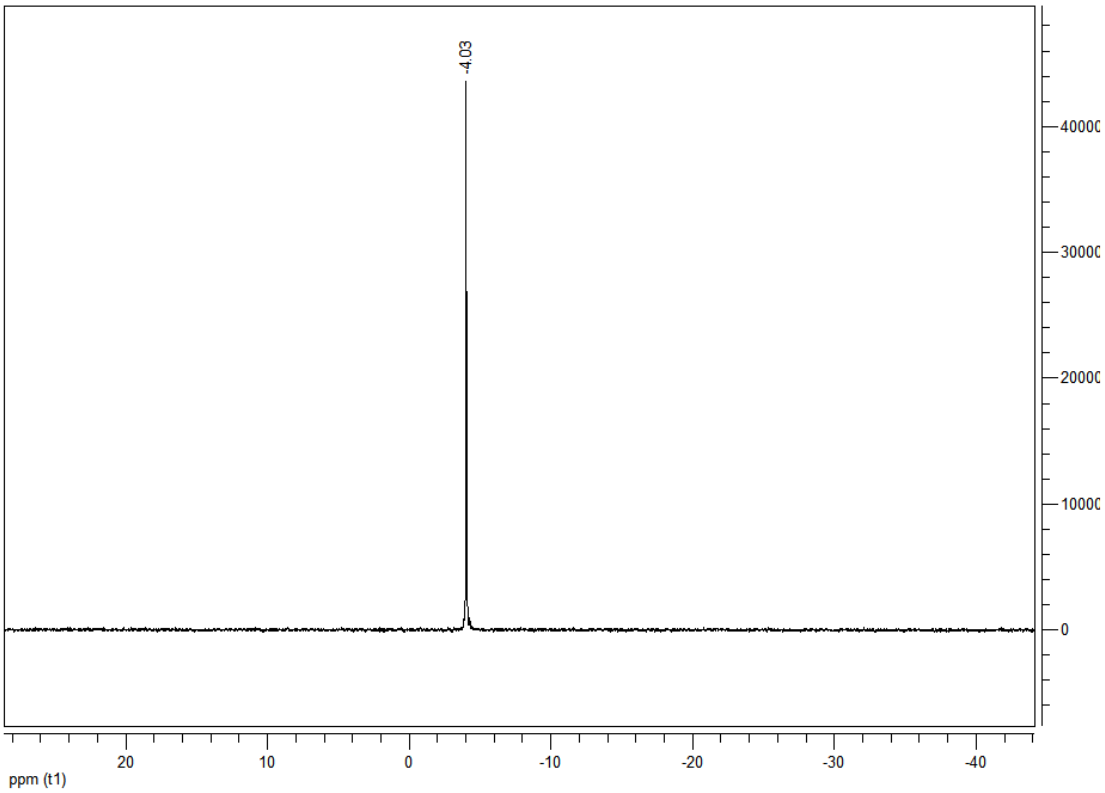

Fig. 127 $CDCl_3$ ^{31}P-NMR of 1,3,5-tris[3′-5′-bis(diphenylphosphano)phenyl]benzene

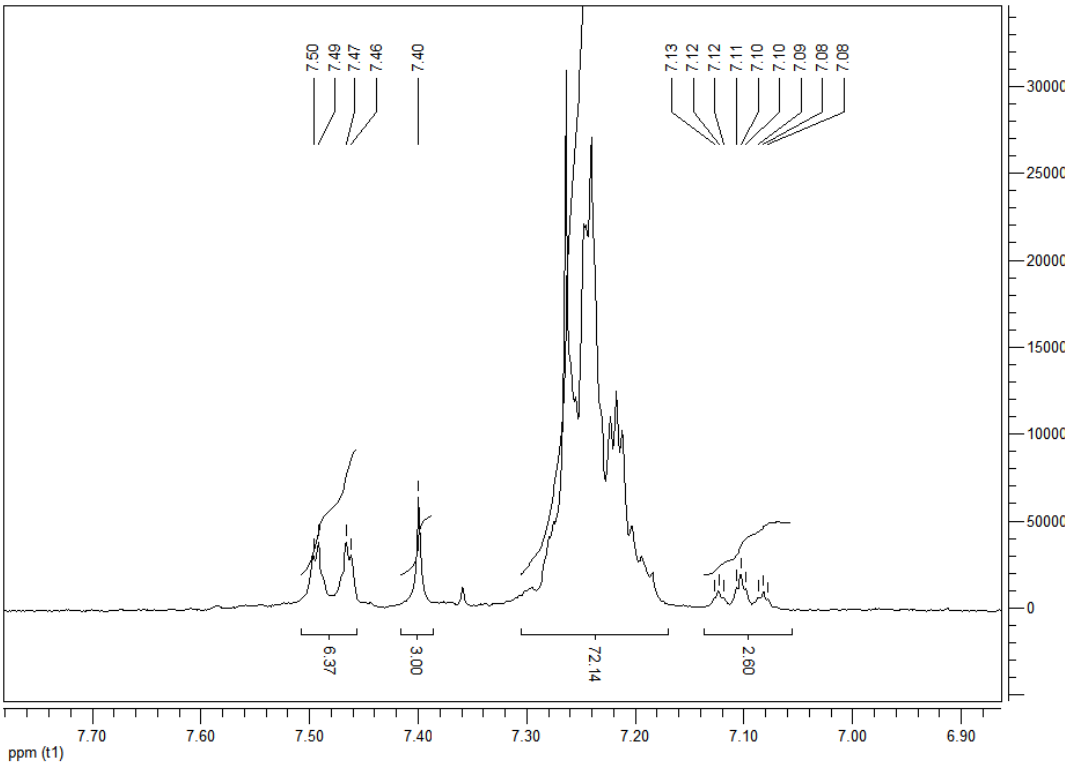

Fig. 128 $CDCl_3$ ^{1}H-NMR of 1,3,5-tris[3′-5′-bis(diphenylphosphano)phenyl]benzene

Finally in Fig. 129 the excitation and emission spectra of 120hexaphos, registered in degassed dichloromethane, are reported.

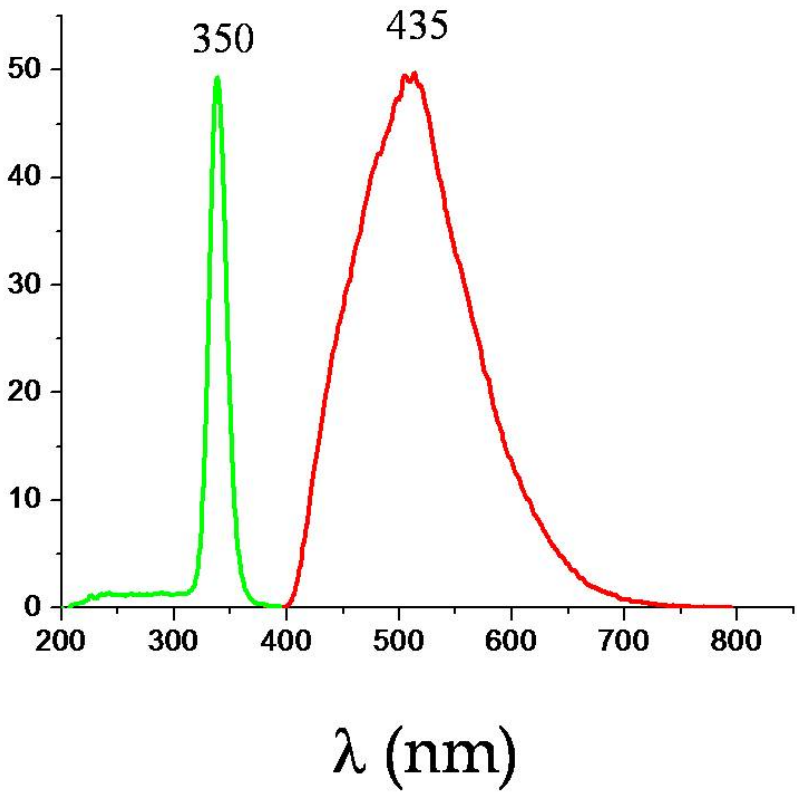

Fig. 129 Excitation (green) and emission (red) spectra of 120hexaphos

Tetrakis[4'-(diphenylphosphanophenyl)]methane (t4dpppm)

This species has been obtained by lithiation with *n*BuLi followed by electrophilic substitution with PPh_2Cl, while the tetrabromo derivative has been prepared as reported in the literature.[164]

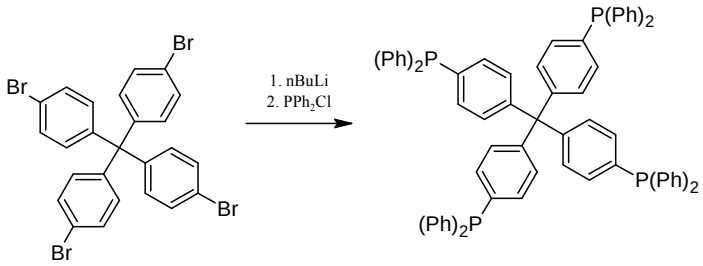

In Fig. 131 is reported the ^{1}H-NMR of t4dpppm. The integration is not consistent with what we expert. This is probably due to the hindrance of the molecule that influences the relaxion time of the protons. The same phenomenon is observed for the two following ligands, which have the same structure based on a central C atom and four bulky substituents.

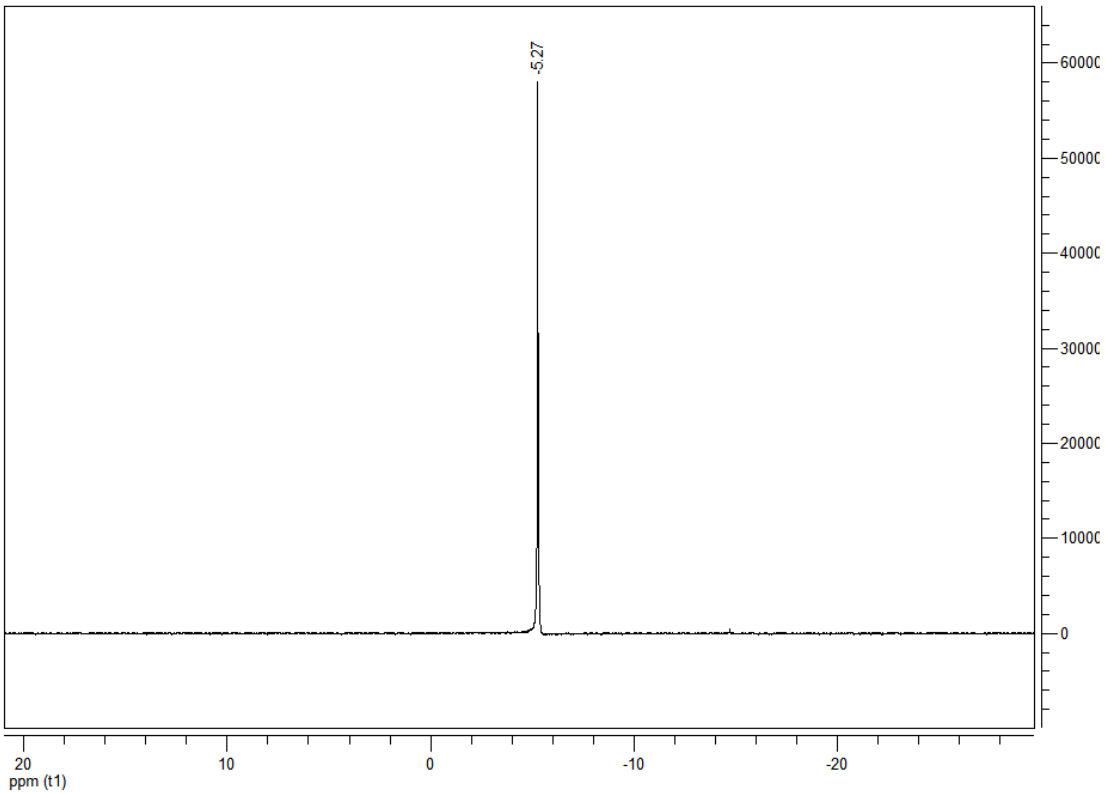

Fig. 130 $CDCl_3$ ^{31}P-NMR of tetrakis[4'-(diphenylphosphanophenyl)]methane

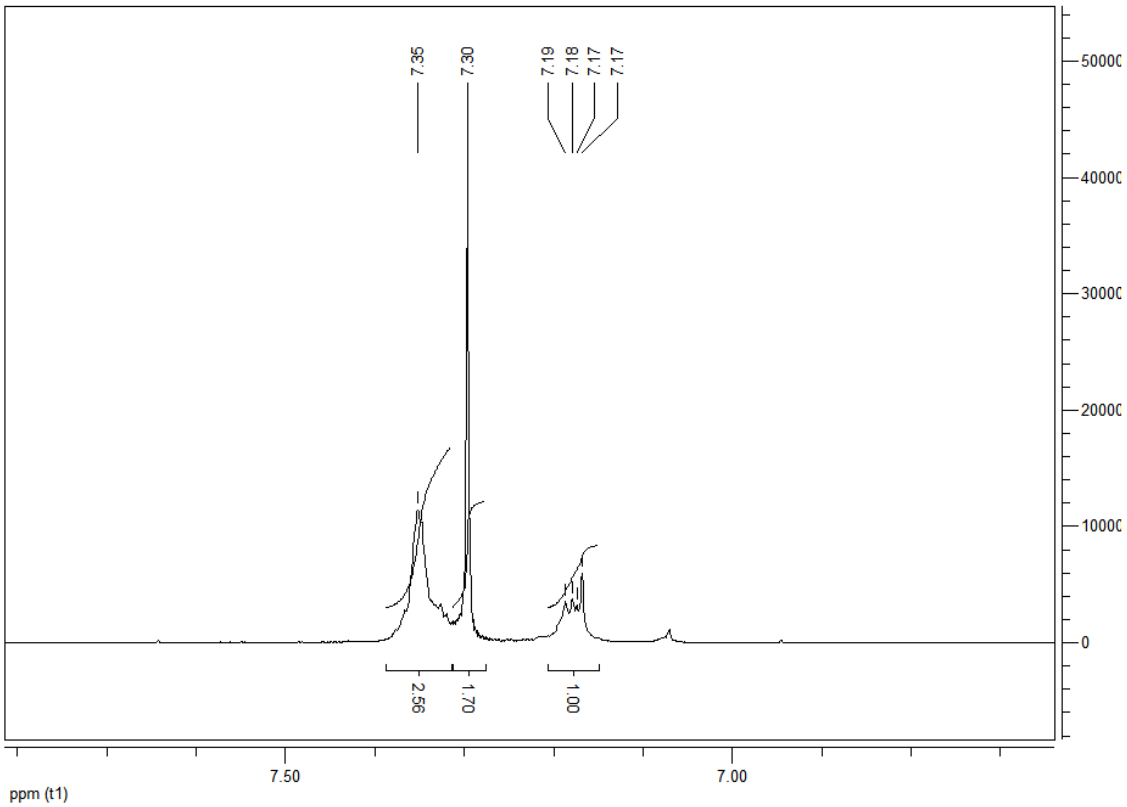

Fig. 131 $CDCl_3$ ^{1}H-NMR of tetrakis[4′-(diphenylphosphanophenyl)]methane

In Fig. 132 are reported the excitation and emission spectra of t4dpppm (degassed dichloromethane as solvent).

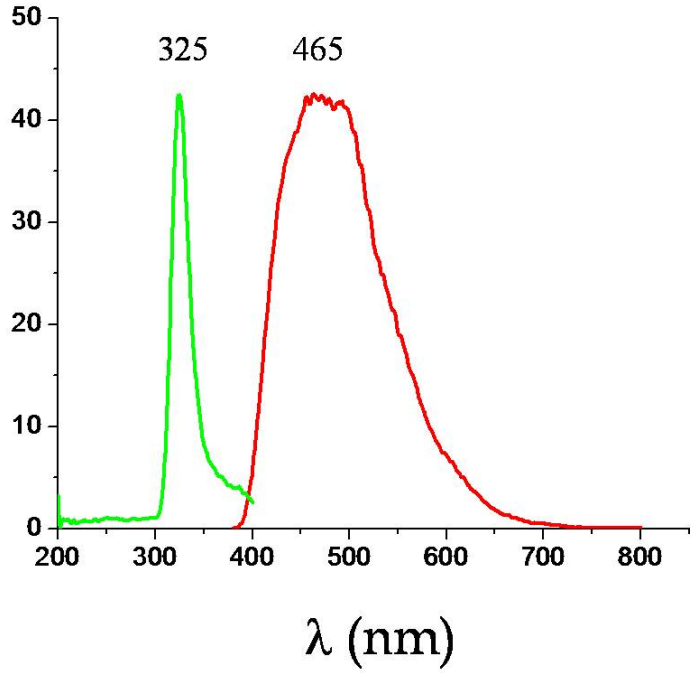

Fig. 132 Excitation (green) and emission (red) spectra of t4dpppm

Tetrakis[3′-(diphenylphosphano)biphenyl]methane (t3′dppbm)

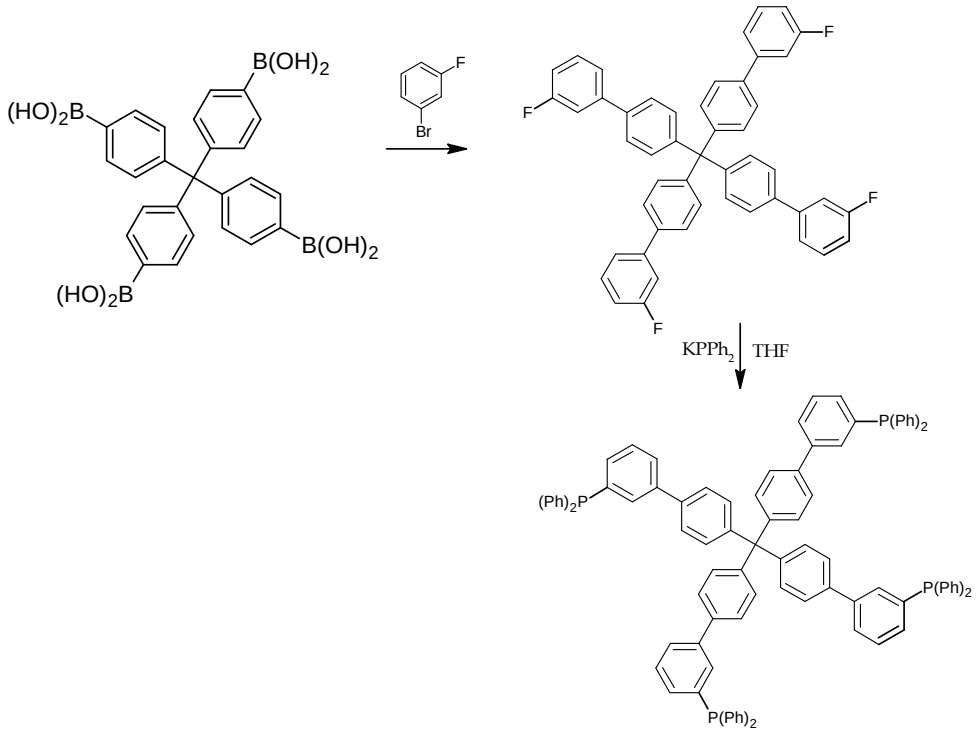

The tetrafluoro derivative has been obtain with Suzuky coupling, while the phosphane has been prepared through reaction with $KPPh_2$ as usual. In the following figures NMR spectra are reported.

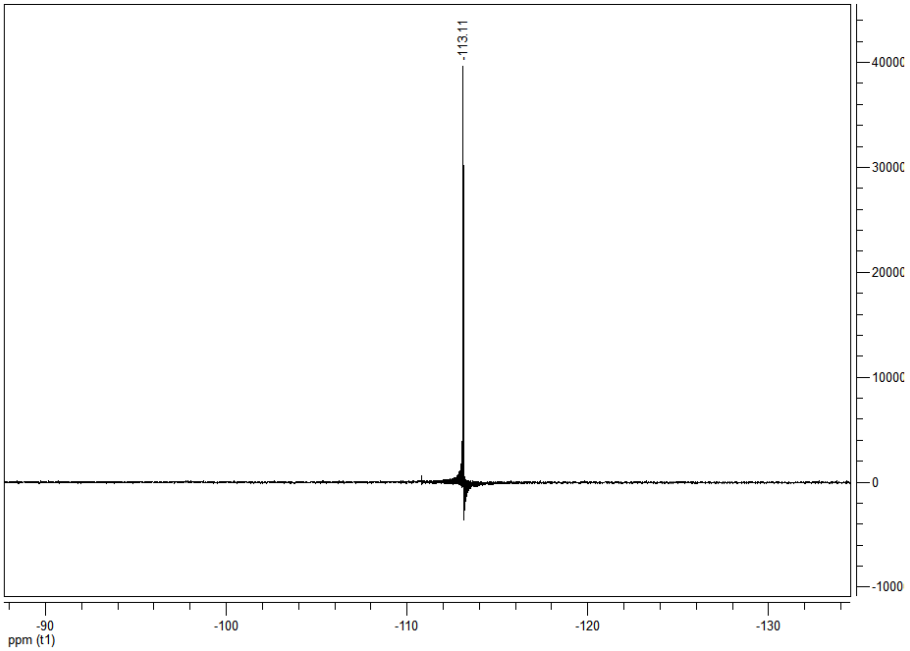

Fig. 133 $CDCl_3$ ^{19}F-NMR of tetra(3′-fluorobiphenyl)methane

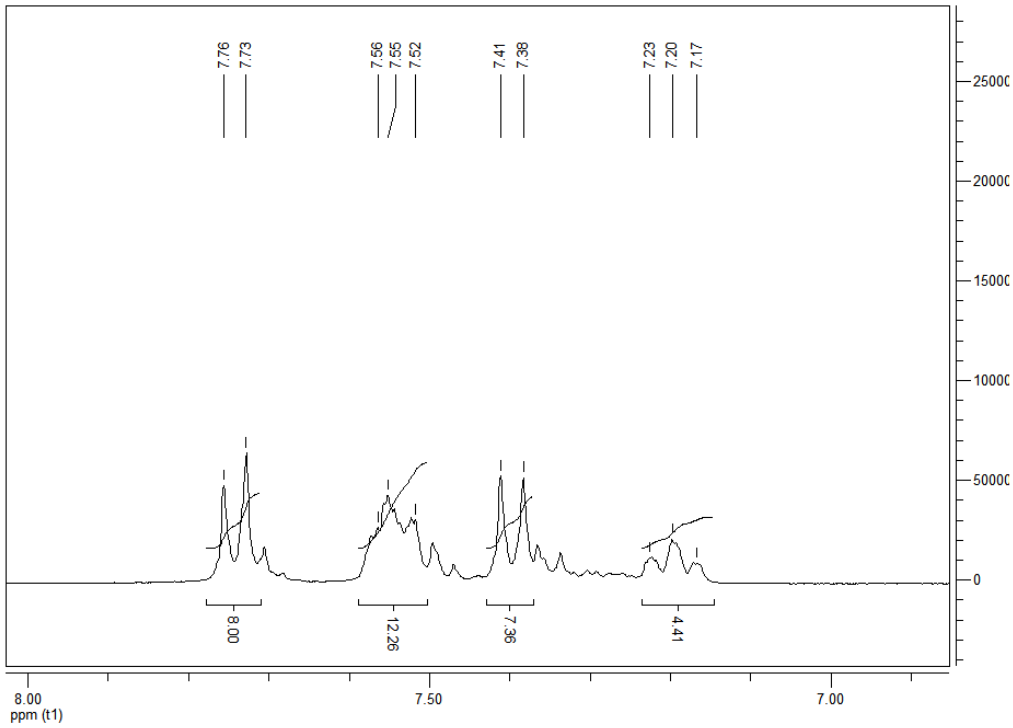

Fig. 134 $CDCl_3$ ^{1}H-NMR of tetra(3′-fluorobiphenyl)methane

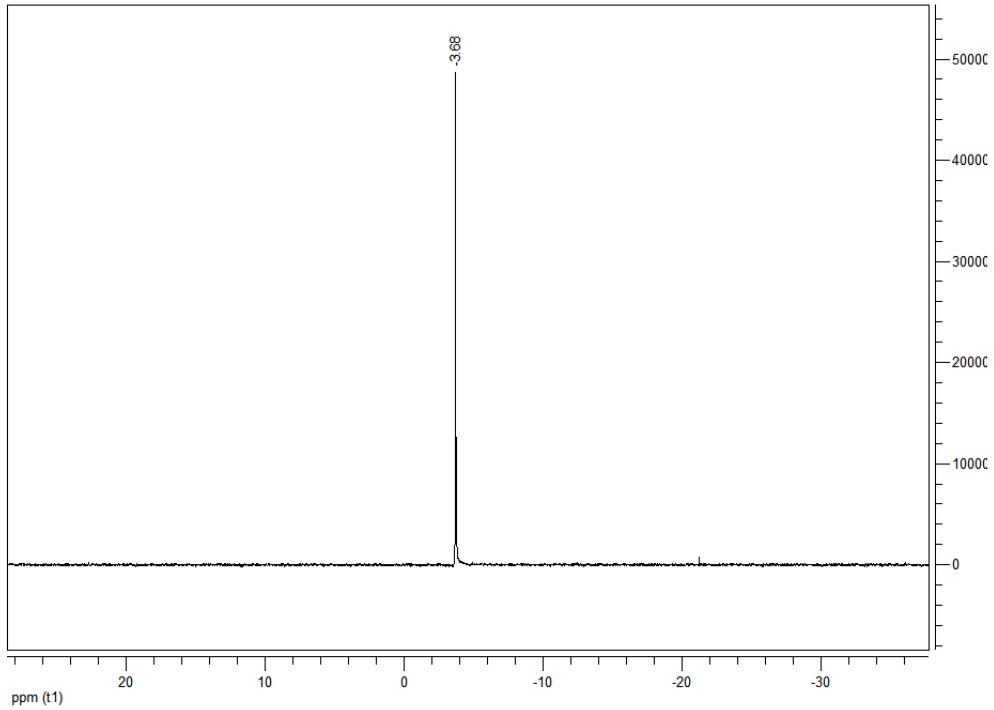

Fig. 135 $CDCl_3$ ^{31}P-NMR of tetrakis[3′-(diphenylphosphano)biphenyl]methane

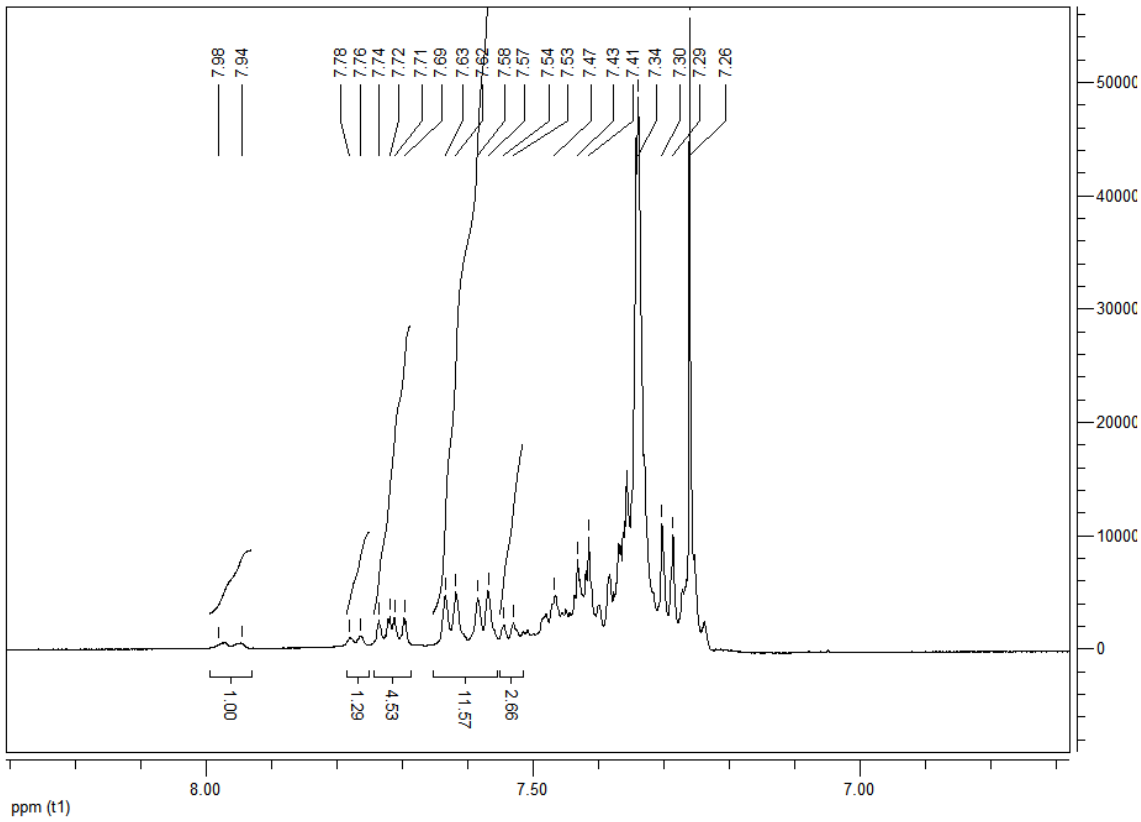

Fig. 136 $CDCl_3$ ^{1}H-NMR of tetrakis[3'-(diphenylphosphano)biphenyl]methane

Finally, excitation and emission spectra of t3'dppbpm, registered in degassed dichloromethane, are reported in Fig. 137

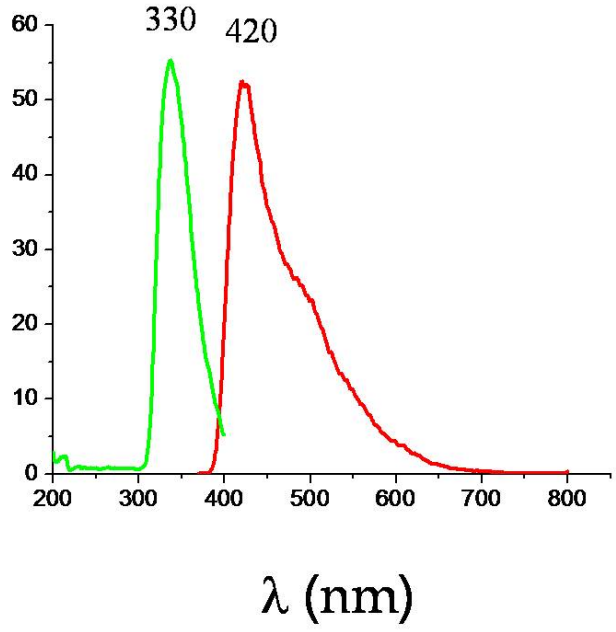

Fig. 137 Excitation (green) and emission (red) spectra of t3'dppbpm

Tetrakis[3'-5'-bis(diphenylphosphano)biphenyl]methane (t3′5′dppbpm)

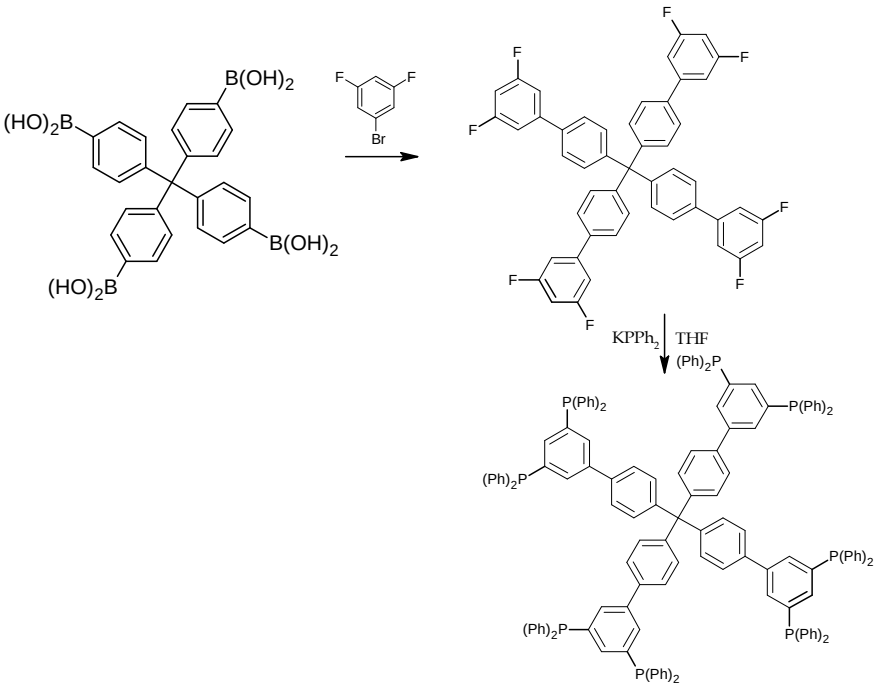

The usual synthesis strategy resulted successful also in the case of this last ligand, although the yields were lower than in other cases.

In the following figures NMR and excitation-emission spectra are reported.

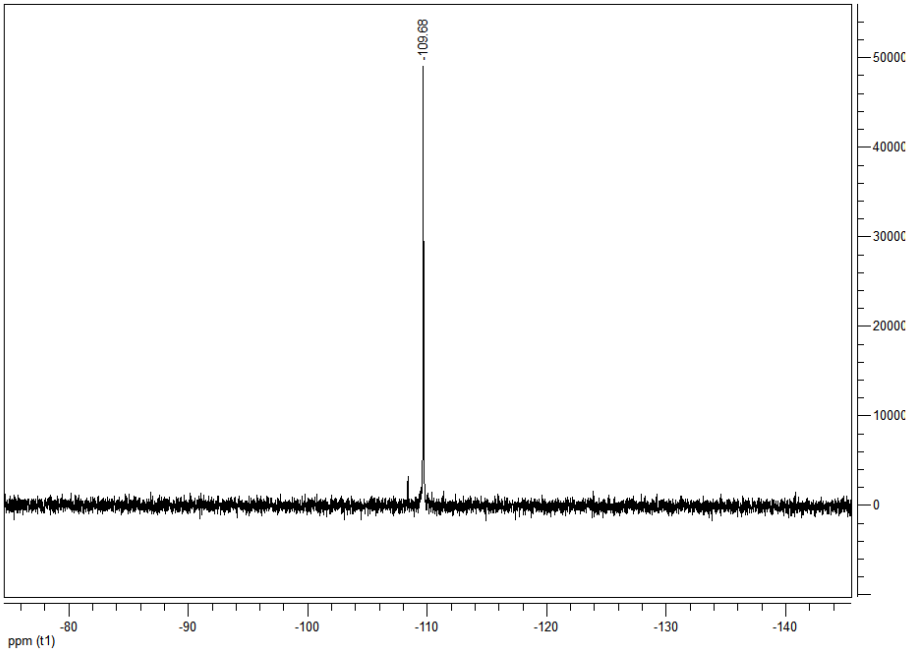

Fig. 138 $CDCl_3$ ^{19}F-NMR of tetra(3'-5'-difluorobiphenyl)methane

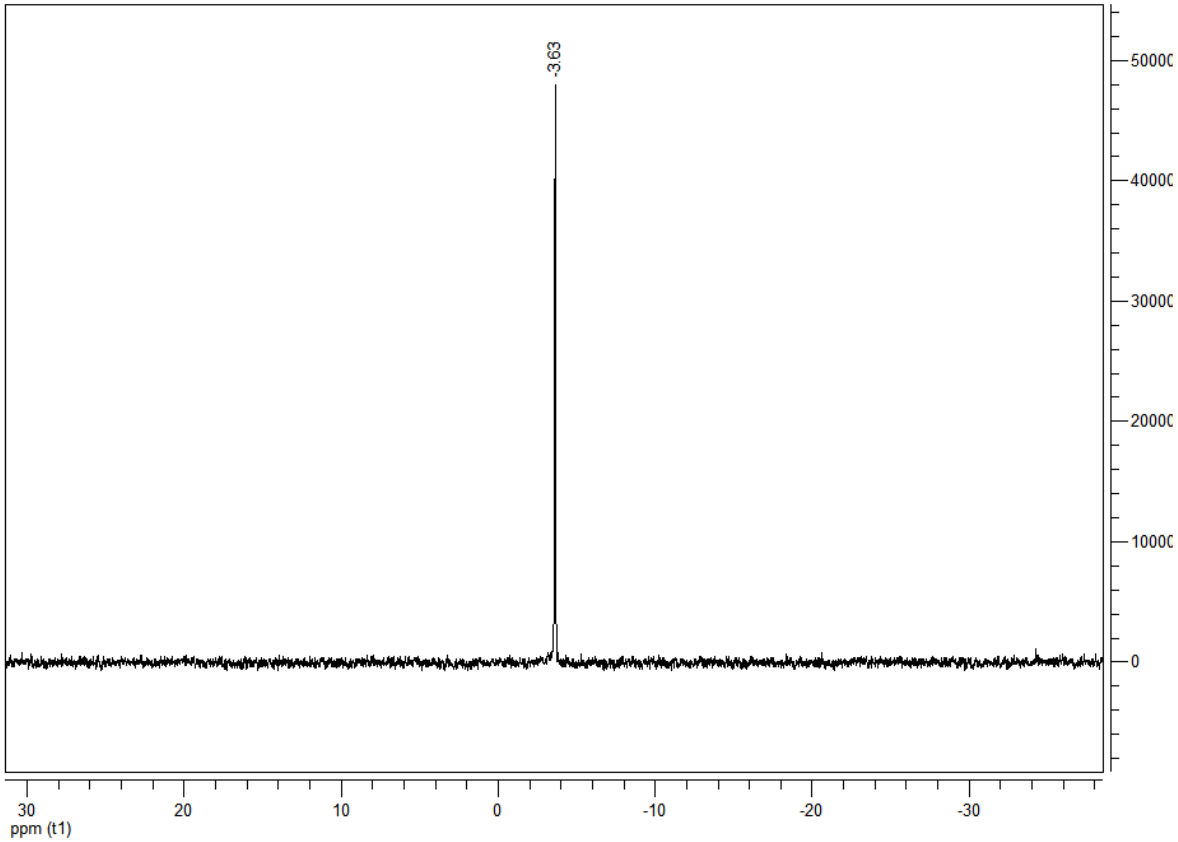

Fig. 139 $CDCl_3$ ^{31}P-NMR of tetrakis[3'-5'-bis(diphenylphosphano)biphenyl]methane

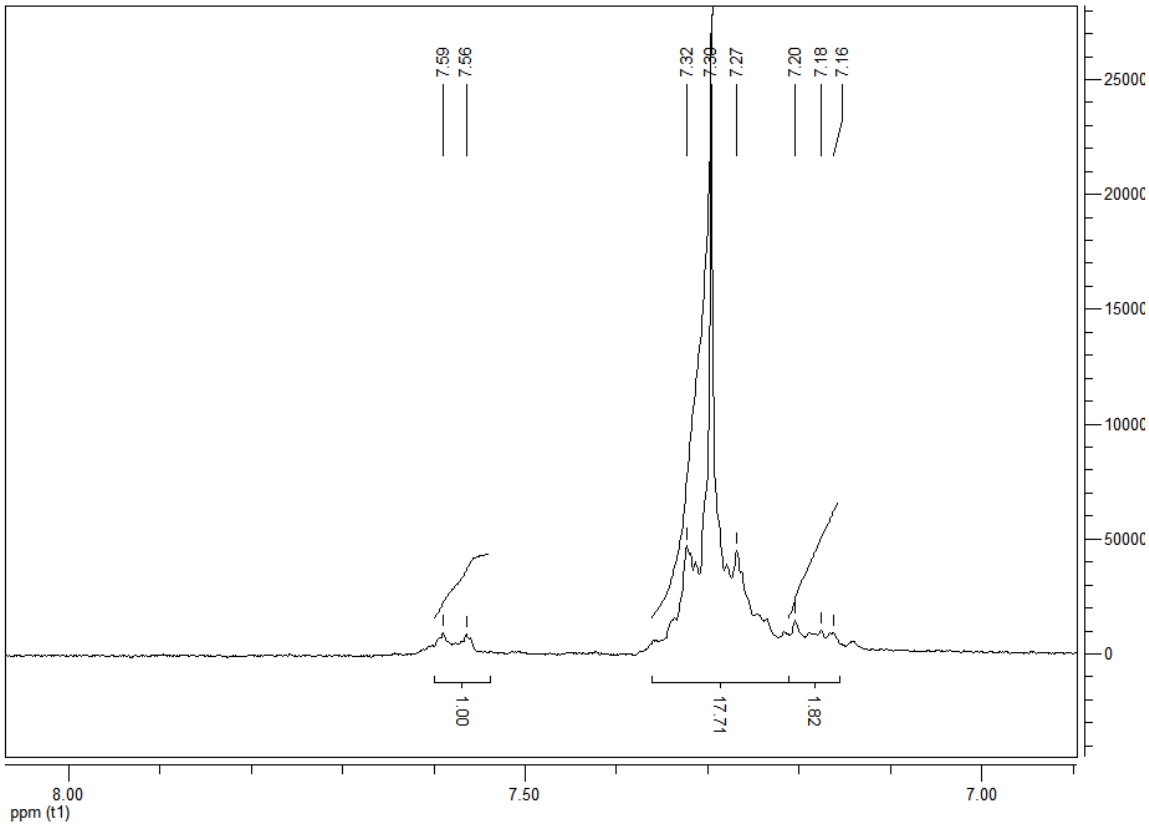

Fig. 140 $CDCl_3$ ^{1}H-NMR of tetrakis[3'-5'-bis(diphenylphosphano)biphenyl]methane

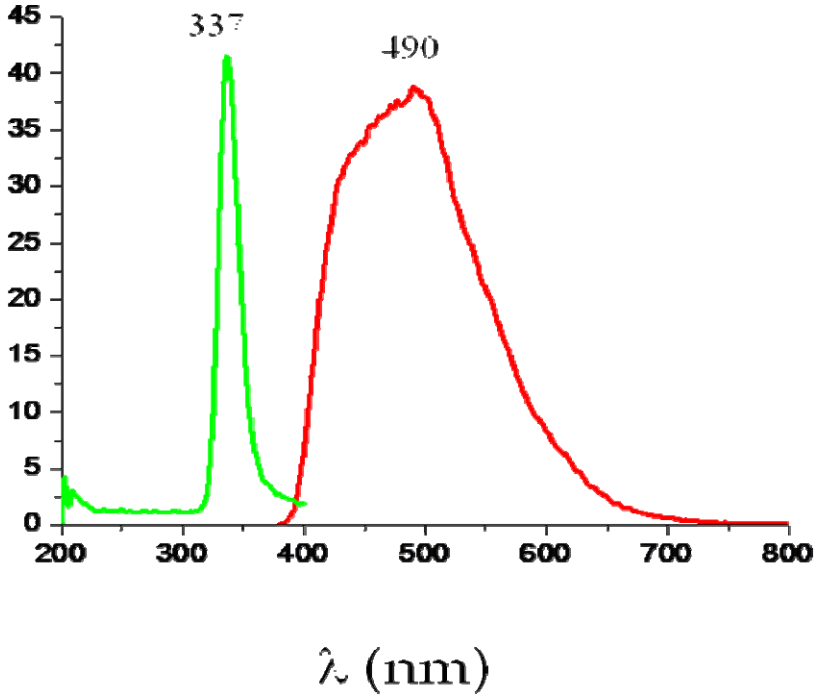

Fig. 141 Excitation (green) and emission (red) spectra of t3'5'tdppbpm

Reactivity of rigid poliphosphanes and $[MCl_2(CO)_2]^-$ (M = Rh, Ir)

We have explored the reactivity of the rigid multiphosphanes towards $[MCl_2(CO)_2]^-$ (M= Rh, Ir) in a suitable molar ratio: M:L = 2:1 for 1, 2, 4 (L^4) and 5, 3:1 for 3 (L^6) and 4:1 for 6 (L^8). As the halocarbonyls are known to react with phosphanes by coordinating two of them and substituting one CO and one Cl^-, those ratios should saturate the coordination sites with the minimum number of ligands.

Air stable, insoluble products have been obtained in all cases and the elemental analyses are in accordance with an hypothetical formula $[\{MCl(CO)\}_{n/2}(L^n)]_m$.

Unfortunately we were unable to grow crystals of these compounds.

Anyway we can suppose their structure on the basis of the ligands and complex geometrical constraints. For example in the case of 120hexaphos (Fig. 142), the molecule should contain cyclic dimers as repeating motif.

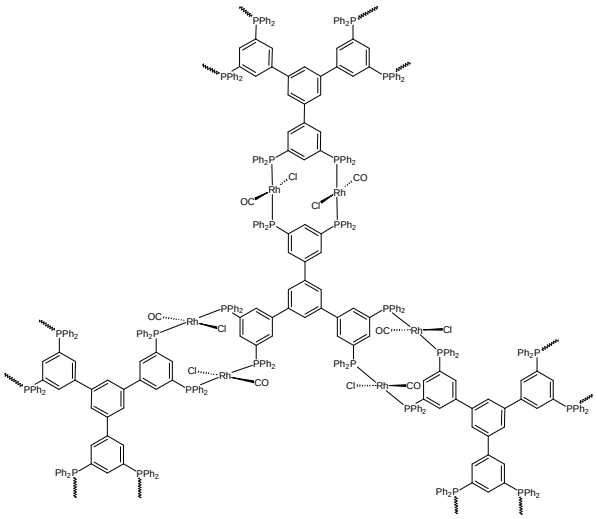

Fig. 142 Proposed structure for $[\{RhCl(CO)\}_3(120hexaphos)]_n$

In a typical reaction, the halocarbonyl is dissolved in dichloromethane or chloroform in $10^{-.3}$ M molar concentration and then the ligand is added. So the precipitatation of a yellow solid quickly occurs, that is isolated and washed with the same solvents used for the reaction.

The reaction is followed by IR spectroscopy: after the addition of the ligands carbonyl stretching bands at 2070, 1990 cm^{-1} of the starting material are substituted by one band in

the range of 1957-1970 cm^{-1}, according to the phosphane. At the end of the reaction, the concentration of the species this band is due to is negligible. So we can argue it is an intermediate that than evolves to the final product. Elemental analyses are in agreement with the formula $[\{MCl(CO)\}_{0.5n}(L^n)]_m$.

ATR-IR (Attenuated Total Reflectance – Infra Red) spectra of the products show, in the carbonyl region, one sharp band, as we esxpect basing on the formulated hypothesis.

In the following figures, ATR-IR spectra are reported.

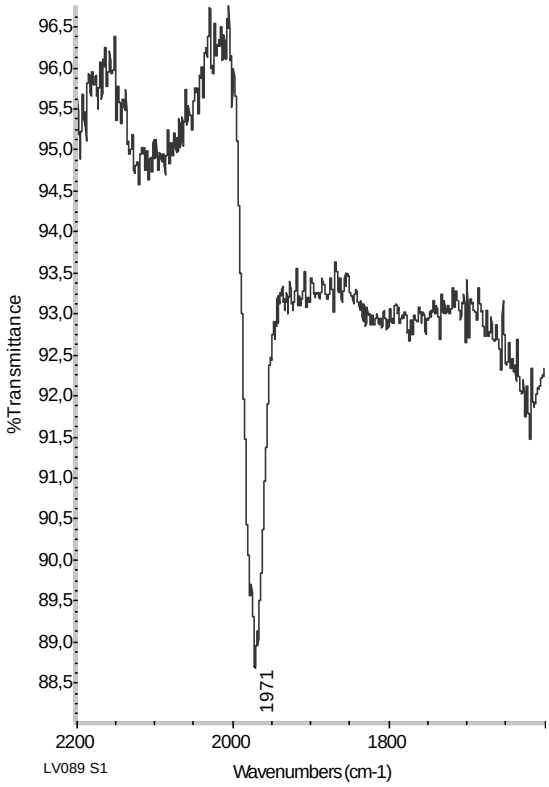

a)

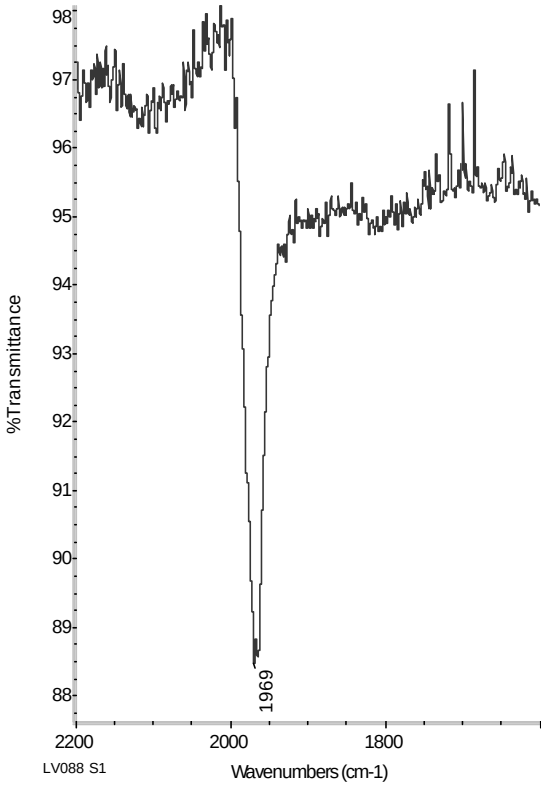

b)

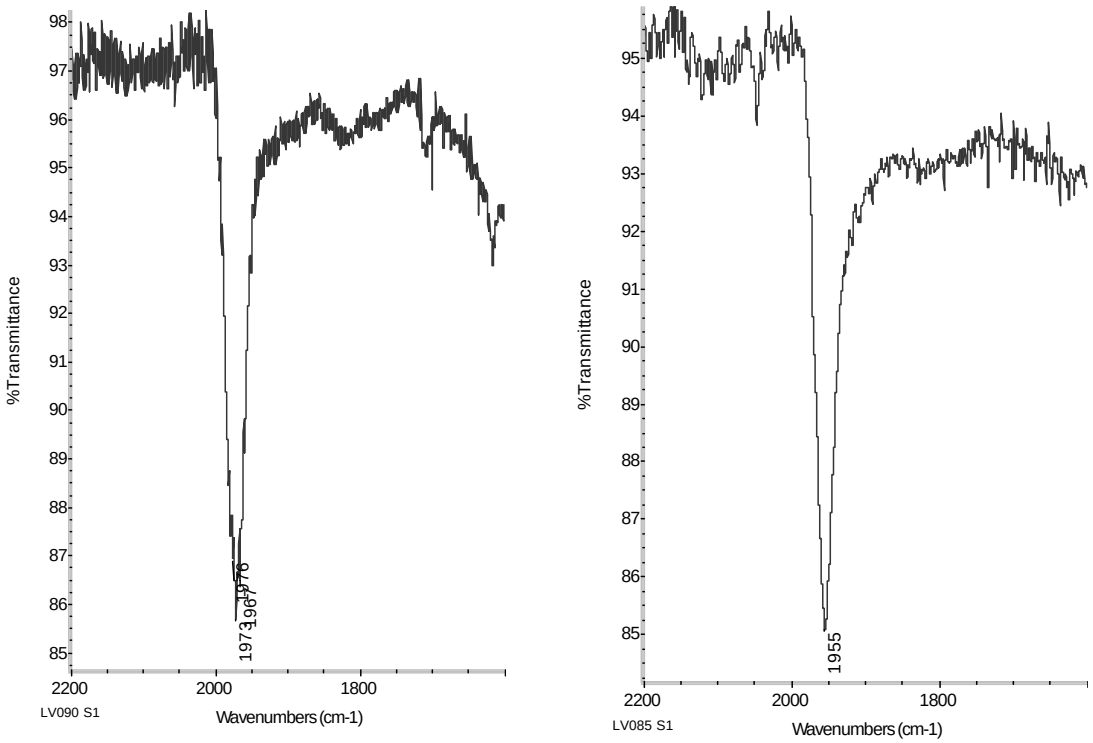

c) **d)**

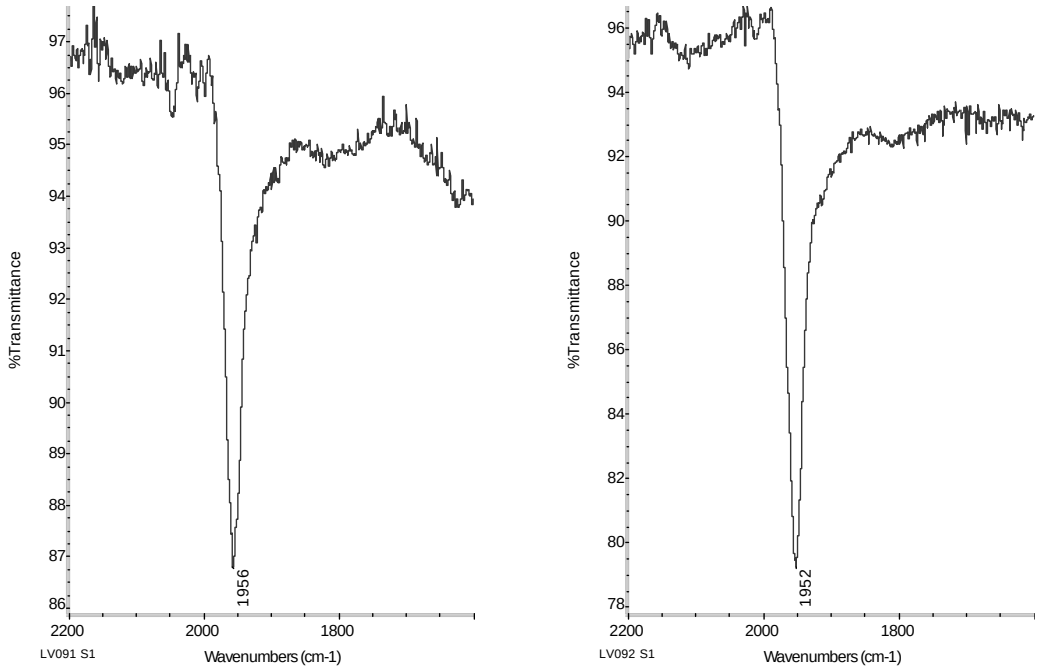

e) **f)**

Fig 11. Spettri ATR-IR di: a) $[[RhCl_2(CO)]_2(180tertetraphos)]_n$, b)$[[RhCl(CO)]_2(180tetraphos)]_n$, c) $[RhCl_2(CO)_2]_3(120hexaphos)]_n$, d) $[[IrCl(CO)]_2(180tertetraphos)]_n$, e) $[[IrCl(CO)]_3(120hexaphos)]_n$, f) $[[IrCl(CO)]_2(180tetraphos)]_n$

All the products are completely insoluble in all common organic solvents and so it is not possible to re-crystallize them once they are obtained as powder.

We tried to get crystals directly during the formation of the products. Halocarbonyl has been dissolved in a solvent and this solution has been layered with a ligand solution, made using a miscible and less dense solvent. In this way the reactants are allowed to slowly react at the interphase. This technique resulted successful for these carbonyls and other diphosphanes in many cases. Nevertheless, in this case it was not possible to get crystals suitable for X-ray analysis.

Anyhow, it is possible to propose an hypothesis about the structure of these compound, basing on the geometrical constraints of the complexes and the ligands. For example, in the case of 120hexaphos, the structure should contain cyclic dimer as repeating motif, adopting an honeycomb like geometry.

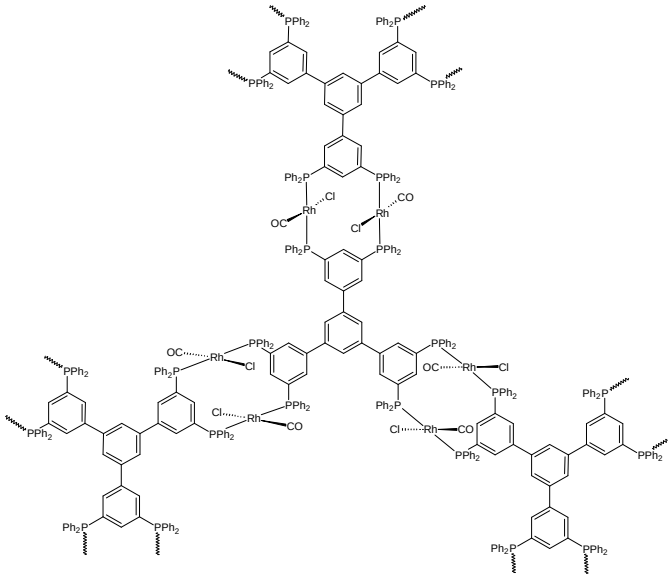

Fig. 143 Supposed structural motif adopted by $[RhCl_2(CO)_2]_3$(120hexaphos)$]_n$

Reactivity of rigid poliphosphanes and $[Ir_4Br(CO)_{11}]^-$

With the aim to aggregate metal carobyl clusters by using poliphosphane ligands, I have continued to exploit tetrahedral iridium cluster.

Our research group developed considerable expertise in the synthesis, characterization and reactivity of these carbonylic cluster.

The founder of this compound family is $[Ir_4(CO)_{12}]$ (Fig. 144), that has been presented in the introduction.

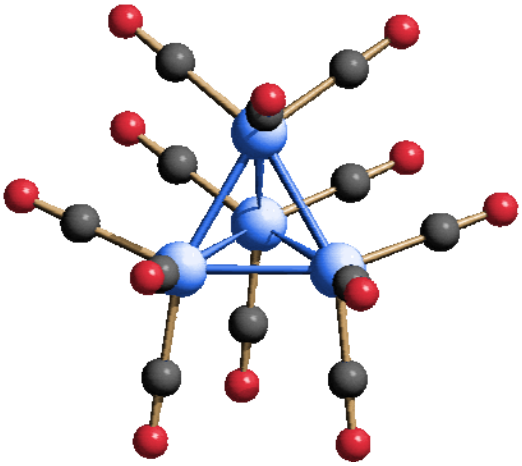

Fig. 144 Solid state structure of $[Ir_4(CO)_{12}]$

The compound is a yellow air-stable powder and it is prepared by reductive carbonylation in an autoclave starting from $IrCl_3 \cdot 3H_2O$ and formic acid.[165]

Its almost complete insolubility in all common organic solvent represents an hindrance in its reactivity which is possible to remedy only in drastic condition (refluxing in high boiling solvents). It is than known, from kinetic studies, that the CO substitution rate increases with the increasing of the substitution degree.[166] With P-donor ligands and isonitriles tri and tetrasubstituted products have been mainly obtained[167] in place of monosubstituted products.[168] The introduction of an halide or a pseudohalide (Cl^-, Br^-, I^-, CN^-, SCN^-) radically changes the situation: it is possible to isolate product that are soluble in basic solvent and can easily give substitution reactions.

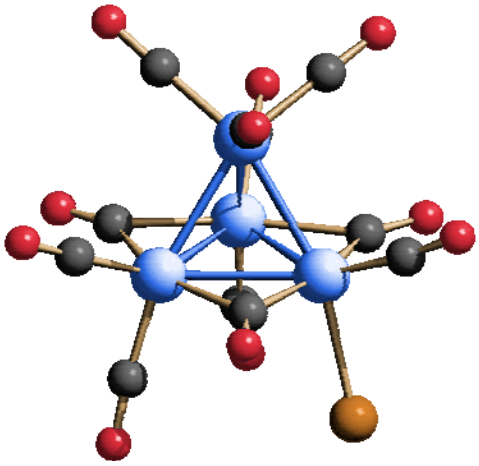

Fig. 145 Solid state structure of $[Ir_4Br(CO)_{11}]^-$

So we have used $[Ir_4Br(CO)_{11}]^-$ (Fig. 145) as starting material, that can be obtained with different ammonium or phosphonium cations, by treating $[Ir_4(CO)_{12}]$ with an excess of LiBr in refluxing THF for some days. The product is precipitated with an aqueous (or alcohol) solution of the desired cation and it is used in inert atmosphere.

The synthetic work, conducted with $[Ir_4Br(CO)_{11}]^-$ and the rigid multiphosphanes, leaded to polimetallic dendrimers which are soluble in solvents like chloroform, tetrahydrofuran and toluene, example of which are rarely reported in literature.

In particular, their dimension above the nanometer, the potential behaviour to undergo to redox processes and the segregation of the metal clusters, made by the ligand organic scaffold, let to define these molecules as "compartmental nanocapacitors".[169]

Nanometric metal carbonyl clusters, showing the ability to reversibly acquire or to give electrons, so without destroy the metal cage, can be defined as nanocapacitors and some examples from the Ceriotti's, Longoni's and Zanello's research group have been reported.[170]

Nowadays, only few examples of self-assembled materials containing metal carbonyl clusters are known.[171,172] Generally, self-assembly is mainly obtained through the formation of M-M bonds (for example $[Pt_{24}(CO)_{48}]^{2-}{}_\infty$ and $[Pt_{18}(CO)_{36}]^{2-}{}_\infty$)[173,174] or M-M' (for example $\{Ag^+[Rh_6C(CO)_{15}]^{2-}\}_n$ and $\{Ag^+[Ru_6C(CO)_{15}]^{2-}\}_\infty$).[175,176]

So far, the use of multidentate ligands to connect clusters together have received less attention and only few example of oligomers $(\{[Rh_5(CO)_{15}]_2(H_2N(CH_2)_4NH_2)\}^{2-}$,[177] $\{[Rh_6(CO)_{14}]_2(dpbp)\}$ and $\{[Ru_6C(CO)_{15}(dpbp)]_3[Ir_4(CO)_8]\}$[178] (dpbp = 2,2'-

bis(diphenylphosphano)-4,4'-bipyridine)) and only one 1D polymer, containing $Fe_4Cu_2(\mu_6\text{-}C)(CO)_{12}$ cluster units linked by N donor ligands.[179]

The use of poliphosphanes was not so far explored, although many clusters substituted by phosphanes are known and the CO substitution reactions have been studied since '70 and '80 of the XX Century.

Synthesis and characterization of $[\{Ir_4(CO)_{11}\}_4(180tetraphos)]$

The reaction is performed dissolving the ligand in chloroform and adding to the resulting solution fuor equivalents of $[PPh_4][Ir_4Br(CO)_{11}]$. The starting orange solution turns to yellow as the reaction is completing.

$$4\ [PPh_4][Ir_4Br(CO)_{11}] + 180tetraphos \longrightarrow [\{Ir_4(CO)_{11}\}_4(180tetraphos)] + 4PPh_4Br$$

The reaction is followed by IR spectroscopy: in Fig. 141a is reported the carbonylic region of $[PPh_4][Ir_4Br(CO)_{11}]$ IR spectrum, the most significant for our aims, while in the Fig. 146b there is the final spectrum. A shift to higher wave numbers occurred, as we expect moving from an anionic to a neutral species.

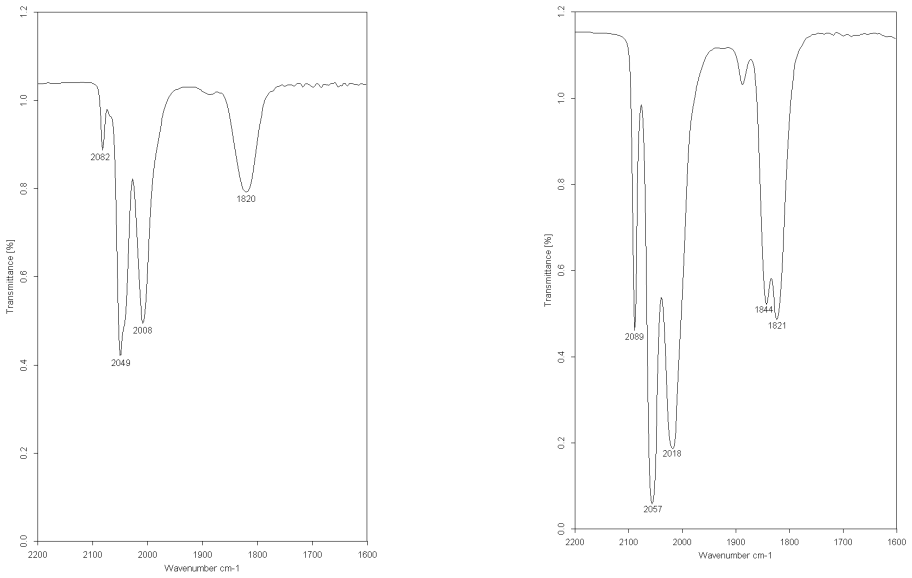

Fig. 146 $CHCl_3$ IR spectrum of a) $[PPh_4][Ir_4Br(CO)_{11}]^-$ and b) $[\{Ir_4(CO)_{11}\}_4(180tetraphos)]$

RT ^{31}P-NMR, registered in $CDCl_3$, is shown in Fig. 147.

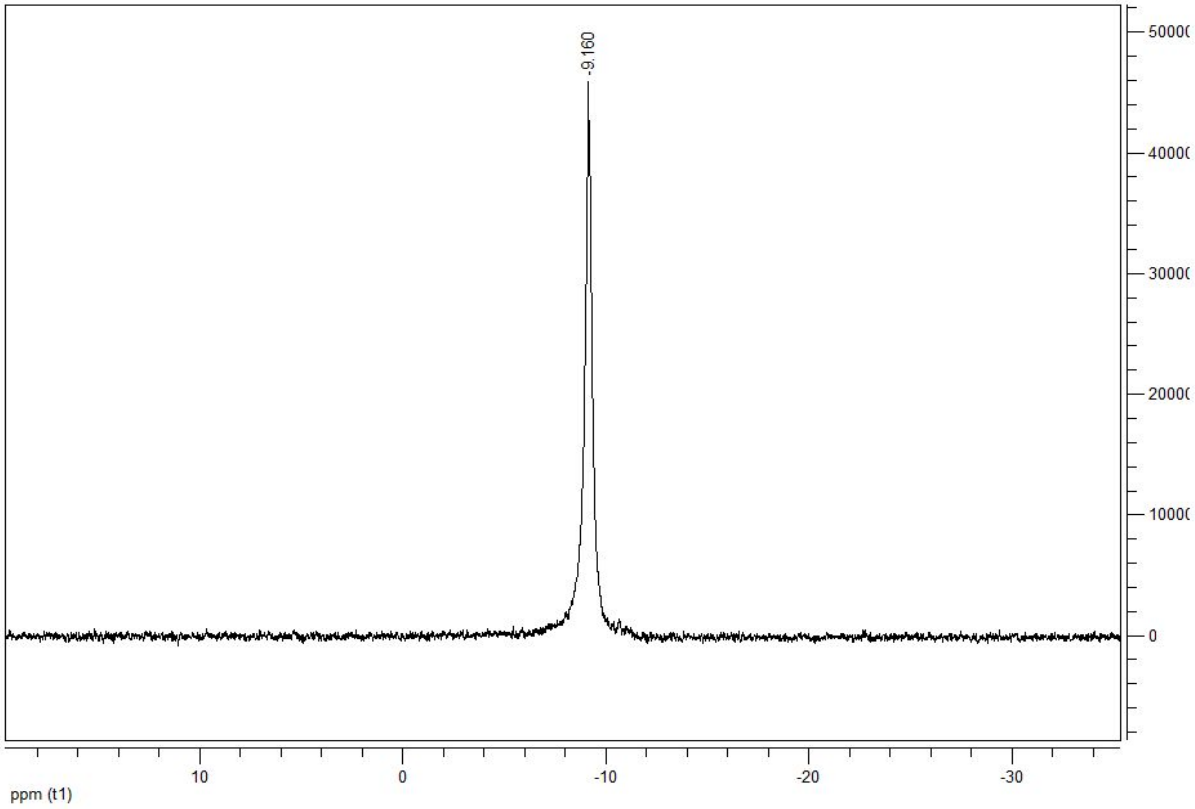

Fig. 147 $CDCl_3$ ^{31}P-NMR of [{$Ir_4(CO)_{11}$}$_4$(180tetraphos)]

There is only one singlet at -9,16 ppm,while the free ligand chimica shift is -3,85 ppm. This means that all the phosphorus atoms have the same chemical environment. The chemical shift is in agreement with an axial coordination of the phosphane groups.

Solid state structure

The solid state structure was obtained from single crystals X-ray diffraction, Fig. 143. The crystals were grown by layering a chloroform solution of the product with 2-propanol. It consists of four [$Ir_4(CO)_{11}$] fragments assembled through a 180tetraphos molecule. All the phosphane groups are axially coordinated and this is consistent with the ^{31}P-NMR spectrum, confirming that the structure in solution is the same than in solid.

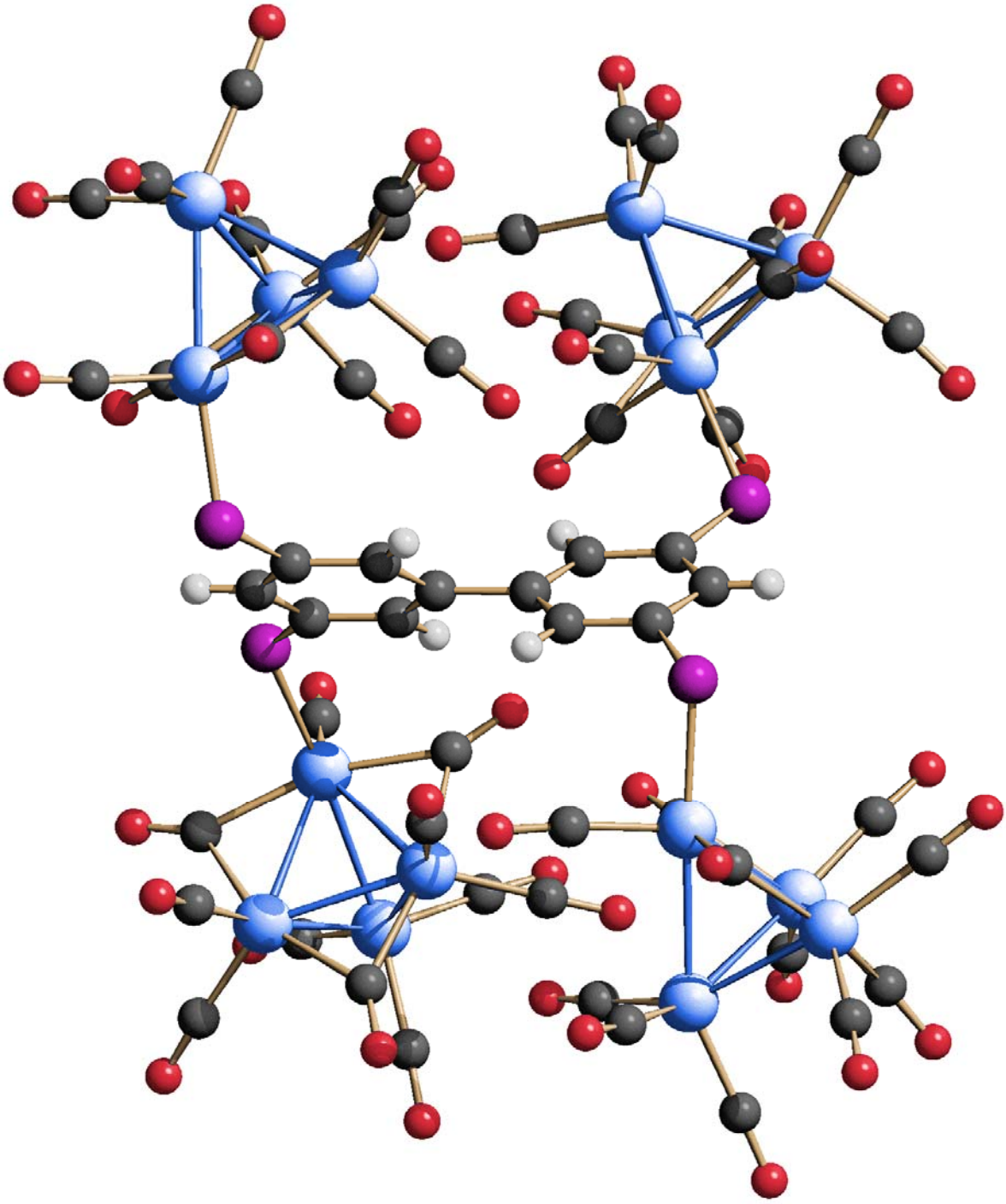

Fig. 148 SC X-ray diffraction of [{$Ir_4(CO)_{11}$}$_4$(180tetraphos)]

From Fig. 149 it is possible to see how the four clusters are on the vertex o fan irregular tetrahedrom. The distances among the metal atoms, excluding the coordinated CO spheres are included between 10,819 and 14,986 Å, so the molecule has nanometric size.

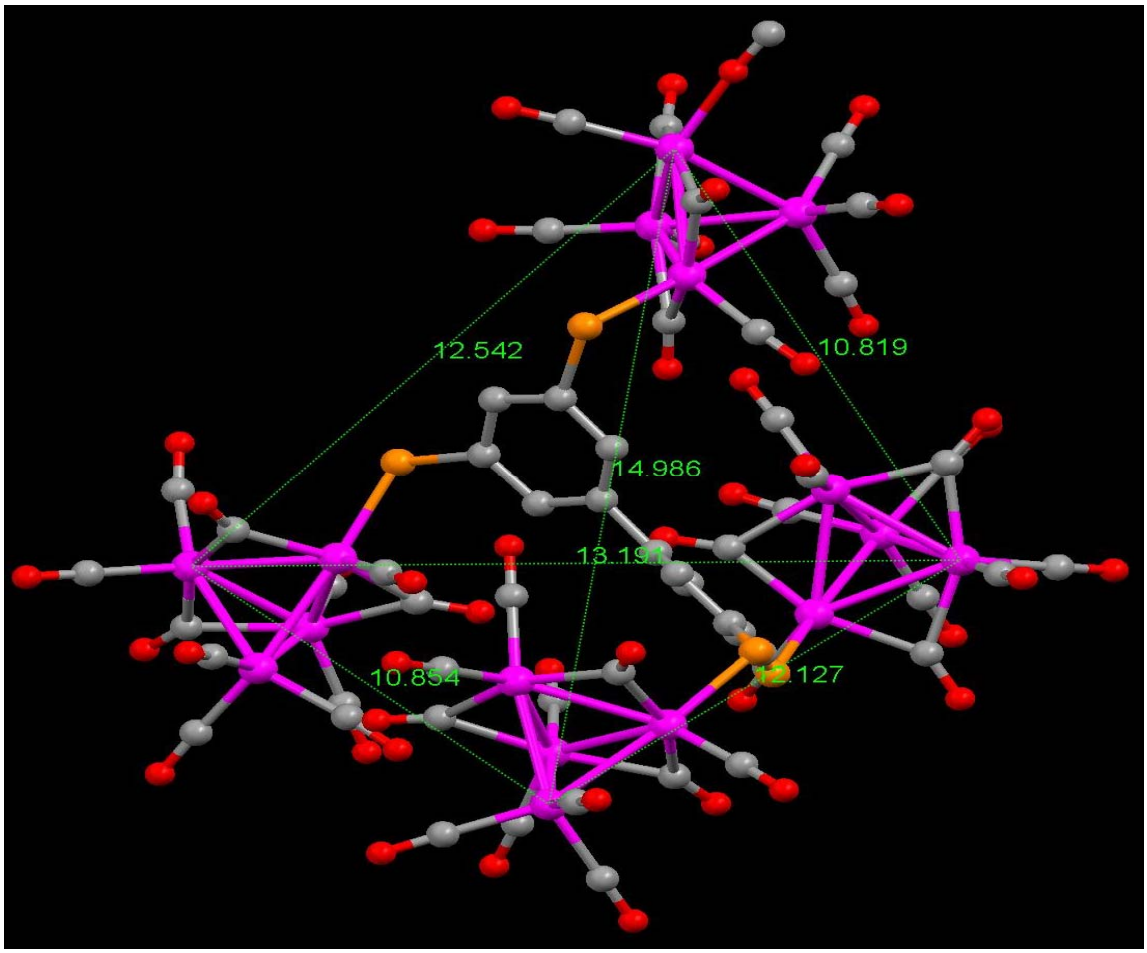

Fig. 149 Another view of [{$Ir_4(CO)_{11}$}$_4$(180tetraphos)]

Electrochemistry

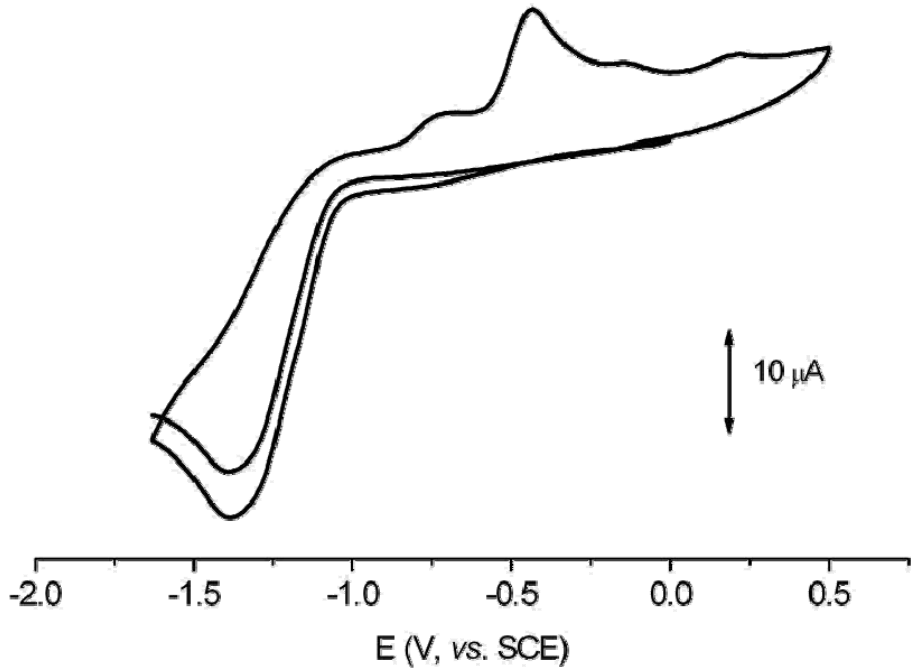

Fig. 150 Cyclic voltammetric responses recorded at a Pt electrode in THF solution of [{$Ir_4(CO)_{11}$}$_4$(180tetraphos)]. NBu_4PF_6 as supporting electrolyte.

An electrochemical study has been conducted on [{$Ir_4(CO)_{11}$}$_4$(180tetraphos)]. The compound exhibits an irreversible reduction at -1,37 V. After this process, the resulting species is adsorbed on the electrode and redox active breaking down products are formed. From the voltammetric profile it is evident that some of them give adsorbtion processes too.

During the electrolysis the solution gradually changes color, moving from yellow to dark red and the process appears to be multielectronic.

Synthesis and characterization of [{$Ir_4(CO)_{11}$}$_4$(180tertetraphos)]

The synthesis of this species has followed the same procedure of the previous derivative. The IR spectrum is nearly superimposable while the ^{31}P-NMR is shown in Fig. 151

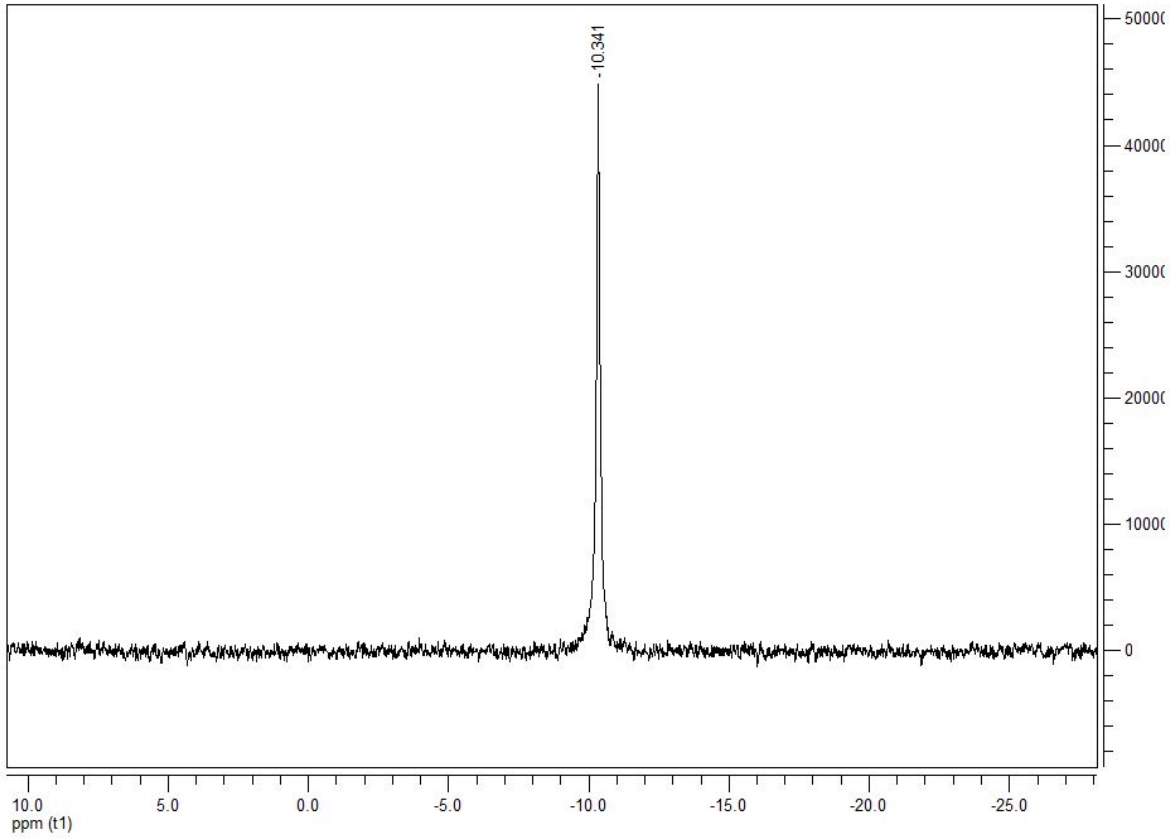

Fig. 151 $CDCl_3$ ^{31}P-NMR of [{$Ir_4(CO)_{11}$}$_4$(180tertetraphos)]

It is present a singlet at -10,34 ppm, agreeing with axially coordinated P atoms, as for [{$Ir_4(CO)_{11}$}$_4$(180tetraphos)], only slightly shifted to higher field.

Solid state structure

The solid state structure was obtained from single crystal X ray diffraction (Fig. 152).
As in the previous case, a tetraphosphane molecule assemble four tetrairidium cluster, which coordinate the ligand arms in axial position respect to the base of the tetrahedron.

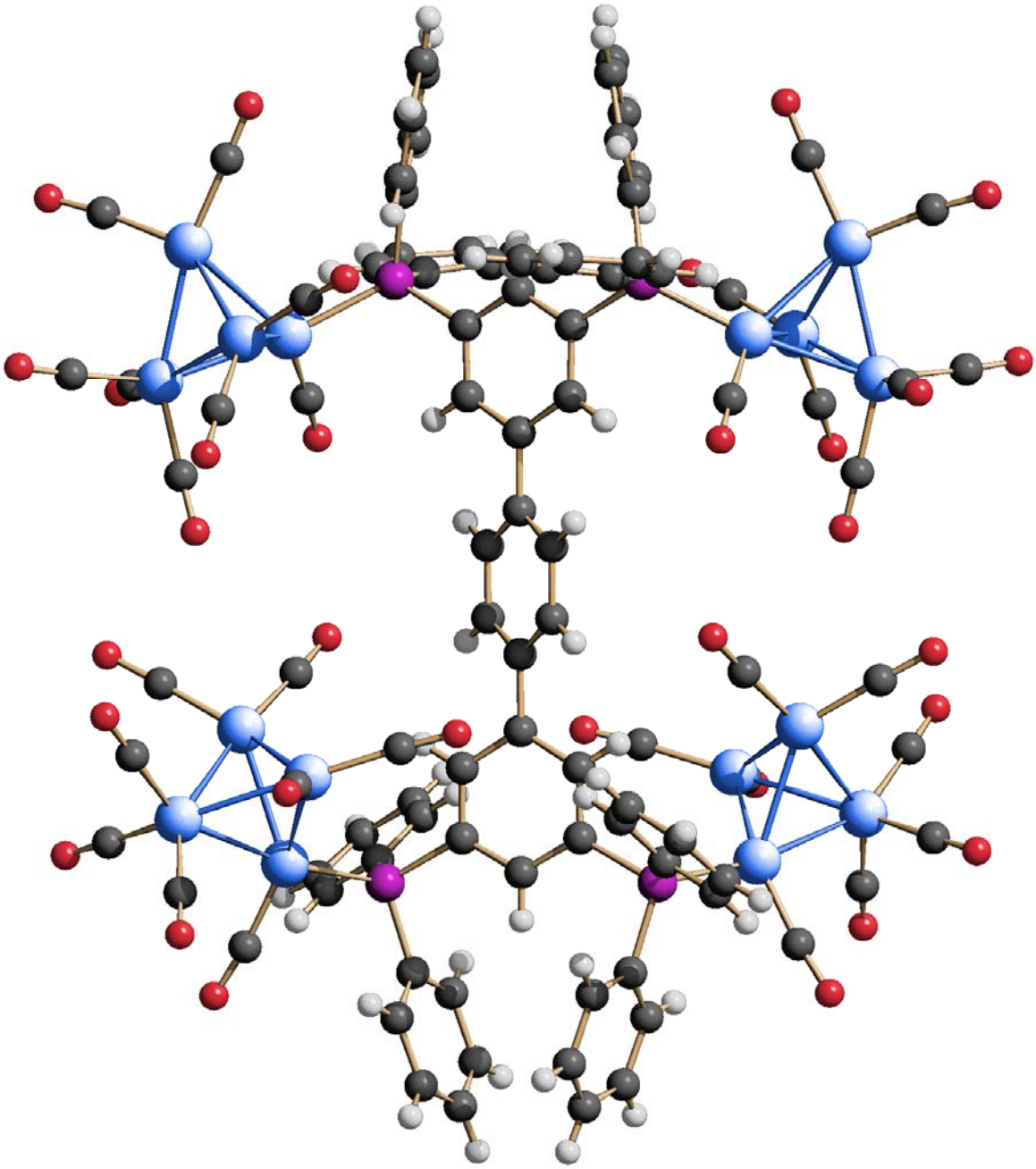

Fig. 152 SC X-ray diffraction of [{$Ir_4(CO)_{11}$}$_4$(180tertetraphos)]

From Fig. 153 it is possible to note that the four clusters occupy the vertex of a distorted isosceles trapezium, existing a torsion angle of 17.69°.

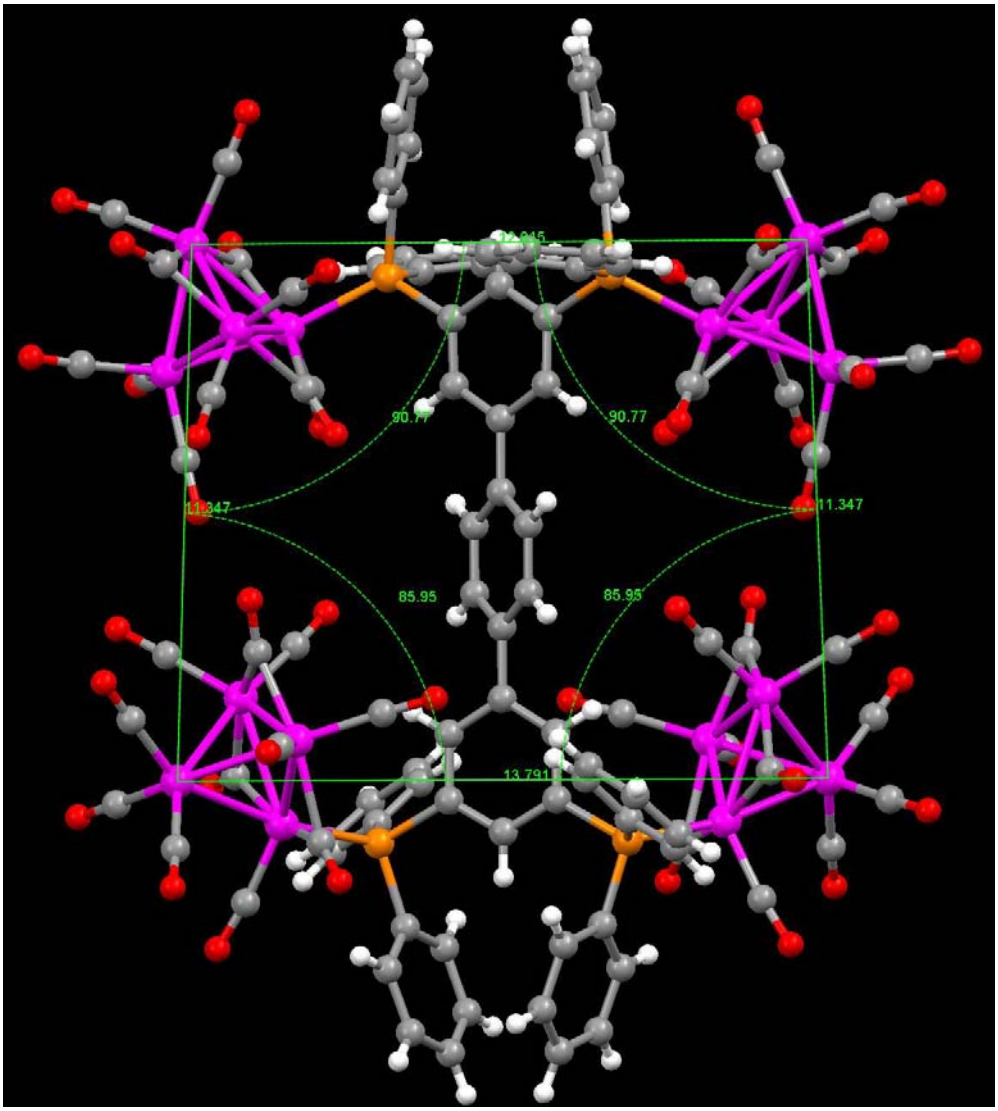

Fig. 153 Another view of [{$Ir_4(CO)_{11}$}$_4$(180tertetraphos)]

Reactivity of $[Ir_4Br(CO)_{11}]^-$ with the other rigid multiphosphanes

Also with the remaining ligands, we exploited the high easiness and selectivity of bromine substitution in $[Ir_4Br(CO)_{11}]^-$ by phosphane ligands to obtain the compounds where a $[Ir_4(CO)_{11}]$ fragment is bonded to each available phosphorous atom.
If we schematize our multidentate ligands having n PPh_2 groups as L^n, the general reaction is the following:

$$n\ [PPh_4][Ir_4Br(CO)_{11}] + L^n \longrightarrow [\{Ir_4(CO)_{11}\}_n(L^n)] + n\ [PPh_4]Br$$

Elemental analyses, IR and ^{31}P-NMR spectra are in agreement with the expected formula $[\{Ir_4(CO)_{11}\}_n(L^n)]$. In particular the chemical shifts are always in the region of axially coordinated PAr_3 groups. These data, together with the two previous presented X-ray structures, support us in stating the similarity of all these products.
In the following figures, ^{31}P-NMR are reported.

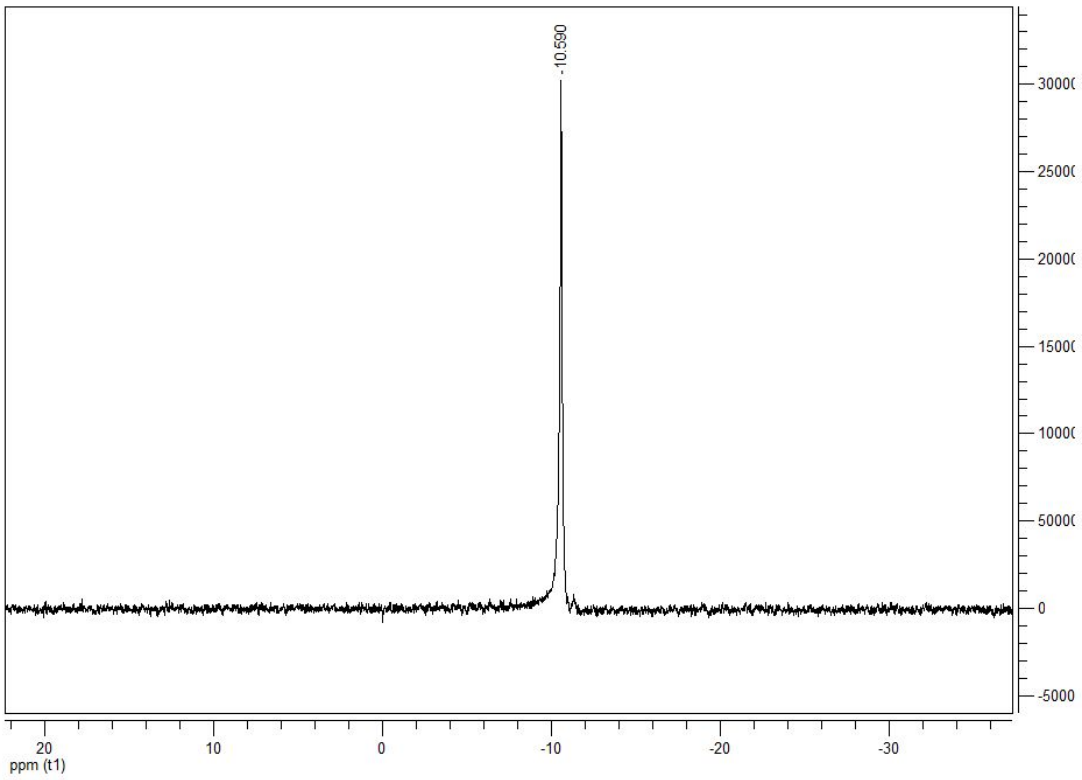

Fig. 154 $CDCl_3$ ^{31}P-NMR of $[\{Ir_4(CO)_{11}\}_6$(120hexaphos)]

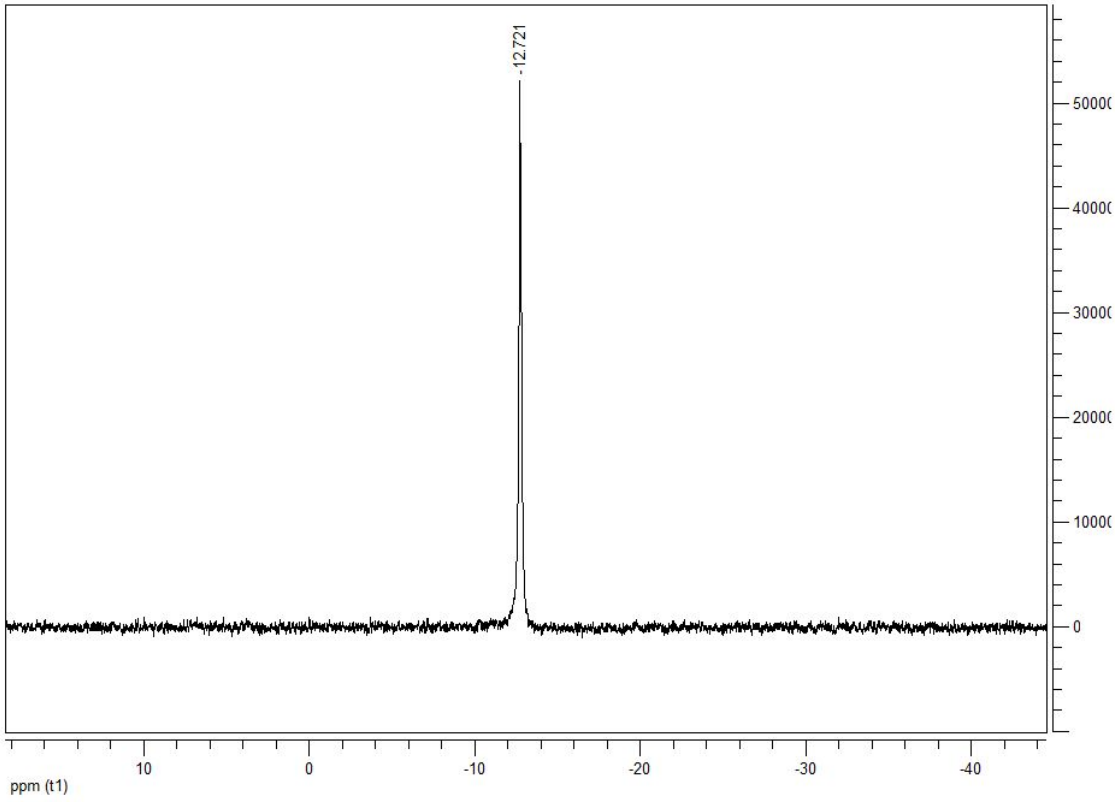

Fig. 155 $CDCl_3$ ^{31}P-NMR of [{$Ir_4(CO)_{11}$}$_4$(t4dpppm)]

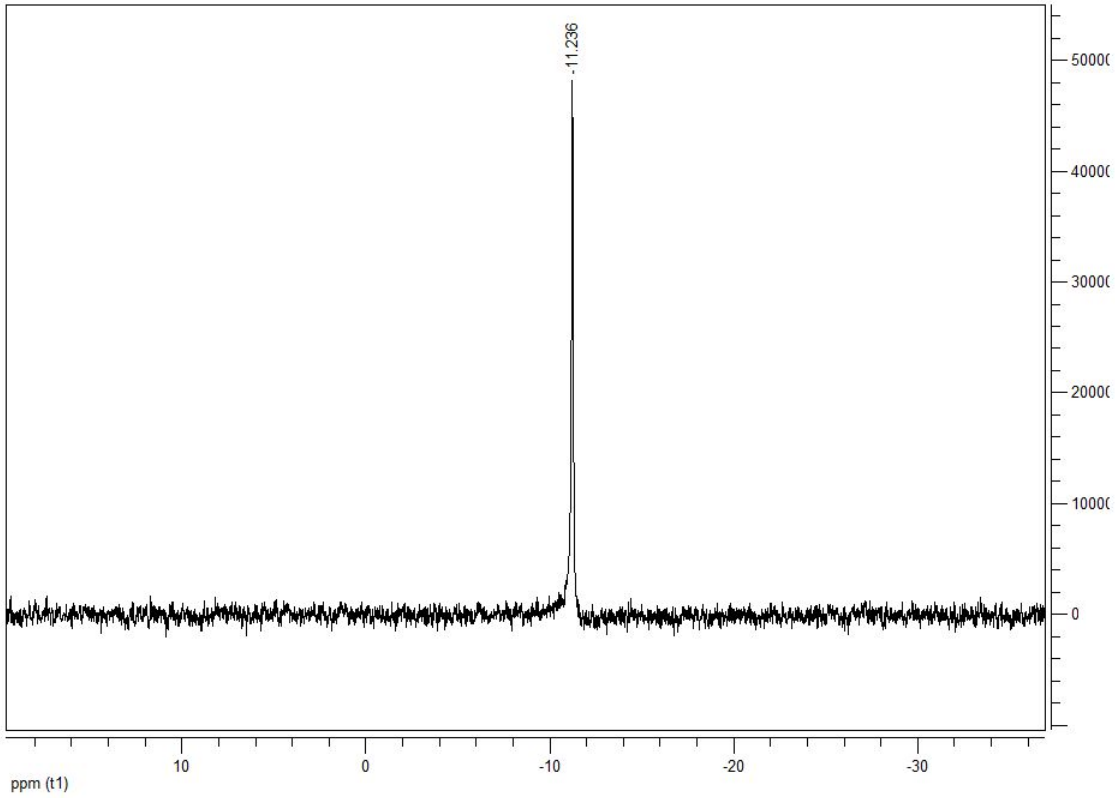

Fig. 156 $CDCl_3$ ^{31}P-NMR of [{$Ir_4(CO)_{11}$}$_4$(t3′dppbm)]

Reactivity of rigid multiphosphanes with [AuCl(THT)]

We have then used AuCl(THT) (THT = tetrahydrothiophene) with the different ligands in order to obtain the species where one fragment AuCl is coordinated to each P atom. THT is a labile ligand and it is easily substituted by the phosphane. For example in the case of 180tetraphos:

$$4[AuCl(THT)] + 180tetraphos \longrightarrow [(AuCl)4(180tetraphos)] + 4THT$$

With the only exception of the product obtained starting from t3'dppbpm, which is very sensible to oxidation, all the others are air and light stable and they are prepared in good yields. ^{31}P-NMR spectra show onle singlet shifted to lower field respect of the corresponding uncoordinated ligands, Figg. 157-161

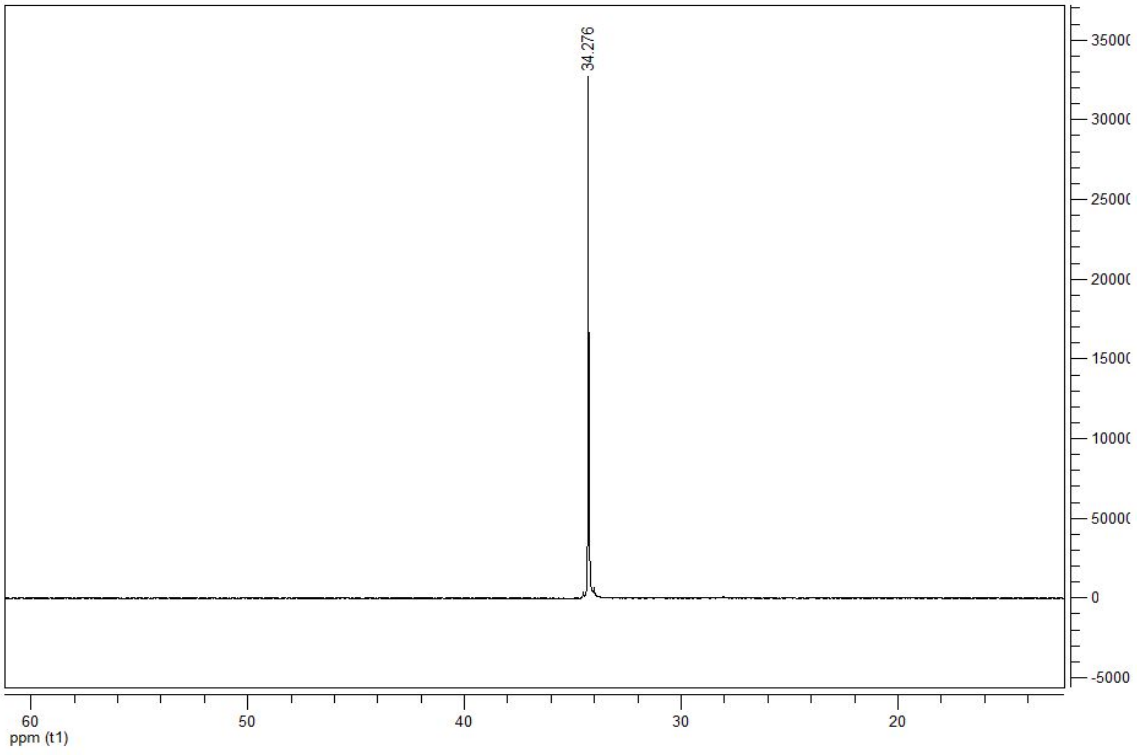

Fig. 157 $CDCl_3$ ^{31}P-NMR spectra of $[(AuCl)_4(180tetraphos)]$

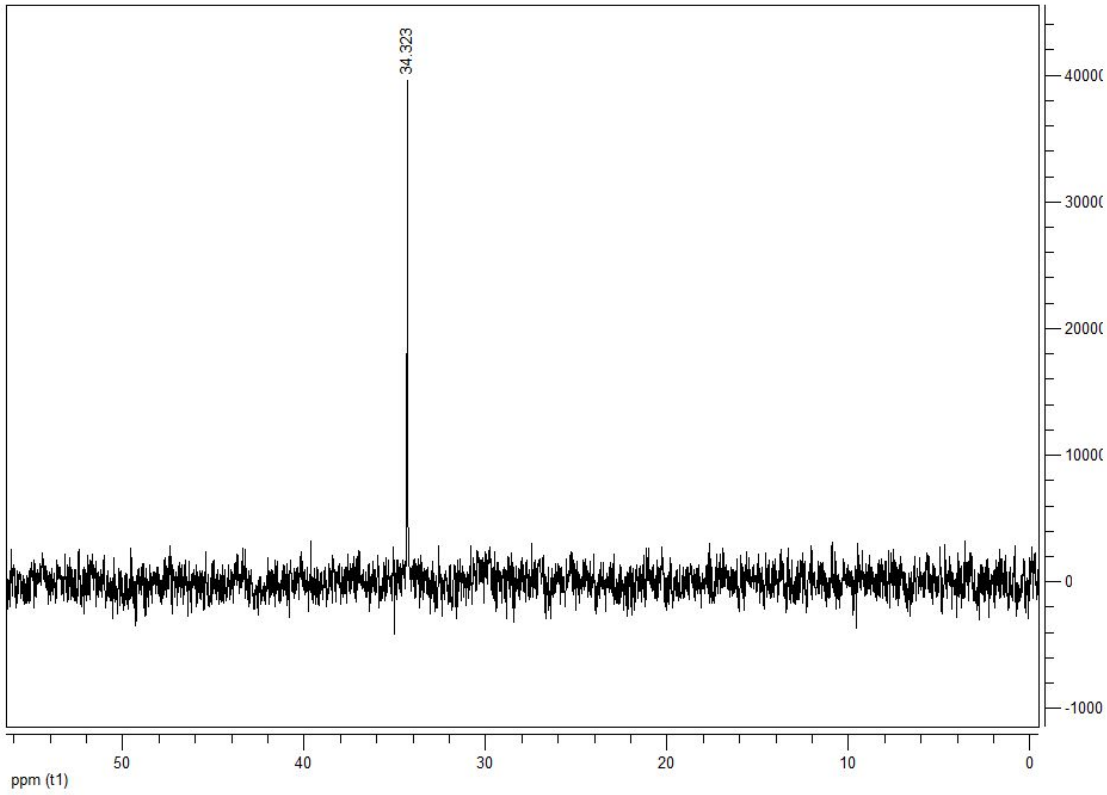

Fig. 158 $CDCl_3$ ^{31}P-NMR spectra of [$(AuCl)_4$(180tertetraphos)]

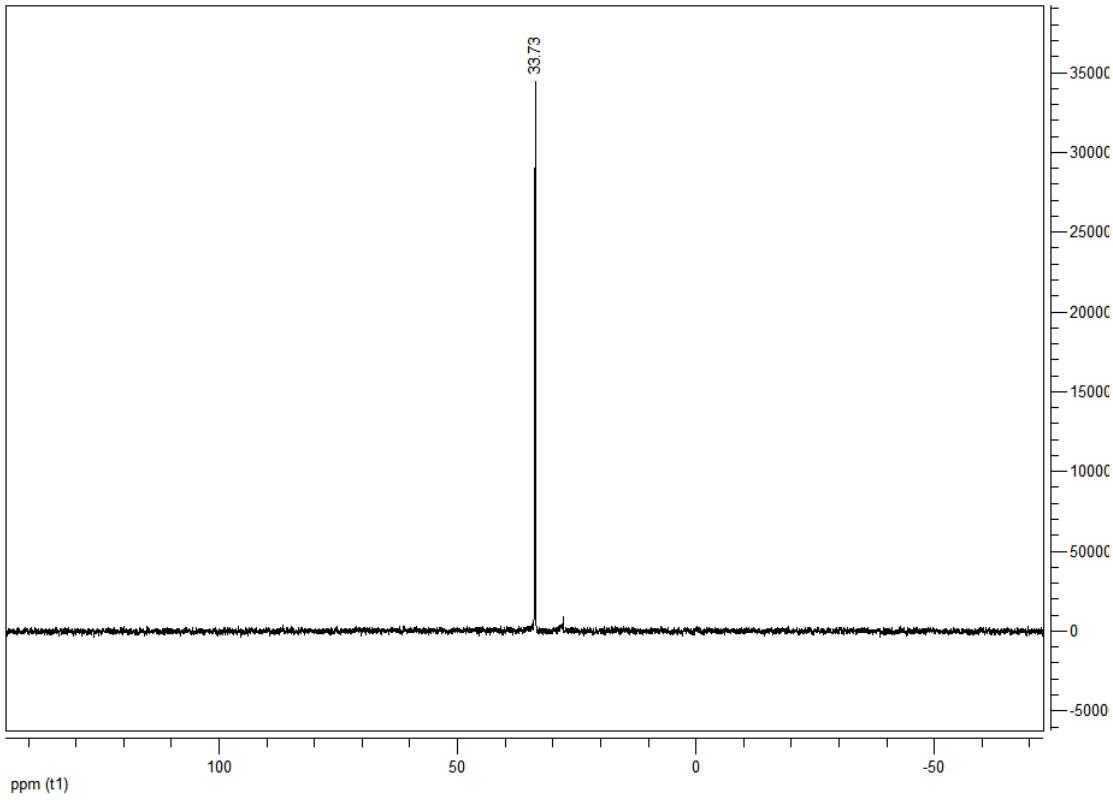

Fig. 159 $CDCl_3$ ^{31}P-NMR spectra of [$(AuCl)_6$(120hexaphos)]

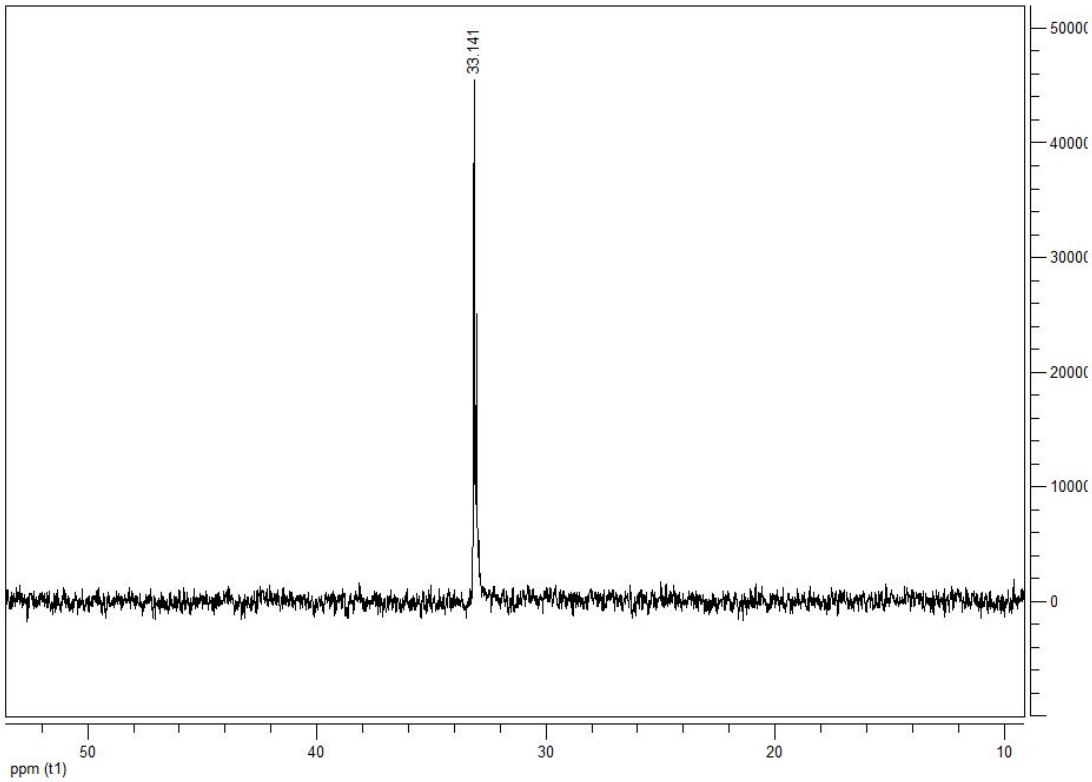

Fig. 160 $CDCl_3$ ^{31}P-NMR spectra of [$(AuCl)_4$(t4dpppm)]

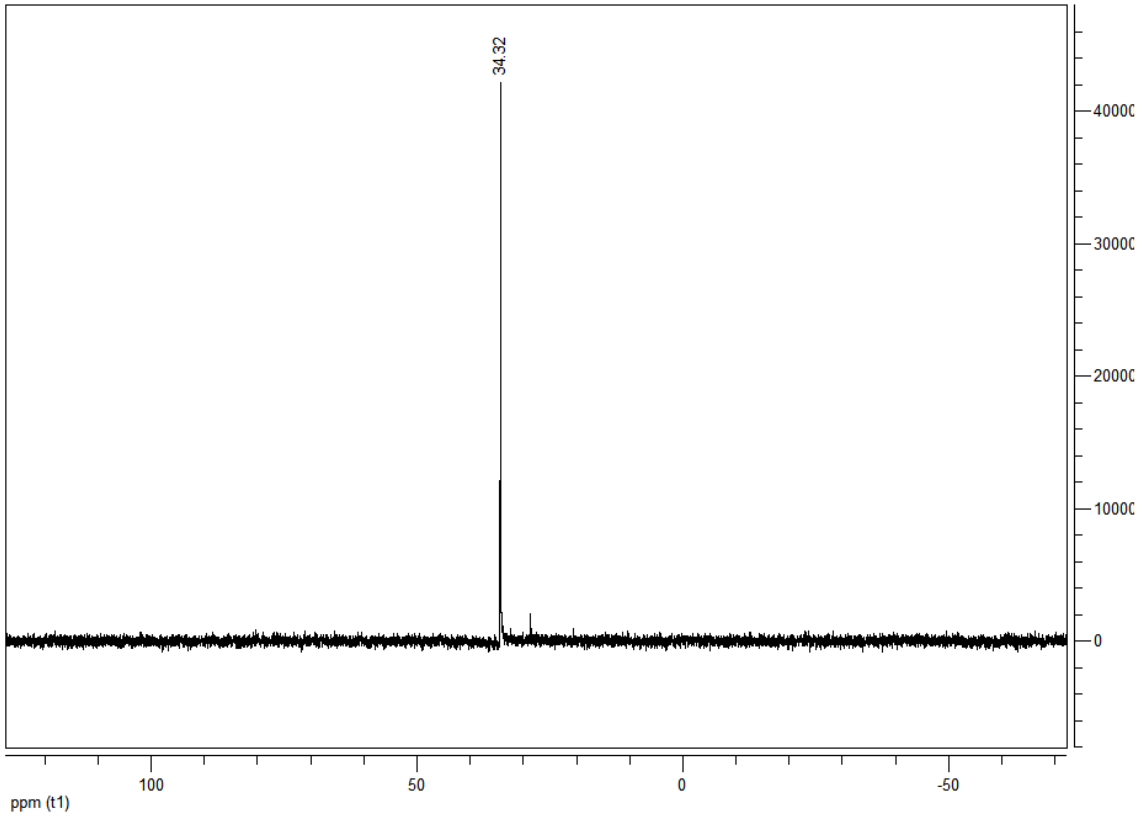

Fig. 161 $CDCl_3$ ^{31}P-NMR spectra of [$(AuCl)_8$(t3′5′tdppbpm)]

Emission spectra of Au(I) phosphanes complexes, registered in chloroform, are here reported. A shift to lower wavelenghts, respect to the free ligands, is observed in all cases.

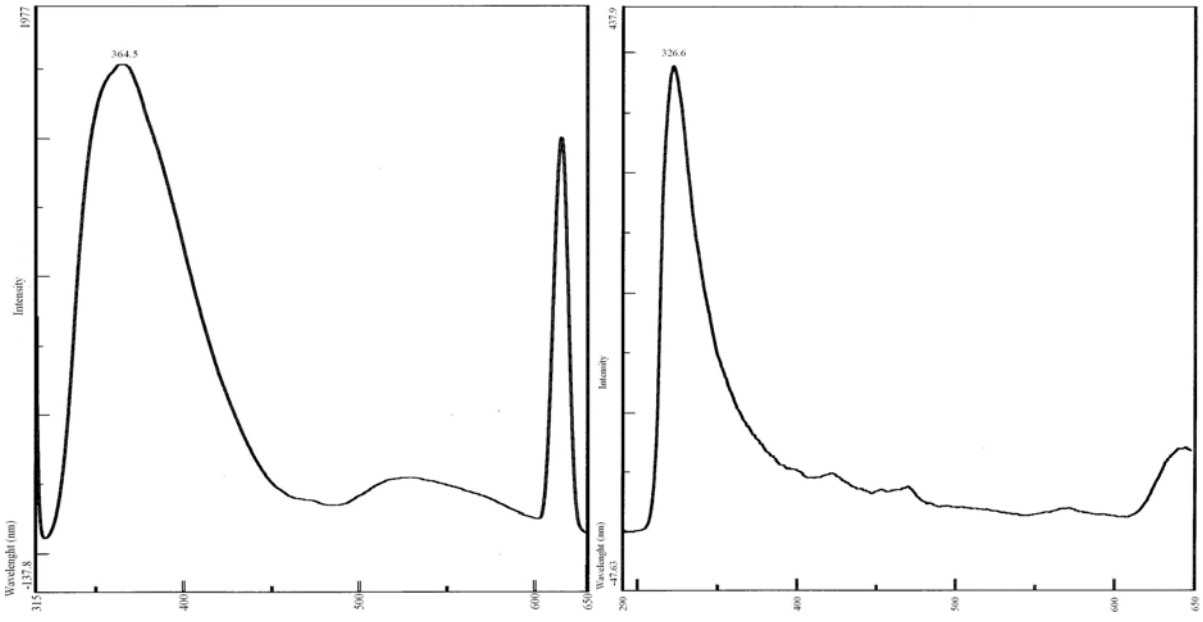

a **b**

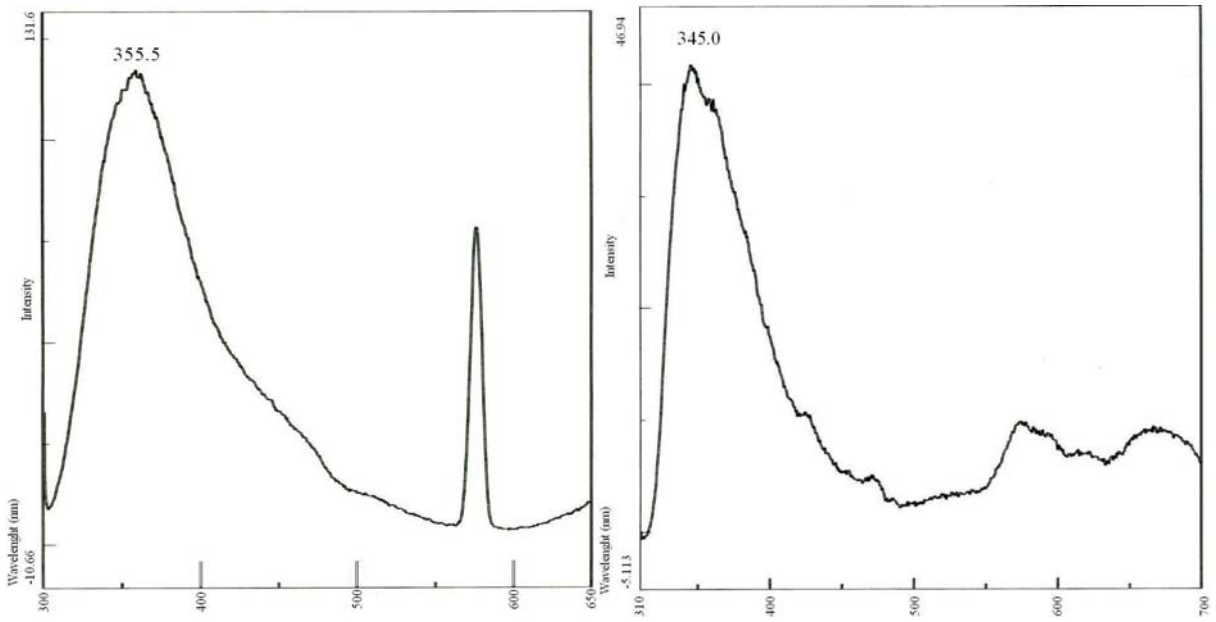

c **d**

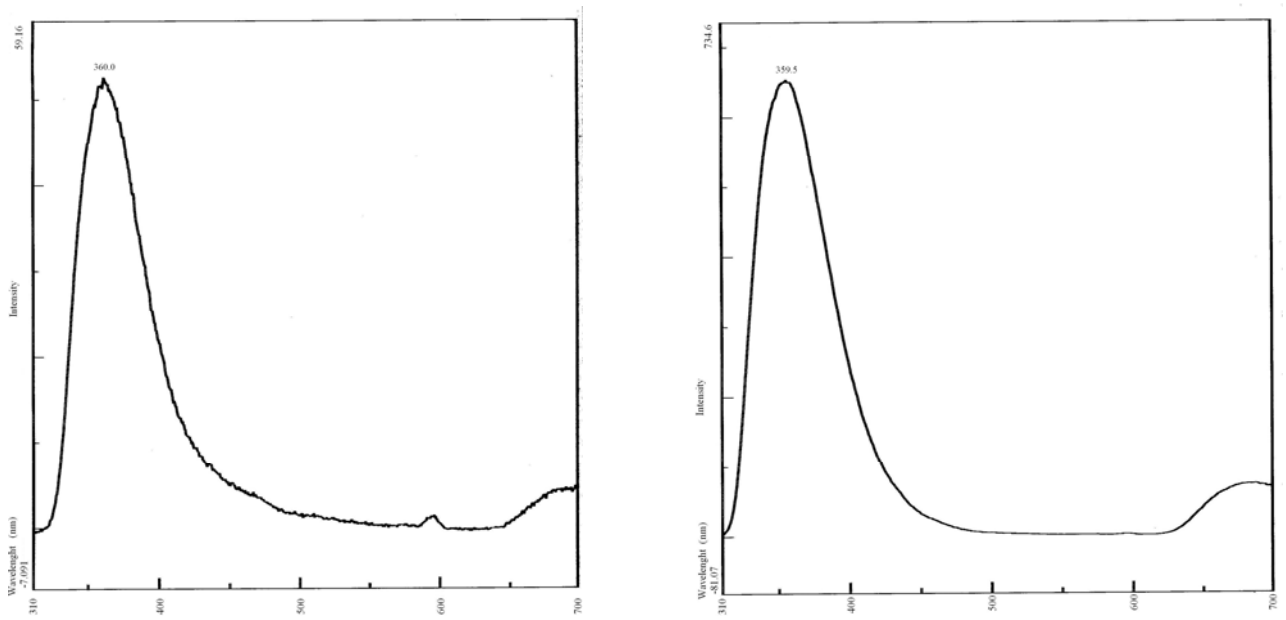

e **f**

Fig. 162 $CHCl_3$ emission spectra of a) $[(AuCl)_4$(180tetraphos)] b) $[(AuCl)_4$(180tertetraphos)] c) $[(AuCl)_6$(120hexaphos)] d) $[(AuCl)_4$(t4dpppm)] e) $[(AuCl)_4$(t3′dppbpm)] f) $[(AuCl)_8$(t3′5′tdppbpm)]

Reaction of 180tetraphos, 180tertraphos and 120hexaphos with $NiBr_2$

We tested $NiBr_2$ with rigid multiphosphanes with the aim to obtain analogous polymers to those hyphotized for Rh(I) and Ir(I) and characterized in the case of these metals and rigid or flexible diphosphanes.[180]

So we have used a 2:1 M:L molar ratio for tetra- phosphanes and 3:1 for hexa- phosphane.

In a typical reaction, the nickel salt is dissolved in acetone and this solution is added under stirring to a solution of the ligand in chloroform. We have conducted the reaction in a mixture of solvents as there is not a solvent suitable for both the reagents.

A green solid, which then reveals to be insoluble in all organic solvents, was precipitating after some minutes from the addition. The colour of the solid is important because it gives us an indication about the geometry of the metal centres.

In fact, it is known that a tetra-coordinated Ni(II) can adopt a square planar geometry in a low spin complex or a tetrahedral geometry in a high spin complex. In the first case the products are yellow whereas in the latter they are green.

Crystals suitable for X-ray analysis have been obtained in the case of 180tetraphos by layering an acetone solution of the salt on a solution of the ligand in chloroform. The structure is shown in Fig. 163.

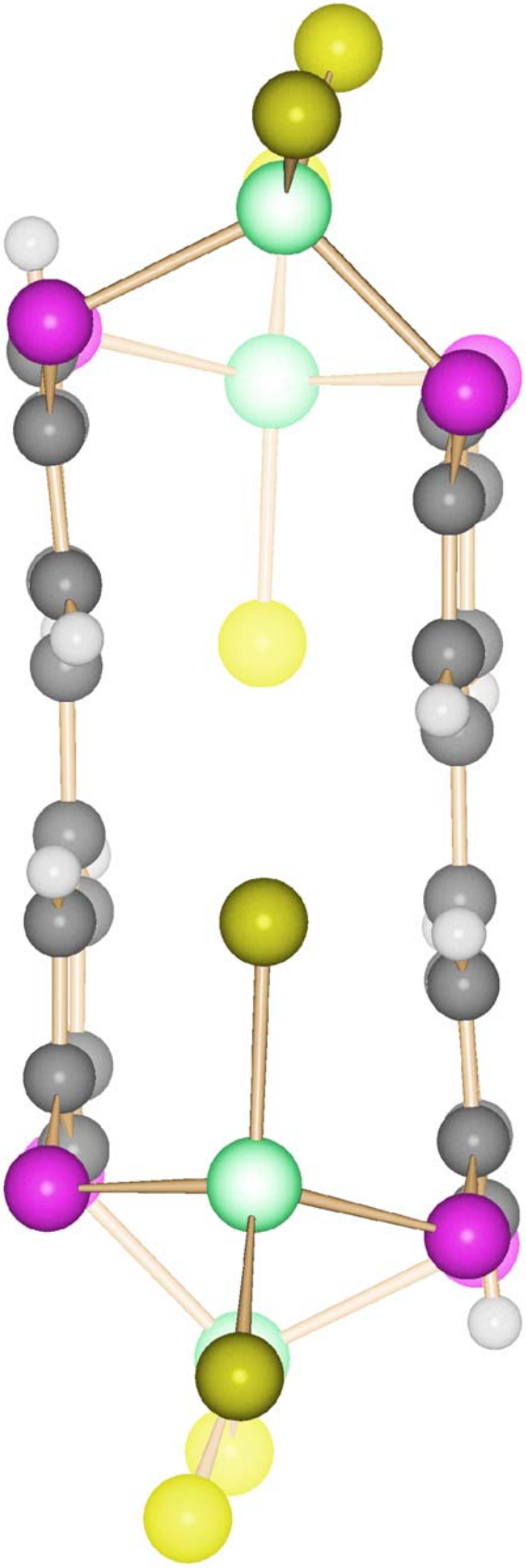

Fig. 163 SC X-ray diffraction structure of [{$NiBr_2$}$_4$(180tetraphos)$_2$]

It consists of two ligand molecules facing parallelly joined by four Ni(II) centres coordinating two P atoms and two bromidres in tetrahedral geometry.

Elemental and XRPD analyses conducted on the microcrystalline products obtained by reaction have confirmed its identity with the crystalline product obtained by stratification.

With regard to the products obtained with the other phosphanes, elemental analyses agree with a M:L 2x : 1x molar ratio for 180tertetraphos and 3x: 1x for 120hexaphos.

We can hypothesize that analogous species to the structurally characterized are formed, although we can not exclude other possibilities including a coordination polymer.

Magnetic measurements on [{$NiBr_2$}$_4$(180tetraphos)$_2$]

We have conducted magnetic measurements in collaboration with Prof. Riccò of the "Università degli Studi di Parma" using a SQUID equipment.

[{$NiBr_2$}$_4$(180tetraphos)$_2$] magnetic signal is intense and it has been measured in different conditions.

The measure as fuction of field at 300 K (Fig. 164) shows that the sample has a paramagnetic behaviour, with an additional little ferromagnetic contribution, consistent with some traces of ferromagnetic impurities (most likely metallic nickel).

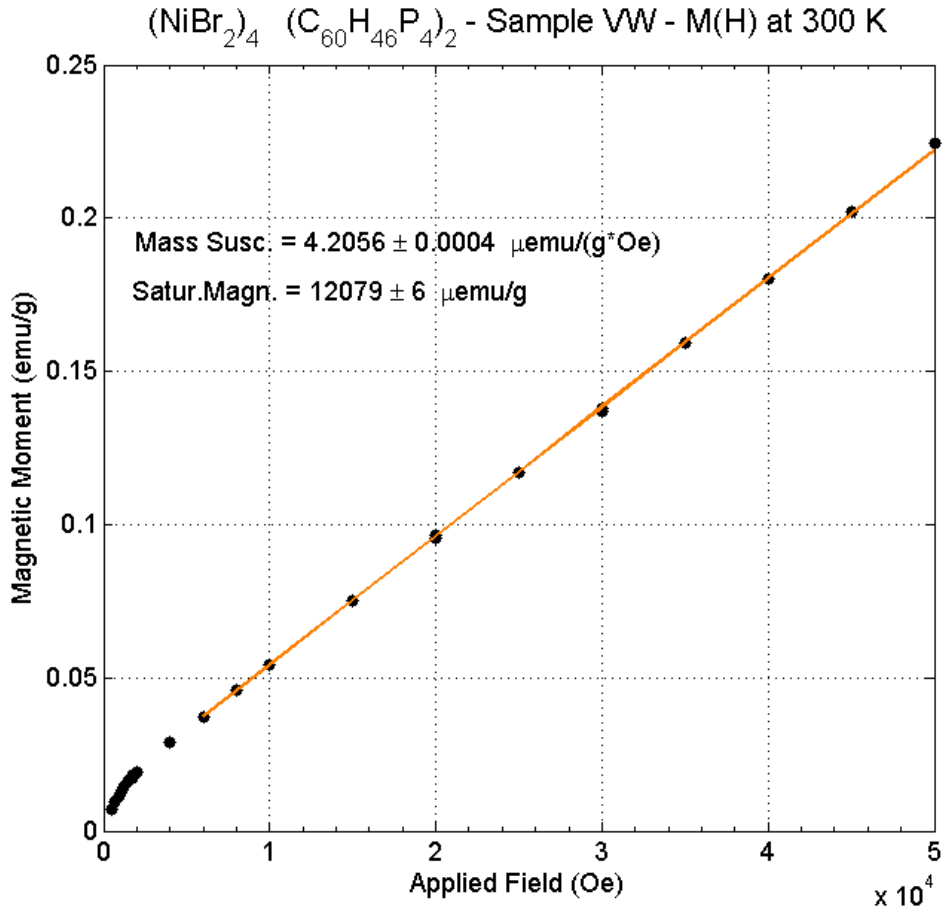

Fig. 164 Applied field *vs* magnetic moment measure trend of [{$NiBr_2$}$_4$(180tetraphos)$_2$]

The measurements depending on temperature (Fig. 165) show the Curie-Weiss behaviour typical of paramagnets and they indicate that the four nickel atoms do not interact one to each other. Instead, each of them behaves as an isolated spin with a magnetic moment of

3,21 Bohr magnetons. This value is in good agreement with the tabulated experimental value for a Ni(II) of 3,12 Bohr magnetons.[181]

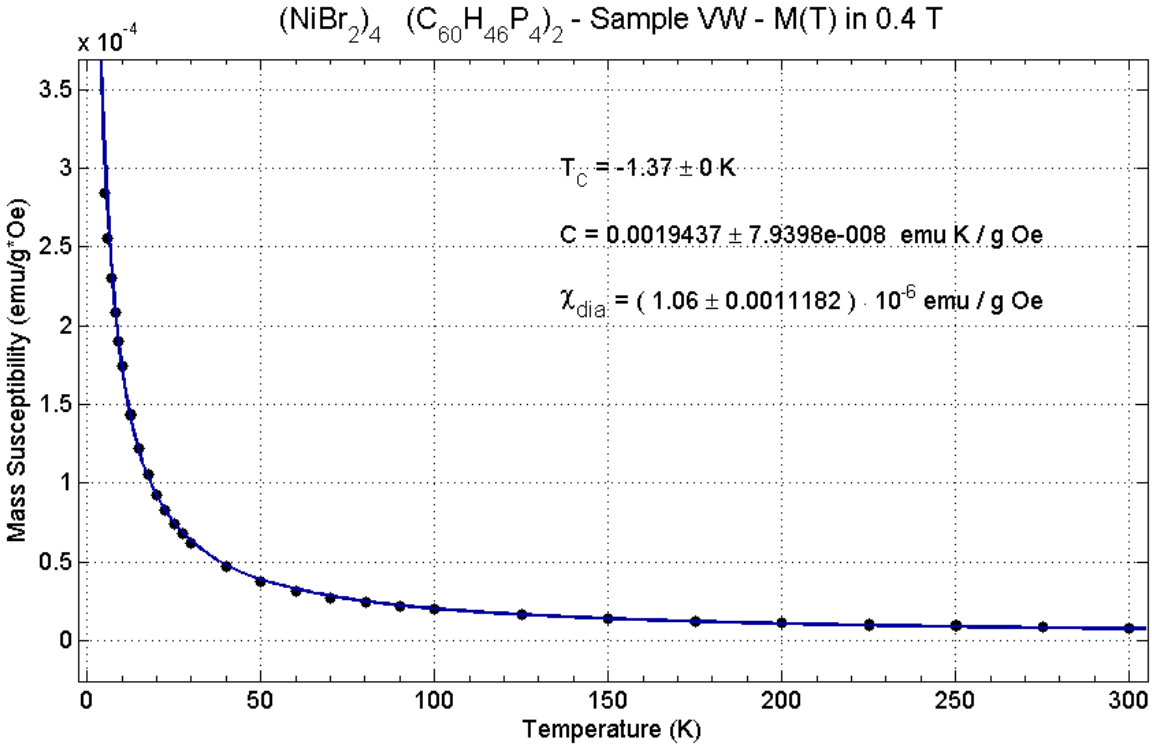

Fig. 165 Mass susceptibility of [{$NiBr_2$}$_4$(180tetraphos)$_2$] as a function of temperature

This magnetic moment grossly corresponds to a J = 1 state of spin which should be well recognizable by the shape of the magnetization curve as a function of the field at low temperature. Actually a pure J = 1 state of spin should have a magnetic moment of 3,00 Bohr magneton.

We performed this measurement at 2 K (Fig. 166) but the teoric curve that is obtained by attributing a J = 1 spin to each Ni corresponds to a magnetization higher than the experimental one. This reduced magnetization indicates the presence of magnetic anisotropy in the system.

It is not possible to attribute a J_{TOT} to the whole molecule becuase the spins of the single Ni centres can not be combined as the centres are too far to interact.

We can otherwise state that the total magnetic moment is equivalent to that one of eight unpaired electrons.

In fact, if we consider eight spin per molecule, the experimental magnetic moment is 1,6 μB for each spin, while the value for a single electron is 1,73 μB.

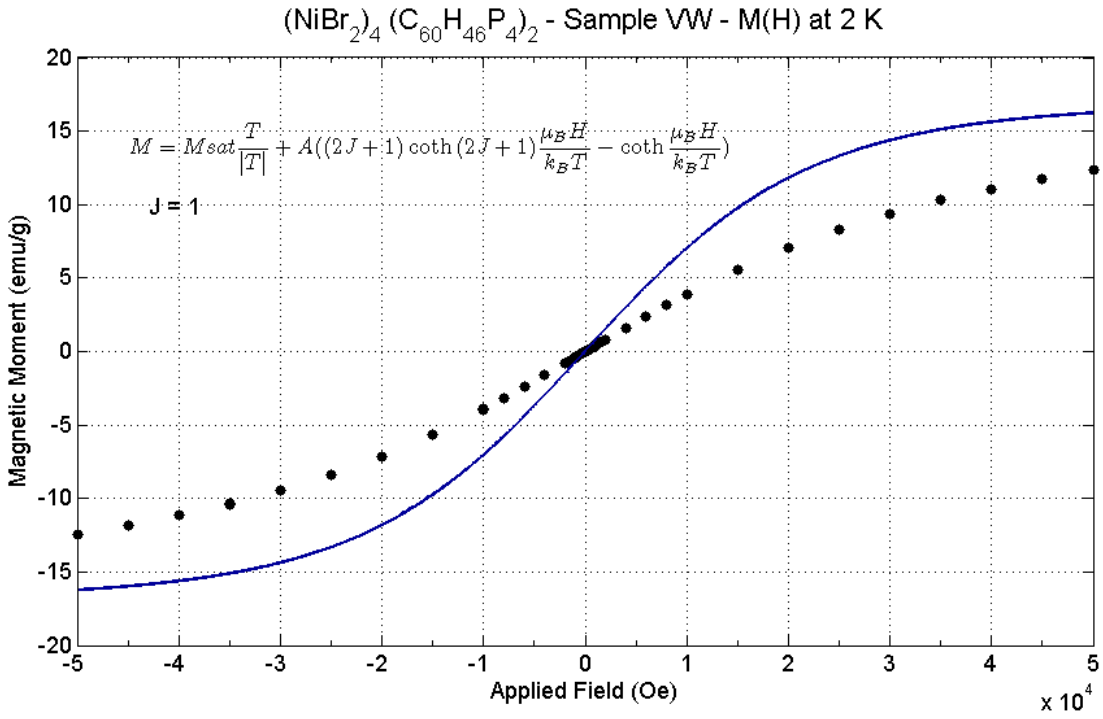

Fig. 166 Experimental magnetization curve (dots) as a function of field of at 2 K and theoric curve (line) for an eight J = 1 spins system [{$NiBr_2$}$_4$(180tetraphos)$_2$]

Reaction between rigid poliphosphanes and $[Pt_{19}(CO)_{22}]^{4-}$

Tetrairidium carbonyl cluster revealed to be too small to bear a change in oxidation state reversibly, as we confirmed through cyclovoltammetry of $[\{Ir_4(CO)_{11}\}_4(180tetraphos)]$.
So we decided to try with bigger cluster, as it is known that the higher the nuclearity is, the closer the energetic levels are and the metal core can assume different charges without substantial structural changes.
$[Pt_{19}(CO)_{22}]^{4-}$ [182]has a special role among metal carbonyl clusters, since it remained for a long time as the largest structurally characterized one. Studies on its reactivity have been slowed down by difficulties in the characterization of its unstable products. An example is the one obtained by simple exposure to CO atmosphere, which presents an unusual down-shift of the original stretching bands. This fact indicates that the metal-to-ligand backdonation is increased, suggesting that this uncharacterized species would be a good electron donor toward electrophiles.
$[Au(PPh_3)]^+$ fragment has been proved to stabilize $[Pt_{19}(CO)_{22}]^{4-}$ and the series $[Pt_{19}(CO)_{22}(AuPPh_3)n]^{n-4}$ (n = 1, 2) and $[Pt_{19}(CO)_{24}(AuPPh_3)m]^{m-4}$ (m = 3, 4) have been prepared and structurally and electrochemically characterized.[183]
So, following the idea of compartmental capacitors, we used our gold(I) poliphosphane complexes to assemble Pt_{19} clusters.

Synthesis

$$n\,[Pt_{19}(CO)_{22}]^{4-} + [Au_nL^n]^{n+} \xrightarrow{CO} [\{Pt_{19}Au(CO)_{24}\}_n(L^n)]^{3n-}$$

We found that a dehalogenation step of the gold-phosphanes (made with Ag^+) has been necessary as the reaction occurred.
A solution of the gold phosphane complex in THF has been added to a solution of $[Pt_{19}(CO)_{22}]^{4-}$ in acetone and the resulting solution has been put in CO atmosphere and stirred for some hours.
The CO stretching bands pattern is similar to that of $[Pt_{19}(CO)_{22}(AuPPh_3)]^{3-}$

We focused our attention expecially on 180tetraphos and 120hexaphos. In both cases elemental analyses are in good accordance with the above proposed formula, giving $[NBu_4]^+$ as cation.

We grow some crystals for these products but unfortunaly they were geminate or their unit cell was too big and so it was not possible to get the structure. Actually the crystallization of such big species as $[NBu_4]_{18}[\{Pt_{19}Au(CO)_{24}\}_6(120hexaphos)]$ can be really challenging.

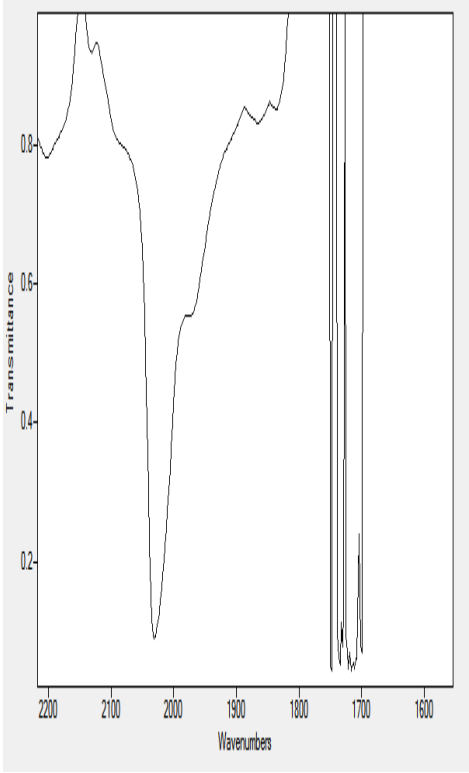

Fig. 167Acetone IR spectrum of $\{Pt_{19}Au(CO)_{24}\}_6(120hexaphos)]^{18-}$

Reaction between rigid poliphosphanes and $[Ir_6(CO)_{15}]^{2-}$

Cluster aggregates based on tetrahedral Ir_4 described above appear to show irreversible reduction in the cyclovoltammetry. So, their behaviour as "compartmental nanocapacitors" is inficied by the lack of cyclability of the charge-discharghe process.
On its hand, the anionic $[Ir_6(CO)_{15}]^{2-}$ is known to show reversible redox processes. This difference arises from the presence of quasi-degenerate orbitals in the hexanuclear cluster that allows to catch or to loose electrons without a change in the structure.
We are currently investigating redox behaviour with electrochemical analysis.

Synthesis

The reaction is conducted under CO atmosphere and the de-halogenation of the gold-phosphane ligand is necessary. A solution of the ligand in stoichiometric amount is added to a solution of the cluster, both in THF.

$$4\ [Ir_6(CO)_{15}]^{2-} + [Au_4(180tetraphos)]^{4+} \xrightarrow{CO} [\{Ir_6Au(CO)_{15}\}_4(180tetraphos)]^{4-}$$

After one hour stirring the reaction is completed, as checked by IR spectroscopy. Elemental analyses and ^{31}P-NMR spectroscopy agree with the proposed formulation. We performed the reaction in nitrogen atmosphere too. The resulting product is not as pure as in the case of CO atmosphere, as revealed by elemental analysis where the found Carbon exceeds 2% the calculated one.
We have compared our spectroscopic data with those ones reported in literature for the simpler species $[Ir_6(CO)_{15}(AuPPh_3)]^{4-}$, finding a strict similarity, as we would expected. The only substantial difference is that the literature species shows fluxionality at room temperature in the ^{31}P-NMR, while our molecule does not.
In the following figures IR and ^{31}P-NMR, registered in THF, are shown.
We are currently investigating electrochemical behaviour of this promising species.

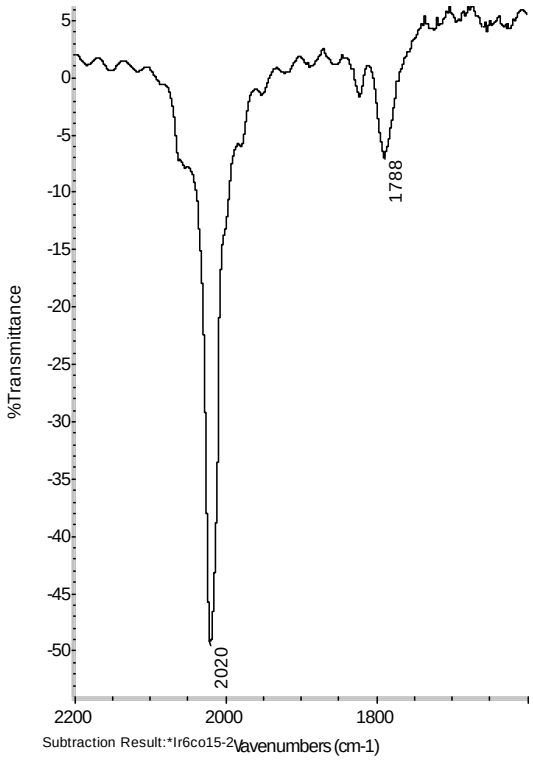

Fig. 168 THF IR spectrum of $[\{Ir_6Au(CO)_{15}\}_4(180tetraphos)]^{4-}$

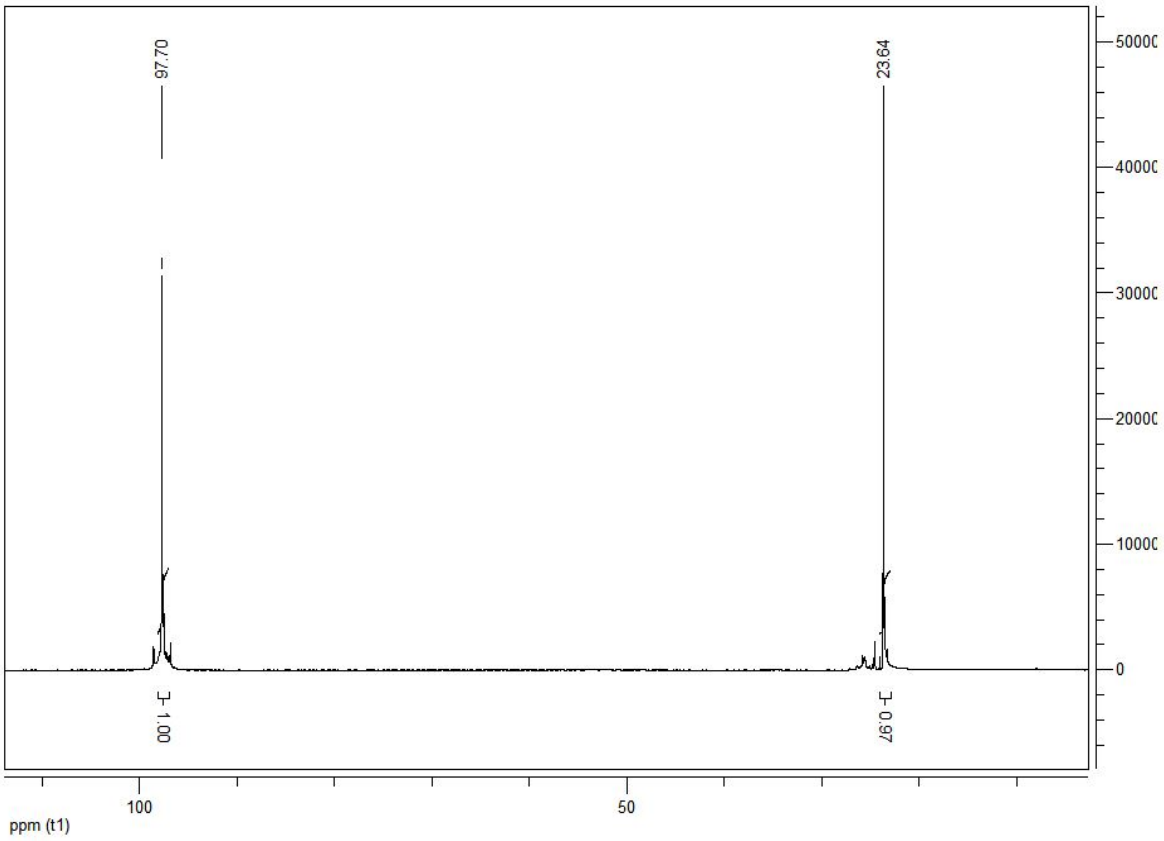

Fig. 169 THF ^{31}P-NMR spectrum of $[PEtPh_3]_4[\{Ir_6Au(CO)_{15}\}_4(180tetraphos)]$

Chapter three - Experimental section

All air-sensitive operations were carried on under nitrogen atmosphere by using standard Schlenk technique. Syntheses involving Au(I) complexes were made far from light. All the commercially available reagents were purchased from Sigma-Aldrich, Acros or FluoroChem and used as received.

Syntheses of the starting materials

$[PPh_4][RhCl_2(CO)_2]$

In a two necks, 250 mL flask 1,580 g of $RhCl_3 \cdot 3H_2O$ ($6{,}0 \cdot 10^{-3}$ mol), 70 mL of ethanol and 2 mL of H_2O have been introduced and CO has been bubbled at RT for some minutes. Then the solution has been heated under CO flux at 40°C for 20 hours. During this time the dark red solution turns to orange and finally yellow.

A solution prepared from tetraphenylphosphonium chloride (4,63 g) and 100 mL of 2-propanol has been then added, observing the precipitation of a fine yellow solid. It was filtered under nitrogen atmosphere, washed with 2-propanol (2x35 mL) and finally dried under vacuum pump.

CH_2Cl_2, IR spectrum shows two carbonyl stretching bands: ν_{CO} 2069 cm^{-1} e 1991 cm^{-1}

$[PPh_4][IrCl_2(CO)_2]$

In a 250 mL two necks flask 1,01 g of $IrCl_3 \cdot 3H_2O$ ($2{,}87 \cdot 10^{-3}$ mol), 50 mL di methanol and 1 mL of H_2O have been introduced. Then CO has been bubbled in the solution for some minutes at RT. The solution has been heated under CO flux at 70°C for 20 hours. During this time the brown solution turns to orange and finally yellow.

A solution prepared from tetraphenylphosphonium chloride (3,33 g) and 70 mL of 2-propanol has been then added, resulting in the precipitation of a gray fine solid. It has

been filtered under nitrogen atmosphere, washed with 2-propanol (2x35 mL) and dried under vacuum pump.

CH_2Cl_2 IR spectrum shows two carbonyl stretching bands: ν_{CO} 2055 cm^{-1} e 1971 cm^{-1}

$[Ir_4(CO)_{12}]$

In a glass 8,69 g of $IrCl_3 \cdot 3H_2O$ ($2{,}46 \cdot 10^{-2}$ mol) and about 300 mL of formic acid (98%) was introduced. The glass has been than put in its autoclave. It was then heated under stirring at 130°C for 12 hours, allowing then to cool for 24 hours. The resulting suspension, made of a pale yellow solid and a uncoloured solution (in the best case) has been poured in about 2 L of water. The resulting suspension has been filtered over Buchner and the product has been washed with methanol (200 mL) and acetone (200 mL).

Obtained 5,52 g, 81%, yield.

ATR-IR ν_{CO} 2053, 2018, 2002, 1995 cm^{-1})

Estimate of the pressure inside the autoclave

For the synthesis of $[Ir_4(CO)_{12}]$, two extreme stoichiometry are possible, while the real one is intermediate.

A

$4IrCl_3 \cdot 3H_2O + 18HCOOH \rightarrow Ir_4(CO)_{12} + 6COCl_2 + 30H_2O$

B

$4IrCl_3 \cdot 3H_2O + 18HCOOH \rightarrow Ir_4(CO)_{12} + 12HCl + 24H_2O + 6CO_2$

In our autoclave there was a free volume of about 0,133 L. We have overlooked that HCl, CO_2, and $COCl_2$ are partially dissolved in formic. We have considered an intermediate stoichiometry between A and B, by assuming that 9,75 moles of gas are formed per mole of $IrCl_3 \cdot 3H_2O$, so ¼[(36+42)/2], where 36 are the moles of gases forming per 4 moles of iridium trichloride in A and 42 those of B.

So the pressure inside the autoclave, at a given temperature, is:

$$P = \frac{nRT}{V_0\left(1+\frac{p_s}{RT(d_s/M_s - p_s/RT)}\right)} + p_s$$

where

n = moles of gases forming during the reaction

R = gas constance, 0,082 atm·l/mol·K

T = temperature, K

V_0 = starting free volume in the autoclave, L

p_s = solvent vapour tension at T, atm

d_s= solvent density at T, g/L

M_s= solvent molar mass, in g/mol

In the reported synthesis, at 120°C the resulting pressure is 67,8 atm

$[PPh_4][Ir_4Br(CO)_{11}]$

In a 250 mL two necks flask, $[Ir_4(CO)_{12}]$ (1,52 g, $1{,}38\cdot10^{-3}$ mol), LiBr (0,72 g, $8{,}26\cdot10^{-3}$ mol) and THF (40 mL) was introduced. This suspension has been beate at 75°C in nitrose atmosphere for 10 hours. During this times the suspension turns into a red solution. A solution obtained from 1,64 g of tetraphenylphosphonium bromide and 100 mL of 2-propanol has been added and the resulting solution has been concentrated in order to remove most of THF. This allowed an orange solid to precipitate, that has been filtered under nitrogen and washed with 2-propanol (4x25 mL).

Obtained 1,12 g, 55% yield.

CH_2Cl_2 IR: ν_{CO} 2081-2050-2042-2007-1821 cm^{-1}

$[PPh_4]_2[Ir_6(CO)_{15}]$

In a 250 mL two necks flask, $[Ir_4(CO)_{12}]$ (0,5 g, $4{,}52 \cdot 10^{-4}$ mol), $[PPh_4][Ir(CO)_4]$ (0,5 g, $7{,}7 \cdot 10^{-4}$) and THF (40 mL) and the resulting suspension was refluxed under nitrogen atmosphere until the $[Ir_4(CO)_{12}]$ was consumed. Sometimes a further addition of $[PPh_4][Ir(CO)_4]$ is necessary. This red solution was added to a solution prepared from PPh_4Br (0,5 g) and 2-propanol (80 mL). After partial remotion of the solvents by vacuum pump, the precipitated solid was filtered under nitrogen and washed with 2.propanol.

THF IR: ν_{CO} 1980(s), 1770(m) cm^{-1}

$[PPh_4][Ir(CO)_4]$

In a 300 mL Schlenk tube DMSO (30 mL) is degassed and put under CO atmosphere. Then $IrCl_3 \cdot 3H_2O$ is dissolved and triturated KOH (3-4 tablets) is added. The resulting suspension is stirred under CO for 3-4 days, adding further amounts of KOH once a day. When the reaction is completed (IR ν_{CO} 1890 cm^{-1}) a solution of PPh_4Cl (1 g) in water (100 mL) is added before some solid NaCl. This allowed a beige solid to precipitate, which is filtered under nitrogen and washed with water

THF IR: ν_{CO} 1890 cm^{-1}

$[NBu_4]_4[Pt_{19}(CO)_{22}]$

$[NBu_4]_2[Pt_9(CO)_{18}]$ is dissolved in CH3CN (~100 mL) and the resulting purple solution is heated at 80°C under nitrogen atmosphere for about 5 hours. Then the solvent is removed by vacuum pump and the remaining dark brown solid is washed with methanol (3 x 20 mL) and dried.

CH3CN IR: ν_{CO} 2005(s), 1800(m) cm^{-1}

$[NBu_4]_2[Pt_9(CO)_{18}]$

In a 500 mL 2 necks flask, a solution made from NaOH (8 g) and methanol (120 mL) is put under CO atmosphere for about 30 minutes. Na_2PtCl_4 (10 g) is added and the resulting orange suspension is stirred under CO for about 24 hours. Then the suspension is filtered

and to the violet solution is added a solution made from NBu_4Cl (2 g) and water (100 mL). This allowed the product to precipitate, which is filtered under nitrogen and washed with water.

THF: ν_{CO} 2030(s), 1855(m) cm^{-1}

[AuCl(THT)]

$NaAuCl_4$ (0,5 g) is dissolved in ethanol (30 mL) under nitrogen and tetrahydrotiofene (THT) is dropwise added far from light until the white desired product precipitates. It is filtered under nitrogen, washed with ethanol and ethyl ether (20+20 mL), dried and maintained far from light.

1,4-bis(diphenylphosphanomethyl)benzene

In a Schlenk tube a red 0,5 M THF of $KP(C_6H_5)_2$ (11,5 mL). After cooling to -10°C, a solution prepared with 4 mL of freshly distilled THF and 1,4-bis(chloromethyl)benzene (0,505 g) has been dropwise added under stirring. After some minutes the red colour has lightened and a white solid has precipitated. After fifteen minutes the solution has been allowed to get room temperature and it has been stirred for two hours. The 40 mL of water have been added and after 30 minutes the resulting suspension has been filtered over Buchner. The white solid has been washed with water (30 mL) and methanol (40 mL).

Obtained 1,04 g, 76% yield

Elemental analysis. Calculated for $C_{30}H_{24}P_2$ C 80,34% H 5,32 %, found C 81,00 % H 5,95%

^{31}P-NMR: -9,74(s) ppm (CD_2Cl_2)

4,4'-bis(diphenylphosphano)biphenyle

In a Schlenk tube 4,4'-dibromobiphenyle (2,064 g, 6,61 $\cdot 10^{-3}$ mol) and freshly distilled THF (65 mL) have been introduced. The resulting bright yellow solution has been cooled to -78°C and n-buthyl lithium (5,3 mL, 2.5 M in hexanes) has been carefully dropwise added under vigorous stirring. During the addition a white solid has precipitated and the solution has become light yellow. This suspension has been stirred for two hours and then

$P(C_6H_5)_2Cl$ (2,5 mL, $1{,}35 \cdot 10^{-2}$ mol) have been slowly added. After some minutes a clear yellow solution has formed. It has been allowed to get room temperature and then it has been stirred for 24 hours. A saturated aqueous solution of NH_4Cl (70 mL) has been added and the organic phase has been separated. The aqueous phase has been extracted twice with CH_2Cl_2 (30 mL). All the organic phases have been dried over $MgSO_4$ and then the solvents was evacuated with a vacuum pump. dopo alcuni minuti di agitazione la fase organica è stata separata. La fase acquosa è stata estratta 2 volte con 30 ml di CH_2Cl_2 e queste fasi, riunite con la soluzione di THF, sono state anidrificate con $MgSO_4$. The resulting white solid, wet by $CH_3(CH_2)_3Br$, has been suspended in CH_3CH_2OH (60 mL) and the suspension filtered over Buchner.

Obtained 2,20 g, 64% yield

^{31}P-NMR: -5,55(s) ppm (CD_2Cl_2)

Elemental analysis: calculated for $C_{36}H_{28}P_2$ C 82,74 % H 5,40, found C 81,72% H 5,32 %

4,4'-bis(diphenylphosphanomethyl)biphenyle

In a Schlenk tube $KP(C_6H_5)_2$ (9,6 mL, $4{,}80 \cdot 10^{-3}$ mol, 0,5 M in THF) has been introduced and cooled at -10°C. Then a solution made from 4,4'-bis(chloromethyl)diphenyle (0,604 g, $2{,}41 \cdot 10^{-3}$ mol) and freshly distilled THF (5 mL) was dropwise added under stirring. After some minutes the red solution has turned in light yellow and a white solid has precipitated. This suspension has been allowed to get RT and the it has been warmed at 70°C for 1h30min. Then it has been filtered over Buchner and washed with water (30 mL) and methanol (40 mL). Finally the solid has been then digested in methanol for three hours and filtered over Buchner

Obtained 1,04 g, 78,5% yield

^{31}P-NMR: -9,56(s) ppm (CD_2Cl_2)

Elemental analysis: calculated for $C_{38}H_{32}P_2$ C 82,89% H 5,86%, found C 81,38% H 5,52%

1,8-bis(diphenylphosphano)octane

In a Schlenk tube $KP(C_6H_5)_2$ (26,3 mL, 0.5 M in THF) have been introduced and cooled at -78°C. A solution prepared from 1,8-dichlorooctane (1,23 g, $6{,}72 \cdot 10^{-3}$ mol) and THF (1.5 mL) has been dropwise added under stirring, getting to the precipitation of a white solid. After one hour 15 mL of water have been added and the suspension vigorously stirred. Then the organic phase has been separated, the solvent evacuated and the resulting white solid has been dissolved in toluene (45 mL) and dried with Na_2SO_4. Methanol (100 mL) has been added to the toluene solution, allowing the precipitation of the product as a white powder, that has been filtered over Buchner and washed with methanol.

Obtained 2.1 g, 65% yield

^{31}P-NMR: -15,74(s) ppm (CD_2Cl_2)

Elemental analysis: calculated for $C_{32}H_{36}P_2$ C 79,66% H 7,89%, found C 79,64% H 7,52%

1,10-bis(diphenylphosphano)decane

In a Schlenk tube $KP(C_6H_5)_2$ (23 mL, 0.5 M in THF) have been introduced and cooled at -78°C. A solution prepared from 1,10-dichlorodecane (1,20 g, $5.67 \cdot 10^{-3}$ mol) and THF (1.5 mL) has been dropwise added under stirring, getting to the precipitation of a white solid. After one hour 15 mL of water have been added and the suspension vigorously stirred. Then the organic phase has been separated, the solvent evacuated and the resulting white solid has been dissolved in toluene (50 mL) and dried with Na_2SO_4. Methanol (100 mL) has been added to the toluene solution, allowing the precipitation of the product as a white powder, that has been filtered over Buchner and washed with methanol.

Obtained 2.35 g, 81% yield

^{31}P-NMR: -15,74(s) ppm (CD_2Cl_2)

Elemental analysis: calculated for $C_{34}H_{40}P_2$ C 80,01% H 8,03%, found C 79,97% H 7,90%

1,12-bis(diphenylphosphano)dodecane

In a Schlenk tube $KP(C_6H_5)_2$ (16.3 mL, 0.5 M in THF) have been introduced and cooled at -78°C. A solution prepared from 1,12-dichlorododecane (1,01 g, $4.24 \cdot 10^{-3}$ mol) and THF (1.5 mL) has been dropwise added under stirring, getting to the precipitation of a white solid.

After one hour 15 mL of water have been added and the suspension vigorously stirred. Then the organic phase has been separated, the solvent evacuated and the resulting white solid has been dissolved in toluene (35 mL) and dried with Na_2SO_4. Methanol (80 mL) has been added to the toluene solution, allowing the precipitation of the product as a white powder, that has been filtered over Buchner and washed with methanol.

Obtained 1.55 g, 68% yield

^{31}P-NMR: -15,63(s) ppm (CD_2Cl_2)

Elemental analysis: calculated for $C_{36}H_{44}P_2$ C 80,48% H 8,70%found C 80,27% H 8,23%

Syntheses of the new species

[{Ir$_4$(CO)$_{11}$}$_2$(dppa)]

To a solution prepared with [PPh$_4$][Ir$_4$Br(CO)$_{11}$] (0,176 g, 1,2·10^{-4} mol) and acetonitrile (15 mL) dppa (0,024 g, 6,1·10^{-5} mol) has been added under stirring. A yellow microcrystalline solid has quickly precipitated and it has been separated and washed with acetonitrile.

Obtained 0,11 g, 72% yield.

ATR IR ν_{CO}: 2091, 2047, 2030, 2002, 1987,1959, 1845, 1827 cm^{-1}

Nujol ν_{CO}: 2092, 2048, 2036, 2019, 2006 cm^{-1}

Elemental analysis C 22,65%, H 0,81%

Crystals suitable for X-ray analysis have been obtained by layering a solution made from[PPh$_4$][Ir$_4$Br(CO)$_{11}$] (0,061 g, 4,1·10^{-5} mol) and dichloromethane (4 mL) with a solution made from dppa (0,008 g, 2,1·10^{-5} mol) and *n*-eptano + di diclorometano (4 mL + 0,5 mL)

Obtained 0,025 g, 48% yield.

[{Ir$_4$(CO)$_{11}$}$_2$(t-dppethe)]

In a Schlenk tube $[PPh_4][Ir_4Br(CO)_{11}]$ (0,074 g, $4{,}9\cdot10^{-5}$ mol) has been dissolved in acetonitrile (4 mL). The addition of *t*-dppethe (0,024 g, $2{,}7\cdot10^{-5}$ mol) has yielded to the precipitation of the product as a yellow microcrystalline solid separated and washed with acetonitrile.

Obtained 0,048 g, 70% yield

ATR-IR ν_{CO}: 2089, 2043, 2035, 2002, 1974, 1958, 1842, 1821 cm^{-1}

Nujol ν_{CO}: 2091, 2048, 2035, 2010, 1994, 1973 cm^{-1}

Crystals suitable for X-ray analysis have been obtained maintaining for 3 days at 3°C a solution obtained dissolving $[PPh_4][Ir_4Br(CO)_{11}]$ (0,08 g, $5{,}3\cdot10^{-5}$ mol) in dichloromethane (4 mL), adding *t*-dppethe (0.011 g, $2{,}7\cdot10^{-5}$ mol) and stirring for 1 hour.

$[RhCl(CO)(dppmb)]_n$

In a Schlenk tube $[PPh_4][RhCl_2(CO)_2]$ (0,044 g, $7{,}8\cdot10^{-5}$ mol) has been dissolved in dichloromethane (2 mL). The addition of dppmb (0,074 g, $1{,}6\cdot10^{-4}$ mol) has yielded to the precipitation of the product as a yellow microcrystalline solid separated and washed with dichloromethane.

Obtained 0,051 mg

ATR-IR ν_{CO}: 1964 cm^{-1}

Elemental analysis: calculated for $RhC_{33}H_{28}ClOP_2$ C 61,85% H 4,40. Found C 59,93%, H 5,15%

$[IrCl(CO)(dppmb)]_n$

In a Schlenk tube $[PPN][IrCl_2(CO)_2]$ (0,061 g, $7{,}1\cdot10^{-5}$ mol) has been dissolved in dichloromethane (3 mL). The addition of dppmb (0,067 g, $1{,}4\cdot10^{-4}$ mol) has yielded to the precipitation of the product as a yellow microcrystalline solid separated and washed with dichloromethane.

Obtained 0,055 mg

ATR-IR ν_{CO}: 1953 cm^{-1}

Elemental analysis: calculated for $IrC_{33}H_{28}ClOP_2$ C 54,28% H 3,86. Found C 52,59%, H 4,40%

$[RhCl(CO)(dppmb)]_2$

Crystals of this product have been collected by layering a solution made from 1,4-bis(diphenylphosphanomethyl)benzene (dppmb) (115 mg, 0,24 mmol) and CH_2Cl_2 (6 mL) with a solution prepared with $[PPh_4][RhCl_2(CO)_2]$ (69 mg, 12 mmol) and ethanol (15 mL). Crystals of the product was accompanied with other labile crystals, likely of $[RhCl(CO(dppmb)]_n$.

$[RhCl(CO)(dppbp)]_n$

In a Schlenk tube $[PPh_4][IrCl_2(CO)_2]$ (0,042 g, $7,5 \cdot 10^{-5}$ mol) has been dissolved in dichloromethane (2,5 mL). The addition of dppmb (0,071 g, $1,4 \cdot 10^{-4}$ mol) has yielded, after about twenty hours, to the precipitation of the product as a yellow microcrystalline solid separated and washed with dichloromethane.

Obtained 0,051 mg

ATR-IR ν_{CO}: 1966 cm^{-1}

$[IrCl(CO)(dppbp)]_n$

In a Schlenk tube $[PPN][IrCl_2(CO)_2]$ (0,080 g, $9,3 \cdot 10^{-5}$ mol) has been dissolved in dichloromethane (3 mL). The addition of dppmb (0,098 g, $1,9 \cdot 10^{-4}$ mol) has yielded to the precipitation of the product as a yellow microcrystalline solid separated and washed with dichloromethane.

Obtained 0,092 mg

ATR-IR ν_{CO}: 1981(w), 1960(vw), 1922(vs), 1989(vw) cm^{-1}

$[RhCl(CO)(dppmbp)]_2$

In a Teflon® line steel vessel a solution of $[PPh_4][RhCl_2(CO)_2]$ (51,2 mg, 0,090 mmol) in CH_2Cl_2 (10 mL) has been put together with 4,4'-bis(diphenylphosphanomethyl)biphenyle. The autoclave has been heated at 90°C for 10 hours and then it has been cooled at 0,1°C/min rate. Crystals of the product have been so collected and washed with dichloromethane.

Obtained 26 mg, 40,3% yield

ATR-IR ν_{CO} 1965 cm^{-1}

Elemental analysis: calculated for $C_{28}H_{64}Cl_2O_2P_4Rh_2$: C 64,17% H 4,05%, found C65,33%, H 4,50%

$[IrCl(CO)(dppmbp)]_2$

In a Teflon line steel vessel a solution made from $[PPh_4][IrCl_2(CO)_2]$ (46 mg, 0,054 mmol) and CH_2Cl_2 (8 mL) has been added with 31 mg (0,054 mmol) di 4,4'-bis(diphenylphosphanomethyl)biphenyle. The autoclave has been heated for 1h30min at 70°C and the cooled at 0,2°C/min. rate. Crystals has been so recovered and washed with dichloromethane.

ATR-IR ν_{CO} 1956 cm^{-1}

Elemental analysis: calculated for $C_{28}H_{64}Cl_2O_2P_4Ir_2$: C 58,10% H 4,00% found C 58,61% H 4,41%

$[\{Ir_4(CO)_{11}\}_2(dppmb)]$

To a solution prepared from $[PPh_4][Ir_4Br(CO)_{11}]$ (0,063 g, 4,2 10^{-5} mol) and dichloromethane (5 mL) dppmb (0,011 g, 2,2 $\cdot 10^{-5}$ mol) has been added and the resulting solution has been stirred for 18 hours. Then the solvent has been removed and the product has been extracted from the resulting solid with toluene (2x3 mL). Then the solvent has been evaporated and the product has been washed with 2-propanol (5 mL).

Obtained 0,037 g, 67% yield

IR (CH_2Cl_2) ν_{CO} (CH_2Cl_2): 2087(m), 2055(vs), 2018(s), 1843(m),1818(m) cm^{-1}

Elemental analysis: calculated for $C_{54}H_{28}Ir_8O_{22}P_2$ C 24,48% H 1,07%, found C 25,96% H 1,58%

TLC: R_f = 0,38 (CH_2Cl_2/n-hexane 2:3)

$[Ir_4(CO)_{11}(dppmb)]$

A solution made from $[PPh_4][Ir_4Br(CO)_{11}]$ (0,051 g, 3,4 10^{-5} mol) and dichloromethane (4 mL) has been cooled to -10°C. then dppmb has been added. The solution has been stirred for 18 hours during which the temperature slowly raise to RT. Then the solvent has been evacuated and the resulting solid washed twice with acetonitrile (3 mL).

Obtained 0,016 g

ν_{CO} (CH_2Cl_2): 2087(m), 2055(vs), 2018(s), 1843(m),1818(m) cm^{-1}

Elemental analysis: calculated for $C_{43}H_{28}Ir_4O_{11}P_2$ C 33,29% H 1,82%, found C 26,62% H 1,94%

TLC: R_f = 0,42 (CH_2Cl_2/n-hexane 2:3)

$[\{Ir_4(CO)_{11}\}_4(dppmb)_6]$

Method A: $Ir_4(CO)_{12}$[184] (60 mg, $5.5 \cdot 10^{-5}$ mol) and 1,4-bis(diphenylphosphinomethyl) benzene[185] (80 mg, $1.7 \cdot 10^{-4}$ mol) were kept in a 23 ml teflon lined steel vessel and suspended in a mixture of ethanol (5 ml) and toluene (3 ml). The vessel was then heated in an oven at 130°C for 14 hours. After ca 8 hours (rate of cooling 0.2°C/min), orange crystals of the product were recovered and washed with dichloromethane. Obtained 50 mg, 52% yield.

Method B: $[PPh_4][Ir_4Br(CO)_{11}]$ [186] (96 mg, $6.4 \cdot 10^{-5}$ mol) and dppmb (31 mg, $6.5 \cdot 10^{-5}$ mol) were dissolved in dichloromethane (3 ml) and the solution was stirred for 1h 15min at room temperature. Then the solvent was removed under vacuum and the remaining solid was extracted with toluene (2 x 2.5 ml). The resulting solution was refluxed with dppmb (31 mg, $6.5 \cdot 10^{-5}$ mol) for 14 hours obtaining precipitation of the desired product as a microcrystalline powder, which was filtered, washed with toluene (10 ml) and dried.

Obtained 75 mg, 68% yield.

ATR-IR ν_{CO} 2040(m), 1981(s), 1965(s) cm^{-1} (terminal COs) and 1792(s), 1775(s), 1755(vs) cm^{-1} (edge-bridged COs).

Elemental analysis. Calculated for $Ir_{16}C_{228}H_{168}O_{36}P_{12}$: C 39,51%, H 2,44%. Found: C 37,12%, H 2,73%.

$[\{Ir_4(CO)_{11}\}_2(dppbp)]$

To a solution of $[PPh_4][Ir_4Br(CO)_{11}]$ (0,079 g, 5,3 10^{-5} mol) in dichloromethane (5 mL) dppbp (0,013 g, 2,5 $\cdot 10^{-5}$ mol) has been added under stirring. After 18 hours the solvent has been evacuated and the resulting solid washed twice with acetonitrile (3 mL).

Obtained 0,038 g, 54% yield.

Elemental analysis: calculated for $C_{58}H_{28}Ir_8O_{22}P_2$ C 26,03% H 1,05%, found C 26,65% H 1,75%

IR ν_{CO} (CH_2Cl_2): 2088(m), 2054(vs), 2017(s), 1843(m),1822(m) cm^{-1}

TLC: R_f = 0,6 (CH_2Cl_2/n-hexane 1:1)

$[Ir_4(CO)_{11}(dppbp)]$

To a solution of $[PPh_4][Ir_4I(CO)_{11}]$ (0,046 g, 2,9 10^{-5} mol) in acetonitrile (3 mL) dppbp (0,016 g, 3,1 10^{-5} mol) has been added. The resulting suspension has been stirred for two hours. Then the precipitated yellow solid has been separated and washed with acetonitrile.

Obtained 0,023 g, 48% yield

Elemental analysis: calculated for $C_{47}H_{28}Ir_4O_{11}P_2$ C 35,29% H 1,76 %, found C 35,12 % H 2,34%

ν_{CO} (CH_2Cl_2): 2088(m), 2056(vs), 2019(ms), 1844(m),1822(m) cm^{-1}

TLC: R_f = 0,4 (CH_2Cl_2/n-hexane 1:1)

$[RhCl(CO)(dppo)]_n$

To a solution of $[PPh_4][RhCl_2(CO)_2]$ (64 mg, 0,135 mmol) in CH_2Cl_2 (2 mL) 1,8-bis(diphenylphosphano)octane (dppo) (146 mg, 0,271 mmol) has been added and the

solution has been stirred for 18 hours. So a yellow microcrystalline solid precipitated which has been washed with dichloromethane. tramite XRPD.

Obtained 28 mg, 39% yield

ATR-IR : ν_{CO} 1978 cm^{-1}

Elemental analysis: calculated for $C_{33}H_{36}RhClOP_2$: C 61,08% H 5,59%, found C 62,89% H 5,83%

Crystals suitable for X-ray analysis have been obtained by two ways:

- To a solution of $[PPh_4][RhCl_2(CO)_2]$ (50 mg, 0,088 mmol) in CH_2Cl_2 (4 mL) dppo (85 mg, 0,16 mmol) have been added and the solution have been stirred for two hours. The solution has been then concentrated and layered with 2-propanol (12 mL). After some hours crystals of the polymer were formed.
- A solution of $[PPh_4][RhCl_2(CO)_2]$ (55 mg, 0,056mmol) in CH_2Cl_2 (0,5 mL) have been layerd with a solution of dppo (95 mg, 0,20 mmol) in THF (1 mL).

$[RhCl(CO)(dppdod)]_2$

To a solution of $[PPh_4][RhCl_2(CO)_2]$ (77 mg, 0,135 mmol) in CH_2Cl_2 (2 ml) 1,12-bis(diphenylphosphano)dodecane (dppdod) (146 mg, 0,271 mmol) have been added and the solution have been stirred for two hours. Then it has been concentrated and layered with 2-propanol (6 mL). After complete diffusion crystals of the product have been recovered.

Obtained 50 mg, 52% yield

CH_2Cl_2 IR in : ν_{CO} 1968 cm^{-1}

^{31}P-NMR: 26,1(d) (J_{Rh-P}125Hz) ppm (CD_2Cl_2)

Elemental analysis: calculated for $Rh_2C_{74}H_{88}Cl_2O_2P_4$: C 63,06% H 6,25%, found C 58,85% H 5,95%

$[RhClI_2(CO)(dppdod)]$

$[PPh_4][RhCl_2(CO)_2]$ (83 mg, 0,146 mmol) has been dissolved in dichloromethane (ν_{CO} 2070, 1990 cm^{-1}) and to this solution dppdod (79 mg, 0,146 mmol) and iodine (75 mg, 0,295 mmol) has been subsequently added. After the addition of the ligand CO stretching bands

of the starting material quickly disappeared for one band at 1969 cm^{-1} which had an upshift to 2083 cm^{-1} after the oxidation with iodine. The final solution has been layered with 2-propanol, obtaining dark crystals of the product.

ATR-IR 2079 cm^{-1}

Elemental analysis: calculated for $RhC_{37}H_{44}ClI_2OP_2$: C 46,35% H 4,63%, found C 43,50% H 4,04%

$[\{Ir_4(CO)_{11}\}_2(dppbut)(dppbut)_2]$

In a Teflon liner steel vessel $[Ir_4(CO)_{12}]$ (51 mg, 0,046 mmol), dppbut (60 mg, 0,14 mmol), CH_2Cl_2 (2,5 mL) and n-heptane (5,5 mL) have been loaded. The vessel has been heated at 130°C for 18 hours and allowed to slowly cool down to room temperature. Orange crystals of the product have been so recovered

Obtained 36 mg

ATR-IR 2040(w), 1980(w), 1954(m), 1789(s), 1771(vs) cm^{-1}

Elemental analysis: calculated for $Ir_8C_{102}H_{84}O_{18}P_6$: C 46,35% H 4,63%, found C 43,50% H 4,04%

$[\{Ir_4(CO)_{11}\}_2(dpphex)]$

To a solution of $[PPh_4][Ir_4Br(CO)_{11}]$ (0,079 g, $5{,}3 \cdot 10^{-5}$ mol) in dichloromethane (2,5 ml), 1,6-bis(diphenylphosphano)hexane (0,013 g, $2{,}6 \cdot 10^{-5}$ mol) was added and the resulting solution was stirred for an hour. Solvent was removed *by vacuum* and the resulting yellow solid was washed with acetonitrile in order to remove PPh_4Br and dried (0,040 g, 58% yield based on Ir). Crystals suitable for X-Ray analysis were grown by layering a solution in CH_2Cl_2 (0,058 g, 3ml) with *n*-heptane (7 ml).

IR ν_{CO} (CH_2Cl_2): 2087(m), 2055(vs), 2018(s) cm^{-1} (terminal COs), 1842(m), 1818(m) cm^{-1} (edge-bridged COs).

^{31}P-NMR (CD_2Cl_2, 213 K): -17,4; -17,2; 6 ppm.

Elemental analysis: calculated for $Ir_8C_{52}H_{32}O_{22}P_2$ C 23,94%, H 1,24%. Found C 24,41%, H 1,47%.

$[Ir_4(CO)_{10}(dpphex)]_2$

$[PPh_4][Ir_4Br(CO)_{11}]$ (0,099 g, $6{,}6 \cdot 10^{-5}$ mol) was solved in dichloromethane (2,5 ml). Then 1,6-bis(diphenylphosphano)hexane was added (0,015 g, $3{,}3 \cdot 10^{-5}$ mol) and the resulting solution was stirred for an hour, resulting in the formation of $[\{Ir_4(CO)_{11}\}_2(dpphex)]$. Then a second amount of dpphex was added (0,015 g, $3{,}3 \cdot 10^{-5}$ mol). This solution was stirred at RT for four days during which a yellow powder of $[Ir_4(CO)_{10}(dpphex)]_2$ precipitated. The solid was filtered, washed with CH_2Cl_2 and dried (3 mg, 3% yield based on Ir). Crystals suitable for X-ray analysis have been obtained by layering a solution of $[PPh_4][Ir_4Br(CO)_{11}]$ (0,080 g, $5{,}3 \cdot 10^{-5}$ mol) in CH_2Cl_2 (5 ml) with a solution of dpphex (0,049 g, $1{,}1 \cdot 10^{-4}$ mol) in *n*-heptane (8 ml).

ATR-IR: 2058(m), 2032(m), 1987(s), 1973(s) (terminal COs) cm^{-1}, 1795, 1771 cm^{-1} (edge-bridged COs).

Crystals suitable for X-ray analysis have been obtained by layering a solution prepared from 0,077 g of $[PPh_4][Ir_4Br(CO)_{11}]$ ($5{,}1 \cdot 10^{-5}$ mol) and dichloromethane (4,5 mL) with a solution prepared starting from 0,047 g of dpphex ($1{,}03 \cdot 10^{-4}$ mol) and *n*-heptane-dichloromethane mixture (5 mL - 1,5 mL). After complete diffusion, yellow crystals have been recovered and washed with dichloromethane.

Elemental analysis: calculated for $Ir_8C_{80}H_{64}O_{20}P_4$ C 31,95%, H 2,15%. Found C 32,05%, H 2,72%.

$[\{Ir_4(CO)_{11}\}_2(dpphex)_3]$

$[Ir_4(CO)_{12}]$ (0,050 g, $4{,}5 \cdot 10^{-5}$ mol) and dpphex (0,061 g, $1{,}3 \cdot 10^{-4}$ mol) were suspended in a CH_2Cl_2 (2,5 ml) *n*-heptane (5,5 ml) mixture and kept in a Teflon lined steel vessel. It was then heated in an oven at 130°C for 18 hours. After *ca* 8 (rate of cooling 0,2°C/min), yellow/orange powder and crystals of $[\{Ir_4(CO)_9\}_2(dpphex)_3]$ were recovered and washed with dichloromethane (40 mg, 52% yield based on Ir).

ATR-IR ν_{CO}: 2037(m), 1994(m), 1972(s), 1952(s) cm^{-1} (terminal COs), 1776(s), 1761(vs) cm^{-1} (edge-bridged COs).

Elemental analysis: calculated for $Ir_8C_{108}H_{96}O_{18}P_6$ C 38,09% H 2,84% Found C 39,41% H 3,40%

3,3′-5,5′-tetrakis(diphenylphosphano)biphenyle (180tetraphos)

To 3,3′-5,5′-tetrafluorobiphenyle[187] (**1a**) (0,813 g, 3,59 mmol) was added a 0,5 M THF solution of $KPPh_2$ (57 ml, 28,5 mmol). The reaction was slightly exotermic and it was stirred at room temperature for an hour and then refluxed at 90°C overnight. The resulting red clear solution was cooled to room temperature and 200 ml of CH_3OH was slowly added. The solution turned pale yellow and a white solid precipitated. The solvents were separated from the solid, 100 ml of CH_3OH added, and the mixture stirred for 30 min. Then the solid was filtered and washed with CH_3OH, obtaining 2,6 g of a white solid. Yield 81%

^{1}H-NMR 300 MHz ($CDCl_3$): 7,41(d) ppm (4H) $^3J_{H-P}$ = 7,8 Hz, 7,31-7,18(m) (40H), 7,14(t) $^3J_{H-P}$ = 6,6 Hz

^{31}P-NMR 127 MHz ($CDCl_3$): -3,85(s) ppm.

Elemental analysis: calculated for $C_{60}H_{46}P_4$ C 80,89%, H 5,20%. Found C 80,62%, H 5,24%

[3,3′-5,5′-tetrakis(diphenylphosphano)biphenyl]tetrakis[chlorogold(I)

180tetraphos (0,100 g, $1{,}1 \cdot 10^{-1}$ mmol) was dissolved in chloroform (3 mL) and [AuCl(THT)][188] (THT = tetrahydrothiophene) (0,144 g, $4{,}5 \cdot 10^{-1}$ mmol) was added. The resulting solution was stirred for 30 min, then the solvent was removed by vacuum and the resulting white powder was washed with ethanol and diethylether (5+5 mL). Obtained 0,150 g, yield 73,6%

^{31}P-NMR 127 MHz 34,3(s) ppm. Elemental analysis: calculated for $C_{60}H_{46}Au_4Cl_4P_4$ C 39,58%, H 2,55%. Found C 38,57%, H 2,70%

3,3′′-5-5′′-tetrafluoro-1,1′:4′.1′′-terphenyl (2a).

Tetrakis(triphenylphosphino)palladium(0) (0,244 g, 0,21 mmol) was dissolved in 20 mL of degassed DMF and 3,5-difluorobromobenzene (1,9 mL, 16,9 mmol), Benzene-1,4-diboronic acid (0,700 g, 4,22 mmol) and Na_2CO_{3aq} 2M (20 ml) were in sequence added. The resulting mixture was stirred at 90°C overnight and the resulting mixture cooled to room temperature, filtered and washed with water. The resulting gray solid was dissolved in

chloroform (50 ml) and filtered over silica gel. The solvent was then removed affording 1,1 g of a white solid, 86% yield. Elemental analysis: calculated for $C_{18}H_{10}F_4$ C 71,52%, H 3,33%. Found C 70,98%, H 3,01%

^{1}H-NMR 300 MHz ($CDCl_3$) 7,68(s) ppm (4H) 7,18(td) ppm (4H) $^3J_{H-F}$ = 8,7 Hz, $^4J_{H-H}$ = 2,4 Hz, 6,85(tt) (2H) $^3J_{H-F}$ = 9 Hz, $^4J_{H-H}$ = 2,4 Hz. ^{19}F-NMR 282 MHz ($CDCl_3$, ^{1}H decoupled) -109,9(s) ppm.

3,3''-5-5''-tetrakis(diphenylphosphino)-1,1':4',1''-terphenyl (2b)

To 3,3''-5-5''-tetrafluoro-1,1':4',1''-terphenyl (0,475 g, 1,57 mmol) was added a 0,5 M THF solution of $KPPh_2$ (25 ml, 12,5 mmol) and the resulting solution stirred at room temperature for an hour. Then it was stirred at 90°C overnight. The resulting suspension was cooled to room temperature and CH_3OH (50 ml) added. After 5 minutes stirring the solvents were removed with a syringe, 100 ml of CH_3OH added and the suspension stirred again for 30 minutes. Then the solid was filtered and washed with additional CH_3OH, affording 1,3 g of a white solid. Yield 87%

^{1}H-NMR 300 MHz ($CDCl_3$) 7,57(d) ppm (4H) $^3J_{H-P}$ = 8,7 Hz, 7,44(s) (4H), 7,33-7,28(m) ppm (40H), 7,19(t) ppm ^{3}JH-P = 6 Hz. ^{31}P-NMR 127 MHz -3,6(s) ppm. Elemental analysis: calculated for $C_{66}H_{50}P_4$ C 81,98%, H 5,21%. Found C 83,09%, H 5,72%

[3,3''-5-5''-tetrakis(diphenylphosphino)-1,1':4',1''terphenyl]tetrakis[chlorogold(I)] (2c)

Compound 2b (0,060 g, $6{,}2 \cdot 10^{-2}$ mmol) was dissolved in chloroform (10 mL) and [AuCl(THT)][188] (THT = tetrahydrothiophene) (0,079 g, $2{,}5 \cdot 10^{-1}$ mmol) was added. The resulting suspension was stirred for 30 min, then the solvent was removed by vacuum and the resulting white powder was washed with ethanol and diethylether (5+5 mL). Obtained 0,060 g, yield 52%

^{31}P-NMR 127 MHz 34,3(s) ppm. Elemental analysis: calculated for $C_{66}H_{50}Au_4Cl_4P_4$ C 41,60%, H 2,66%. Found C 41,65%, H 2,66%

1,3,5-tris(3′-5′-difluorophenyl)benzene (3a).

Tetrakis(triphenylphosphino)palladium(0) (0,160 g, 0,14 mmol) was dissolved in 35 ml of degassed dimethylformamide (DMF) and 3,5-difluorobromobenzene (1,74 ml, 15,11 mmol), benzene-1,3,5-tris-(boronic acid)[189] (0,695 g, 2,46 mmol) and Na_2CO_{3aq} 2M (35 ml) were in sequence added. The resulting mixture was stirred at 90°C overnight. Then the crude was filtered and washed with water, resulting a light brown solid that was suspended in diethyl ether and treated in an ultrasound bath, affording a white solid that was filtered and dried. Obtained 1,0 g, yield 99%.

1H NMR 300 MHz (DMSO, 60°C) 8,13(s) ppm (3H), 7,81(d) ppm (6H) $^3J_{H-F}$ = 8,4 Hz, 7,26(t) ppm $^3J_{H-F}$ = 8,7 Hz ^{19}F-NMR 282 MHz (DMSO, 60°C, ^{1}H decoupled) -110,1(s) ppm. Elemental analysis: calculated for $C_{24}H_{12}F_6$ C 69,57%, H 2,92%. Found C 66,78%, H 3,05%

1,3,5-tris[3′-5′-bis(diphenylphosphano)phenyl]benzene (3b)

To 1,3,5-tris(3′-5′-difluorophenyl) benzene (0,500 g, 1,21 mmol) was added a 0,5 M THF solution of $KPPh_2$ (30 ml, 15 mmol) and the resulting solution stirred at room temperature for an hour. Then it was stirred at 90°C overnight. After re-cooling the solution to room temperature, 60 ml of CH_3OH was added, the red solution turned pale yellow and a white solid precipitated. Then the solvents were removed, 100 ml of CH_3OH were added and this suspension stirred for half an hour, after which the solid was filtered and washed with additional CH_3OH, affording 1,6 g of a white solid, 93% yield.

^{1}H-NMR 300 MHz ($CDCl_3$) 7,48(d) ppm (6H) $^3J_{H-P}$ = 7,8 ppm, 7,40(s) ppm (3H), 7,30-7,25(m) ppm (60H), 7,10(t) ppm (3H) $^3J_{H-P}$ = 6 Hz. ^{31}P-NMR 127 MHz ($CDCl_3$) -4,0(s) ppm. Elemental analysis: calculated for $C_{96}H_{72}P_6$ C 81,69%, H 5,14%. Found C 79,52%, H 6,31%

[1,3,5-tris[3′-5′-bis(diphenylphosphano)phenyl]benzene]hexakis[chlorogold(I)] (3c)

Compound 3b (0,080 g, $5{,}6 \cdot 10^{-2}$ mmol) was dissolved in chloroform (6 mL) and [AuCl(THT)][188] (THT = tetrahydrothiophene) (0,107 g, $3{,}4 \cdot 10^{-1}$ mmol) was added. The resulting solution was stirred for 30 min, then the solvent was removed by vacuum and

the resulting white powder was washed with ethanol and diethylether (5+5 mL). Obtained 0,094 g, yield 57,8%

^{31}P-NMR 127 MHz 33,7 (s) ppm. Elemental analysis: calculated for $C_{96}H_{72}Au_6Cl_6P_6$ C 41,09%, H 2,59%. Found C 40,54%, H 3,10%

Tetra(3'-fluorobiphenyl)methane (4a).

Tetrakis(triphenylphosphano)palladium(0) (0,059 g, 0,05 mmol) was solved in 10 ml of degassed DMF and sequence added 3-fluorobromobenzene (1 ml, 8,95 mmol), Tetra(benzene-4-boronic acid)methane (0,506 g, 1,02 mmol) and Na_2CO_{3aq} 2M (10 ml)were in. The resulting mixture was stirred at 90°C overnight cooled to room temperature, and after adding brine (200 ml), it was extracted with chloroform (3x50 ml). The organic phases were dried over $MgSO_4$ and the solvent was evaporated. Then the resulting brownish solid was solved in dichloromethane (300 ml) and filtered over silica gel. The solvent was then removed affording 0,440 g of a white solid. Yield 62% ^{1}H-NMR 300 MHz, (DMSO) 7,74(d) ppm (8H) $^3J_{H-H}$ = 8,4 Hz, 7,55(m) ppm (12H), 7,40(d) (8H) $^3J_{H-H}$ = 8,4 Hz, 7,20(t) ppm (4H) $^3J_{H-H}$ = 7,5 Hz. ^{19}F-NMR 282 MHz (DMSO, ^{1}H decoupled): -113,1(s) ppm. Elemental analysis: calculated for $C_{49}H_{32}F_4$C 84,46%, H 4,63%. Found C 82,05%, H 5,57%

Tetrakis[3'-(diphenylphosphano)biphenyl]methane (4b)

To tetra(3'-fluorobiphenyl)methane (0,18 g, 0,26 mmol) was added a 0,5 M THF solution of $KPPh_2$ (4,5 ml, 2,25 mmol) and the resulting solution stirred at room temperature for an hour. Then it was stirred at 90°C overnight. Then the resulting suspension was cooled to room temperature and CH_3OH (50 ml) added. After 5 minutes stirring the solvents were removed, 100 ml of CH_3OH added and the suspension stirred again for 30 minutes. Then the solid was filtered and washed with additional CH_3OH, affording 0,290 g of a white solid, 81% yield

^{1}H-NMR 300 MHz ($CDCl_3$) 7,72(t) (4H) ppm, 7,62(d) (8H) ppm, 7,57(d) (8 H) ppm, 7,34(m) (40 H), 7,29(d) (12H) ppm. ^{31}P-NMR 127 MHz -3,68(s) ppm. Elemental analysis: calculated for $C_{97}H_{72}P_4$ C 85,57%, H 5,33%. Found C 82,88%, H 5,67%

[Tetrakis[3'-bis(diphenylphosphano)biphenyl]methane]tetrakis[chlorogold(I)] (4c)

Compound 5b (0,060 g, $2{,}9 \cdot 10^{-2}$ mmol) was dissolved in chloroform (6 mL) and [AuCl(THT)][188] (THT = tetrahydrothiophene) (0,073 g, $2{,}3 \cdot 10^{-1}$ mmol) was added. The resulting solution was stirred overnight, then the solvent was removed by vacuum and the resulting white powder was washed with ethanol and diethylether (5+5 mL). Obtained 0,049 g, yield 42,7%

^{31}P-NMR 127 MHz 33,2(s) ppm. Elemental analysis: calculated for $C_{97}H_{72}Au_4Cl_4P_4$ C 50.85%, H 3.17%. Found C 49.96%, H 3.99%

Tetra(3'-5'-difluorobiphenyl)methane (5a)

Tetrakis(triphenylphosphano)palladium(0) (0,093 g, 0,081 mmol) was solved in 20 ml of degassed DMF and then 3,5-difluorobromobenzene (1,5 ml, 12,9 mmol), Tetra(benzene-4-boronic acid)methane[190] (0,800 g, 1,61 mmol) and Na_2CO_{3aq} 2M (20 ml) were in sequence added. The resulting mixture was stirred at 90°C overnight, cooled to room temperature, and after adding brine (100 ml) the resulting whitish sticky solid was suspended in acetone (150 mL). Filtration and washing with additional acetone leads to a white solid. Obtained 0,765 g, 60,2% yield.

^{19}F-NMR 282 MHz (DMSO, ^{1}H decoupled): -109,7(s) ppm. Elemental analysis: calculated for $C_{49}H_{28}F_8$ C 76,66%, H 3,67%. Found C 75,41% H 3,61%

Tetrakis[3'-5'-bis(diphenylphosphano)biphenyl]methane (5b)

To tetra(3'-5'-difluorobiphenyl)methane (0,500 g, 0,65 mmol) was added a 0,5 M THF solution of $KPPh_2$ (21 ml, 10,5 mmol) and the resulting solution stirred at room temperature for an hour. Then it was stirred at 90°C overnight. Then the resulting suspension was cooled to room temperature and CH_3OH (120 ml) added. After 15 minutes stirring the suspension was filtered and the whitish solid was washed with additional CH_3OH. Then it was solved in chloroform (30 mL) and the solution was treated with activated carbon and filtered over silica. Then the solvent was removed with rotavapor

and the resulting white crystalline solid washed again with methanol. Obtained 0,850 g, yield 62%. ^{31}P-NMR 127 MHz -4,17(s) ppm. Elemental analysis: calculated for $C_{145}H_{108}P_8$ C 83,00%, H 5,19%. Found C 82,31%, H 5,14%

[Tetrakis[3'-5'-bis(diphenylphosphano)biphenyl]methane]octakis[chlorogold(I)] (5c)

Compound 5b (0,060 g, $2{,}9 \cdot 10^{-2}$ mmol) was dissolved in chloroform (6 mL) and [AuCl(THT)][188] (THT = tetrahydrothiophene) (0,073 g, $2{,}3 \cdot 10^{-1}$ mmol) was added. The resulting solution was stirred overnight, then the solvent was removed by vacuum and the resulting white powder was washed with ethanol and diethylether (5+5 mL). Obtained 0,049 g, yield 42,7%

^{31}P-NMR 127 MHz 34,3(s) ppm. Elemental analysis: calculated for $C_{145}H_{108}Au_6Cl_8P_8$ C 44,01%, H 2,75%. Found C 45,59%, H 3,59%

[{$Ir_4(CO)_{11}$}$_4$(180tetraphos)]

In a Schlenk tube 180tetraphos (15 mg, $1.68 \cdot 10^{-2}$ mmol) have been dissolved in chloroform (3 mL) and then TPP[$Ir_4Br(CO)_{11}$] (101 mg, $6.67 \cdot 10^{-2}$ mmol) have been added. The resulting solution was allowed to stir for 24 hours, while it turned from orange to yellow. A TLC (CH_2Cl_2 : hexane 7 : 3) confirmed the presence of a unique product. So the solution has been dried by a vacuum pump and the resulting yellow solid has been washed with acetonitrile (2x5 mL). Obtained 61 mg, yield 69.8%

$CHCl_3$ IR ν_{CO}=2089, 2057, 2019, 1842, 1822 cm^{-1}

^{31}P-NMR: -9.126 ppm.

Elemental analysis: calculated for $Ir_{16}C_{104}H_{46}O_{44}P_4$ C 24.03%, H 0.89%, found C 24.28%, H 1.11%,

[{$Ir_4(CO)_{11}$}$_4$(180tertetraphos)]

In a Schlenk tube 180tertetraphos (15 mg, $1.55 \cdot 10^{-2}$ mmol) have been dissolved in chloroform (5 mL) and then TPP[$Ir_4Br(CO)_{11}$] (92 mg, $6.15 \cdot 10^{-2}$ mmol) have been added.

The resulting solution was allowed to stir for 24 hours, while it turned from orange to yellow. A TLC (CH_2Cl_2 : hexane 5.5 : 4.5) confirmed the presence of a unique product. So the solution has been dried by a vacuum pump and the resulting yellow solid has been washed with acetonitrile (2x5 mL). Obtained 69 mg, yield 87.2%

$CHCl_3$ IR ν_{CO}=2087, 2054, 2016, 1842, 1821 cm^{-1}

^{31}P-NMR: --10.341 δ.

Elemental analysis: calculated for $Ir_{16}C_{110}H_{50}O_{44}P_4$ C 25.02%, H 0.96, found C 25.01%, H 0.97%

[{$Ir_4(CO)_{11}$}$_6$(120hexaphos)]

In a Schlenk tube 120hexaphos (15 mg, $1.05 \cdot 10^{-2}$ mmol) have been dissolved in chloroform (3 mL) and then TPP[$Ir_4Br(CO)_{11}$] (95 mg, $6.35 \cdot 10^{-2}$ mmol) have been added. The resulting solution was allowed to stir for 24 hours, while it turned from orange to yellow. A TLC (CH_2Cl_2 : hexane 7 : 3) confirmed the presence of a unique product. So the solution has been dried by a vacuum pump and the resulting yellow solid has been washed with acetonitrile (2x5 mL). Obtained 56 mg, yield 67.5%

$CHCl_3$ IR ν_{CO}=2089, 2054, 2013, 1841, 1820 cm^{-1}

^{31}P-NMR: -10.597 ppm

Elemental analysis: calculated for $Ir_{24}C_{162}H_{72}O_{66}P_6$ C 24.71%, H 0.92%, found C 25.29%, H 1.10%

[{$Ir_4(CO)_{11}$}$_4$(t4dpppm)]

In a Schlenk tube t4dpppm (15 mg, $1.42 \cdot 10^{-2}$ mmol) have been dissolved in chloroform (3 mL) and then TPP[$Ir_4Br(CO)_{11}$] (85 mg, $5.68 \cdot 10^{-2}$ mmol) have been added. The resulting solution was allowed to stir for 24 hours, while it turned from orange to yellow. A TLC (CH_2Cl_2 : hexane 5.5 : 4.5) confirmed the presence of a unique product. So the solution has been dried by a vacuum pump and the resulting yellow solid has been washed with acetonitrile (2x5 mL). Obtained 58 mg, yield 76.1%

$CHCl_3$ IR ν_{CO}=2088, 2055, 2019, 1844, 1822 cm^{-1}

^{31}P-NMR: -12.723 ppm

Elemental analysis: calculated for $Ir_{16}C_{117}H_{56}O_{44}P_4$ C 26.19%, H 1.05%, found C 25.44%, H 1.19%.

[{$Ir_4(CO)_{11}$}$_4$(t3'dppbpm)]

In a Schlenk tube t3'dppbpm (15 mg, $1.10 \cdot 10^{-2}$ mmol) have been dissolved in chloroform (3 mL) and then TPP[$Ir_4Br(CO)_{11}$] (66 mg, $4.41 \cdot 10^{-2}$ mmol) have been added. The resulting solution was allowed to stir for 24 hours, while it turned from orange to yellow. A TLC (CH_2Cl_2 : hexane 5.5 : 4.5) confirmed the presence of a unique product. So the solution has been dried by a vacuum pump and the resulting yellow solid has been washed with acetonitrile (3x5 mL). Obtained 51 mg, yield 81.1%

$CHCl_3$ IR ν_{CO}=2088, 2055, 2019, 1844, 1822 cm^{-1}

^{31}P-NMR: -11.243 ppm

Elemental analysis: calculated $Ir_{16}C_{144}H_{72}O_{44}P_4$ C 30.31%, H 1.27%, trovato C 31.10%, H 1.48%.

[{$Ir_4(CO)_{11}$}$_4$(t3'5'dppbpm)]

In a Schlenk tube t3'5'dppbpm (15 mg, $7.16 \cdot 10^{-3}$ mmol) have been dissolved in chloroform (3 mL) and then TPP[$Ir_4Br(CO)_{11}$] (85 mg, $5.68 \cdot 10^{-2}$ mmol) have been added. The resulting solution was allowed to stir for 24 hours, while it turned from orange to yellow. A TLC (CH_2Cl_2 : hexane 1 : 1) confirmed the presence of a unique product. So the solution has been dried by a vacuum pump and the resulting yellow solid has been washed with acetonitrile (3x5 mL). Obtained 60 mg, 77.8%

$CHCl_3$ IR ν_{CO}=2089, 2054, 2018, 1842, 1823 cm^{-1}

^{31}P-NMR: -10,409 ppm

Elemental analysis: calculated $Ir_{32}C_{233}H_{108}O_{88}P_8$ C 26.12%, H 1.02%, found C 28.72%, H 2.01%.

$[PPh_4]_4[\{Ir_6Au(CO)_{15}\}_4$(180tetraphos)]

$[\{AuCl\}_4$(180tetraphos)] (40 mg, 0,022 mmol) has been dissolved in THF (15 mL) and $AgCF_3SO_3$ (22 mg, 0,088 mmol) has been added under stirring far from light. The precipitated AgCl has been separated and the resulting solution has been added to a solution prepared from $[PPh_4]_2[Ir_6(CO)_{15}]$ (200 mg, 0,088 mmol) and THF (15 mL) just put under CO atmosphere. After about two hours the reaction was completed as checked bu IR spectroscopy. The solution has been concentrated and 2-propanol (20 mL) added. This has allowed the product to precipitate, which has been then washed with 2-propanol. Obtained 142 mg, 68,8%

THF IR ν_{CO}=2020(vs), 1788(m) cm^{-1}

^{31}P-NMR: 98,5(s) – 23(s) ppm

Elemental analysis: calculated for $Au_4Ir_{24}C_{216}H_{126}O_{60}P_8$ (9332,9) C 27.79%, H 1.36%, found C 29.23%, H 1.94%.

$[NBu_4]_{18}[\{Pt_{19}Au(CO)_{22}\}_6$(120hexaphos)]

$[NBu_4]_4[Pt_{19}(CO)_{22}]$ (316 mg, 0,06 mmol) have been dissolved under nitrogen atmosphere in acetone (10 mL). $[\{AuCl\}_6$(120hexaphos)] (29 mg, 0,01 mmol) have been dissolved in THF far from light and $AgCF_3SO_3$ (15 mg, 0,06 mmol) have been added. After the separation of AgCl, the resulting solution has been added to the Pt19 solution under stirring. The resulting solution has been put under CO atmosphere and stirred for 40 minutes. After this time the reaction was completed as checked by IR spectroscopy. The solvents were removed with vacuum pump, acetone (10 mL) was added and a IR spectrum collected. Then 2-propanol (20 mL) has been added and the solution concentrated, affording to the precipitation of the product as a black powder.

Acetone IR ν_{CO}=2024(vs), 1821(m) cm^{-1}

Elemental analysis: calculated for $Au_6Pt_{114}C_{420}H_{720}O_{122}P_6$ (31746,59) C 15,89%, H 2,28%, N 0,79 found C 16,13%, H 1,96% N 0,66

References

[1] a) A.G. Orpen, *J. Chem. Soc., Chem. Comm*., **1985,** 1310;

b) P.B. Dias, M.E.M. Depiedade, J.A.M. Simoes, *Coord. Chem. Rev*., **2004**, *135*, 737.

[2] C.A. Tolman, *Chem. Rev*., **1977**, *77*, 313

[3] D.R. Anton, R.H. Crabtree, *Organomet*., **1983**, *2,* 621

[4] F. Basolo, *Polyhedron*, **1990**, *9*, 1503

[5] a) J.A.S. Howell, P.M. Burkishaw, *Chem. Rev*., **1983**, *83*, 557;

b) F. Basolo, *Polyhedron*, **1990**, *9*, 1503;

c) D.J. Daresbourg, *Adv. Organomet. Chem*., **1982**, *21*, 11.

[6] a) O. Eisenstein et al., *New J. Chem.* **1990**, *14*, 671;

b) F. Maseras, O. Eisenstein, et al., *New J. Chem.* **1998**, *22*, 1493.

[7] a) R. J. Cross, *Chem. Soc. Rev*. **1985**, *14*, 197;

b) F. Basolo et al., *J. Am. Chem. Soc.* **1966**, *85*, 3929;

c) F. Basolo et al., *J. Am. Chem. Soc.* **1967**, *89*, 4626.

[8] R. G. Pearson, H. B. Gray, and F. Basolo, *J. Am. Chem. Soc.* **1960**, *82*, 787.

[9] a) G. Wilkinson, R. D. Gillard, J. A. McCleverty, *Comprehensive Coordination Chemistry*, Pergamon Press, Oxford, **1987**;

b) E. W. Abel, F. G. A. Stone, G. Wilkinson, *Comprehensive Organometallic Chemistry*, Pergamon Press, Oxford, **1982**;

c) J. A. Osborn, F. H. Jardine, J.F. Young, G. Wilkinson, *J. Chem. Soc. A*, **1966**, 1711;

d) M. Hidai, K. Tominari, Y. Uchida, A. Misono, *J. Chem. Soc. D*, **1969**, *814;*

e) M. Hidai, K. Tominari, Y. Uchida, *J. Chem. Soc.*, **1972**, *94*, 110;

f) R. Noyori, H. Takaya, *Acc. Chem. Res.*, **1990**, *23*, 345;

g) R.Noyori, *Angew. Chem. Int. Ed.*, **2003**, *41*, 2008;

j) W. S. Knowles, *Adv. Synth. Catal.*, **2003**, *345*, 3;

k) R. H. Grubbs, *Adv. Synth. Catal.*, **2007**, *349*, 34;

l) C. Chielini, A. Casini, O. Cochet, C. Gabbiani, G. Alihaud, C. Dani, L. Messori, E. Z. Amri, *Chem. Biodiversity*, **2008**, *5*, 1513;

m) A. E. Finklestein, D. T. Walz, V. Batista, M. Mizraji, F. Roisman, A. Misher, *Ann. Rheum. Dis.*, **1976**, *35*, 251.

[10] K. Biradha, M. Sarkar, L. Rajput, *Chem. Commun*., **2006**, *4169*.

[11] a) H. Willner, F. Aubke et al., *Angew. Chem. Int. Ed.* **1996,** *35*, 1974;

b) H. Willner, F. Aubke et al., *Angew. Chem. Int. Ed.* **2000**, *39*, 168.

[12] F.A. Cotton, Inorg. Chem., **1964**, *3*, 1217

[13] J.J. Raffalko, P.M. Watson, D. H. Malueg, R.E. Davies, B.C. Gates, *Inorg. Chem.*,**1981**, 20, 3540.

[14] M.M. Harding, B.S.Nicholls, A.K. Smith, *J. Chem. Soc*., *Dalton Trans*., **1983**, 1479.

[15] H.-K.Wang, H.W. Choi and E.L.Muetterties, *Inorg. Chem.* **1981**, 20, 2661.

[16] J.P.Collman, *et.al*., *J. Am. Chem. Soc.*, **1983**, 105, 3913.

[17] R.Bau, *et.al*., *Inorg.Chem.*, **1984**, 23, 4758.

[18] G.Ciani, M.Manassero, V.G. Albano, F,Canziani, G.Giordano, S.Martinengo, P.Chini., *J.Organomet. Chem.*, **1978**, 150, C17.

[19] D.M.Vandenberg, T.Chin-Choy, P.C.Ford, *J. Organomet. Chem.*, **1989**, 366, 257.

[20] G.J.Leigh and R.L.Richards, *Comprhensive Organometallic Chemistry-I,* 5, 614

[21] V.G.Albano, D.Braga, S.Martinengo, *J. Chem. Soc, Dalton Trans.*, **1983**, 253.

[22] P.E.Cattermole, K.G.Orrell, A.G.Osborne, *J. Chem. Soc., Dalton Trans.*, **1974**, 328.

[23] Bo Keun Park, Md.A.Miah, Hongkyu Kang, Kwangyeol Lee, Youn-Jaung Cho, D.G.Churchill, Sangwoo Park, Moon-Gun Choi, Joon T.Park, *Organometallics*, **2005**, 24, 675

[24] F.Ragaini, F.Porta and F.Demartin, *Organometallics*, **1991**, 10, 185.

[25] F. A. Cotton, *Inorg. Chem.*, **1966**, *5*, 1083

[26] J. R. Shapley, G. F. Stuntz, M. R. Churchill, H. P. Hutchinson, **1979**, *J. Am. Chem. Soc., 101, 7425-7428*

[27] K.J. Karel and J.R. Norton, *J. Am. Chem. Soc.*, **1974**, 96, 6812.

[28] D.J. Darensbourg, in *"The chemistry of Metal Cluster Complexes", eds. D.W. Shriver, H.D. Kaesz and R. Adams, VHC, New York*, **1990**, 121.

[29]B.E. Mann, B.T. Pickup and A.K. Smith, *J. Chem Soc, Dalton Trans.*, **1989**, 889.

[30] A. Strawczynski, R. Ros and R. Roulet, *Helv. Chim. Acta,* **1988**, 71, 867.

[31] K.J. Karel and J.R. Norton, *J. Am. Chem. Soc.*, **1974**, 96, 6812.

[32] D. Sonnenberger and J.D. Atwood, *Inorg. Chem.,* **1981**, 20, 3243.

[33] M.P. Brown et al., *Inorg. Chim. Acta,* **1989**, 162, 287.

[34] R. Della Pergola, L. Garlaschelli, S. Martinengo, F. Demartin, M. Manassero, M. Sansoni, *Gazz. Chim. Ital.*, **1987**, 117, 245.

[35] D.M.P. Mingos, *Inorg.Chem.*, **1982**, 21, 464.

[36] D.C. Sonninberger, J.D. Atwood, *Organometallics*, **1982**, 1, 694.

[37] A. Orlandi, U. Frey, G. Suardi, A.E. Merbach, R. Roulet, *Inorg. Chem.*, **1985**, 286, C8.

[38] D. Braga, R. Ros, R. Roulet, *J. Organomet. Chem.*, **1985**, 286, C8.

[39] K.J. Karel, J.R. Norton, *J. Am. Chem. Soc.*, **1974**, *96*, 6812

[40] J.R. Shapley, G.F. Stuntz, M.R. Churchill and J.P. Hutchinson, *J. Am. Chem. Soc.*, **1979**, 101, 7425.

[41] P. Braunstein, *J. Organomet. Chem.*, **2004**, *689*, 3953

[42] M. Ichikawa, *Metal Clusters in Chemistry*; P. Braunstein, L. A. Oro, P. R. Raithby; Wiley-VCH: Wienheim, Germany, **1999**, Vol. 3, p 1273.

[43] B. F. G. Johnson, *Coord. Chem. Rev.*, **1999**, *190-192*, 1269.

[44] F. Schweyer-Tihay, P. Braunstein, C. Estournes, J. L. Guille, B. Lebeau, J.-L Palliaud, M. Richard-Plouet, J. Rose; *Chem. Mater.*, **2003**, *15*, 57

[45] A. J. Deeming, *J. Cluster Sci.*, **1992**, *3*, 347.

[46] E. W. Ainscough, A. M. Brodie, R. K. Coll, T. G. Kotch, A. J. Lees, A. J. A. Mair, J. M. Waters, *J. Organomet. Chem.*, **1996**, *517*, 173.

[47] J. Zhang, X. -N. Chen, Y. -Q. Yin, W. -L. Wang, X. -J. Huang, *J. Organomet. Chem.*, **1999**, *582*, 252.

[48] V. Torna, O. Vidoni, U. Simon, G. Schmid, *Eur. J. Inorg. Chem.*, **2003**, *1121*.

[49] L. -C. Song, W. -F. Zhu, Q. -M Hua, H. Wua, G. -A. Yu, *J. Organomet. Chem.*, **2003**, *667*, 143.

[50] A. J. Amoroso, B. F. G. Johnson, J. Lewis, A. D. Massey, P. R. Raithby, W. T. Wong, *J. Organomet. Chem.*, **1992**, *440*, 219.

[51] A. J. Amoroso, A. J. Edwards, B. F. G. Johnson, J. Lewis, M. R. Al-Mandhary, P. R. Raithby, V. P. Saharan, W. T. Wong, *J. Organomet. Chem.*, **1993**, *443*, C11.

[52] C. J. Adams, M. I. Bruce, E. Horn, B. W. Skeleton, E. R. T. Tiekink, A. H. White, *J. Chem. Soc. Dalton Trans.*, **1993**, *3299*.

[53] C. E. Housecroft, A. L. Rheingold, A. Weller, G. P. A. Yap, *J. Organomet. Chem.*, **1998**, 565*, 105*.

[54] M. Ferrer, A. Julia, O. Rossell, M. Seco, M. A. Pelinghelli, A. Tiripicchio, *Organometalics*, **1997**, *16*, 3715.

[55] D. Imhof, U. Burckhardt, K.-H. Dahmen, F, Joho, R. Nesper, *Inorg. Chem.*, **1997**, *36*, 1813.

[56] N. Feeder, J. Geng, P. G. Goh, B. F. G. Johnson, C. M. Martin, D. S. Shephard, W. Zhou, *Angew. Chem., Int. Ed.* **2000**, *39*, 1661.

[57] J. Geng, H. Li, W. T. S. Huck, B. F. G. Johnson, *Chem.Commun.*, **2004**, 2122.

[58] A. Togni, L. M Venanzi, *Angew. Chem., Int. Ed. Engl.* **1994**, *33*, 7.

[59] G. Chelucci, R. P. Thummel, *Chem. Rev.* **2002**, *102*, 3129.

[60] C. Kaes, A. Katz, M. W. Hosseini, *Chem. Rev.* **2000**, *100*, 3553.

[61] A. J. Deeming, R. Peters, M. B. Hursthouse, J. D. J. Backer-Dirks, *J. Chem. Soc., Dalton Trans.* **1982**, 787.

[62] G. A. Foulds, B. F. G. Johnson, J. Lewis, *J. Organomet. Chem*, **1985**, *294*, 123.

[63] W. Y. Wong, S. H. Cheung, S. M. Lee, S. Y. Leung, *J.Organomet. Chem.*, **2000**, *596*, 36.

[64] W. Y. Wong, S. -H. Cheung, X. Huang, Z. Lin, *J. Organomet.Chem.*, **2002**, *655*, 39.

[65] S. Chan, W. T. Wong, *J. Chem. Soc., Dalton Trans.*, **1994**, 1605.

[66] R. Ros, R. Bertani, A. Tassan, D. Braga, F. Grepioni, E. Tedesco, *Inorg. Chim. Acta*, **1996**, *244*, 11.

[67] G. Freeman, S. L. Ingham, B. F. G. Johnsopn, M. McPartlin, I. J. Scowen, *J. Chem. Soc., Dalton Trans.* **1997**, 2705.

[68] S. P. Tunik, I. O. Koshevoy, A. J. Poe, D. H. Farrar, E. Nordlander, M. Haukka, T. A. Pakkanen, *Dalton*, **2003**, 2457.

[69] K. Wajda-Hermanowicz, F. Pruchnik, M. J. Zuber, *J. Organomet. Chem.*, **1996**, *508*, 75.

[70] A. J. Deeming, M. B. Smith, *J. Chem. Soc., Dalton Trans.* **1993**, 3383.

[71] V. I. Ponomarenko, T. S. Pilyugina, V. D. Khripun, E. V. Grachova, S. P. Tunik, M. Haukka, T. A. Pakkanen, *Eur. J. Inorg. Chem.*, in press.

[72] G. Longoni, P. Chini, *J. Am. Chem. Soc.*, **1976**, *98*, 7225.

[73] B.T. Heaton, L. Strona, S. Martinengo, D. Strumolo, V.G. Albano, D. Braga, *J. Chem. Soc. Dalton Trans.*, **1983,** *2175*.

[74] L.H. Gade, B.F.G. Johnson, J. Lewis, M. McPartlin, H.R. Powell, *J. Chem. Soc. Chem. Commun.*, **1990**, *110*.

[75] T. Nakajima, A. Ishiguro, Y. Wakatsuki, *Angew. Chem. Int. Ed.*, **2000**, *39*, 1131.

[76] T. Nakajima, A. Ishiguro, Y. Wakatsuki, *Angew. Chem. Int. Ed.*, **2001**, *40*, 1066.

[77] K.-F. Yung, W.-T. Wong, *Angew. Chem. Int. Ed.*, **2003**, *42*, 553.

[78] F. Demartin, M.C. Iapalucci, G. Longoni, *Inorg. Chem*., **1993**, *32*, 5536.

[79] M.A. Beswick, J. Lewis, P.R. Raithby, M.C. Ramirez de Arellano, *Angew. Chem. Int. Ed*., **1997**, *36*, 291.

[80] M.A. Beswick, J. Lewis, P.R. Raithby, M.C. Ramirez de Arellano, *Angew. Chem. Int. Ed*, **1997**, *36*, 2227.

[81] D.S. Shephard, T. Maschmeyer, B.F.G. Johnson, J.M. Thomas, G. Sankar, D. Ozkaya, W. Zhou, R.D. Oldroyd, R.G. Bell, Angew. *Chem. Int. Ed.*, **1997**, *36*, 2242.

[82] S. Zacchini, in preparation.

[83] A. Fumagalli, M.C. Malatesta, A. Tentori, D. Monti, P. Macchi, A. Sironi, *Inorg. Chem*., **2002**, *41*, 76.

[84] I.O. Koshevoy, M. Haukka, T.A. Pakkanen, S.P. Tunik, P. Vainiotalo, *Organometallics*, **2005**, *24*, 3516.

[85] J.L. Segura, N. Martin, *Chem. Soc. Rev.*, **2000**, *29*, 13.

[86] N. Dragoe, H. Shimotani, M. Hayashi, K. Saigo, A. de Bettencourt-Dias, A.L. Balch, Y. Miyake, Y. Achiba, K. Kitazawa, *J. Organomet. Chem*., **2000**, *65*, 3269.

[87] N. Dragoe, H. Shimotani, J. Wang, M. Iwaya, A. de Bettencourt-Dias, A.L. Balch, K. Kitazawa, *J. Am. Chem. Soc.*, **2001**, *123*, 1294.

[88] K. Lee, H. Song, J. T. Park, *Acc. Chem. Res*., **2006**, *36*, 78.

[89] J.M. Williams, *Adv. Inorg. Chem. Radiochem*., **1983**, *26*, 235.

[90] L. Brossard, M. Ribault, L. Valade, P. Cassoux, *Physica B and C (Amsterdam*), **1986**, *143*, 378.

[91] H. Tajima, M. Inokuchi, A. Cobayashi, T. Ohta, R. Kato, H. Cobayashi, H. Kuroda, *Chem. Lett*., **1993**, 1235.

[92] [208] L.B. Coleman, M.J. Cohen, D.J. Sandman, F.G. Yamagishi, A.F. Garito, A.J. Heeger, *Solid State Commun.*, **1973**, *12*, 1125.

[93] K. Bechgaard, K. Carneiro, F.B. Rasmussen, H. Olsen, G. Rindorf, C.S. Jacobsen, H. Pedersen, J.E. Scott, *J. Am. Chem. Soc.*, **1981**, *103*, 2440.

[94] A.F. Diaz, K.K. Kanazawa, G.P. Gardini, *J. Chem. Soc. Chem. Commun*., **1979**, 635.

[95] J. Roncali, *Chem. Rev.*, **1992**, *92*, 711.

[96] W.A. Little, *Phys. Rev. A*, **1964**, *134*, 1416.

[97] D. Jerome, K. Bechgaard, *Nature*, **2001**, *410*, 162.

[98] J.K. Bera, K.R. Dunbar, *Angew. Chem. Int. Ed*., **2002**, *41*, 4453.

[99] G.M. Finniss, E. Canadell, C. Campana, K.R. Dunbar, *Angew. Chem. Int. Ed. Engl*., **1996**, *35*, 2772.

[100] F. Huq, A.C. Skapski, *J. Cryst. Mol. Struct.*, **1974**, *4*, 411.

[101] F. Bagnoli, D. Belli Dell'Amico, F. Calderazzo, U. Englert, F.Marchetti, G.E. Herberich, N. Pasqualetti, S. Ramello, *J. Chem. Soc. Dalton Trans.*, **1996**, 4317.

[102] F.A. Cotton, E.V. Dikarev, M.A. Petrukhina, *J. Organomet. Chem.*, **2000**, *596*, 130.

[103] F.A. Cotton, E.V. Dikarev, M.A. Petrukhina, *J. Chem. Soc. Dalton Trans*., **2000**, 4241.

[104] P. Klüfers, *Angew. Chem. Int. Ed*., **1985**, *24*, 70.

[105] N. Masciocchi, M. Moret, P. Cairati, F. Ragaini, A. Sironi, *J. Chem. Soc. Dalton Trans*., **1993**, 471.

[106] J.C. Calabrese, L.F. Dahl, A. Cavalieri, P. Chini, G. Longoni, S. Martinengo, *J. Am. Chem. Soc.* **1974**, *96*, 2616.

[107] D. Braga, F. Grepioni, P. Milne, E. Parisini, *J. Am. Chem. Soc*, **1993**, *115*, 5115.

[108] C.J. McNeal, J.M. Hughes, G.J. Lewis, L.F. Dahl, *J. Am. Chem. Soc.*, **1991**i, *113*, 372.

[109] P.M.S. Monk, *The Viologens*, John Wiley and Sons, Chichester, **1998**, and references therein.

[110] D. Collini, C. Femoni, M.C. Iapalucci, G. Longoni, *Proceedings of the II National Conference on Nanosciences and Nanotechnologies*, Bologna, **2004**, P1.12.

[111] R. J. Puddephatt, *Chem. Soc. Rev.*, **2008**, *37*, 2012.

[112] R. J. Puddephatt, *J. Inorg. Organomet. Polym. Mater*., **2005**, *15*, 371.

[113] M. -C. Brandy, R. J. Puddephatt, *Chem. Commun*., **2001**, *1280*.

[114] A. Deák, T. Megys, G. Tárkányi, P. Király, L. Bickóz, G. Pálinkás, P. J. Stang, *J. Am. Chem. Soc.*, **2006**, *128*, 12668.

[115] G. Tárkányi, P. Király, G. Pálinkás, A. Deák, *Mang. Reson. Chem.*, **2007**, *47*, 917.

[116] T. Tunyogi, A. Deák, G. Tárkányi, P. Király, G. Pálinkás, *Inorg. Chem.*, **2008**, *47*, 2049.

[117] J. H. K. Yip, J. Prabhavarty, *Angew. Chem. Int. Ed.*, **2001**, *40*, 2159.

[118] R. Lin, J. H. K. Yip, K. Zhang, L. L. Koh, K. –Y. Wong, K. P. Ho, *J. Am. Chem. Soc.*, **2004**, *126*, 15852.

[119] C. P. MacArdle, M. J. Irwin, M.C. Jennings, R. J. Puddephatt, *Angew. Chem. Int. Ed.*, **1999**, *38*, 3376.

[120] C. P. MacArdle, J. J. Vittal, R. J. Puddephatt, *Angew. Chem. Int. Ed.*, **2000**, *39*, 3819.

[121] a) A. E. Underhill and D. M. Watkins, *Chem. Soc. Rev*., **1980**, *9(4),* 429–448.

b) K. V. Krishnamurty, G. M. Harris and V. S. Sastri, *Chem. Rev*., **1970**, *70(2),* 171–197.

c) K. V. Krishnamurty and G. M. Harris, Chem. Rev., **1961**, *61(3),* 213–246.

[122] a) R. Robson, *Dalton Trans*., **2008**, *38,* 5113–5131.

b) M. J. Zaworotko, *Cryst. Growth Des*., **2007**, *7(1),* 4–9.

c) A. Y. Robin and K. M. Fromm, *Coord. Chem. Rev*., **2006**, *250(15–16),* 2127–2157.

d) S. L. James, *Chem. Soc. Rev*., **2003**, *32(5),* 276–288.

e) B. Moulton and M. J. Zaworotko, *Chem. Rev*., **2001**, *101(6),* 1629–1658.

[123] a) A. F. Wells, in *Structural Inorganic Chemistry,* Oxford University Press, London, 5th edn, **1984**.

b) A. F. Wells, in *Three dimensional Nets and Polyhedra*, Wiley, New York, **1977**

c) A. F. Wells, Acta Crystallogr., **1954**, *7(8–9),* 535–544 and 545-554

[124] a) S. R. Batten, B. F. Hoskins and R. Robson, *J. Chem. Soc., Chem. Commun*., **1991**, *(6),* 445–447.

b) B. F. Abrahams, B. F. Hoskins and R. Robson, *J. Am. Chem. Soc*., **1991**, *113(9*), 3603–3607.

c) B. F. Abrahams, B. F. Hoskins, J. Liu and R. Robson, *J. Am. Chem. Soc*., **1991**, *113(8),* 3045–3051.

d) B. F. Hoskins and R. Robson, *J. Am. Chem. Soc*., **1990**, *112(4),* 1546–1554.

[125] a) K. Biradha and M. Fujita, *Chem. Commun*., **2001**, *1*, 15–16.

b) M. Bertelli, L. Carlucci, G. Ciani, D. M. Proserpio and A. Sironi, *J. Mater. Chem*., **1997**, *7(7),* 1271–1276.

c) L. Carlucci, G. Ciani, D. M. Proserpio and A. Sironi, *Inorg. Chem*., **1997**, *36(9*), 1736–1737.

d) S. Kawata, S. Kitagawa, M. Kondo, I. Furuchi and M. Munakata, *Angew. Chem., Int. Ed. Engl.,* **1994**, *33(17),* 1759–1761.

[126] a) M. Fujita, M. Tominaga, A. Hori and B. Therrien, *Acc. Chem. Res*., **2005,** *38(4),* 371–380

b) M. Fujita, K. Umemoto, M. Yoshizawa, N. Fujita, T. Kusukawa and K. Biradha, *Chem. Commun*., **2001**, *6*, 509–518.

[127] a) A. Michaelides, V. Kiritsis, S. Skoulika and A. Aubry, *Angew. Chem., Int. Ed. Engl*., **1993**, *32(10),* 1495–1497.

b) B. F. Abrahams, M. J. Hardie, B. F. Hoskins, R. Robson and G. A. Williams, *J. Am. Chem. Soc*., **1992**, *114(26),* 10641–10643.

[128] a) G. R. Desiraju, *Angew. Chem., Int. Ed*., **2007**, *46(44),* 8342–8356.

b) G. R. Desiraju, *Angew. Chem., Int. Ed. Engl*., **1995**, *34(21),* 2311–2327.

c) C. B. Aakero¨ y and K. R. Seddon, *Chem. Soc. Rev*., **1993**, *22(6),* 397–407.

[129] a) M. J. Zaworotko, *Chem. Soc. Rev*., **1994**, *23(4),* 283–288.

b) S. B. Copp, S. Subramanian and M. J. Zaworotko, *J. Chem. Soc., Chem. Commun*., **1993**, *13,* 1078–1079.

c) S. B. Copp, S. Subramanian and M. J. Zaworotko, *J. Am. Chem. Soc.,* **1992**, *114(22),* 8719–8720.

[130] a) X. Wang, M. Simard and J. D. Wuest, *J. Am. Chem. Soc*., **1994**, *116(29),* 12119–12120.

b) M. Simard, D. Su and J. D. Wuest, J. Am. Chem. Soc., **1991**, *113(12),* 4696–4698.

c) O. Ermer and A. Eling, *Angew. Chem., Int. Ed. Engl*., **1988**, *27(6),* 829–833.

[131] G. B. Gardner, D. Venkataraman, J. S. Moore and S. Lee, *Nature*, **1995**, *374(6525),* 792–795.

[132] a) O. M. Yaghi, G. Li and H. Li, *Nature*, **1995**, *378(6558),* 703–706.

b) M. Kondo, T. Yoshitomi, K. Seki, H. Matsuzaka and S. Kitagawa, *Angew. Chem., Int. Ed. Engl*., **1997**, *36(16),* 1725–1727.

[133] a) O. M. Yaghi, D. A. Richardson, G. Li, E. Davis and T. L. Groy, *Mater. Res. Soc. Symp. Proc*., **1995**, *371*, 15–19.

b) O. M. Yaghi and H. Li, *J. Am. Chem. Soc*., **1995**, *117(41),* 10401–10402.

[134] a) S. Shimomura, S. Horike and S. Kitagawa, *Stud. Surf. Sci. Catal*., **2007**, *170B*, 1983–1990.

b) S.-i. Noro, S. Kitagawa, M. Kondo and K. Seki, *Angew. Chem., Int. Ed*., **2000**, *39(12),* 2082–2084.

[135] a) G. Férey, C. Mellot-Draznieks, C. Serre, F. Millange, J. Dutour, S. Surble´ and I. Margiolaki, *Science*, **2005**, *309(5743),* 2040–2042.

b) H. K. Chae, B. Y. Siberio-Perez, J. Kim, Y. B. Go, M. Eddaoudi, A. J. Matzger, M. O'Keeffe and O. M. Yaghi, *Nature*, **2004**, *427(6974),* 523–527.

[136] O. M. Yaghi, M. O'Keeffe, N. W. Ockwig, H. K. Chae, M. Eddaoudi and J. Kim, *Nature*, **2003**, *423(6941),* 705–714.

[137] M. Eddaoudi, D. B. Moler, H. Li, B. Chen, T. M. Reineke, M. O'Keeffe and O. M. Yaghi, *Acc. Chem. Res.*, **2001**, *34(4),* 319–330.

[138] a) T. K. Maji and S. Kitagawa, *Pure Appl. Chem*., **2007**, *79(12),* 2155–2177.

b) M. Eddaoudi, J. Kim, N. Rosi, D. Vodak, J. Watcher, M. O'Keeffe and O. M. Yaghi, *Science*, **2002**, *295(5554),* 469–472.

c) M. Eddaoudi, H. Li and O. M. Yaghi, *J. Am. Chem. Soc*., **2000**, *122(7),* 1391–1397.

[139] a) JeongYong Lee, Omar K. Farha, John Roberts, Karl A. Scheidt, SonBinh T. Nguyen and Joseph T. Hupp, *Chem. Soc. Rev*., **2009**, *38*, 1450-1459

b) S.-H. Cho, B. Ma, S. T. Nguyen, J. T. Hupp and T. E. Albrecht- Schmitt, *Chem. Commun*., **2006**, *(24),* 2563–2565.

c) So-Hye Cho, Baoqing Ma, Son Binh T. Nguyen, Joseph T. Hupp and Thomas E. Albrecht-Schmitt, *Chem. Comm*., **2006**, 2563-2565

[140] a) Mohamedally Kurmoo, *Chem. Soc. Rev*., **2009**, *38*, 1353-1379

[141] a) B. Chen, L. Wang, F. Zapata, G. Qian and E. B. Lobkovsky, *J. Am. Chem. Soc*., **2008**, *130(21),* 6718–6719.

b) L. Bastin, P. S. Barcia, E. J. Hurtado, J. A. C. Silva, A. E. Rodrigues and B. Chen, *J. Phys. Chem. C*, **2008**, *112(5),* 1575–1581.

c) C. Sanchez, B. Julian, P. Belleville and M. Popall, *J. Mater. Chem*., **2005**, *15(35–36),* 3559–3592.

[142] a) M. D. Allendorf, C. A. Bauer, R. K. Bhakta and R. J. T. Houk, *Chem. Soc. Rev*., **2009**, *39*, 1330-1352

b) B. Chen, L. Wang, F. Zapata, G. Qian and E. B. Lobkovsky, *J. Am. Chem. Soc*., **2008**, *130(21),* 6718–6719.

c) R. Custelcean and B. A. Moyer, *Eur. J. Inorg. Chem.,* **2007**, *(10),* 1321–1340.

[143] a) Y. Liu, G. Li, X. Li and Y. Cui, *Angew. Chem., Int. Ed*., **2007**, *46(38),* 6301–6304.

b) O. R. Evans and W. Lin, *Acc. Chem. Res*., **2002**, *35(7)*, 511–522.

[144] a) U. Mueller, M. Schubert, F. Teich, H. Pu¨ tter, K. Schierle-Arndt and J. Pastre´ , *J. Mater. Chem*., **2006**, *16(7),* 626–636.

b) S. Kitagawa, R. Kitaura and S.-I. Noro, *Angew. Chem., Int. Ed*., **2004**, *43(18),* 2334–2375.

c) C. Janiak, *Dalton Trans*., **2003**, *14,* 2781–2804.

[145] a) M. J. Zaworotko, *Nature*, **2008**, *451(7177),* 410–411.

b) K. K. Tanabe, Z. Wang and S. M. Cohen, *J. Am. Chem. Soc*., **2008**, *130(26),* 8508–8517.

c) M. J. Ingleson, J. P. Barrio, J.-B. Guilbaud, Y. Z. Khimyak and M. J. Rosseinsky, *Chem. Commun*., **2008**, *23,* 2680–2682.

d) J. S. Costa, P. Gamez, C. A. Black, O. Roubeau, S. J. Teat and J. Reedijk, *Eur. J. Inorg. Chem*., 20**08**, *10,* 1551–1554.

e) Y.-F. Song and L. Cronin, *Angew. Chem., Int. Ed.*, **2008**, *47(25),* 4635–4637.

[146] a) T. Otieno, S. J. Rettig, R. C. Thompson and J. Trotter, *Inorg. Chem*., **1993**, *32(9),* 1607–1611.

b) D. Imhof, U. Burckhardt, K-H. Dahmen, F. Joho, R. Nesper, *Inorg. Chem*., **1997**, *36*, 1813

[147] L. J. Farrugia , A. G. Orpen in "*Metal Cluster in chemistry*", Vol 2, Ed. Wiley-VCH, 1001

[148] A. F.Wells, Three-dimensional Nets and Polyhedra, Wiley, New York, 1977.

[149] M. Stol, D.J.M. Snelders, H. Kooijman, A.L. Spek, G.P.M. van Klink, G. van Koten, *Dalt. Trans*, **2007**, 2589

[150] M. Daghetta, G. Peli, P. Macchi, L. Garlaschelli, A. Sironi, *VIII Congresso del Gruppo Interdivisionale di Chimica Organometallica della Società Chimica Italiana, Perugia (IT) 25-28 giugno 2008,* P7 poster communication

[151] M. Stol, D.J.M. Snelders, H. Kooijman, A.L. Spek, G.P.M. van Klink, G. van Koten, *Dalt. Trans*, **2007**, 2589

[152] a) M. Cowie, S.K. Dwight, *Inorg. Chem*., **1980**, 19(9), 2500 b) A.R. Sanger, *JCS, Chem. Comm*., **1975**, 893 c) A.R. Sanger, *JCS, Dalton Trans*., **1977**, 1971 d) J.T. Mague, J.P. Mitchener, *Inorg. Chem*., **1969**, 8(1), 119

[153] L. J. Farrugia , A. G. Orpen in "*Metal Cluster in chemistry*", Vol 2, Ed. Wiley-VCH, 1001

[154] A. Strawczynski, G. Suardi, R. Ros and R. Roulet. *Helv. Chim. Acta* **1993**, **76**, 2210

[155] M. Daghetta, G. Peli, P. Macchi, L. Garlaschelli, A. Sironi, P7 Communication, *VIII Congresso Interdivisionale di Chimica Organometallica, SCI*, Perugia 25-28/6/2008

[156] a) M. Cowie, S.K. Dwight, *Inorg. Chem*., **1980**, 19(9), 2500 b) A.R. Sanger, *JCS, Chem. Comm*., **1975**, 893 c) A.R. Sanger, *JCS, Dalton Trans*., **1977**, 1971 d) J.T. Mague, J.P. Mitchener, *Inorg. Chem*., **1969**, 8(1), 119

[157] Matteo Daghetta, *Tesi di Laurea triennale*, Milano **2005**

[158] E. Lozano, M. Nieuwenhuyzen and S. L. James, *Chem. Eur. J*., **2001**,**7**, 2644;

[159] F. Leroux, T.U. Hutschenreuter, C. Charrière, R. Scopelliti, R.W. Hartmann, *Helv. Chim. Acta*, **2003**, *86(7)*, 2671

[160] H. Nishide, M. Miyasaka, E. Tsuchida, *J. Org. Chem*., **1998**, *63*, 7399

[161] P.W. Miller, M. Nieuwenhuyzen, J.P.H. Charmant, S.L. James, *Inorg. Chem*., **2008**, *47*, 8367

[162] For an example: C. Ganesamoorthy, J.T. Mague, M.S. Balakrishna, *Eur. J. Inorg. Chem*., **2008**, *4*, 596

[163] R.W. Tilford, W.R. Gemmil, H-C. Zur Loye, J.J. Lavigne, *Chem. Mater*., **2006**, *18*, 5296

[164] R. Rathore, C.L. Burns, I.A. Guzei, *J. Org. Chem*., **2004**, *69*, 1524

[165] F. P. Pruchnik, K. Wajda-Hermanowicz, M. Koralewicz – J. Organomet. Chem., **1990**,384,381

[166] R. B. Jordan in " Reaction Mechanism of Inorganic and Organometallic Systems", Oxford University Press, **1998**.

[167] P: Chini, B. T. Heaton, in "Tetranuclear Carbonyl Cluster", Topics in Current Chemistry, 71, 1, **1977**, Springer-Verlag, Berlino.

[168] J. R. Shapley, G. F. Stuntz, M. R. Churchill and J. P. Huchinson – J.Chem.Soc.Chem.Commun., **1979**, 219.

[169] A. Ceriotti, private communication, **2009**

[170] a) J.C. Calabrese, L.F. Dahl, P. Chini, G. Longoni, S. Martinengo, J. Am. Chem. Soc., **1974**, 96, 2614, b) P. Zanello, Structure and Bonding, , Springer, Berlin, **1992**. Vol. 79, p.101, c) G.J. Lewis, J.D. Roth, R.A. Montag,

L.K. Safford, X. Gao, S.-C. Chang, L.F. Dahl, M.J. Weaver, J. Am. Chem. Soc. **1990**, 112, 2831, d) J.D. Roth, G.J. Lewis, L.K. Safford, X. Jiang, L.F. Dahl, M.J. Weaver, J. Am. Chem. Soc. **1992**, 114, 6159

[171] C. Femoni, M. C. Iapalucci, F. Kaswalder, G. Longoni and S. Zacchini, Coord. Chem. Rev., 2006, 1580-1604.

[172] B. F. G. Johnson, Coord. Chem. Rev., 1999, **190-192**, 1269-1285.

[173] C. Femoni, F. Kaswalder, M.C. Iapalucci, G. Longoni, M. Mehlstaubl, S. Zacchini and A. Ceriotti, Angew. Chem. Int. Ed., 2006, **45**, 2060-2062.

[174] C. Femoni, F. Kaswalder, M. C. Iapalucci, G. Longoni and S. Zacchini, Eur. J. Inorg. Chem., 2007, 1483-1486.

[175] B. T. Heaton, L. Strona, S. Martinengo, D. Strumolo, V. G. Albano and D. Braga, J. Chem. Soc. Dalton Trans., 1983, 2175.

[176] T Nakajima, A. Ishiguro and Y. Wakatsuki, Angew. Chem. Int. Ed., 2001, **40**, 1066-1067.

[177] A. Fumagalli, M. C. Malatesta, A. Tentori, D. Monti, P. Macchi and A. Sironi, Inorg. Chem., 2002, **41**, 76-85.

[178] I. O. Koshevoy, M. Haukka, T. A. Pakkanen, S. P. Tunik and P. Vainiotalo, Organometallics, 2005, **24**, 3516-3526.

[179] C. Femoni, R. Della Pergola, M. C. Iapalucci, F. Kaswalder, M. Riccò and S. Zacchini, Dalton Trans., 2009, 1509-1511.

[180] a) G. Peli, S. Rizzato, S. Cassese, L. Garlaschelli, M. Manassero, *CrystEngComm* , **2005**, *7*, 575-577, b) N. Janjic, G. Peli, L. Garlaschelli, A. Sironi, P. Macchi, *Cryst. Growth and Des*., **2008**, *8(3)*, 854

[181] S.Blundell, *Magnetism in Condensed Matter*, Oxford Univ. Press

[182] D.M. Washecheck, E.J.Wucherer, L.F. Dahl, A. Ceriotti, G. Longoni, M. Manassero M. Sansoni, P. Chini, *J Am Chem Soc.,* **1979**, 101, 6110

[183] S. El Afefey, A. Ceriotti, M. Daghetta, P. Zanello, S. Fedi, P. Macchi, R. Della Pergola, A. Sironi, XXXVIII Congresso Nazionale della Divisione di Chimica Inorganica della società Chimica Italiana (Trieste 13-16 September 2010), poster communication P22

[184] M.M. Harding, B.S. Nicholls, K. Smith, *J. Chem. Soc., Dalton Trans*, 1983, 1479

[185] D. Imhof, U. Burckhardt, K-H. Dahmen, F. Joho, R. Nesper, *Inorg. Chem.*, 1997, **36**, 1813

[186] P. Chini, G. Ciani, L. Garlaschelli, M. Manassero, S. Martinengo, A. Sironi, F. Canziani, J. *Organomet. Chem*., 1978, **152(2)**, C35-C38

[187] F. Leroux, T.U. Hutschenreuter, C. Charrière, R. Scopelliti, R.W. Hartmann, *Helv. Chim. Acta*, **2003**, *86(7)*, 2671

[188] R. Uson, A. Laguna and M. Laguna, Inorg. Synth., **1989**, *26*, 85

[189] R.W. Tilford, W.R. Gemmill, H-C. zur Loye, J.J. Lavigne, *Chem. Mat.*, **2006**, *18*, 5296

[190] J.H. Fournier, T. Maris, J.D. Wuest, W. Guo, E. Galoppini, *J. Am. Chem. Soc.*, **2003**, *125*, 1006